

**Studies on the separation of rare earths using solid phase
extraction and liquid membrane techniques**

By

Kartikey Kumar Yadav

CHEM01201104023

Bhabha Atomic Research Centre, Mumbai

A thesis submitted to the

Board of Studies in Chemical Sciences

In partial fulfillment of requirements

For the Degree of

DOCTOR OF PHILOSOPHY

of

HOMI BHABHA NATIONAL INSTITUTE

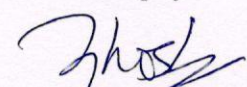


October, 2016

Homi Bhabha National Institute

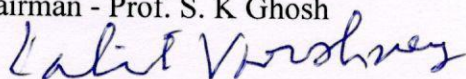
Recommendations of the Viva Voce Committee

As members of the Viva Voce Committee, we certify that we have read the dissertation prepared by **Shri Kartikey Kumar Yadav** entitled "**Studies on the separation of rare earths using solid phase extraction and liquid membrane techniques**" and recommend that it may be accepted as fulfilling the thesis requirement for the award of Degree of Doctor of Philosophy.



Chairman - Prof. S. K. Ghosh

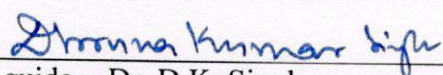
Date: 14/10/2016



14/10/2016

Guide / Convener - Prof. Lalit Varshney

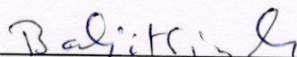
Date:



14/10/2016

Co-guide - Dr. D.K. Singh

Date:



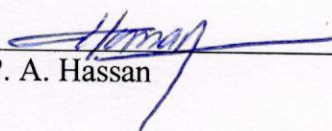
Examiner - Prof. Baljeet Singh

Date: 14/10/2016



Member 1- Dr. Manmohan Kumar

Date: 14-10-2016



Member 2- Dr. P. A. Hassan

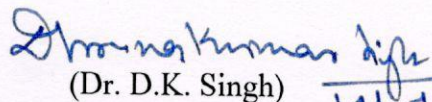
Date: 14-10-2016

Final approval and acceptance of this thesis is contingent upon the candidate's submission of the final copies of the thesis to HBNI.

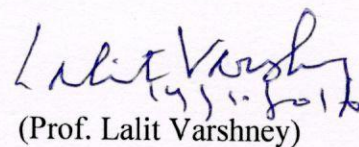
I hereby certify that we have read this thesis prepared under our direction and recommend that it may be accepted as fulfilling the thesis requirement.

Date: 14/10/2016

Place: RTDD,
BARC


(Dr. D.K. Singh)

Co-guide


(Prof. Lalit Varshney)

Guide

STATEMENT BY AUTHOR

This dissertation has been submitted in partial fulfillment of requirements for an advanced degree at Homi Bhabha National Institute (HBNI) and is deposited in the Library to be made available to borrowers under rules of the HBNI.

Brief quotations from this dissertation are allowable without special permission, provided that accurate acknowledgement of source is made. Requests for permission for extended quotation from or reproduction of this manuscript in whole or in part may be granted by the Competent Authority of HBNI when in his or her judgment the proposed use of the material is in the interests of scholarship. In all other instances, however, permission must be obtained from the author.

Kartikey Kumar Yadav

DECLARATION

I, hereby declare that the investigation presented in the thesis has been carried out by me.
The work is original and has not been submitted earlier as a whole or in part for a degree /
diploma at this or any other Institution / University.

Kartikey Kumar Yadav

List of Publications arising from the thesis

Publications in Refereed Journal:

a. Published: 04

1. Studies on separation of rare earths from aqueous media by polysulfone beads containing D2EHPA as extractant, **Kartikey K. Yadav**, D.K. Singh, M. Anitha, L. Varshney and H. Singh, **Separation and Purification Technology**, 118 (2013) 350-358.
2. Solvent impregnated carbon nanotube embedded polymeric composite beads: An environment benign approach for the separation of rare earths, **Kartikey K. Yadav**, K. Dasgupta, D.K. Singh, M. Anitha, L. Varshney and H. Singh, **Separation and Purification Technology**, 143 (2015) 115-124.
3. Dysprosium sorption by polymeric composite bead: Robust parametric optimization using Taguchi method, **Kartikey K. Yadav**, K. Dasgupta, D. K. Singh, L. Varshney, H. Singh, **Journal of Chromatography A**, 1384 (2015) 37-43.
4. Sorption behavior of Y(III) from chloride medium with polymer composites containing di-2-ethyl hexyl phosphoric acid and multiwall carbon nanotube, **Kartikey K. Yadav**, K. Dasgupta, D.K. Singh, M. Anitha, R.K. Lenka, L. Varshney, H. Singh, **Separation Science and Technology**, 50 (2015) 463-470.

b. Accepted: None

c. Communicated: 2

d. Other Publications: 16

BARC News Letter:

1. Thermal analysis of polyethersulfone based composite beads encapsulated with di-2-ethyl hexyl phosphoric acid, **Kartikey K. Yadav**, D.K. Singh S. Francis and L. Varshney, H. Singh, BARC Newsletter, Founder's Day Special Issue (2013), p. 358.
2. Studies on CNT doped D2EHPA impregnated polymeric beads for yttrium extraction, **Kartikey K. Yadav**, K. Dasgupta, D.K. Singh, M. Anitha, L. Varshney and H. Singh, BARC Newsletter, Founder's Day Special Issue (2013), p. 361.

International Conferences:

1. Recovery of uranium from phosphoric acid medium by polymeric composite beads encapsulating organophosphorus extractants, D.K. Singh, **Kartikey K. Yadav**, Lalit Varshney and H. Singh, GLOBAL-2013: International Nuclear Fuel Cycle Conference, September 29 – October 3, 2013, Salt Lake City, Utah, USA

SYMPOSIA:

1. Green separation process for rare earths by extractant encapsulated polymeric composite beads, D.K.Singh, **Kartikey K. Yadav**, International Conference on Frontiers at the Chemistry-Allied Science Interface (FCASI-2016), University of Rajasthan, Jaipur, April 25-26, 2016, IL-10, p.13.
2. Polymeric composite materials for rare earths separation, D.K. Singh, **Kartikey K Yadav**, 4th National Conference on Recent Advances in Chemical & Environmental Sciences: Emphasis on Material Science (RACE-2016), ITM University, Gwalior, March 4-5, 2016, IT 1, p.PL1.

3. Preparation and evaluation of PC88A encapsulated polymeric beads doped with carbon nanotube for Yttrium separations, **Kartikey K. Yadav**, K. Dasgupta, M Anitha, D.K. Singh and J.K. Chakravartty, ARRMA 2016, BARC Mumbai, p. 130
4. Equilibrium and kinetic studies of dysprosium sorption by D2EHPA impregnated polymeric composite beads; **Kartikey K Yadav**, K. Dasgupta, D.K. Singh, M. Anitha, L. Varshney, J.K. Chakravartty; ICSTAR 2015, Kovalam, Kerala, p.71.
5. Sorption behavior of Y(III) from chloride medium with polymer composites containing D2EHPA and CNT, **Kartikey K. Yadav**, K. Dasgupta, D. K. Singh, M. Anitha, L. Varshney, H. Singh, SESTEC 2014, BARC Mumbai, SNFC-35, p.83.
6. Separation of yttrium using carbon nanotube doped polymeric beads impregnated with D2EHPA; K. Dasgupta, **Kartikey K. Yadav**, D. K. Singh, M. Anitha, H. Singh; Proceedings of Chemcon 2013. Institute of Chemical Technology, Mumbai, 2013.
7. Studies on CNT doped D2EHPA impregnated polymeric beads for yttrium extraction, **Kartikey K. Yadav**, K. Dasgupta, D.K. Singh, M. Anitha, L. Varshney and H. Singh, Proceedings of DAE-BRS 4th Interdisciplinary Symposium on Materials Chemistry (ISMC-2012), p.87. (**Awarded Paper**)
8. Studies on the effect of additives on the microstructure and metal ion extractability of polymeric beads encapsulating PC88A, **Kartikey K. Yadav**, D.K. Singh, K. Dasgupta, M. Anitha, R.K. Lenka, L. Varshney and H. Singh, NUCAR 2013, Jabalpur, MP, p. 335-336.
9. Development of polysulfonic composite beads for extraction and separation of rare earths, **Kartikey K. Yadav**, D.K. Singh, H. Singh and L. Varshney, SESTEC-2012, Mumbai, Paper No.SSRM-7, p.37.

10. Preparation and characterization of polysulfonic composite beads encapsulated with di-2-ethyl hexyl phosphoric acid, **Kartikey K. Yadav**, D.K. Singh, S. Francis, L. Varshney and H. Singh, SESTEC 2012, Paper No.SSRM-16, p. 46.
11. Thermal analysis of polysulfone based composite beads encapsulated with di-2-ethyl hexyl phosphoric acid, **Kartikey K. Yadav**, D.K. Singh, S. Francis, L. Varshney and H. Singh, THERMAS 2012, HBNI, Mumbai, India, p.274. (**Awarded Paper**)
12. A novel polymeric composite for separation of Yttrium from chloride medium, **Kartikey K. Yadav**, D.K.Singh, M.K. Kotekar, H. Singh and L. Varshney, Proceedings of Science, STAR-2011 Munnar, Kerala, P-04, p. 25.
13. Development of polysulfonic based polymeric composite beads encapsulated with di-2-ethyl hexyl phosphoric acid for the separation of yttrium and neodymium, **Kartikey K. Yadav**, D.K. Singh, H. Singh and L. Varshney, NUCAR 2011, Vol.1, p. 202.

ACKNOWLEDGEMENTS

I owe a deep sense of gratitude to the Almighty God (Parampita Parmeshwar) whose divine light and warmth provided me the faith and strength to carry on even when the going got tough.

It gives me an immense pleasure in expressing deep sense of reverence to my supervisor Prof. Lalit Varshney for his valuable guidance, enthusiastic interest throughout my research work. His affectionate treatment and magnanimity made it feasible to bring the present work to conclusion. I am grateful to him for articulating this path and being a constant source of inspiration. It gives me prodigious gratification to enunciate my profound gratitude to my mentor Dr. Dhruva Kumar Singh for his meticulous guidance, invigorating discussions and constant encouragement which I received so spontaneously and lavishly throughout the work of dissertation. His intellectual inspiration and moral encouragement will have a niche in my memory as I continue to probe further and deeper in this field in the years to come.

The Chairman and members of doctoral committee are deeply acknowledged for their critical analysis and valuable suggestions provided during the review presentations and pre-synopsis viva-voce. I pay my profound gratitude to Shri Harvinderpal Singh, former Head, Rare Earths Development Section for his constant encouragement which I received throughout the work of dissertation. I am grateful to Dr. M. Anitha for sharing her expertise, experience along with continued assistance during this work. Thanks are also due to Smt. R. Vijayalakshmi and Dr. M. Kotekar for their encouraging discussions and help during the course of my doctoral research. Further I extend thanks to all the members of Rare Earths Development Section with special mention to Shri Jaiprakash R. and Shri Mahesh Z. Jambu for their cooperation throughout my research work.

The list of acknowledgement would be incomplete without the mention of Dr. Kinshuk Dasgupta and Shri Ram Avtar Jat. Their selfless advice, constant motivating support and amiability enabled me to successfully face the challenging times. I owe both of them my sincere gratitude for their generous and timely help.

I take this opportunity to express my love and gratitude to my father who has been my inspiration in all walks of life. It was his teachings of dedication, discipline and passion for the work which always drives me to put more and more efforts towards my duties. My vocabulary fails to express my sense of gratitude to my mother. From the day of my birth, it was my mother's insistence and efforts against all the odds to make me successful person in life. Without

my mother's determination, motivation and affection, I would not have been a bit of what I am today. No words articulate to acknowledge the didactic guidance rendered by my loving parents. I find myself lucky to have an energetic, caring and motivating younger brother like Ashwani with whom I shared my memorable childhood. His puerile and affable attitude will always remain a pleasant part of my life. Last but not the least, expressions of encomium is also due to my in-laws (father & mother) for their constant moral support and blessings.

And most of all for my loving, supportive and encouraging wife Dr. Sanghamitra (Rani) who has left all the luxuries of her life to be with me sharing all the difficulties of my life without complaining even once. She has been by my side throughout this PhD, living every single minute of it. She, being an excellent researcher and achiever, has never let me feel any less and always supported me through her constant motivation and realistic push towards the excellence. I deeply appreciate her unrelenting help, constant encouragement and unending support.

The chain of gratitude would be definitely incomplete if I would forget to thank all my relatives for their blessings, benevolence, benign attitude and unsparing affection. Finally, I wish to thank all those whose names have not figured but have helped during my research work in one way or the other, as the list is more of omission than inclusion. Really this dissertation would not have been completed without any one of you.

(Kartikey K. Yadav)

CONTENTS

Synopsis	i
List of Figures	xii
List of Tables	xviii
Chapter 1: Introduction	1
1.1 Rare Earths	2
1.2 Electronic configuration and properties of rare earths	4
1.2.1 Electronic Configuration and oxidation state:	4
1.2.2 Lanthanide Contraction	7
1.2.3 Physicochemical Properties of Rare Earth	9
1.3 Application and importance of rare earth elements	11
1.3.1 Metallurgy and Machinery	12
1.3.2 Petroleum and Chemical Industry	13
1.3.3 Glass and Ceramics	13
1.3.4 Phosphors	14
1.3.5 Permanent Magnets	15
1.4 Rare earths crisis	15
1.5 Rare earths resources	18
1.5.1 Monazite	19
1.5.2 Bastnaesite	19
1.5.3 Xenotime	20
1.5.4 Secondary Resource	20
1.6 Separation and purification of rare earths	22
1.6.1 Selective Oxidation	22
1.6.2 Selective Reduction	23
1.6.3 Fractional Crystallization	23
1.6.4 Fractional Precipitation	24
1.6.5 Ion Exchange	25
1.6.6 Solvent extraction	27
1.7 Limitation of conventional method and scope of alternative methods	30
1.7.1 Use of hazardous diluents in L-L extraction	30
1.7.2 Limitation of organic extractants	31
1.7.2.1 Saponification	31
1.7.2.2 Complex Process	31

1.7.2.3 Relatively Low Separation Factor	32
1.7.3 Alternative methods	32
1.7.3.1 Membrane based separation	33
1.7.3.1.1 Flat-Sheet Supported Liquid Membrane (FSSLM)	33
1.7.3.1.2 Hollow Fibre Liquid Membrane (HFSLM)	34
1.7.3.2 Solvent impregnated/encapsulated resins	36
1.8 Scope of thesis	39
CHAPTER 2: Experimental and Techniques	43
2.1 Materials	44
2.1.1 Polyethersulfone (PES)	44
2.1.2 N-methyl pyrrolidone (NMP)	44
2.1.3 Di-(2-ethylhexyl) phosphoric acid	45
2.1.4 2-Ethylhexyl 2-ethylhexyphosphonic acid (EHEHPA)	45
2.1.5 Diluents	45
2.1.6 Polyvinyl alcohol	46
2.1.7 Rare earths oxides	46
2.1.8 Multiwall Carbon Nanotube (MWCNTs)	47
2.1.9 Others	47
2.2 Method	47
2.2.1 Preparation of polymeric beads	47
2.2.2 Metal ion sorption studies	48
2.2.3 Sorption isotherms	49
2.2.3.1 Langmuir isotherm	49
2.2.3.2 Freundlich isotherm	51
2.2.4 Sorption Kinetics	52
2.2.4.1 Pseudo first-order kinetic model	53
2.2.4.2 Pseudo second-order kinetic model	54
2.2.4.3 Kinetic steps	55
2.2.4.4 Intraparticle diffusion model	56
2.2.4.5 Boyd's plot	56
2.2.5 Column studies	57
2.2.6 Experimental design to optimize parameters	58
2.2.6.1 Trial-and-error approach	58
2.2.6.2 Design of experiments	58
2.2.6.3 Taguchi Method	59
2.2.6.3.1 Static Problems	59
2.2.6.3.1.1 Batch Process Optimization	59
2.2.6.3.1.2 Dynamic Problems:	60
2.2.7 Membranes based studies	61

2.3 Analytical Instruments/Techniques	64
2.3.1 Inductively Coupled Plasma-Atomic Emission Spectroscopy (ICP-AES)	64
2.3.2 Thermogravimetric analysis (TGA)	66
2.3.3 Scanning electron microscopy (SEM)	66
2.3.4 Fourier transform infra-red spectroscopy (FT-IR)	66
CHAPTER 3: Preparation, characterization and evaluation of D2EHPA encapsulated beads for rare earth sorption	68
3.1 D2EHPA encapsulated beads for rare earths separation	71
3.1.1 Synthesis of PES/D2EHPA beads	71
3.1.2 Characterization	72
3.1.3 Metal ion sorption studies	72
3.1.4 Morphology: Role of additives	73
3.1.5 Thermogravimetric Studies	75
3.1.6 Functional group analysis	79
3.1.7 Effect of additives in polymeric beads on Y(III) sorption	80
3.1.8 Effect of Yttrium ion concentration	82
3.1.9 Effect of aqueous phase acidity	83
3.1.10 Influence of temperature	85
3.1.11 Sorption of Y(III) in the presence of other rare earth ions	86
3.1.12 Sorption isotherms	87
3.1.13 Sorption kinetics	90
3.1.13.1 Pseudo-first order model	91
3.1.13.2 Pseudo-second order model	93
3.1.14 Sorption mechanism	95
3.1.15 Column study (sorption and desorption of yttrium)	98
3.1.16 Stability of composite beads	100
3.1.17 Monitoring of D2EHPA loss	102
3.1.18 Conclusions	104
3.2 Optimization of parameters by Taguchi method for Dysprosium sorption by D2EHPA beads	105
3.2.1 Taguchi method	106
3.2.2 Selection of parameters for Taguchi optimization	108
3.2.3 Preparation and evaluation of polymeric beads	109
3.2.4 Taguchi Analysis on sorption	111
3.2.5 Conclusions	118

CHAPTER 4: Synthesis and evaluation of EHEHPA encapsulated beads for rare earths separation	120
4.1 Synthesis of PES/EHEHPA beads	123
4.2 Effect of additives on beads morphology	123
4.3 Thermogravimetric Analysis	125
4.4 Functional group studies	127
4.5 Effect of additives in polymeric beads on Y(III) extraction	128
4.6 Effect of extractant concentration	130
4.7 Effect of Yttrium ion concentration	132
4.8 Effect of aqueous phase acidity	133
4.9 Y(III) extraction mechanism from aqueous medium	135
4.10 Influence of temperature	136
4.11 Extraction of Y(III) w.r.t. competing rare earth ions: individual and mixture	137
4.12 Yttrium recovery from loaded EHEHPA beads:	139
4.13 Reusability and stability of EHEHPA composite beads	141
4.14 Conclusions	142
 Chapter 5: Transport studies on rare earths by Hollow Fibre Liquid membrane	 144
5.1 Batch Extraction of Dy(III) by EHEHPA	148
5.2 Membrane based transport studies	149
5.2.1 Non-dispersive solvent extraction by hollow fibre membrane:	149
5.2.1.1 Effect of aqueous phase acidity on Dy extraction	150
5.2.1.2 Effect of flow rate	151
5.2.1.3 Effect of Dy(III) concentration	153
5.2.1.4 Influence of organic extraction on Dy(III) extraction	154
5.2.1.5 Effect of phase ratio	155
5.2.1.6 Effect of competing metal ions	156
5.2.1.7 Stripping of Dy(III) from loaded PC88A by HFM:	157
5.2.2 Hollow Fibre supported liquid membrane studies:	158
5.2.2.1 Effect of aqueous Feed Acidity.	161
5.2.2.2 Effect of Carrier Concentration	162
5.2.2.3 Effect of competing metal ions on Dy transport in HFSLM mode:	163
5.2.2.4 Evaluation of permeation coefficient for Dy transport	165
5.3 Conclusion:	166
Chapter 6: Summary and Conclusions	168
References	173

SYNOPSIS

The rare earth elements are a group of 17 elements which have, to a large extent, chemically similar characteristics. Scandium and yttrium, although not part of the lanthanide series are included in the group. Rare earth finds utilization in the arena of modern electronics, high end engineering products, alloys, catalysts, hybrid and electric cars, compact fluorescent lamps, wind turbines, data storage devices, optical glasses etc. majority of these application utilizes unique properties of magnetism, and luminescence associated with rare earths. These interesting properties are attributed to partially occupied 4f orbital electrons. The supply of these elements is abundant as of now, but negative and erratic supply pattern not conducive of assured availability, due to various geopolitical as well as environmental reasons. As a consequence, reopening of old mines and erections of new processing plants are underway throughout the world [1, 2]. Further, supply risk of rare earths have necessitated the need of recovering rare earths from e-wastes, end of life rare earth product, tailing of mines and lean solutions of processing plants to augment the supply through regular mines [3]. Due to the similar valence and ionic radii separation and purification of individual rare earth is one of the most challenging tasks in analytical chemistry. Solvent extraction technique has been in use on industrial scale to separate rare earths from various sources [4]. This technique uses large inventories of hazardous organic extractants, diluents and modifiers, contributing to environmental concerns [5]. Alternative techniques based on membrane technology, such as supported liquid membrane, emulsion liquid membrane, polymer inclusion membrane etc. has been reported to separate metal ions from aqueous solutions. These technique use controlled amount of organic extractants and solvents without significantly affecting the extraction efficiency and environment [6]. However, the stability of these membranes, applicability in continuous large scale and loss of extractants after repeated

use remain major concerns. The last decade has also seen phenomenal growth in the use of ionic liquids in this field [5]. However their physical properties, toxicity and cost remain a challenge for sustainable industrial applications [7]. These factors have led to research and development of new extraction system with improved efficiency and lower secondary organic waste [8]. In this context, reusable solvent encapsulated resins/beads are being developed as attractive alternatives in separation technology. These beads offer high surface area, eliminate the need of organic diluents, ease in phase separation and have the dual advantage of solvent extraction and ion exchange with relatively better selectivity and mass transfer respectively [9]. Similarly separation of metal ions by employing Hollow Fibre Membrane (HFM) have drawn considerable attention, as this module requires less amount of organic extractant for metal ion separation due to the advantage of simultaneous extraction and stripping. The arena of exploring these techniques for rare earths separation is still wide open.

Scanty reports are available in literature for the separation of rare earths by solvent encapsulated beads. The reported solvent encapsulated beads are mainly based on polystyrene, polyether ether ketone, and alginate types of polymer and have sizes in micron to sub-millimeter range [10]. These beads suffer from the drawbacks such as low holding capacity of extractants and susceptible to the leaching of encapsulated or impregnated extractants during repeated cycle of operations. These factors adversely affect the efficiency, reusability and stability of the beads. Therefore, it is desirable to develop novel polymeric beads which not only overcome these drawbacks but also result in enhanced extraction/sorption of metal ions from aqueous solution. In the present study, various polymers were evaluated to select the suitable matrix material for solvent encapsulated beads. Polyethersulfone has been found to be most suited matrix material to prepare the polymeric beads which can encapsulate the desired extractant during phase inversion.

Subsequently, the developed composite beads were evaluated for the sorption of rare earths under variable experimental conditions. The present work also emphasizes on the importance of optimization of various variables i.e. system compositions (polymer, additive, extractants etc.), preparatory parameters and process variables (aqueous media, metal ion, temperature, solid to liquid ratio etc.) to obtain the best engineered beads by innovative design of experiments. Taguchi, which is a multi-parameter optimization procedure, was employed in the present study to identify and optimize process parameters with a minimum number of experiments. Based on the batch experimental results, it was also of interest to employ these polymeric beads for the recovery of rare earths in continuous column operation mode, which established the materials possibility to scale up to industrial level.

Another important objective of the present thesis was to develop separation scheme for rare earths from aqueous solution by utilizing hollow fibre membrane module. Experimental evaluations of various process variables i.e. organic extractant, concentration (aqueous, metal ion, organic), flow rate and strippents on the transport of rare earths were performed. As a result of this study, experimental parameters were optimized to maximize the recovery of rare earths (Dy, La, Sm) from the acidic solution by carrier (organic extractant) facilitated liquid membrane technique.

The result of the studies in this thesis has been organized into six chapters.

Chapter 1: Introduction

The introductory chapter of the thesis gives an overview about the rare earths elements their resources and application for material production in different fields. Conventional techniques such as solvent extraction, ion-exchange, and precipitation etc., used in the purification of rare earths from different sources have been discussed. This chapter elaborates the

difficulty in separation and purification of individual rare earth elements. along with the comprehensive literature survey in the field of hydrometallurgy of rare earths separation. The chapter also shed some light on the use, importance and advantages of alternative separation techniques such as solvent encapsulated beads and hollow fibre supported liquid membranes over other conventional techniques for the purification of metal ions from aqueous systems. Possibility and advantages of applying above mentioned techniques in separating the rare earths from different aqueous streams have been discussed in this chapter. Importance of operational parameters optimization in process development and experimental design using Taguchi method, which is a multi-parameter optimization procedure, is also described in this chapter [11].

The chapter lists the motivation, aim and objectives of the present investigation along with the current research scenario in the field.

Chapter 2: Experimental and Techniques

A general outline about different instrumentations and experimental techniques, used in this work, has been elaborated in this chapter. General methods used for the synthesis of solvent encapsulated polymeric beads as well as the techniques which have been used for the characterization of the synthesized materials are discussed. The synthesized bead materials have been characterized ed, by various techniques, such as infrared spectroscopy, scanning electron microscopy (SEM) and thermal analysis. The basic principle and working of the characterization equipment's have been elaborated in this Chapter. The experimental conditions and procedure to evaluate rare earths sorption by various types of polymeric beads has been elaborated in this chapter. Principle and application of ICP-AES for rare earth analysis in aqueous phase samples is discussed in this chapter.

The details regarding hollow fibre supported liquid membrane and loading of carrier solvent in the pores of the hollow fibre have been described in this Chapter. Two different experimental methods namely supported liquid membrane and non-dispersive liquid-liquid extraction using HFM are described. These techniques have been explored for rare earth transport studies.

Chapter 3: Preparation, characterization and evaluation of Di-2-ethyl hexyl phosphoric acid (D2EHPA) encapsulated beads for rare earth sorption

This chapter deals with the studies carried out on the preparation of polyethersulfone beads encapsulating organophosphorus type of extractants by phase inversion method. It elaborates the synthesis, characterization and application of polyethersulfone based organophosphorus extractant encapsulated beads. The chapter comprises two sections, depicting the synthesis of D2EHPA encapsulated beads and its application for rare earths separation from aqueous media. The first section describes the synthesis and Y(III) sorption studies performed with D2EHPA PES beads, while second section deals with optimization of experimental parameters for Dy(III) sorption by D2EHPA –PES beads by employing Taguchi method.

Section 1: D2EHPA encapsulated beads for rare earths separation

A method has been developed for the preparation of D2EHPA encapsulated beads by phase inversion technique, using polyethersulfone as the polymer matrix. The internal microstructure and surface morphology of PES beads has been modified by introducing various types of additives, namely, polyvinyl alcohol (PVA), multiwall carbon nanotube (MWCNT), lithium chloride (LiCl) and polyethelene glycol (PEG).. The developed composite beads were characterized by techniques like Thermogravimetry (TG), Scanning Electron Microscopy (SEM) and Fourier Transform Infra-Red (FTIR) spectroscopy. Subsequently, all the types of D2EHPA

encapsulated composite beads have been evaluated for the sorption of rare earths under comparable experimental conditions. The porosity and pore structure of D2EHPA/PES beads were controlled through different additives, of which, polyvinyl alcohol and multiwall carbon nanotubes proved to be the most efficacious. The influence of various process parameters, namely, aqueous phase acidity, metal ion concentration, presence of other competitive ions and temperature on the separation of representative yttrium ion has been elaborated in the present section. Equilibrium data are found to be represented well by the Langmuir isotherm equation, with a sorption capacity of 44.09 mg/g of the swollen beads. Kinetic modeling analysis, by fitting the data in the pseudo first-order, pseudo second-order, and intraparticle diffusion equations, show that the pseudo second order equation is the most appropriate model for the description of sorption of yttrium ions onto the composite beads. The experimental results attribute to the excellent stability and reusability of the developed beads. The feasibility of employing this novel technology in large scale has been established by successful operation in continuous column mode.

Section 2: Optimization of parameters by Taguchi method for Dysprosium sorption by D2EHPA beads

This section deals with the optimization of experimental parameters for Dysprosium sorption by the developed D2EHPA – PES beads. There are many variables involved which influence the rare earths sorption by polymeric beads from aqueous streams thus it is very difficult to arrive at an optimum condition for maximum sorption and recovery unless adopt a design of experiments. If a full factorial design, where all possible variable combinations are taken into account, is used to find out the effects of parameters on the metal ion sorption capacity of polymeric beads, several hundreds of experiments need to be carried out. For k parameters at

n different levels the total number of combinations using a full factorial design is n^k . On the other hand Taguchi method [11] can help in sorting out the most influential parameters with minimum number of experiments. In the present work, Taguchi approach has been adopted to arrive at the optimum conditions for effective sorption of Dy(III) by the D2EHPA encapsulated polymeric beads. Seven parameters, namely, contact time of the beads with the solution, nature of additive, the concentration of Dy(III) in the feed solution, aqueous phase molarity, stirring speed of the agitator, polymer to extractant ratio and the temperature have been selected and varied in three different levels. Another parameter, liquid to solid phase ratio (w/w), has been varied in two levels. Apparently, this is an eight factor mixed (two and three) level system. Adoption of Taguchi method, allowed us to carry out only eighteen experiments in order to get the required optimization. In this section the effects of various operational and structural parameters have been analyzed by Taguchi method using L18 orthogonal array. Feed concentration of Dy(III) has been observed to be the most influential factor for equilibrium sorption capacity, whereas aqueous phase acidity significantly influences the percentage recovery. The analysis of variance predicted the optimum conditions with maximum performance and minimum standard deviation. Experiments carried at optimum conditions verified the predicted data.

Chapter 4: Synthesis and evaluation of EHEHPA encapsulated beads for Y(III) sorption

This chapter deals with the preparation, characterization of polyethersulfone beads encapsulating EHEHPA an organophosphonic acid type of extractant by phase inversion method. This chapter also elaborates the attempts made to modify the internal morphology of polymeric beads by adding different additive materials such as PVA, MWCNT, LiCl, PEG etc in the polymer matrix. The developed EHEHPA/PES beads were characterized by various techniques. Subsequently, all the developed EHEHPA beads were evaluated for their suitability for the

separation of rare earths from various aqueous media. Effect of various additives on the morphology and metal ion sorption capacity was also discussed in the chapter taking into account cross-sectional SEM images of these beads. Except nitrate medium, the extraction of rare earths was found to be comparable in perchlorate, chloride and sulphate medium and the results have been described in detail. Effect of aqueous phase acidity, rare earth concentration in aqueous feed, concentration of EHEHPA inside the beads, extractant to polymer ratio, liquid to solid (L/S) ratio, additive concentration, and temperature on the extraction of rare earths (Yttrium) have been discussed. Recovery of rare earths from loaded EHEHPA beads was found to be effective (>90%) with 40% HCl and 30% H₂SO₄. The results shown in this chapter emphasizes the applicability of polymeric beads in wide range of experimental variables.

Chapter 5: Transport studies on rare earths by Hollow fibre liquid membrane

This chapter describes the transport behavior of rare earths (Dy, La, Sm etc) in Hollow Fibre Membrane. The Non-dispersive solvent extraction (NDSX) and supported liquid membrane (HFSLM) are the two mode of operation evaluated for these transport studies. The batch solvent extraction experiments suggested that PC88A in petroffin is a suitable carrier solvent for polypropylene hollow fibre membrane. Various experiments were carried out to evaluate the effect of feed acidity, metal ion concentration, carrier concentration, feed composition, flow rates and phase ratio on the transport of rare earths metal ions across the membrane. The experimental findings discussed in this chapter revealed that in non-dispersive mode of operation with 0.5M EHEHPA as carrier solvent, ~98% of Dy(III) in aqueous feed has been transported across the membrane. Similarly, in the case of stripping of loaded carrier by this mode resulted in ~96% recovery in 1hour under optimized condition. In another set of experiments Dy(III) transport has been investigated by Hollow fibre supported liquid membrane

containing EHEHPA as carrier solvent. Various process variables such as feed acidity, metal ion concentration, carrier concentration, feed composition, flow rates and phase ratio were altered to achieve an optimized experimental conditions to achieve maximum Dy(III) recovery. Under optimized experimental condition >94% recovery of Dy(III) from aqueous feed solution can be attained in 2 hours of operation.

Quantitative transport of rare earths was also achieved during non-dispersive as well as supported liquid membrane mode of operation, when EHEHPA was used as a carrier. Studies on the effect of interfering rare earth ions on the transport of Dy(III) has been also discussed in this chapter.

Chapter 6: Summary and conclusions

Rare earths are in great demand due to the unique properties they bring to the material on addition. Scarcity of resources needs their separation process to be more efficient and environment friendly. Recycling and reusability of rare earth based materials has become much more relevant in the present scenario. In this context the present thesis summarizes the importance and use of rare earths based materials along with commonly practiced separation and purification techniques such as solvent extraction and ion exchange. The research work presented in the thesis lead to the process development for the separation of rare earths by employing synthesized polyethersulfone beads embedded with suitable organic extractant such as D2EHPA, EHEHPA. The developed polymeric beads are environment friendly due to the elimination of hazardous organic diluents and prevention of significant organic extractant loss during the process of recovery of rare earths from aqueous media. The polymeric beads not only address the environmental issues but also offer selective and efficient separation of rare earths. Moreover, the beads have added advantage of extraordinary stability and recyclability as

compared to the other conventional techniques. The developed beads were found to be excellent in the separation of rare earths such as Yttrium, Dysprosium from aqueous phase under optimized experimental condition. The developed beads were also satisfactorily employed for the recovery in continuous column operation mode and have promising potential to scale up to industrial level. This chapter also summarizes the experimental finding of rare earths (La, Sm, Dy) separation by employing carrier (D2EHPA, EHEHPA) facilitated hollow fibre membrane set up. A hollow fibre supported liquid membrane method has been developed for theseparation of rare earths from aqueous stream on 500 to-5000ml scale.

The major findings of the present research work are summarized in this Chapter along with the future perspectives

References

- [1] Rare earth element, global supply chain, M. Humphries, Congressional research service. (2011) 3-6.
- [2] U.S. Department of the Interior and U.S. Geological Survey, Mineral commodity summaries 2010, United State Government Printing Office, Washington, 2010.
- [3] K. Binnemans, P. T. Jones, B. Blanpain, T. Gerven, Y. Yang, A. Walton, M. Buchert, Journal of Cleaner Production, 51 (2013) 1-22.
- [4] J. Bochinski, M. Smutz, F. H. Spedding, Industrial Engineering and Chemical Research, 50 (1958) 157-160.
- [5] S. Wellens, R. Goovaerts, C. Möller, J. Luyten, B. Thijs, K. Binnemans, Green Chemistry, 15 (2013) 3160-3164.
- [6] P. R. Danesi, Separation Science and Technology, 19 (1984) 857-894.
- [7] G. Cevasco, C. Chiappe, Green Chemistry, 16 (2014) 2375-2385.

- [8] X.Q. Sun, H.M. Luo, S. Dai, Chemical Review, 112 (2012) 2100-2128.
- [9]A. Warshawsky, Talanta 21 (1974) 962-965.
- [10] X. C. Gong, G. S. Luo, W. W. Yang, F. Y. Wu, Separation and Purification Technology, 48 (2006) 235-243.
- [11] Taguchi, G.; Konishi, S. Orthogonal Arrays and Linear Graphs, MI:ASI Press: Dearborn, MI, 1987.

LIST OF FIGURES

Fig. 1.1: Positions of Seventeen Rare Earth Elements in Periodic Table.....	4
Fig. 1.2: Atomic and ionic radii of the rare earth elements.....	9
Fig. 1.3: Sector wise applications of Rare Earth Elements.....	12
Fig. 1.4: Medium term criticality matrix depicting the five most critical REEs (by DOE).....	17
Fig. 1.5: Solvent Extraction: Mixer-Settler Assembly for Yttrium Purification.....	29
Fig 1.6: Hollow Fibre Supported Liquid Membrane Module.....	35
Fig. 2.1: Structure of Polyethersulfone.....	44
Fig 2.2: Structure of N-methyl pyrrolidone.....	45
Fig. 2.3: Structure of di(2-ethylhexyl)phosphoric acid (D2EHPA).....	45
Fig. 2.4: Structure of 2-Ethylhexyl 2-ethylhexyphosphonic acid.....	45
Fig. 2.5: Structure of poly vinyl alcohol.....	46
Fig. 2.6: Preparation set up for extractant encapsulated PES based polymeric beads.....	48
Fig. 2.7: Schematic diagram of Hollow Fibre Membrane contactor employed in the present work.....	63
Fig. 2.8: Hollow Fibre Membrane contactor used in the present work.....	64
Fig. 2.9: Inductively Coupled Plasma-Atomic Emission Spectroscopy (ICP-AES) employed for the analysis of rare earth elements.....	65
Fig. 3.1: Optical images of PES/D2EHPA, PES/PVA/D2EHPA and PES/PVA/MWCNT/D2EHPA.....	74

Fig.3.2: SEM images of cross-section of PES bead (a)PES blank, (b)PES/D2EHPA, (c)PES/PVA/D2EHPA, (d)PES/PEG/D2EHPA, (e)PES/LiCl/D2EHPA, (f)PES/PVA/MWCNT/D2EHPA.....	75
Fig. 3.3: TGA of blank polymer bead, PES/D2EHPA beads having different extractant to polymer ratios of 1:4, 1:5, 1:7.5, 1:10, 1:15 and D2EHPA (3M)	76
Fig. 3.4: TG profiles of (a) PES bead (b) PES/D2EHPA/PVA (c) PES/D2EHPA/PVA /MWCNT bead and (d) D2EHPA (3M).....	77
Fig. 3.5: FTIR spectra of (a) D2EHPA, (b) Blank PES bead (c) PES/D2EHPA/PVA/ MWCNT bead.....	79
Fig. 3.6: Effect of additives in polymeric composite beads on weight distribution ratio of Y(III) by PES/D2EHPA beads.....	81
Fig. 3.7: Effect of additives in polymeric composite beads on the rate of sorption of Y(III) from aqueous media by PES/D2EHPA beads.....	82
Fig.3.8 Effect of Y(III) concentration in feed solution on sorption of Y(III) by PES beads (a)PES-I (b) PES-II beads.....	83
Fig. 3.9: Effect of aqueous phase acidity and Y(III) concentration in aqueous phase on Y(III) sorption by PES-II beads.....	84
Fig. 3.10: Plots of Y(III) sorption as a function of temperature by (a) PES-I beads (b) PES-II beads.....	86
Fig. 3.11: Effect of competing rare earth ions (La, Sm) on Y(III) sorption by PES-II beads.....	87
Fig. 3.12: Langmuir plot for the sorption of Y(III) on the PES-I (a) and PES-II(b) beads, aqueous phase: 0.5 M HCl, temperature: 28°C.....	88

Fig. 3.13: Freundlich plot for the sorption of Y(III) on the D2EHPA containing PES beads, aqueous phase: 0.5 M HCl, temperature: 28°C.....	90
Fig. 3.14: Pseudo-first order plot for yttrium ion sorption by polymeric beads, at four different initial concentration of Y(III)	92
Fig. 3.15: Pseudo-second-order plot for yttrium ion sorption by polymeric beads, at four different initial concentration of Y(III).....	94
Fig. 3.16: Intraparticle diffusion plot for Y(III) sorption by polymeric beads, at different Y(III) concentration in feed.....	96
Fig. 3.17: Boyd's plot for Y(III) sorption by polymeric beads.....	98
Fig.3.18: (a) Breakthrough profile of Y(III) uptake by a)PES-I (b) PES-II, Feed: 160 mg/L Y(III) in 0.5M HCl, Flow rate: 2ml/min. (b) Elution profiles of loaded Y(III) beads using 40% HCl from column containing a)PES-I (b) PES-II beads.....	99
Fig. 3.19: Effect of different aqueous media on sorption of Y(III) extraction by polymeric bead.....	101
Fig. 3.20: Periodic stability of (a)PES-I (b) PES-II beads in 6M HCl.....	102
Fig. 3.21: Effect of sorption and desorption of Y(III) from PES beads on cumulative percentage loss of encapsulated D2EHPA.....	103
Fig. 3.22: Plot of S/N ratios for different factors for R.....	114
Figure 3.23: Variation Reduction plot for R.....	115
Fig. 3.24: Plot of S/N ratios for different factors for q_e	117
Fig.4.1: SEM images of cross-section of PES based bead (a) PES blank, (b) PES/PC88A, (c) PES/PVA/PC88A, (d) PES/PEG/PC88A, (e) PES/LiCl/PC88A, (f) PES/PVA/MWCNT/PC88A.....	124

Fig. 4.2: TG of PES/PC88A bead, PC88A (3M), Blank polymer bead.....	126
Fig. 4.3: FTIR spectra of PC88A (3M), PES/PC88A (15:1) bead, PES/PC88A (5:1) bead, blank PES beads.....	127
Fig. 4.4 (a): Effect of additives in polymeric composite beads on sorption of Y(III) by PES/PC88A beads	129
Fig. 4.4 (b): Effect of additives in polymeric composite beads on equilibrium sorption capacity of Y(III) by PES/PC88A beads	130
Fig. 4.5: Effect of extractant (PC88A) concentration inside the bead on Y(III) extraction.....	131
Fig. 4.6: Effect of Y(III) concentration in feed solution on equilibrium sorption capacity of Y(III) by PES/PVA/MWCNT/PC88A beads.....	133
Fig. 4.7(a): Plots of Y(III) uptake as a function of aqueous phase hydrochloric acid concentration and Y(III) concentration in aqueous phase by PES/PVA/MWCNT/PC88A beads	134
Fig. 4.7 (b): Effect of aqueous feed acidity in terms of HCl concentration on Y(III) sorption capacity by PES/PVA/MWCNT/PC88A beads	135
Fig. 4.8: Effect of temperature on Y(III) equilibrium sorption capacity by PES/PVA/MWCNT/PC88A beads.....	137
Fig. 4.9: Equilibrium sorption capacity for different rare earths (La, Nd, Sm, Dy, Y) sorption by PES/PVA/MWCNT/PC88A beads.....	138
Fig. 4.10: Equilibrium sorption capacity(mg/g) for different rare earths (La, Nd, Sm, Dy, Y) sorption by PES/PVA/MWCNT/PC88A beads from Mixed RE feed.....	139
Fig. 4.11: Effect of stripping agent on Y(III) stripping from loaded beads.....	140
Fig. 4.12: Effect of sorption and desorption of Y(III) from PES/PC88A beads on cumulative percentage loss of encapsulated PC88A and on equilibrium sorption capacity(q_e)	141

Fig. 5.1: Effect of Aqueous phase acidity on the extraction of Dy(III) by 0.5 M PC88A; aqueous phase: 1000mg/l; flow rate: 100mL/min, Phase ratio: 1:1.....	151
Fig. 5.2: Effect of organic phase flow rate on the percentage extraction of Dy(III) at fixed aqueous phase flow rate.....	152
Fig. 5.3: Effect of Dy(III) concentration on its extraction by 0.5M PC88A organic phase and 0.1M HNO ₃ aqueous phase at flow rates of 100 mL/min for both the phases.....	153
Fig. 5.4 Effect of Dy(III) concentration on its extraction by 0.5M PC88A organic phase and 0.1M HNO ₃ aqueous phase at flow rates of 100 mL/min for both the phases.....	154
Fig. 5.5: Extraction of Dy(III) at different organic to aqueous phase volume ratios; organic phase:0.5M PC88A; aqueous phase: 1.0 g/L Dy(III) at 0.3M HNO ₃ ; flow rate:100 mL/min....	156
Fig. 5.6: Extraction of Dy(III) in presence of competing rare earths ions.....	157
Fig. 5.7: Stripping of Dy(III) from loaded 0.5 M PC88A phase; strip phase: 1.5 M HNO ₃ ; flow rate:100 mL/min, phase ratio 1:1, organic phase 0.5 M PC88A having 3.3g/L Dy(III)	158
Fig. 5.8: Simultaneous extraction and stripping of Dy by PC88A as carrier in HFSLM mode Carrier: 0.5 M PC88A in petroffin; feed, 1 g/L Dy (400 mL); strippant, 3M HNO ₃ (400 mL); flow rate, 100 mL/min; temperature, 25 °C.....	160
Fig. 5.9: Influence of feed acidity on the permeation of Dy(III) by HFSLM. Carrier, 0.5 M PC88A in petroffin; feed, 1 g/L Dy (400 mL); strippant, 3M HNO ₃ (400 mL); flow rate, 100 mL/min; temperature, 25 °C.....	161
Fig. 5.10: Effect of extractant Concentration on the permeation of Dy(III) by HFSLM. Aqueous feed : 0.1 M HNO ₃ consisting 1 g/L Dy (400 mL); strippant, 3M HNO ₃ (400 mL); flow rate, 100 mL/min; temperature, 25 °C.....	163

Fig. 5.11: Transport of Dy(III) in presence of competing rare earths ions; organic carrier phase:0.5M PC88A; aqueous feed phase: 1.0 g/L of Dy(III), La(III) and Sm(III) each in 0.3M HNO ₃ ; flow rate:100 mL/min, strip phase 3 M HNO ₃	164
Fig. 5.12: Evaluation of P values for Erbium and Dy transport permeability coefficient.....	166

LIST OF TABLES

Table 1.1: Electronic configurations rare earth elements and ions in the ground state.....	6
Table 1.2: Atomic radii and effective ionic radii of the rare earth elements (in nm).....	8
Table 1.3: Rare earth world scenario: resource and production.....	18
Table 1.4: Recycling potential for rare earths by 2020.....	21
Table 2.1: Characteristic properties of petroffin.....	46
Table 2.2: Details of hollow fibre membrane contactor (Liqui-Cel X50: 2.5x8 Membrane Contactor).....	62
Table 3.1: Parameters of Langmuir isotherm model for the sorption of Y(III) by PES/D2EHPA beads, Aqueous phase: 0.5N HCl, Temperature: 28°C.....	89
Table 3.2: Pseudo-First-Order, Pseudo-Second-Order, and Intraparticle Diffusion Constants and values of R ² for the sorption of Yttrium.....	91
Table 3.3: Selection of parameters and their levels for Taguchi method.....	109
Table 3.4: Design of L-18 orthogonal array for experiments.....	110
Table 3.5: Percentage recovery (<i>R</i>) and equilibrium sorption (<i>e_q</i>) data for L-18 arrays and corresponding S/N ratio.....	112
Table 3.6: Effect of different parameters on the percentage recovery (<i>R</i>) of Dy(III).....	113
Table 3.7: Effect of different parameters on the equilibrium sorption (<i>q_e</i>) of Dy(III).....	116
Table 5.1: Distribution Coefficient (<i>D</i>) for Dy(III) extraction by EHEHPA from different aqueous phase acidities: organic Phase: 0.5M EHEHPA, aqueous phase: 1089 mg/L Dy.....	149
Table 5.2: Permeability Coefficient (<i>P</i>) of Dy(III) and Er(III) by HFSLM System	166



Chapter 1

INTRODUCTION

1 Introduction

1.1 Rare Earths

Over the last five years, not only researcher and scientists but more and more people from different walk of society also became aware of the term rare earths elements (REE). This awareness did not originate because of their surprisingly large number of application but rather due to the supply restrictions on REE and related ores owing to geopolitical reasons which resulted in panic like situation from producers to end users of these elements. This period, of scarcity of REE, starting in 2009 known as the “Rare Earth Crisis,” made many people around the world aware of this peculiar group of elements [1].

The name rare earths was originally used to assign the lanthanoids in 4f block elements of the modern periodic table which also consists oxides of scandium (Sc, 21), yttrium (Y, 39), lanthanum (La, 57) and the 14 elements starting from cerium (Ce, 58) to lutetium (Lu, 71) in the periodic table of elements [2]. Yttrium’s geochemical behaviour is very similar to the lanthanides, which is why it is considered to be a REE. Scandium, however shows geochemical behaviour that is much more similar to that of the ferromagnesian transition elements (Fe, V, Cr, Co and Ni) due to its smaller atomic radius. This is also due to a different coordination in the crystal lattices of minerals. Therefore, scandium is often considered not to be a rare earth element, but a ferromagnesian trace element. However, in aqueous media, scandium behaves more like the other REEs [3]. The history of the discovery of these elements has given this group of elements the name rare earth elements. These elements are never existed in the earth’s crust as pure minerals of individual rare earths and also do not exist as free metals in any deposit. These rare earth elements are found as oxides which have proved to be particularly difficult to separate from each other, especially to 18th and 19th century chemists. The term earths coined by Greeks

means, materials that could not be changed further by sources of heat, and these oxides seemed to fit that definition. There is still an ambiguity on why Rare Earth term consists 'rare' as some believe, that the rare part of rare earth refers to the difficulty in separating the pure elements, and did not refer to their relative abundances in the Earth's crust [4]. Although the ore deposits of REE are quite restricted in numbers, but the abundance of the elements is quite large. The most common rare earth element is cerium (Ce), which is, with a crustal abundance of 60 ppm, the 27th element in the earth's crust, and has a larger abundance than, for instance, lead (Pb), the 37th element, which has a crustal abundance of 10 ppm. One of the least common rare earth elements (lutetium, abundance 0.5 ppm), has a crustal abundance of about 200 times that of gold (0.0031 ppm) [5].

The discovery of the rare earth elements started at the end of the 18th century with Yttrium was the first element to be discovered, by Johan Gadolin of Finland [6-9]. By the end of the 19th century, most of the rare earth elements had been discovered. Lutetium was discovered in 1907, and the last one promethium only after the discovery of nuclear reactions [10]. The rare earth elements are: scandium (Sc), yttrium (Y), lanthanum (La), cerium (Ce), praseodymium (Pr), neodymium (Nd), promethium (Pm), samarium (Sm), europium (Eu), gadolinium (Gd), terbium (Tb), dysprosium (Dy), holmium (Ho), erbium (Er), thulium (Tm), ytterbium (Yb), and lutetium (Lu). The 17 original rare earth elements along with atomic number are summarized in figure 1.1.

[illegible]

1.2 Electronic configuration and properties of rare earths

1.2.1 Electronic Configuration and oxidation state

4

elements share the xenon core, [Xe], corresponding to $1s^2 2s^2 2p^6 3s^2 3p^6 3d^{10} 4s^2 4p^6 4d^{10} 5s^2 5p^6$. The remaining electrons, the valence electrons, are then placed in the 6s orbital and, with exception of La, Ce, Gd, and Lu, in the 4f orbital, since the energy difference between the 4f and 5d orbitals is large. Thus, all the rare earth elements belong formally to group 3 of the periodic table. In the neutral rare earth elements, the 5d and 4f electrons have almost similar energies. This fact explains the occurrence of the typical electronic configuration referred to above within the lanthanide series (see Table 1.1), whereby the configurations $4f^7$ (half-filled orbital) and $4f^{14}$ (completely filled orbital) are preferred owing to the high thermodynamic stability of such states. The irregularity of the configurations of the two elements immediately before the middle and the end of the lanthanide series, Eu and Yb, are characteristic of the neutral atoms and the mono- and divalent oxidation state. However, in the case of the trivalent ions, the 4f orbital is filled in a completely regular manner. The energy of the 4f orbital decreases with increasing atomic number and increasing ionic charge, so that when the oxidation number is 3+, which is characteristic of the rare earth elements, the 4f electrons represent well-defined “inner electrons” that take virtually no part in chemical bonding due to their proximity to the nucleus and shielding by the 8 electrons of 5 shell. Therefore, the regular filling of the 4f orbital from Ce^{3+} to Lu^{3+} determines the chemical properties, as the resulting electronic configurations resemble those of the rare gases, and lead to the great similarity of the Ln^{3+} compounds to each other, to the corresponding compounds of La^{3+} , Y^{3+} , and, to a limited extent, to those of Sc^{3+} . The regular filling of the 4f orbital is accompanied by a steady reduction in the Ln^{3+} ionic radii (Table 1.2, and Figure 1.2) – the so-called lanthanide contraction [11-13]. This steady shrinkage of the inner electron shell is mainly caused by the incomplete mutual shielding of the 4f electrons against the increasing attraction of the nucleus. The peculiarities of the electronic structure of the rare earth elements

described here lead to periodic changes in some physical and chemical properties of these elements and their compounds in the series La to Lu, while other properties show a steady or non-periodic change. The typical similarity of the rare earth elements to each other, which is often emphasized, is in essence only exhibited for the non-periodic properties. Thus, the regular change in the RE^{3+} radii leads to largely non-periodic changes in properties that depend on ion size, such as solubility, basicity, normal potential, and enthalpy of hydration.

Table 1.1 Electronic configurations rare earth elements and ions in the ground state

Rare earths element	Element Symbol	Atomic number	Electronic configuration
Lanthanum	La	57	$[Xe] 4f^0 5d^1 6s^2$
Cerium	Ce	58	$[Xe] 4f^1 5d^1 6s^2$
Praseodymium	Pr	59	$[Xe] 4f^2 5d^1 6s^2$
Neodymium	Nd	60	$[Xe] 4f^3 5d^1 6s^2$
Promethium	Pm	61	$[Xe] 4f^4 5d^1 6s^2$
Samarium	Sm	62	$[Xe] 4f^5 5d^1 6s^2$
Europium	Eu	63	$[Xe] 4f^6 5d^1 6s^2$
Gadolinium	Gd	64	$[Xe] 4f^7 5d^1 6s^2$
Terbium	Tb	65	$[Xe] 4f^8 5d^1 6s^2$
Dysprosium	Dy	66	$[Xe] 4f^9 5d^1 6s^2$
Holmium	Ho	67	$[Xe] 4f^{10} 5d^1 6s^2$
Erbium	Er	68	$[Xe] 4f^{11} 5d^1 6s^2$
Thulium	Tm	69	$[Xe] 4f^{12} 5d^1 6s^2$
Ytterbium	Yb	70	$[Xe] 4f^{13} 5d^1 6s^2$
Lutetium	Lu	71	$[Xe] 4f^{14} 5d^1 6s^2$
Yttrium	Y	39	$[Kr] 4d^1 5s^2$
Scandium	Sc	21	$[Ar] 3d^1 4s^2$

1.2.2 Lanthanide Contraction

Both the atomic radii and trivalent ionic radii of the lanthanide elements decrease with the increase in atomic number (Table 1.2), this phenomenon is called lanthanide contraction [14-16]. The reason for this contraction is due to the weak shielding effect of the 4f electrons to the nuclear charge, causing the increase of the effective nuclear charge with the increase in atomic number, thus increasing the attraction to the electrons in the outer shell. There are only two conductive electrons ($6s^2$) for europium and ytterbium, while the other lanthanide elements have three conductive electrons ($6s^2 4f^1$). This explains why the atomic radius of europium and ytterbium are far greater than those of the other lanthanide elements. As a result of the lanthanide contraction, the radii of RE^{3+} decreases from 1.061 Å (La^{3+}) to 0.848 Å (Lu^{3+}). The average of the radii changes between two neighbour RE^{3+} ions is 0.0152 Å. The tiny radii discrepancy makes the lanthanide elements able to substitute each other in the crystal lattice of their minerals, i.e., the isomorphism. Also as a result of the lanthanide contraction, yttrium has an ionic radius comparable to that of the heavier REE species in the holmium-erbium region. If the effective ionic radius [16] of Y^{3+} is plotted (0.90 Å), it plots in between element 67 (Ho) and 68 (Er). Scandium (effective ionic radius is 0.745 Å), plots outside of the Lanthanide series. As also the outermost electronic arrangement of yttrium is similar to the heavy rare earths, the element behaves chemically like the heavy rare earths

Lanthanide contraction is the property which makes their separation possible. The lanthanide contraction results in the steady property variation of the lanthanides with their atomic number. With the increase of their atomic number, their radii decrease, making the coordination ability of some of the ligands with lanthanide cations increase. Taking these subtle differences of the coordination ability, SX and IX technologies are able to separate REEs to produce high purity single rare earth oxides.

Table 1.2 Atomic radii and effective ionic radii of the rare earth elements (in nm)

Symbol	Atom	Re[+3]
Sc	0.1654	0.0730
Y	0.1824	0.0892
La	0.1884	0.1061
Ce	0.1825	0.1034
Pr	0.1836	0.1013
Nd	0.1829	0.0995
Pm	0.1825	0.0979
Sm	0.1814	0.0964
Eu	0.1984	0.0950
Gd	0.1817	0.0938
Tb	0.1803	0.0923
Dy	0.1796	0.0908
Ho	0.1789	0.0894
Er	0.1780	0.0881
Tm	0.1769	0.0869
Yb	0.1932	0.0858
Lu	0.1760	0.0848

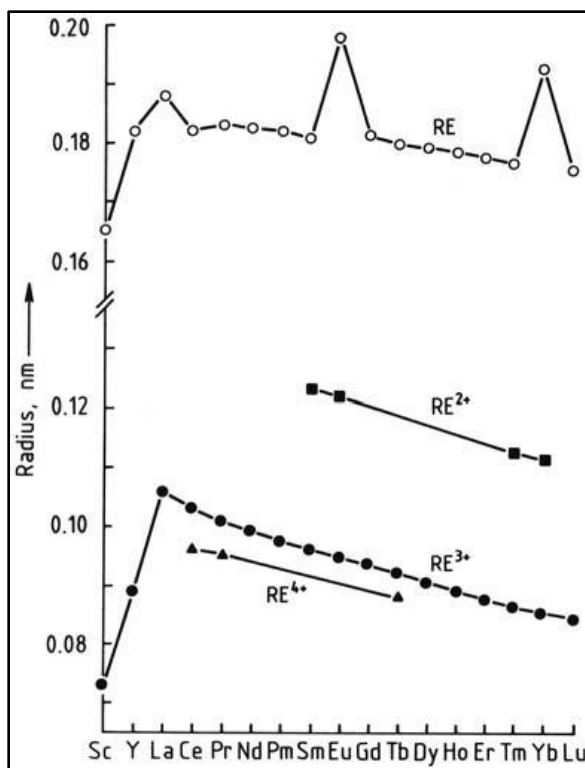


Fig. 1.2 Atomic and ionic radii of the rare earth elements

1.2.3 Physicochemical Properties of Rare Earth

The rare earth elements are very electropositive, and, as a consequence, they generally form ionic compounds. REEs therefore form oxides, halides, carbonates, phosphates and silicates, borates or arsenates, but not sulphides [18]. Rare earth metals in pure form are silvery in appearance with the exception of Pr and Nd that are pale yellow and rather soft, but become harder across the series. Most of them occur in more than one crystallographic form, of which hexagonal close packed structure is the most common. In this respect they are more related to calcium in behavior. They react readily with oxygen, moisture and mineral acid so have to be kept in kerosene to prevent oxidation from air and moisture. The reactivity of rare earth elements increases in the order of Sc, Y, and La, but decreases from La to Lu. The ignition point of rare earth metals is very low. It is 165, 290, and 270 °C for Ce, Pr, and Nd, respectively.

Therefore, the Ce-based mixed light rare earth metals are used as the pyrophoric alloy, such as flint. Apart from oxygen rare earth metals readily react with hydrogen, halogen, sulfur, nitrogen, and carbon, forming stable compounds.

Sm, Eu and Gd have very high thermal neutron absorption capture cross sections and are being used as thermal neutron absorption capture materials in nuclear reactors. Rare earth metals have low conductivities. However, La shows superconductivity at 47 K. The electronic configurations and spectroscopic terms of the Ln^{3+} ions are largely unaffected by the type of compound in which they are situated, owing to the shielding of the 4 f electrons from the chemical environment by the $5s^2 p^6$ octet. For these ions, with the exception of Sm^{3+} and Eu^{3+} , it is characteristic that the values of the total spins J applicable to the spectroscopic term of the ground state differ from each other fairly widely so that in the ground state practically only one J value is occupied. This peculiarity has interesting consequences for the magnetic properties of these ions. While Sc^{3+} , Y^{3+} , La^{3+} and Lu^{3+} are diamagnetic due to their closed shells, the remaining Ln^{3+} ions are paramagnetic, with Gd, Tb, Dy, and Tm having ferromagnetism [19].

Most lanthanide ions absorb electromagnetic radiation, particularly in the visible region of the spectrum, exciting the ion from its ground state to a higher electronic state, as a consequence of the partly filled 4f sub shell. The f-f transitions are excited both by magnetic dipole and electric dipole radiation. Except Y(III), La(III) and Lu(III) all other tri-positive rare earth ions absorb electromagnetic radiation in wavelength range of 2000 to 10000Å. A number of RE ions have striking colors as they absorb in visible region [20]. The average life of some excited states of the REE cations is very long and up to 10^{-6} to 10^{-2} s, which is much longer than that of the general cations (10^{-10} to 10^{-8} s). The REEs with this property are used to produce the long afterglow luminescent materials. They react with water and inorganic acids as well. Rare

earth metals form various intermetallic compounds with many metals. The rare earth permanent magnets (Sm-Co alloys and Nd-Fe-B alloys) and the rare earth hydrogen storage material (RENi5) are two classes of the rare earth intermetallic compounds [21].

The physical, chemical, and above all structural properties of the rare earth compounds indicate that these elements exhibit mainly ionic bonding. In solution and in crystalline compounds, the RE^{3+} ions (except Sc^{3+}) generally have coordination numbers >6 . For scandium compounds, which can also be regarded as homologues of aluminum, coordination numbers >6 do not occur. In general, the tendency of the lanthanides, including Y and La, to form complexes is smaller than for the d-transition elements, as the shielded 4 f orbitals are not available for forming the hybrid orbitals that form covalent bonds. Also, the very large size of the Ln^{3+} ions compared with other triply charged cations leads to smaller electrostatic forces of attraction.

1.3 Applications of Rare Earth Elements

The applications for the REE cover a huge field as all 17 elements have to be considered. Despite their chemical similar characteristics, they have diverging applications (Fig. 1.3). Rare earth metals and their compounds are in immense demand, and are often critical for, a wide range of applications that rely upon their electrical, magnetic, chemical, catalytic, and optical properties. Rare earths are also widely employed for conventional fields consisting metallurgy, petroleum, textiles, and agriculture. These elements are also becoming critical in various high-tech large scale application and products such as hybrid and electric cars, wind turbines, and compact fluorescent lights, flat screen televisions, mobile phones, disc drives, and defense products/technologies [22,23]

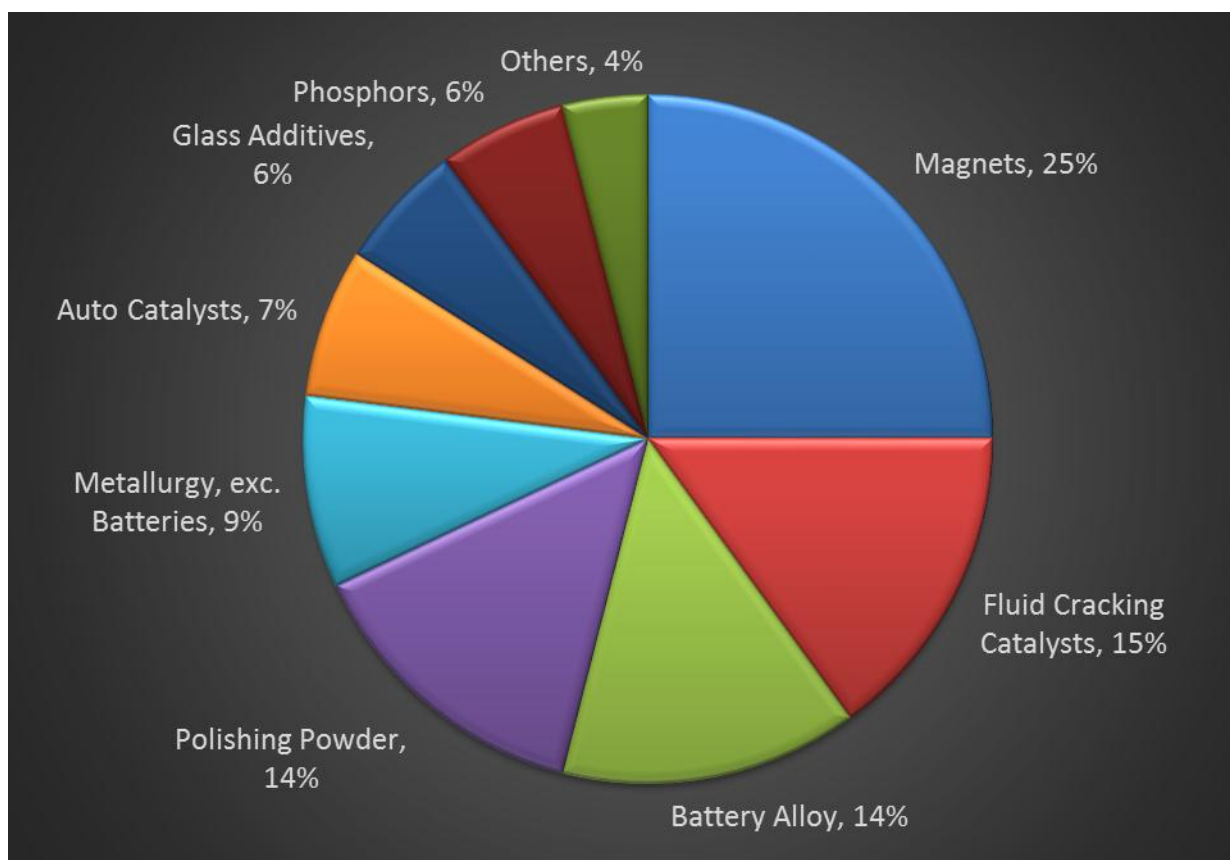


Fig. 1.3 Sector wise applications of Rare Earth Elements

1.3.1 Metallurgy and Machinery

Metallurgical properties play a key role in the development of rare earth alloy-based compounds as they are best suited for the development of a special product with unique performance capabilities. About 10% of rare earth production is used in these alloys. Since the early 1900s the primary commercial form of mixed rare– earth metals has been misch metal, an alloy of 50% cerium, 25% lanthanum, 15% neodymium and 10% other rare–earth metals and iron [24]. This misch-metal has been used extensively by the metallurgy industry to enhance the strength, oxidation, corrosion resistance, and malleability and creep resistance of various steels and other iron–based alloys. Other elemental rare earths are used as alloy additives in particular, praseodymium is used in high–strength, low–creep magnesium alloys for jet engine parts.

Precision castings of aluminium and magnesium have also been reported to be improved by the addition of other rare earths. The application of cerium and iron alloy which emits sparks when struck started the flint industry, leading to the purification of large inventory each year of the cerium-laden mineral monazite. Rare earth metals and alloys can be used to purify the molten metal or alloy by removal of the impurities such as oxygen and sulphur, modify the configuration and distribution of the impurities, reduce the size and amount of inclusions, and make the grains finer. REEs in the cast iron change the graphite into spherical particles, thus forming the so-called nodular cast iron. The nodular cast iron has excellent mechanical properties and machinability. Cerium is the most effective rare earth element for this function. REEs in non-ferrous metals significantly improve their machinability and physical properties [23].

1.3.2 Petroleum and Chemical Industry

One of the principal industrial uses of the rare earths, involving millions of tons of raw material each year, is in the production of catalysts for the cracking of crude petroleum. Rare earth elements are also used as catalysts for alkylation, isomerization, hydrogenation, dehydrogenation, dehydration, reforming of hydrocarbons, polymerization, oxidation of CO and hydrocarbons and reduction of the concentration of nitrogen oxides in automobile exhaust gases. One such application is fluid cracking catalysts (FCCs), materials which are used in the petroleum-refining industry, to convert heavy crude oil into gasoline and other valuable products [25].

1.3.3 Glass and Ceramics

Another important use of rare earth elements is in the glass and ceramic industries. Rare earth oxides in their naturally-occurring composition or with an increased CeO_2 content (or pure CeO_2) are used as polishing agents in the glass industry. Due to their intrinsic crystal structures,

chemical reactivity and the colours of some REE cations, REEs are widely applied in glass clarification, decolouring/colouring, polishing as well as ceramic pigments [26]. The REEs used in these areas include cerium, lanthanum, praseodymium, neodymium, samarium, erbium, and yttrium. Significant amounts of CeO_2 (with some La_2O_3 and Nd_2O_3) are utilized in the polishing of glass, mirrors, TV screens, computer displays and the wafers used to produce silicon chips. When used in a fine-powder form, the REOs react with the surface of the glass to form a softer layer (mechano-chemical effect), thus making it easier to polish the surface to a high-quality finish. Cerium dioxide has completely replaced toxic white arsenic (arsenic trioxide) for this use. REEs make the glass with different colours or with different specialties. CeO_2 and La_2O_3 are used as additives in the glass industry. Neodymium glass is a very good laser material and is used in large-scale and high power laser devices. REEs in the ceramics and enamels enable the ceramics with rich colours and increase the cracking resistance of the enamels [1].

1.3.4 Phosphors

Phosphors are the major application of the high purity single rare earth oxides. Stimulation by UV, X-rays, or electron beams causes certain rare earth elements to emit light of a definite wavelength. Liquid crystal displays (LCDs) and plasma screen displays, light-emitting diodes (LEDs) and compact fluorescent lamps (CFLs) all utilize rare earth based materials. Compounds containing europium (Eu), yttrium (Y) and Tb are frequently used to produce phosphors, and are fine-tuned for particular colour outputs. Since much more of the electrical energy is converted into light than with conventional light sources, phosphor materials are significantly more energy-efficient than older technologies, requiring a lot less electricity to produce the same outputs. The spectral position of the emission lines of rare earths is almost independent of the host lattice which is not the case in transition elements. Rare earth ions such

as Tb^{3+} and Eu^{3+} emit at frequencies that enable high lumen efficacies and a good quality of white light [27,28]. Commercial plasma screens have used yttrium tantalates activated by thulium (YTbO_4 : Tm) or niobium (YTbO_4 : Nb) [29,30].

1.3.5 Permanent Magnets

The use of REEs in magnetic alloys has enhanced the possibility to prepare permanent-magnet materials which can not only generate very strong magnetic fields but also able to strongly resist being demagnetized when exposed to other magnetic fields, or to increases in temperature. The REEs used in these alloys are neodymium (Nd), praseodymium (Pr), samarium (Sm), dysprosium (Dy) and terbium (Tb), which supplement the inherent ferromagnetism of transition metals such as iron (Fe) and cobalt (Co). These characteristics have revolutionized the field of magnetics design in recent years, in the production of high-performance electric motors, which convert electricity into mechanical motion, and electric generators. Rare-earth permanent-magnet materials have also reduced the size of the motors, loudspeakers, hard-disk drives, cordless power tools and other applications that use permanent magnets to operate, while maintaining the same or better output characteristics as other technologies. Sm, Eu, Gd, and Dy have high thermal neutron capture cross sections. Eu and Dy can take up five neutrons in succession [31-32]. Therefore, they have a low rate of burn off when used in control rods or in ceramics for radiation protection [33].

1.4 Rare earth crisis

The rare-earth elements (REEs) are becoming increasingly important in the transition to a green economy, due to their essential role in permanent magnets, lamp phosphors, catalysts, rechargeable batteries etc. With China presently producing more than 90% of the global REE output and its increasingly tight export quota, the rest of the world is confronted with a REE

supply risk. Consequentially, as the global demand for hybrid and electric cars, wind turbines, and compact fluorescent lamps rises, so does the price of REEs. As such, the European Commission labeled the REEs as the most critical raw materials group in its landmark report Critical Raw Materials for the European Union [34]. Likewise, the US Department of Energy (DOE) acknowledged the critical importance of REEs in their Critical Materials Strategy report by listing REEs in their medium term criticality matrix (Fig. 3.1) [35]. Furthermore, the US DOE labeled neodymium (Nd), europium (Eu), terbium (Tb), dysprosium (Dy), and yttrium (Y) as the five most critical REEs. The demand for Nd and Dy is anticipated to increase by 700 % and 2600% in the next 25 years, respectively [22]. Presently, China produces over 90 % of the global REE supply, although less than 40 % of the known REE supply is located in China. This is due to the specialization China has achieved in last 4 decades of expertise in downstream activities, such as the separation of rare earth oxides into individual elements, processing elements into rare-earth metals, and the production of rare-earth permanent magnets and lamp phosphors. Moreover, in order to accommodate increased domestic demand, China decreased its export quota from 50145 tons to 31130 tons between 2009 and 2012 [36]. Mining companies are now actively seeking new exploitable REE deposits while some old mines are being reopened because of the above mentioned crisis. The absence of economical and/or operational primary deposits on their territory, many countries will have to rely on recycling of REEs from pre-consumer scrap, industrial residues and REE-containing End-of-Life products [37, 38].

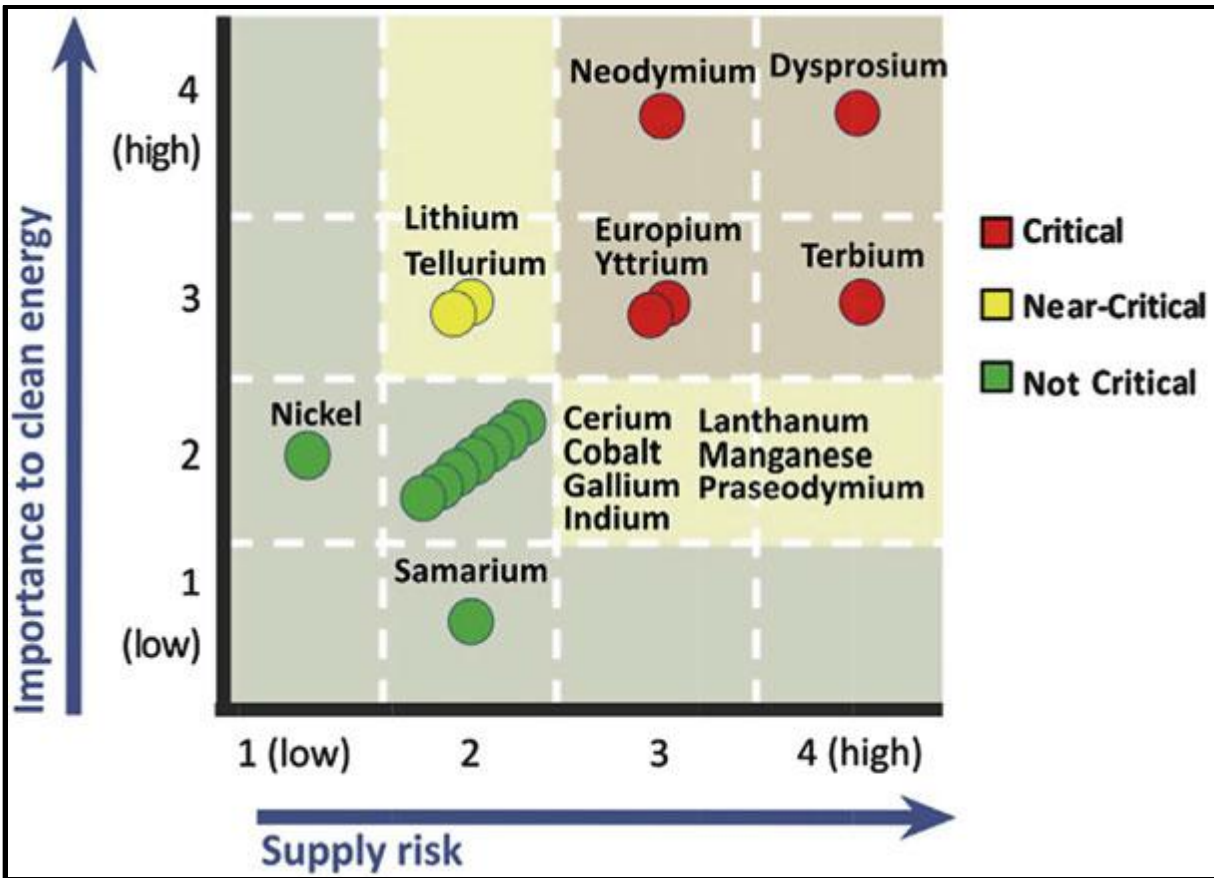


Fig. 1.4 Medium term criticality matrix depicting the five most critical REEs (DOE)

REE recycling is also recommended in view of the so-called “balance problem”. For instance, primary mining of REE ores for neodymium generates an excess of the more abundant elements, lanthanum and cerium. Therefore, recycling of neodymium can reduce the total amount of REE ores that need to be extracted. Despite a vast, mostly lab-scale research effort on REE recycling, up to 2011 less than 1% of the REEs were actually recycled. This is mainly due to inefficient collection, technological problems and, especially, a lack of incentives. A drastic improvement in the recycling of REEs is, therefore, an absolute necessity [39,40]. This can only be realized by developing efficient, fully integrated recycling routes, which can take advantage of the rich REE recycling literature [41].

1.5 Rare Earth Resources

The rare earth elements are lithophilic and are therefore concentrated in oxidic compounds such as carbonates, silicates, titanotantaloniobates, and phosphates, or form minerals of these types on their own [42,43]. The formation of the minerals is influenced by variations in ionic radii, crystallochemical factors such as coordination number, basicity, potential for isomorphic replacement, tendency to form complexes, and differences in oxidation states. More than 250 rare earth minerals have been identified. However, only about a few of them have important industrial value (Table 1.3): bastnaesite, monazite, xenotime, fluocerite, parasite, fergusonite, gadolinite, aeschynite, synchysite, samarskite, polycrase, and loparite. Among these, the first four are the major industrial rare earth minerals [44, 45]. In addition to the rare earth minerals in Table 1.5, ion-adsorption type rare earth clay is the major source of current heavy rare element production. It was first discovered in China's Jiangxi Province in 1969.

Table 1.3 Rare earth world scenario: resource and production

Country	Mine Production (metric tons)	% of total	Reserves (million metric tons)	% of total	Reserve Base ^a (million metric tons)	% of total
United States	none		13.0	13	14.0	9.3
China	105,000	95	55.0	50	89.0	59.3
Russia			19.0	17	21.0	14
(and other former Soviet Union countries)						
Australia	2,200	2.0	1.6	1.5	5.8	3.9
India	2,800	2.5	3.1	2.8	1.3	1
Brazil	250	0.22	Small			
Malaysia	280	0.25	Small			
Other	NA		22.0	20	23	12.5
Total	111,000		110.0		154	

Source: U.S. Department of the Interior, Mineral Commodity Summaries, USGS, 2013.

The REEs are adsorbed on the surface of clays in the form of ions. The REO grade in the ion-adsorbing type clay is 0.05–0.3 %. Of the REO up to 60 % are heavy rare earth elements. The ore composition is relatively simple in comparison to the coastal placers. Presently, the main ore minerals for the REEs are monazite, bastnaesite, and xenotime. The first REE mineral to be used was gadolinite, and from this mineral, several of the REE were first isolated, but it was not applied on an industrial scale. So it can be safely said that the first REE ore mineral from which REE were extracted for industrial use was monazite.

1.5.1 Monazite

Monazite is one of the most important rare earth minerals and it was the first rare earth mineral recovered for industrial application. Monazite has a generalized chemical formula LaPO_4 [46]. The name is devised from the Greek monazeis, meaning “to be alone” because of the isolated crystals of monazite, and the fact that it was quite rare when first found. Monazite primarily consist light rare earth elements: La, Ce, Pr, Nd, and Sm, however, a mix of all the rare earths is present in low concentration. It usually also contains Th and/or U, but the amounts in monazite are generally too low to be extracted as a valuable by-product. It is widely distributed across the world. Australia, Brazil, India, and China are all important monazite producers. Monazite reserves in India are poor in europium and other heavy rare earths compared to all other types of monazite found across the world which makes them disadvantageous for producing HRE.

1.5.2 Bastnaesite

Bastnaesite is the most industrially important rare earth mineral, containing 67–73 % REO. It is the major source of light rare earth elements. The chemical composition of bastnaesite is relatively simple in comparison with other rare earth minerals with general formula of

$\text{Ce}(\text{CO}_3)\text{F}$. At present the basic origin for Bastnaesite is from two countries USA and China. Among the HREEs, only Y is constantly found in Bastnaesite. Bastnaesite, containing neither U nor Th, has replaced monazite as the primary LREE-ore mineral. Related minerals may arise from substitution of the fluorine and carbonate ions. Bastnaesite is a widespread mineral, but never occurs in large quantities.

1.5.3 Xenotime

Xenotime is a rare earth phosphate mineral with its major component yttrium orthophosphate (YPO_4). It is one of the important sources of heavy rare earth elements. Xenotime was first described by Berzelius in a specimen from Hydra (Hitterø), Flekkefjord, Vest-Agder, Norway [47]. The generalized chemical formula of xenotime is (YPO_4). Xenotime, in contrast to monazite and bastnaesite, generally contains, besides Y, appreciable amounts of the HREE (Heavy Rare Earth Elements: Y, Tb, Dy, Ho, Er, Tm, Yb, and Lu). Xenotime usually consists up to 67 % REO, mostly the heavier elements [8].

1.5.4 Secondary Resource

With the dramatically increasing application, global RE consumption has exhibited significant growth in recent years. As an important non-renewable natural resource, a stable supply of RE raw materials is crucial. In addition to mineral resource, secondary resource also has tremendous potential. It is estimated that the current recycling rates of REs are less than 1%. An assessment of recycling potential global REs for the year 2020 is outlined, which includes most extensively used permanent magnets, nickel-metal-hydride batteries, and lamp phosphors, as shown in Table 1.4 [36]. The so-called urban mining can make a significant contribution to the overall RE supply, which means the process to recover the compounds and materials from products at their end of life.

Table 1.4 Recycling potential for rare earths by 2020

Rare Earth Application	Estimated RE stocks in 2020 (tonnes)	Estimated average lifetime of the products	Predicted RE scarp by 2020 (tonnes)
RE Magnets	300000	15	20000
Lamp Phosphors	25000	6	4167
Nickel Metal Hydride Batteries	50000	10	5000
Total	375000	-	29167

Recently, with large amounts of RE accumulation in “urban mines” and highlighted supply problems, the recycling of urban mining has become an important source for stabilizing supplies, especially for the regions without sufficient economic and/or operational primary RE deposits. On the other hand, RE recycling is so meaningful which can not only balance the REs’ supply and demand relation but also reduce environmental pollution. Overall, the transition from a linear to a circular approach is the most effective strategy in the future. The main characteristic of secondary resource is the widely dispersed RE concentrations, from 0.1 to 30 %, and no radioactive Th and U compared with the primary ores. Similarly, they contain abundant Nd and Dy. Thus, what is urgently needed in RE recycling is a highly selective and efficient extractant which can obtain individual REs and useful concomitant elements at the same time [39-41, 48].

1.6 Separation and purification of rare earths

The separation of the rare earth elements poses one of the most difficult problems in inorganic chemistry as well as analytical chemistry. Due to the great similarity of the chemical properties, the methods are generally not very selective. In a few cases, better separation can be achieved by the variation of oxidation state of high stability ($\text{Ce}^{3+} \rightarrow \text{Ce}^{4+}$, $\text{Eu}^{3+} \rightarrow \text{Eu}^{2+}$). A further difficulty is presented by the unfavorable distribution of concentrations of individual rare earth metals in the common minerals. Initially rare earth elements are separated in groups of elements that resemble each other very closely. Several processes exist for separation of the naturally occurring rare earths from one another. They all utilize the small differences in basicity resulting from the decrease in ionic radius from lanthanum to lutetium. The basicity differences cause several effects: such as variation in solubility of salts, differences in the hydrolysis of ions and order of formation of complex species. These differences form the basis of the separation procedures by fractional crystallization, fractional precipitation and ion exchange and solvent extraction. Also, some trivalent rare earths (Ce, Pr, Tb) may also become tetravalent, and some others (Sm, Eu, Yb) may become divalent. This creates the possibility to use selective oxidation or reduction of these elements to separate them, because the divalent and tetravalent state the elements show marked differences in behavior from the trivalent state [9].

1.6.1 Selective Oxidation

The most abundant rare earth, Cerium can be removed from the rare earths mixture relatively easily after oxidizing naturally occurring Ce(III) to Ce(IV). This valence change occurs, when a common cerium ore, bastnaesite is heated in air at 650 °C, or when the rare earth hydroxides are dried in air at temperatures of 120–130°. In aqueous hydroxide solution, oxidation can be achieved by chlorination or electrolysis. Cerium can also be oxidized by

hypochlorite, hydrogen peroxide, atmospheric oxygen, or electrolytically at a suitable pH, precipitating it as cerium(IV) oxide hydrate. By adding chlorine and sodium hydroxide solution to a solution of cerium earth chlorides, cerium(IV) oxide hydrate is precipitated. This can lead to a 90% pure cerium oxide that is suitable for use as a polishing material. A very effective way is air oxidation and solvent extraction. It has become apparent that TBP (tributyl phosphate) is the best extractant for large scale operations [9]

1.6.2 Selective Reduction

It is easily possible to remove Sm(III), Eu(III) and Yb(III) from the trivalent rare earths mixture by reducing them to the divalent state. Divalent europium (Eu) has properties similar to those of the alkaline earths, especially strontium (insoluble sulfate, soluble hydroxide, etc.). The rare earth metals are usually reduced in hydrochloric acid solution by zinc amalgam or sodium amalgam. The subsequent precipitation of europium sulfate from the very dilute solution can be improved by co-precipitation of strontium or barium sulfate. The europium can be further purified by precipitating trivalent elements as their hydroxides by using ammonia. Samarium and ytterbium can also be easily separated from the trivalent rare earths mixture after reducing them to a divalent state. Unlike cerium, these elements are much less abundant, and separation using reduction is carried out only after they have been enriched by other procedures. Finally, there is a method of separating samarium, europium and ytterbium based on the fact that the metals Sm, Eu, and Yb cannot be produced by metallothermic reduction of their halides [9].

1.6.3 Fractional Crystallization

Fractional crystallization was the first process for separating the rare earth elements, both in the laboratory and on the industrial scale [49]. In Fractional crystallization, a part of a salt in solution is precipitated by a change in temperature or by evaporation of the saturated solution. If

the solubility of the various compounds of the solution differs, the composition of the crystalline precipitate will not be the same as the composition of the original solution. The least soluble substance will be the first to crystallize. The most suitable compounds are ammonium nitrates (for La, Pr, and Nd) and double magnesium nitrates (for Sm, Eu, Gd). Manganese nitrates have also been used for separation of lanthanides of the cerium group (La–Nd). Other chemicals applied include a sodium rare earth EDTA salt for separating gadolinium, terbium, dysprosium, and yttrium. For these rare earths, a purity of 99% has been reached with this method. Fractional crystallization works best for the lanthanum end of the series, as there the differences in ionic radius are the largest. Fractional crystallization is very slow for the heavy rare earths and in the Sm(III)–Gd(III)—region, because the differences in properties between the rare earths decrease as the atomic number increases [49].

1.6.4 Fractional Precipitation

Fractional precipitation denotes the removal of part of the rare earths from solution by the addition of a chemical reagent to form a new, less soluble compound. The rare earths still remaining in solution are recovered either by further precipitation as the same compound or by complete precipitation as the oxalate, hydroxide, or other compound. Fractional precipitation was only used for separating the rare earth elements into groups, due to filtration difficulties and the slow establishment of equilibrium [50]. In this respect, it is different from fractional crystallisation, where no other compound is introduced in the solution. Hydroxides and double sulphate have extensively been used, as well as double chromate. The latter one has been used for the separation of yttrium from the other rare earths. The addition of sodium sulphate to the rare earth solution leads to the precipitation of double sulphates. The elements La, Ce, Pr, Nd and Sm form poorly-dissolvable double sulphates, whereas Ho, Er, Tm, Yb, Lu and Y form well-

dissolvable double salts. The salts of Eu, Gd and Dy form salts of intermediate solubility. Generally, the use of this method crudely separates the rare earth mixture into three groups, although separation of La and Y is very well possible [9].

1.6.5 Ion Exchange

In ion exchange, there is an adsorption stage and an elution stage. In the first, the ions from the solution get loaded on the exchanger, and in the latter, as a consequence of a change of conditions, the ions desorb from the exchanger and go again into solution. For the rare earths, this was first attempted in the late 19th century (1893) for the separation of yttrium and gadolinium using activated carbon. Later the separation of the rare earths was also tried using other exchangers.

However, current ion exchange process is based on the work carried out on the separation of rare earth elements produced by uranium fission, and formed part of the Manhattan Project. The principles of separation by elution were developed by Boyd and coworkers in the Oak Ridge National Laboratory. Spedding et al had investigated the production of rare earth metals on a large scale by displacement elution [51]. Attempts to develop ion exchange column chromatography into a continuous process were realized with the development of the continuous annular chromatograph by researchers in the mid-1970s. However, the process was designed for analytical requirements with low loading of the columns and was therefore not commercialized [52-54]. A relative better method termed as continuous column chromatography showed promise for better separation and industrial application [55]. In the above mentioned method the exchange of ions between two electrolytes or between an electrolyte solution and a usually solid material called an ion exchanger. Generally, an ion with a higher charge will replace an ion with a lower charge. When the ions have the same charge, the ion with the larger ionic radius displaces the

onewith the smaller radius according to the laws of mass action. At first ion exchange seemed not very promising, as the affinity of the chemically closely related rare earth elements for the applied exchangers was not sufficiently different to result in a satisfactory separation. The separation factors for adjacent rare earths were found to be close to unity. For example, sulfonated polystyrene ion exchange resins, which possess high chemical stability, can combine with 0.5 – 0.8 mole of rare earth elements per moleof resin. However, differences in the affinities of the rare earth elements for the resin are very small, and the separation factor for two neighboring rare earth elements is only 1.08 [56]. The scenario of RE separation changed with the application of complexing agents in ion exchange process, which couldenhance separation factors. Later, the invention of the band-displacementtechnique has enhanced separation [57]. The most useful commercialcomplexing agents are EDTA and HEDTA.EDTA can effectively separate most of the rare earths from each other with exception forthe pairs Eu–Gd, Dy–Y, and Yb–Lu. The band-displacement technique with ammonium-ethylene-diamine-tetraacetateas the complexing agent has made ion exchange the most-used commercialprocess for rare-earth-element separation since the mid-1950. The advantages offered by ion exchange technique aremany like this method can separateindividual rare earth from the mixture of 15 rareearths with 99.99%purity in one pass through the system, it offers potential up scaling to large quantities.The technique is still used today, even with the possibility of solvent extraction, whichis discussed in the next section.

Even though ion exchange method offers high purity rare earths as product but it still possessesvarious disadvantages i.e. Chelating agents required in ion exchange are expensive along with their recovery is difficult and requires a large number of batch operations. Also, the low solubility of rare earths leads to very dilute solutions of the REE (2 – 10 g REO/L), whereas

with liquid – liquid extraction 10 –50 times more concentrated solutions may be used. These high dilutions lead to bulky equipment and handling losses. Rare earths separation by ion exchange techniques has various drawbacks such as considerable increase in plate height when it is applied to industrial scale operation.

1.6.6 Solvent Extraction

The liquid – liquid extraction process for the separation of the rare earth elements was discovered by Fischer et al. who showed that extraction of rare earth metal solutions in hydrochloric acid with an alcohol, ether, or ketone gives separation factors of up to 1.5 [58-60]. The ability of metal ions to distribute themselves between an aqueous solution and an immiscible organic solution has long been utilized by hydro-metallurgists to transfer the valuable metals from the aqueous solution to the organic solution and leave the unwanted metals and impurities in the aqueous solution. The aqueous solution, normally the feed, contains the valuable metals, free acid, and impurities dissolved in water. In the liquid – liquid extraction process used today, the organic phase usually consists of two or more substances. The active extractant has complexing properties and is mainly responsible for the transfer of the dissolved rare earth elements from the aqueous to the organic phase. In most of the cases, as active extractants are usually highly viscous or even solid so must be dissolved in a solvent to ensure good contact between the two phases. Suitable solvents i.e. diluents are kerosene and aromatics. A third phase between aqueous and organic phases is often formed in solvent extraction operation which is related to the solubility of the metal–extractant complex in the organic solution. The third phase can cause significant processing challenges and lead to organic loss. The addition of a modifier to the organic phase is also an effective approach to minimize the formation of the third phase. The objective of extraction is to partially or entirely transfer the valuable solute from the aqueous

solution to the organic solution and leave the undesirable solutes in the aqueous solution. A solute with a higher distribution ratio is easier to be extracted. A single stage extraction requires one time of contact (or mixing) of organic and aqueous solutions. A two stage extraction requires two times of contact of the two solutions. A multi stage extraction needs multi times of contact of the two solutions in order to complete the extraction of the valuable solute(Fig. 1.5). The organic solution will be loaded with the valuable solute after extraction and usually is called loaded organic solution. There will be only small amount of the valuable solute left in the aqueous solution after extraction. The aqueous solution containing only undesirable solutes and impurities is called raffinate. Separation of the rare earths by solvent extraction is currently the most favoured method to obtain pure fractions of every rare earth. There are many advantages to the use of solvent extraction for the separation of the rare earths. One major advantage of solvent extraction process is that the rare earth loading in the organic extractant can be very high. Aqueous solutions with up to 130 grams of rare earth oxide per liter can be used [9]. Another added advantage is relatively simple equipment and rather quickly, high purity products can be achieved [61]. Purities of >99.9 %, reached almost exclusively with solvent extraction, are reported in Gupta and Krishnamurthy (2005). As evident from above extractants, metals of interest, the nature of aqueous solution, etc. Rare earth solvent extraction systems are also introduced according to the extractants. The selection of extractant is critical in developing a rare earth solvent extraction process. The rule of thumb in selecting an industrial extractants includes; the extractant has at least one functional group that can form extractable complex with metal ions. Common functional groups contain O, N, P, and/or S elements. The extractant has a relatively long hydrocarbon chain or contains benzene/ substituted ring. This is to increase the solubility of the extractant and metalextractant complex in organic phase. Apart from this the

extractant should have good selectivity towards the metal of interest along with good chemical and thermal stability. The extractant should also have low tendency to form emulsion in extraction and stripping operations. This requires the extractant to have low density, low viscosity, and large surface tension.



Fig. 1.5 Solvent Extraction: Mixer-Settler Assembly for Yttrium Purification

The commonly used rare earth extractants include all the types of extractant ranging from acidic to basic and neutral extractants as well. 2-ethyl hexylphosphoric mono- 2-ethylhexyl ester (HEH/EPH, EHEHPA, P507), di-(2-ethylhexyl) phosphoric acid (D2EHPA, HDEHP, P204), di-(2,4,4-trimethylpentyl) phosphinic acid (HBTMPP), tributylphosphate(TBP), di-(1-methylheptyl) methyl-phosphonate (P350), Cyanex 923, naphthenic acid, and amines are commonly used extractants[23]. These extractants can be used alone or together depending upon the need and ease of operation. Although solvent extraction industrially accepted process for rare

earths separation but this technique is also not free from difficulties and disadvantages. Few of them are listed in the upcoming sections.

1.7 Limitation of conventional method and scope of alternative methods

Since 1950's solvent extraction process came in to the picture for RE separation and due to the obvious advantages such as simple operation, mild process conditions, and fast, continuous, and economical handling of large quantities of materials, solvent extraction gradually replaced the ion exchange. Up to now, the separation and purification of REs have heavily relied on solvent extraction from lab to industrial scale, which became the predominant RE separation technology, but there also exist some unavoidable issues relating to the environment.

1.7.1 Use of hazardous diluents in L-L extraction

Solvent extraction of REs is similar to other two-phase liquid-liquid extraction processes, which generally requires an abundance of nonpolar organic diluents (or solvents) to dilute the organic extractant. In RE separation process, the most widely used diluents are petrochemical products like kerosene, n-paraffin and n-heptane, which are used to dissolve and dilute organic extractants to reduce the viscosity of the extracted complexes, but most organic diluents are highly volatile and flammable. Therefore, strict standards for fire hazard and explosion are severely needed in industrial process which not only increase the cost of operation but also enhance the risk to environment. Overall, the large-scale use of volatile solvents is a great threat to safe operation, not only because of their toxic and flammable nature but also due to the obvious health problems associated with them [62]. Therefore, it is crucial to seek safer replacements or development of methods/techniques which require nil/less diluents for operation.

1.7.2 Limitation of organic extractants

P507 popularly known as 2-ethylhexyl phosphoric acid mono (2-ethylhexyl) ester or PC88A was successfully synthesized on an industrial scale in the 1980s by Shanghai Institute of Organic Chemistry, Chinese Academy of Sciences (CAS) [63]. Today P507, is the most widely used organic extractant for RE separation on industrial scale in China. Although PC88A of P507 offers various advantages over other solvents such as high β value, high extraction capacity, and easy stripping but it is not free from disadvantages at operation as well as environmental level.

1.7.2.1 Saponification

In rare earths separation hydrometallurgy, P507 required to be saponified by ammonia water, NaOH, or $\text{Ca}(\text{OH})_2$ not only to break hydrogen bonds in the dimers of extractant but also to keep the acidity of aqueous phase approximately constant during extraction process leading to enhance the cation exchange of REs. However, this process leads to production of corresponding ammonia nitrogen, Na^+ , or Ca^{2+} ions in discharged wastewater. It was reported by Sun et al that the RE industry produced over 20 million tons of wastewater, and approximately over 9 million tons of high ammonia nitrogen wastewater was released in 2011 [64]. Recently, saponification by ammonia is gradually being replaced by sodium, which is also creating aqueous phase salinity problems.

1.7.2.2 Complex Process

The selection of organic extractant is a tough process, owing to the complicated organic synthesis process, difficult impurity-removing process, and high preparation and evaluation cost. Some problems about P507 have been shown, but no suitable replacement has been found, even though lots of efforts have been made. Bis(2,4,4-trimethylpentyl) phosphinic acid (Cyanex 272), has the higher β for heavy REs is obtained, but the preparation cost is high, and this system

is difficult to control owing to low extraction capacity and easy emulsification phenomenon along with phase separation issues.

1.7.2.3 Relatively Low Separation Factor

When separation factor values, for the selectivity of heavy REs is compared with the lighter ones they were found to generally lower in the P507 system, e.g., Tm/Er (3.34), Yb/Tm (3.56), and Lu/Yb (1.78) [65]. Another significant deficiency in P507 is that it is difficult to strip heavy REs completely, especially for Tm(III), Yb(III), and Lu (III), and require relatively higher acidity.

1.7.3 Alternative methods

After carefully examining the current scenario in the field of rare earth separation and purification which includes environmental concerns, there is an eminent need to develop effective and efficient processes which not only maximizes the separation but also minimizes the environmental hazard associated with the conventional processes. In recent years, various alternative techniques such as

- (a) Membrane based separation methods i.e. hollow fibre membrane, emulsion liquid membrane etc.
- (b) Solvent impregnated resins/ extractant encapsulated beads i.e. Polystyrene XAD, Poly ether ether Ketone and Polysulfone based solvent encapsulated resins/beads.

The above stated methods have shown tremendous potential to RE green separation. These techniques either require relatively less amount of organic extractant and offers simultaneous extraction and stripping of rare earths or eliminate the use of organic diluents in the process of recovering rare earth values from aqueous phase.

1.7.3.1 Membrane based separation

A membrane is a semipermeable barrier between two phases. If one component of a mixture moves through the membrane faster than another mixture component, a separation can be accomplished. Polymeric and inorganic membranes are used commercially for many applications including gas separations, water purification, particle filtration, and macromolecule separations [66-75]. The membrane techniques offer attractive advantages over conventional methods due to the following reasons i.e. low operating costs, low capital costs, continuous operation. In liquid membrane separation methods, organic phase is kept in between the two aqueous phases; one phase containing metal ion (feed or source phase) and the other which receives the metal ion (strip or receiver phase). Several types of membranes are extensively studied such as: supported liquid membranes and non-supported liquid membranes. Supported liquid membranes consists a polymeric matrix which is used as solid support for organic solvent and is placed in between the feed and strip solutions. The stability of membrane depends upon various factors like nature of polymer and solvent, the pressure difference across the liquid membrane, the solubility of carrier extractant in the aqueous phases, etc. Two types of supported liquid membranes are commonly used i.e. flat sheet supported liquid membrane and hollow fibre supported liquid membrane.

1.7.3.1.1 Flat-Sheet Supported Liquid Membrane (FSSLM)

The term liquid membrane transport includes processes incorporating liquid-liquid extraction (LLX) and membrane separation in one continuously operating device. It utilizes an extracting reagent solution, immiscible with water, stagnant or flowing between two aqueous solutions (or gases), the source or feed and receiving or strip phases. In Flat-Sheet supported liquid membrane (FSSLM), a polymer sheet is placed between the two compartments, one

containing the feed solution while the other containing the receiver or strip solution. The polymer sheet is impregnated with the organic carrier solution and the phases are continuously stirred using magnetic stirrers to reduce the aqueous boundary layer resistance for mass-transfer. Since the small surface area is available for mass-transfer, hence the mass fluxes are lower. Also, this technique cannot be applied on larger scale because a small pressure difference in that case would result in the blowing out of the organic solvent from the pores of liquid membrane. Hence, FSSLM's have been applied on small scales only (generally, few mL to several hundred mL).

1.7.3.1.2 Hollow Fibre Liquid Membrane (HFLM)

As described in the above section, the limitations of FSSLM include lower transport fluxes and physical instability of membrane at higher volumes and pressure of feed and strip phase. The limitation related to mass fluxes can be fixed with increase in the surface area of contact per unit volume. In this regard, Hollow Fibre Supported Liquid Membrane (HFSLM) is an attractive configuration for higher flux. HFSLM module (Fig. 1.6) consists of thousands of single hollow fibres which are cylindrical in geometry. The feed and strip solutions are passed through the inside and outside of hollow fibres. Due to compactness of the system, a very large surface area per unit volume is available which provides larger mass fluxes using HFSLM technique. The presence of tubular porous membrane give rise to two modes of operation: first is in SLM mode where solvent can be loaded in the pores of membrane and subsequently feed and strip phase can be run through the shell and lumen side of tubular membrane second when tubular membrane can be used as interface with feed and organic phase can be passed through shell and lumen sides respectively (non-dispersive mode).

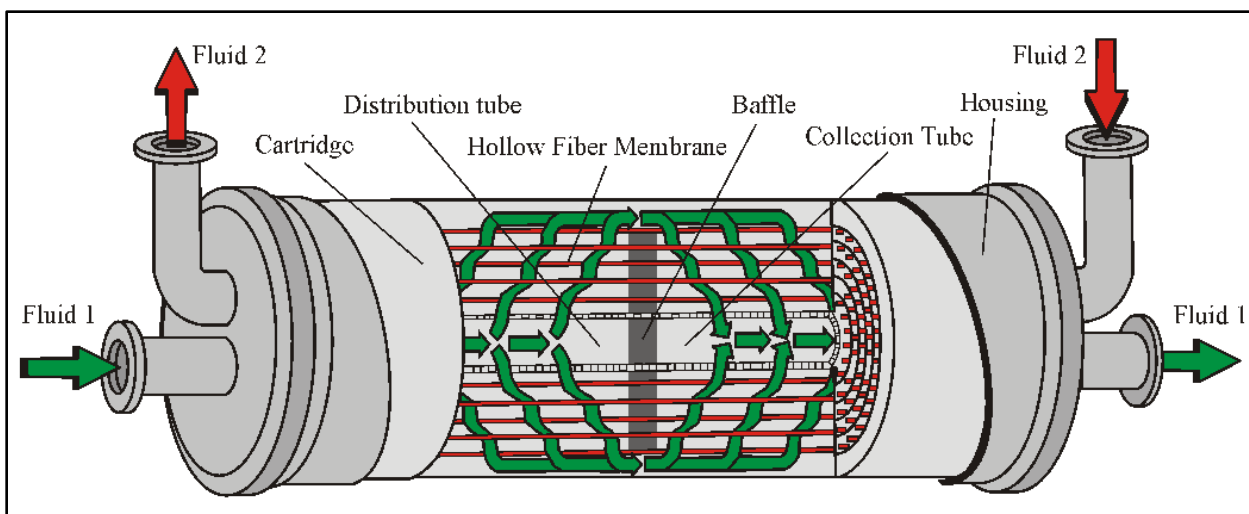


Fig 1.6 Hollow Fibre Supported Liquid Membrane Module

Hollow fibre membrane modules promise more rapid mass transfer than is commonly possible in conventional equipment. For example, mass transferred per equipment volume is about thirty times faster for gas absorption in hollow fibres than in packed towers [76-77]. Liquid extraction is 600 times faster in fibres than in mixer settlers [78-82]. This fast mass transfer in hollow fibres is due to their large surface area per volume, which is typically 100 times bigger than in conventional equipment. In addition, membrane contactors fit the process intensification approach for liquid–liquid extractions, scrubbing, or stripping by permitting independent variation of flow rates without problems of flooding, eliminating post process separations. Contactors show potential for membrane crystallizers using membrane distillation to produce crystals from supersaturated solutions, concentrating the solution and removing solvent in the vapour phase. Membrane crystallizers fit the process intensification scheme with a larger mass transfer area enclosed in a smaller volume than conventional crystallizers. Extensive studies on hollow fiber membrane based separation technology (HFMST) were reported for efficient removal of toxic heavy metals like Cr(VI), Cd, Zn, Ni, separation and concentration of gold from alkaline hydrometallurgical solution [83-87]. Further, recovery of valuable solutes from aqueous

phases for example, citric acid, carboxylic acid, amino acids, and L-phenylalanine [88] such as removal of phenol from industrial waste water [89] are well demonstrated by using this technology.

The faster transport rate and ease of scaling up of process makes it a promising option for using this technology in the separation of rare earths and various researchers around the world have been exploring the possibility to recover and purify rare earths values by HFM based methods.

1.7.3.2 Solvent impregnated/encapsulated resins

Although solvent extraction has been widely applied in the field of RE separation, there exist some shortcomings. Hydrometallurgical operations based on liquid- liquid extraction generally require intimate contact of organic solvents with various types of aqueous solutions in extraction, scrubbing and stripping circuits, which often result in the loss of organic solvents due to entrainment and then inherit solubility characteristic in aqueous solution. In plant scale operations, where large volumes of organic solvents and aqueous solutions are involved, loss of organic solvents would be substantial, if not recovered. Regardless of how well the solvent extraction system operates, the raffinate contains entrained solvent. Another shortcoming with the process requires more reagents and consumes more energy when solvent extraction is used directly to recover rare earths from lean source. To overcome these drawbacks some interesting studies have been focused on solid-liquid separation systems [90]. These systems, consumes minimal amount of extractant, and the extraction and stripping steps can be coupled into a single step. Unfortunately, the industrial use of solid-liquid separation systems is limited by their instability and short lifetime of solid adsorption materials. One such type of method is solvent impregnated resins (SIRs) which are commercially available (macro)porous resins impregnated

with a solvent/an extractant. In this approach, a liquid extractant is contained within the pores of (adsorption) particles having the organic extractant in liquid phase. Its purpose is to extract one or more dissolved components from a surrounding aqueous environment. The basic principle combines adsorption, chromatography and liquid-liquid extraction. The principle of Solvent Impregnated Resins was first shown in 1974 by Abraham Warshawsky[91]. This first venture was aimed at the extraction of metals. Ever since then, SIRs have been mainly used for metal extraction, be it heavy metals or specifically radioactive metals. Sorbents containing immobilized extractants can be classified into two basic types: (1) solvent-impregnated resins prepared by adsorption of an liquid extractant on polymer supports; and (2) resins with liquid extractant encapsulated within polymer matrix during polymerization step or solidification of the matrix[92-96].

However, lately investigations also go towards using SIRs for the separation of natural compounds, and even for separation of biotechnological products. While during conventional liquid-liquid extraction the solvent and the extractant have to be dispersed, in a SIR setup the dispersion is already achieved by the impregnated particles. This also prevents an additional phase separation step, which would be necessary after the equilibration occurring in liquid-liquid extraction. Also, the impregnation step decreases the solvent loss into the aqueous phase compared to liquid-liquid extraction. This decrease of extractant loss is contributed to either physical sorption of the extractant on the particle surface, or encapsulation of extractant by polymer matrix which means that the extractant inside the pores does not entirely behave as a bulk liquid. However, the possible decrease of extractant loss depends largely on the pore size and the water solubility of the extractant. Nonetheless, SIRs have a significant advantage over e.g. custom made ion-exchange resins with chemically bonded ligands. SIRs can be reused for

different separation tasks by just rinsing one complexing agent out and re-impregnating them with another more suitable extractant. This way, potentially expensive design and production steps of e.g. affinity resins can be avoided. Finally, by filling the whole volume of the particle pores with an extractant (complexing agent), a higher capacity for solutes can be achieved than with ordinary adsorption or ion exchange resins, where only the surface area is available. However, there are possible drawbacks of SIR technology, such as leaching of the extractant or clogging of a fixed bed by attrition of the particles. These might be remedied by choosing the proper particle-extractant-system. This implies selecting a suitable extractant with low water solubility, which is sufficiently retained inside the pores, and selecting mechanically stable particles as a solid support for the extractant.

In terms of actual applicability of these SIR's which are also known as solvent encapsulated beads or polymeric beads requires a suitable organic extractant. Normally various types of organic compounds such as LIX 79, Cyanex 272, TBP, Aliquat 336, di-2-ethyl hexyl phosphoric acid (D2EHPA) and 2-ethyl hexyl phosphonic acid (PC88A) have been encapsulated or adsorbed inside/on the matrix due to the advantages associated with the extractant used i.e. stability, high distribution ratio for metal extraction, low water solubility and selectivity for metal ions. Extensive literature survey unveils that various attempts have been made by researchers worldwide to study the preparation conditions for polymer (polysulfone, styrene/ di vinyl benzene, poly ether ether ketone etc.) based microcapsules/beads and membranes which can encapsulate desired extractant. As far as its use in solvent extraction process is concerned most of the metal ion separation studies were performed by microcapsules/beads composed of chitosan, styrene, divinyl benzene which are commercially known as amberlite XAD[97- 118]. In this regard polyethersulfone (PES) which is one of the most important polymeric materials

and is widely used in separation fields shows outstanding oxidative, thermal and hydrolytic stability as well as good mechanical property [119-121]. Various types of membranes are being prepared by phase inversion method using PES for wide spectrum of applications. The structure of membrane of PES is influenced by the composition (concentration, solvent, additives) and temperature of PES solution, the non-solvent or the mixture of non-solvents, and the coagulation bath or the environment, and so on [122]. Considering the advantages offered by polyethersulphone (PES) for its applicability in preparation of polymer supported extraction systems, like membranes, exploring the possibility of using the same PES as matrix material for preparation of extractant encapsulated polymeric beads seems to be worthy exercise. The target of the present work encompasses preparation of such type of solvent encapsulating beads which not only combine the advantages of solvent extraction and ion exchange but also provide benefits with the simplicity of operating condition with solid phase ion exchange process. The advantage of the application of polymeric beads over other processes should consists large surface area, minimal use of organic solvents (environment friendly) and absence of phase separation phenomenon.

1.8 Scope of thesis

As discussed above in this chapter that, the most commonly used hydrometallurgical concentration and purification methods in the mining industry for rare earth separation are precipitation, liquid- liquid extraction and ion exchange. The traditional solvent extraction process also has limitation such as large volumes of organic solvents are required, especially when processing dilute solutions, which is not environmentally friendly. Further the method can be tedious and time consuming in those cases when many steps are needed to reach a sufficient

separation. Another drawback is that the method is difficult to automate and that the liquid phases may form emulsions that at times make it difficult to separate the two phases.

The last decade has seen phenomenal growth in the use of ionic liquids in this field. Though ionic liquids have shown promising results for selective separation but its physical properties, toxicity and cost remains a challenge for sustainable industrial applications[123]. Developing a new extraction system, including novel extraction material, synergistic extraction system, membrane based techniques and ionic liquid extraction, with improved efficiency and elimination of organic waste release in aqueous streams has always been challenging and thereby attracts researchers worldwide to tackle the vexed problem of separation of rare earths. In this context, solvent impregnated resins/beads are being developed as attractive alternatives in separation technology nowadays. They offer high surface area, eliminate the need of organic diluents, ease in phase separation and have the dual advantage of solvent extraction and ion exchange with relatively faster mass transfer kinetics and higher selectivity. Similarly, membrane based techniques in particularly HFM has been drawn considerable, as this technique requires less amount of organic extractant for carrying out separation studies and offers added advantage of simultaneous extraction and stripping. Due to limited literature availability, the arena of exploring these techniques for rare earths separation is still wide open.

Scanty reports are available in literature for the separation of rare earths by solvent impregnated resins [112,114]. The reported solvent impregnated beads are mainly based on polystyrene, polyether ether ketone, and alginate types of polymer and have sizes in micron to sub-millimeter range. These beads suffer from the drawbacks such as low holding capacity for extractants and observed to be susceptible to the leaching of impregnated extractants during repeated cycle of operations. These factors adversely affect the reusability and stability of the

beads. Therefore, it is desirable to develop novel polymeric beads which not only overcome these drawbacks but also result in enhanced extractaion/sorption of metal ions from aqueous solution. After careful screening of different polymers for matrix material, polyethersulfone has been found to be suitable to prepare the polymeric beads encapsulating extractant with improved characteristics. Subsequently, the aim of the present work is to evaluate the developed composite beads for the sorption of rare earths under variable experimental conditions. The present work also emphasizes on the importance of optimization of various variables i.e. system compositions (polymer, additive, extractants etc.), preparatory parameters and process variables (aqueous media, metal ion, temperature, solid to liquid ratio etc.) to obtain the best suited beads by intelligent design of experiments. Taguchi, which is a multi-parameter optimization procedure, is employed in the present developmental work to identify and optimize process parameters with a minimum number of experiments. Based on the batch experimental results, it was also of interest to employ these polymeric beads for the recovery of rare earths in continuous column operation mode, which may establish the materials potential to industrial level scale up.

Another important objective of the present thesis is to develop separation scheme for rare earths separation from aqueous solution utilizing hollow fibre membrane module. The present work also focuses on the efforts to utilize the importance of liquid membrane technique which requires a very less amount of solvent for carrying out rare earth separation studies with added advantage of simultaneous extraction and stripping. The present work encompasses the development of rare earth recovery (Dy, La, Sm) process by employing hollow fibre membrane contactor module with organophosphorus type of extractant. The objective also include the evaluation of two modes of operation i.e. non dispersive solvent extraction and hollow

fibresupported liquid membrane in which the module can used. This work also aims to evaluate the experimental process variables to optimize the rare earth recovery and purification process.



Chapter 2

EXPERIMENTAL AND TECHNIQUES

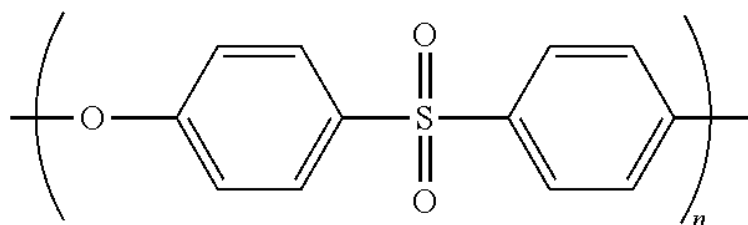
2 Experimental and Techniques

Organic solvent encapsulated beads have been synthesized for potential application in the removal of rare earth values from aqueous phase. Membrane based techniques were also explored for possible separation and purification of rare earths from different aqueous streams. This chapter elaborates the method that was used for the synthesis of polymeric beads, application of synthesized polymeric beads under variable experimental condition and details of hollow fibre supported liquid membrane techniques utilized for studying the transport behaviour of rare earth elements by organophosphorus type of extractants under various experimental conditions. Various reagents used in these studies and the techniques involved throughout the work have been discussed in this Chapter.

2.1 Materials

2.1.1 Polyethersulfone (PES)

PES (average molecular weight of 30,000) was obtained from Gharda Chemicals, India and used as received.



Polyethersulfone (PES)

Fig. 2.1 Structure of Polyethersulfone

2.1.2 N-methyl pyrrolidone (NMP)

1-Methyl-2-pyrrolidone or N-Methyl-2-pyrrolidone, NMP (formula weight: 99.13g/mol) having purity of 98.5% was obtained from Sigma- Aldrich, India and used as received.

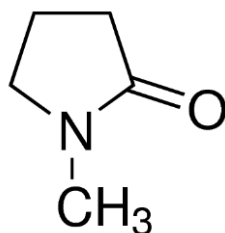


Fig 2.2: Structure of N-methyl pyrrolidone

2.1.3 Di-(2-ethylhexyl) phosphoric acid

Di-(2-ethylhexyl) phosphoric acid (DEHPA or HDEHP) is an organophosphorus compound. The yellow liquid is a diester (purity of 94.8%) of phosphoric acid and 2-ethylhexanol. It was obtained from Heavy Water Board, India and was used without any further purification for preparing composite beads.

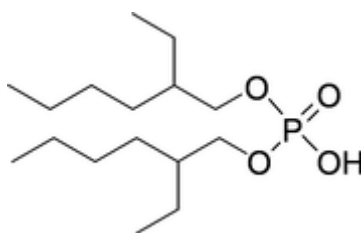


Fig.2.3 Structure of di(2-ethylhexyl)phosphoric acid (D2EHPA)

2.1.4 2-Ethylhexyl 2-ethylhexyphosphonic acid (EHEHPA)

2-Ethylhexyl 2-ethylhexyphosphonic acid also known as PC88A having molecular weight of 306.4 and purity of 95% has been received from Heavy Water board and used as it is.

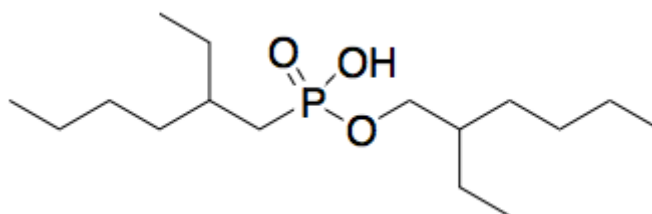


Fig.2.4 Structure of 2-Ethylhexyl 2-ethylhexyphosphonic acid

2.1.5 Diluent

Experiments performed during the recovery of rare earth by employing hollow fibre membrane required organic extractant to be used as carrier phase. The extractant needs to be

diluted so that the hydrodynamic conditions can be optimized for favorable metal ion extraction. Petroffin (Heavy Normal Paraffin) having following specification has been used as diluent.

Table 2.1 Characteristic properties of petroffin

Characteristics	Specifications
Density (at 15 ° C)	0.75±.01
Purity	99%
Carbon Distribution	
C11	20-30 %
C12	25-35 %
C13	20-30 %
C14	20-25 %
Flash point	70 ° C

2.1.6 Polyvinyl alcohol

Polyvinyl alcohol is a water-soluble synthetic polymer having molecular weight in the range of 31,000–50,000 was used as received from Merck India.

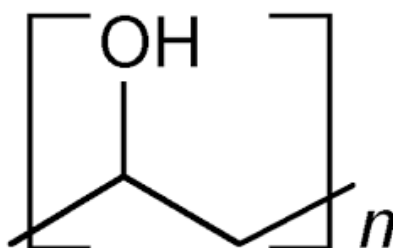


Fig. 2.5 Structure of poly vinyl alcohol

2.1.7 Rare earths oxides

Rare earth (such as Y(III), Sm(III), La(III), Dy (III), Nd(III), Pr(III) etc.) solutions were prepared by dissolving their oxides (>99% purity, received from Indian rare Earth Limited,

India) in hydrochloric acid and individual working solution were prepared by the appropriate dilution of the stock solutions.

2.1.8 Multiwall Carbon Nanotube (MWCNTs)

MWCNTs was having an average diameter of 20nm were prepared in our (REDS) laboratory by chemical vapour deposition method. Purification of MWCNT was achieved by treating it with hydrochloric acid (HCl) following thermal oxidation prior to its use in the present investigation [123].

2.1.9 Others

All the other chemicals and reagents used during the present investigation such as polyethylene glycol (PEG), poly acrylic acid (PAA), ethyl alcohol and LiCl were procured from Merck and were having LR grade purity.

2.2 Method

2.2.1 Preparation of polymeric beads

An experimental set up similar to Gong's approach was prepared for synthesis of extractant encapsulated polymeric beads [Fig 2.6] [116]. Initially, a PES solution was prepared by dissolving polymer in NMP in a desired w/v ratio. This prepared solution was then added to organic extractant at definite polymer to extractant ratio under stirring condition. Due to low solubility and inherent water content in the organic solvent the mixed solution of polymer and organic extractant appear like an emulsion or partially mixed solution. The mixed polymer solution was gradually dropped into the anti-solvent (deionized water) bath through a nozzle of syringe needle at an appropriate height. In the anti-solvent bath, the instantaneously formed droplets slowly precipitated due to the phase inversion of relatively dense polymeric backbone resulting in the formation of PES beads impregnating extractant. During this preparation, the temperature of the water was kept constant at 30°C using a thermostatic unit. These beads were then immersed and stabilized in the water bath

for 24 hours prior to their use. Various types of polymeric composite beads with different additives were prepared by the above mentioned method under optimized preparatory conditions (10-15% w/w PES in NMP with 1:5 D2EHPA to polymer solution).

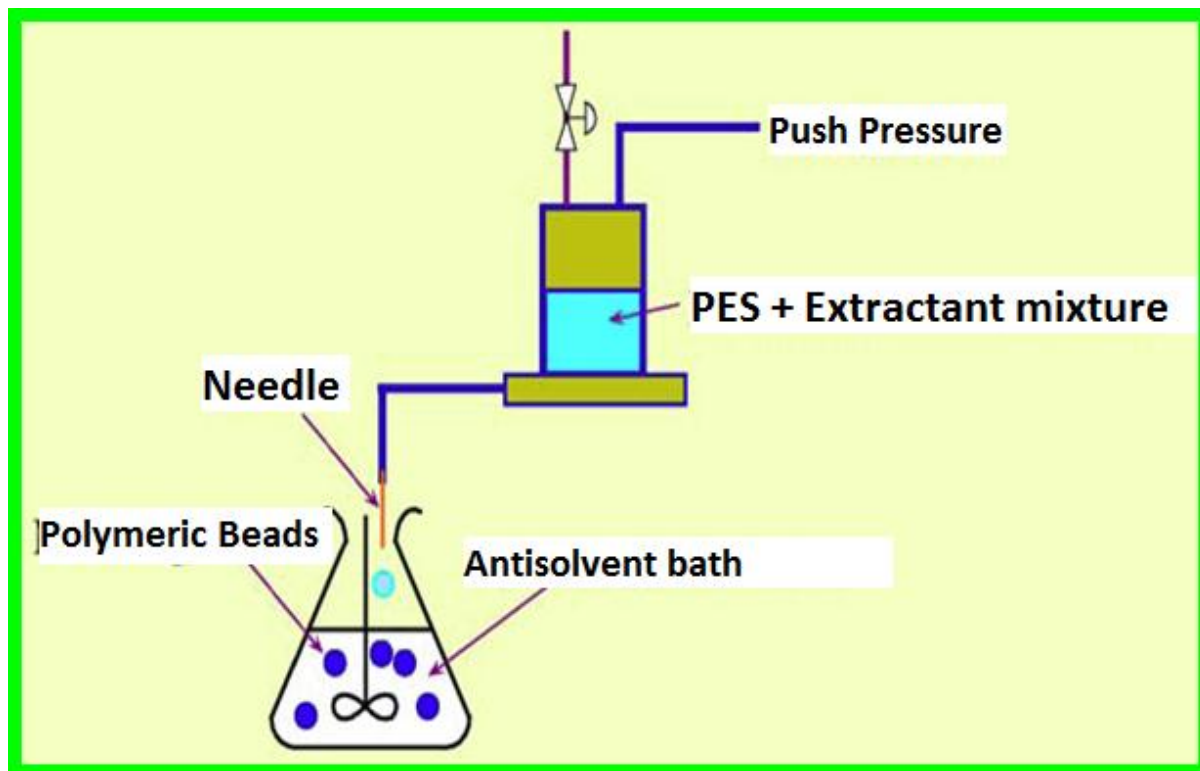


Fig. 2.6 Preparation set up for extractant encapsulated PES based polymeric beads

The concentration of the constituents was optimized in such a way that the resultant composite beads resulted in spherical shape. The concentrations of additives in different polymeric beads were 1.5, 0.25, 1, and 1 % w/w for PVA, MWCNT, PEG and LiCl respectively.

2.2.2 Metal ion sorption studies

Sorption (uptake) study of rare earths by polymeric beads was investigated in batch as well as column mode. In the case of batch mode, sorption studies have been performed by contacting known amount of all types of polymeric beads separately with aqueous solutions containing rare earths (80 to 3300 mg/L) at varying concentrations at an appropriate solid to liquid ratio for 24 hours to make sure that the system had reached the equilibrium. The solid –

liquid mixture was stirred constantly to avoid mass transfer resistance. In general, the experiments were performed at ambient temperature ($30\pm1^\circ\text{C}$), except for temperature variation study. To study the effect of a particular experimental parameter on sorption of rare earth elements, sorption test was carried out in similar way by keeping the other variables constant. Once the system reached the equilibrium the polymeric beads were removed and the aqueous phase was analyzed for its metal ion content by ICP-AES (JY Ultima 2) described in section 2.3.1. The concentration of sorbed metal ion was determined by the difference in the initial and equilibrium concentration in aqueous solution. For material balance the composite beads sorbed with metal ions were stripped either with suitable strippents i.e. 40 % HCl or 25% H_2SO_4 and analyzed for metal ion content by ICP-AES. The equilibrium adsorption (q_e) in mg/g and weight distribution coefficient, K_d were evaluated using following equations:

$$q_e = (C_o - C_e) \frac{V}{w} \quad (2.1)$$

$$K_d = \left(\frac{C_o - C_e}{C_o} \right) \frac{V}{w} \quad (2.2)$$

Where C_o , and C_e are concentration of Y(III) in mg/L or ppm at initial time and at equilibrium, respectively; w is the weight of polymeric beads (polymer and extractant); and V is the volume of aqueous phase in liters for q_e and mL for K_d evaluation.

2.2.3 Sorption isotherms

There are different theoretical models present, to describe the sorption process in detail. By evaluating the experimental data and applying these models, various important parameter and process mechanism can be determined, which help in understanding about the sorption of rare earths by polymeric beads under investigation.

2.2.3.1 Langmuir isotherm

Langmuir was the first to propose a coherent theory of sorption onto a flat surface based on a kinetic viewpoint [124]. The Langmuir sorption model is one of the best known and most frequently applied isotherms. The Langmuir equation initially was formulated on

the basis of a dynamic equilibrium between the sorbent and the sorbate, that is, the rate of sorption (which is the striking rate at the surface multiplied by a sticking coefficient, sometimes called the accommodation coefficient) is equal to the rate of desorption from the surface.

Langmuir proposed that the rate at which the sorbate molecules (B) strike a surface of a sorbent (A) is proportional to the product of the concentration of the sorbent and the fraction of the surface remaining uncovered by sorbate. To derive Langmuir Equation, a parameter 'θ' is introduced. Let θ be the fraction of the number of the sites on the surface which are covered with sorbate molecules. Therefore, the fraction of surface which is unoccupied will be (1 – θ). Now, the rate of the forward direction depends upon two factors: The fraction of sites available on the surface of sorbent, (1-θ), and the concentration, C. Therefore, the rate of the forward reaction is directly proportional to both the mentioned factors.

$$\text{Rate of sorption} \propto C (1-\theta) \quad (2.3)$$

$$\text{Rate of Sorption} = K_a C (1-\theta) \quad (2.4)$$

Similarly, the rate of the backward reaction or rate of desorption depends upon number of the sites occupied by the sorbate molecules on the sorbent,

$$\text{i.e. Rate of desorption} \propto \theta \quad (2.5)$$

$$\text{Rate of desorption} \propto K_d \theta \quad (2.6)$$

At equilibrium, the rate of sorption is equal to the rate of desorption.

$$K_a C (1-\theta) = K_d \theta \quad (2.7)$$

On solving the above equation for θ, we get

$$\theta = \frac{K_a C_e}{K_d + K_a C_e} \quad (2.8)$$

On rearranging the above equation, and substituting K_a/K_d with K_L (Langmuir constant)

$$\theta = \frac{K_L C_e}{1 + K_L C_e} \quad (2.9)$$

This is known as Langmuir sorption equation. θ can be expressed in terms of equilibrium sorption capacity, q_e , and maximum monolayer capacity, q_m , as given in equation (2.9)

$$\theta = \frac{q_e}{q_m} \quad (2.10)$$

Therefore, on substituting θ from equation (2.8), and rearranging, equation (2.9) becomes

$$q_e = q_m \frac{K_L C_e}{1 + K_L C_e} \quad (2.11)$$

The linearized form of the Langmuir sorption isotherm can be presented as

$$\frac{1}{q_e} = \frac{1}{q_m} + \frac{1}{K_L C_e q_m} \quad (2.12)$$

From the linear plot of $1/q_e$ vs $1/C_e$, the values of q_m and K_L can be calculated from the intercept and the slope, respectively. The basic characteristics of Langmuir equation have been often represented in terms of a dimensionless separation factor, (R_L), defined as

$$R_L = \frac{1}{1 + K_L C_0} \quad (2.13)$$

The value of parameter R_L indicates the nature of the isotherm as given below.

$R_L > 1$ unfavorable sorption

$0 < R_L < 1$ favorable sorption

$R_L = 0$ irreversible sorption

$R_L = 1$ linear sorption

2.2.3.2 Freundlich isotherm

Freundlich isotherm is an empirical equation. This equation is also one among the most widely used isotherms for the description of sorption equilibrium [125]. In contrast to the Langmuir equation, the Freundlich isotherm assumes sorption onto sorbent surfaces, which are characterized by heterogeneous sorption sites. It is also assumed that the stronger

binding sites are occupied first, and that the binding strength decreases with increase in the degree of site occupation. At low concentration, the amount of the sorbate sorbed is directly proportional to concentration of the sorbate (raised to power one).

$$q_e \propto C_e \quad (2.14)$$

At high concentration, the amount of the sorbate sorbed is independent of concentration, i.e., C_e raised to power zero

$$q_e \propto C_e^0 \quad (2.15)$$

Therefore, at an intermediate value of concentration, sorption is directly proportional to the concentration raised to power $1/n$. Here, n is a variable, the value of which is greater than one.

$$q_e = K_F C_e^{1/n} \quad (2.16)$$

The above equation is known as Freundlich sorption equation. The linearized form of the above equation can be represented as

$$\log q_e \propto \log K_F + \frac{1}{n} \log C_e \quad (2.17)$$

The linear plot of $\log q_e$ versus $\log C_e$ has a slope of $1/n$ and an intercept of $\log K_F$. However, in other case, when $1/n \neq 1$, the K_F value depends on the units in which q_e and C_e are expressed. On average, a favorable sorption tends to have Freundlich constant n between 1 and 10. Larger value of n (smaller value of $1/n$) implies stronger interaction between the sorbate and the sorbent, while $1/n$ equal to 1 indicates linear sorption, leading to identical sorption energies for all the sites.

2.2.4 Sorption Kinetics

Sorption kinetics describes the time-dependent evolution of the sorption process until equilibrium is reached. Such studies yield information about the possible mechanism of the sorption and the different transition states involved on the way to the formation of the final sorbate-sorbent complex. The results of such study help to develop appropriate mathematical

models, to describe the interactions. Among the most popular kinetic models/equations are the so-called “pseudo first-order” and “pseudo second order” rate expressions.

2.2.4.1 Pseudo first-order kinetic model

Lagergren equation is probably the earliest known one, describing the rate of sorption in the liquid-phase systems [126]. This equation is called the pseudo first-order equation, or the Lagergren’s rate equation, and can be written as

$$\frac{dq_t}{dt} = k_1(q_e - q_t) \quad (2.18)$$

Where q_t is the amount of sorbate sorbed at time t , and k_1 is the rate constant of the first order sorption. After integration and applying the boundary conditions, $q_t = 0$ at $t = 0$, the equation (2.18) can be written as

$$\log(q_e - q_t) = \log q_e - \frac{k_1}{2.303} t \quad (2.19)$$

The values of k_1 and q_e can be determined from the slope and intercept, respectively, of the straight line plot of $\log (q_e - q_t)$ versus t . Determining q_e accurately is a difficult task, because, in many sorbate-sorbent interactions, the chemisorption becomes very slow, after the initial fast response, and it is difficult to ascertain whether equilibrium is reached or not. Therefore, it has been reported that, many sorption processes follow Lagergren pseudo first-order model only for the initial 20 to 30 min of interaction. The value of k_1 parameter, also called time-scaling parameter, decides how fast the equilibrium in the system can be reached. The experimental studies have confirmed that the value of k_1 parameter can be both dependent and independent of the applied operating conditions. Its value depends on the initial concentration of the sorbate. It usually decreases with the increasing initial sorbate concentration in the bulk phase. Since the model does not describe the interactions for the whole range of contact time, in many cases, higher order kinetic models are employed to analyze the experimental results.

2.2.4.2 Pseudo second-order kinetic model

The pseudo second-order kinetics is usually associated with the situation, when the rate of direct sorption/desorption process (seen as a kind of chemical reaction) controls the overall sorption kinetics [126, 127]. The pseudo second-order kinetic model is expressed as

$$\frac{dq_t}{dt} = k_2(q_e - q_t)^2 \quad (2.20)$$

Where k_2 is the rate constant of the pseudo second-order sorption. After integration and applying the similar boundary conditions, the equation (2.20) can be written as

$$\frac{t}{q_t} = \frac{1}{k_2 q_e^2} + \frac{1}{q_e} t \quad (2.21)$$

The above equation can be further simplified by substituting h for $k_2 q_e^2$, where h can be considered as the initial sorption rate, when, and hence the final form of the equation can be written as

$$\frac{t}{q_t} = \frac{1}{h} + \frac{1}{q_e} t \quad (2.22)$$

The plot of t/q_t vs t gives a straight line, from the slope and intercept of which, the values of q_e and h , respectively, can be determined. Once the value of h is known, the value of k_2 can be determined there from. Many reports are available in literature, indicating that the value of k_2 has strong dependence on the applied operating conditions, such as the initial solute concentration, pH of solution and temperature, etc. The value of k_2 is usually strongly dependent on the applied initial solute concentration, and it decreases with the increase in C_o , i.e., the higher is the C_o value, the longer time is required to reach an equilibrium. The sorption kinetics is very complex in nature, and the importance of the various factors varies from one system to another. Any change in the pH and temperature brings about the changes in the equilibrium state. Due to these reasons, the influence of pH and temperature on the k_2 value has not yet been theoretically studied.

2.2.4.3 Kinetic steps

Mass transport, or migration, of the sorbate can be divided into four consecutive steps until it reaches the interior surface of the pores.

i. Bulk transport

This is transport of the sorbate from the solution phase to the subsurface, which is built up around the sorbent. This step is usually very rapid due to mixing of the flow.

ii. Film transport

This step involves diffusion of the solute across the so-called liquid film/sub surface surrounding the sorbent particles. This step is also known as external diffusion.

iii. Intraparticle transport

The third step in sorption involves the transport or diffusion of the solute in the liquid contained in the pores of sorbent particle, and along the pore walls.

iv. Sorption of the solute on active sites

This is the final step in the sorption process, and involves sorption and desorption of the solute molecules on/from the sorbent surface, which is quite fast.

The overall sorption rate may mainly be governed by any one of these steps, or a combination of two or more steps. Usually, the sorbate-sorbent system is under rapid mechanical mixing, and hence, the effect of the transport in the solution is eliminated. Therefore, the involvement of bulk transport step on the overall sorption rate can be neglected. Thus, the sorption rate is governed by external diffusion or internal diffusion. Internal diffusion step actually involves intraparticle diffusion and inter crystalline diffusion, or the sorption of the solute on the active sites. Generally, the control by liquid-phase mass transfer/film diffusion is favoured by

- low liquid-phase concentration (small driving force in the liquid)
- high ion-exchange capacity (large driving force in the exchanger)

- small particle size (short mass transfer distances in the bead)
- open structure of the exchanger, e.g., low cross-linking (little obstruction to diffusion in the exchanger)
- Ineffective agitation of the liquid (low contribution of convection to liquid-phase mass transfer).

All of these mechanisms may also occur in parallel, which makes the determination of the dominating step difficult. In order to determine the contribution of the steps involved, numerous kinetic models have been compared to predict the behaviour of the experimental data.

2.2.4.4 Intraparticle diffusion model

This model is represented by the following equation

$$q_t = k_{id}t^{1/2} + I \quad (2.23)$$

where k_{id} is the intraparticle diffusion rate parameter and I (mg/g) is a constant that gives an idea about the thickness of the boundary layer. The values of k_{id} and I can be determined from the slope and the intercept, respectively, of the plot of q_t vs $t^{1/2}$. Intraparticle diffusion process involves the migration of ions into the internal surface of the sorbent particles through pores of different sizes. Boundary layer diffusion and the rate of surface sorption affect the intraparticle diffusion. These factors, along with the intraparticle diffusion rate, are dependent on surface characteristics of the sorbent.

2.2.4.5 Boyd's plot

Boyd expression was used to analyze the sorption kinetic data to determine that whether sorption of Y(III) by beads proceeds via film diffusion or intraparticle diffusion mechanism [128]:

$$F = 1 - \frac{6}{\pi^2} e^{(-Bt)} \quad (2.24)$$

Where F is the fraction of solute sorbed at different time t and Bt is a mathematical function of F .

$$F = \frac{q_t}{q_e} \quad (2.25)$$

Where, q_t and q_e represent the amount sorbed (mg/g) at any time t and at infinite time (in the present study 1400 min.), respectively. Solutions to eq. (2.24), depending on the value of F , are given as equation (2.26) and (2.27).

$$Bt = 2\pi - \frac{\pi^2 F}{3} \quad (2.26)$$

$$Bt = 0.4977 - \ln(1 - F) \quad (2.27)$$

Bt can be calculated using both the equations (2.26) & (2.27). Equation (2.26) is used when F is upto 0.085, when it is higher > 0.85 , Eq. (2.27) is used. The linearity of Bt versus t plot provides useful information to distinguish between the film diffusion and the intraparticle diffusion mechanism of sorption. A straight line passing through the origin is indicative of the sorption processes only governed by intraparticle diffusion mechanisms; otherwise, it is governed by film diffusion [127-129].

Though the sorption of Y(III) by D2EHPA follows the mechanism of ion exchange, when it is encapsulated inside porous beads, adsorption into the pores comes in the picture, Therefore the isotherms is applicable in this case.

2.2.5 Column studies

Column studies were performed on PES/D2EHPA beads. Sorption study of Y(III) in the continuous column operation mode was performed in a glass column ($d=10\text{mm}$, $h=350\text{mm}$) filled with 15g of both the beads separately. Top and bottom of columns were filled with glass wool to prevent the floating of beads. The Y(III) solution at 160 mg/L Y(III) in 0.5M HCl was passed through the columns with the help of peristaltic pump at an optimum flow rate of 1.5mL/min. The solutions coming out from the columns were taken out periodically and analyzed for Y(III) content till its concentration was found to be equal to the inlet feed so

that breakthrough point can be determined. Desorption study of rare earth loaded composite beads were also carried out with either with 50% HCl solutions in the same column.

Batch as well as column tests were carried out in duplicate for reproducibility of the data. The experimental data were within the average error limit of 4.5%.

2.2.6 Experimental design to optimize parameters

The present work also emphasizes on the importance of optimization of various variables i.e. system compositions (polymer, additive, extractants etc.), preparatory parameters and process variables (aqueous media, metal ion, temperature, solid to liquid ratio etc.) to obtain the best suited beads by intelligent design of experiments. Every experimenter has to plan and conduct experiments to obtain enough and relevant data so that he can infer the science behind the observed phenomenon. This can be done by

2.2.6.1 Trial-and-error approach

This method requires making measurements after every experiment so that analysis of observed data will help in deciding what to do next - "Which parameters should be varied and by how much". Many a times such series does not progress much as negative results may discourage or will not allow a selection of parameters which ought to be changed in the next experiment. The data is insufficient to draw any significant conclusions and the main problem still remains unsolved.

2.2.6.2 Design of experiments

A well planned set of experiments, in which all parameters of interest are varied over a specified range, is a much better approach to obtain systematic data. Mathematically, such a set of experiments ought to give desired results. Usually the number of experiments and resources required are large. However, it does not easily lend itself to understanding of science behind the phenomenon. The analysis is not very easy and thus effects of various parameters on the observed data are not readily apparent. In many cases, particularly those in

which some optimization is required, the method does not point to the best settings of parameters due to limitation imparted by range of data [130].

2.2.6.3 Taguchi Method

Dr. Taguchi has envisaged a new method of conducting the design of experiments which are based on well-defined guidelines [131]. This method uses a special set of arrays called orthogonal arrays. These standard arrays stipulate the way of conducting the minimal number of experiments which could give the full information of all the factors that affect the performance parameter. The crux of the orthogonal arrays method lies in choosing the level combinations of the input design variables for each experiment. "Orthogonal Arrays" (OA) provide a set of well balanced (minimum) experiments and Dr. Taguchi's Signal-to-Noise ratios (S/N), which are log functions of desired output, serve as objective functions for optimization, help in data analysis and prediction of optimum results. Taguchi Method treats optimization problems in two categories,

2.2.6.3.1 Static Problems

Generally, a process to be optimized has several control factors which directly decide the target or desired value of the output. The optimization then involves determining the best control factor levels so that the output is at the the target value. Such a problem is called as a "Static Problem".

2.2.6.3.1.1 Batch Process Optimization

There are 3 Signal-to-Noise ratios of common interest for optimization of Static Problems;

(a) Smaller-The-Better:

$$n = -10 \log_{10}[\text{mean of Sum Of Squares}]$$

This is usually the chosen S/N ratio for all undesirable characteristics like “defects” etc. for which the ideal value is zero. Also, when an ideal value is finite and its

maximum or minimum value is defined (like maximum purity is 100%) then the difference between measured data and ideal value is expected to be as small as possible. The generic form of S/N ratio then becomes,

$$n = -10 \log_{10}[\text{mean of sum of squares of \{measured - ideal\}}]$$

(b) Larger-The-Better:

$$n = -10 \log_{10}[\text{mean of sum squares of reciprocal of measured data}]$$

This case has been converted to Smaller-The-Better by taking the reciprocals of measured data and then taking the S/N ratio as in the smaller-the-better case.

(c) Nominal-The-Best:

$$n = -10 \log_{10} \frac{[\text{Square of mean}]}{[\text{Variance}]}$$

This case arises when a specified value is MOST desired, meaning that neither a smaller nor a larger value is desirable.

2.2.6.3.1.2 Dynamic Problems

If the product to be optimized has a signal input that directly decides the output, the optimization involves determining the best control factor levels so that the "input signal / output" ratio is closest to the desired relationship. Such a problem is called as a "Dynamic Problem".

In Taguchi Method, the word "optimization" implies "determination of BEST levels of control factors". In turn, the BEST levels of control factors are those that maximize the Signal-to-Noise ratios. The Signal-to-Noise ratios are log functions of desired output characteristics. The experiments, that are conducted to determine the BEST levels, are based on "Orthogonal Arrays", are balanced with respect to all control factors and yet are minimum in number. This in turn implies that the resources (materials and time) required for the experiments are also minimum. In the present work I aimed for optimizing the recovery and equilibrium sorption of Rare earths values from aqueous phase by developed polymeric beads

and for that larger-the-better type of objective function has been used. The effects of various operational and structural parameters in process of recovering rare earths by polymeric beads have been analyzed by Taguchi method using L18 orthogonal array [132].

2.2.7 Membrane based studies

Application of membrane based rare earths separation was demonstrated by employing hollow fibre membrane contactor (HFM) fig 2.7. HFM contactor (Liqui Cell 2.5×8) used in the present work was procured from Polypore, USA and made up of hydrophobic microporous polypropylene hollow fibres enclosed in a polypropylene shell of 2.5" × 8" dimension (Fig. 2.8) [133-135]. The module contained about 10,000 fibres of 40 % porosity and had an effective surface area of 1.4 m². The complete specification has been given in Table 2.2. To perform experiments in supported liquid membrane mode organic phase was pumped through the lumen side of the HFM contactor at a pressure above 3 psi in recycling mode. To confirm the complete filling of membrane pores with organic extractant, the organic extractant was circulated for ~30 minutes when the extractant started leaching from lumen side to shell side. After complete soaking of the membrane pores, the excess extractant was washed out by water wash through both lumen and shell side. Subsequently the feed solution was passed through lumen side and strip solution was passed through the shell side of the module in all the experiments. The flow rates of feed and strip solution were kept at 100 ml/min with the help of gear pumps (cole-palmer). In the case of metal ion transport by HFM experiments were performed in non-dispersive mode, organic extractant was circulated in recycling mode in shell side in place of stripping phase along with feed phase in lumen side. All the other experimental parameters and procedure were more or less same to SLM mode of operations.

Table.2.2 Details of hollow fibre membrane contactor (Liqui-Cel X50: 2.5x8 Membrane Contactor)

Parameter	Specification
Fibre material	Polypropylene
Number of fibres	9950
Fibre internal diameter (μm)	240
Fibre outer diameter (μm)	300
Fibre wall thickness (μm)	30
Effective pore size (μm)	0.03
Porosity (%)	40
Tortuosity	2.5
Effective fibre length (cm)	15
Effective surface area (m^2)	1.4

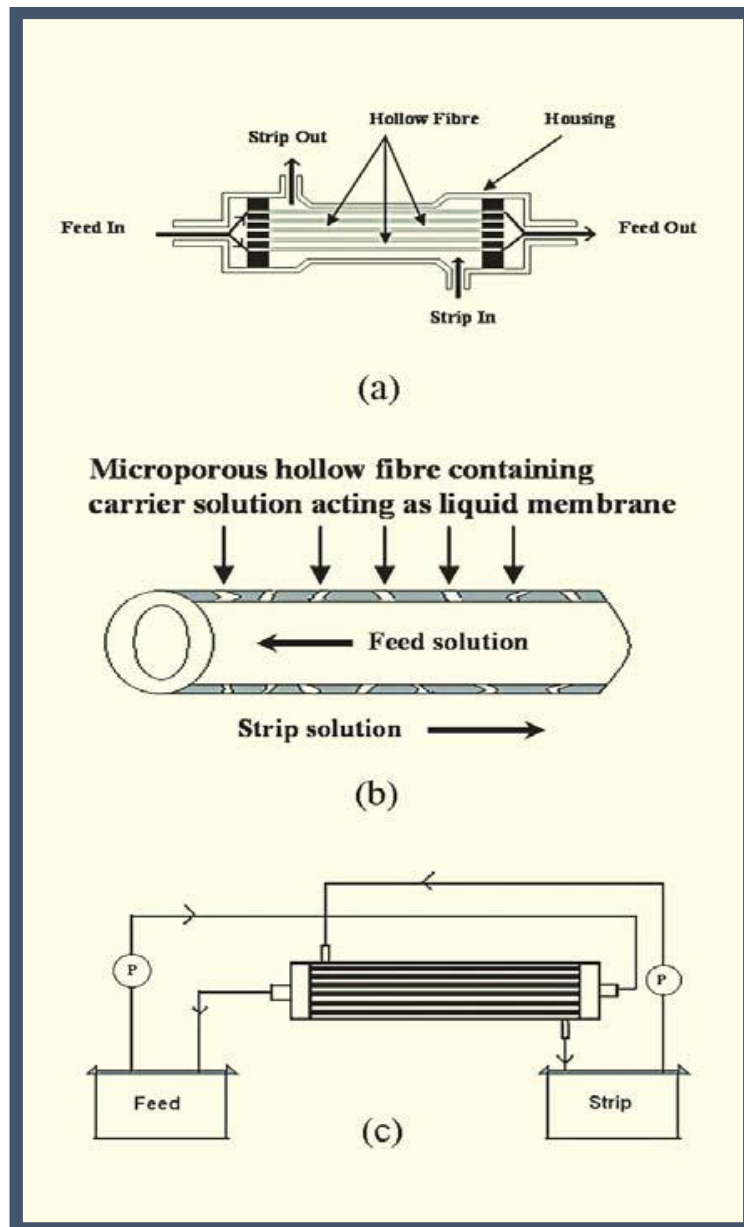


Fig. 2.7 Schematic diagram of Hollow Fibre Membrane contactor employed in the present work



Fig. 2.8 Hollow Fibre Membrane contactor used in the present work

2.3 Analytical Instruments/Techniques

2.3.1 Inductively Coupled Plasma-Atomic Emission Spectroscopy (ICP-AES)

Inductively Coupled Plasma-Atomic Emission Spectrometry (ICP-AES) is an emission spectrophotometric technique, working on the fact that the excited electrons emit energy at a given wavelength as they return to ground state after excitation by high temperature Argon Plasma [136,137]. The fundamental characteristic of this process is that each element emits energy at specific wavelengths peculiar to its atomic character. The energy transfers for electrons when they fall back to ground state is unique to each element as it depends upon the electronic configuration of the orbital. The energy transfer is inversely proportional to the wavelength of the electromagnetic radiation,

$$E = hc/\lambda \quad (2.28)$$

(where h is Planck's constant, c the velocity of light and λ is wavelength), and hence the wavelength of light emitted is also unique. Although each element emits energy at multiple

wavelengths, in the ICP-AES technique it is most common to select a single wavelength (or a very few) for a given element. The intensity of the energy emitted at the chosen wavelength is proportional to the amount (concentration) of that element in the sample being analyzed. Thus, by determining which wavelengths are emitted by a sample and by determining their intensities, the analyst can qualitatively and quantitatively find the elements from the given sample relative to a reference standard. The wavelengths used in the AES measurements ranges from the upper part of the vacuum ultraviolet (160 nm) to the limit of visible light (800 nm). As borosilicate glass absorbs light below 310 nm and oxygen in air absorbs light below 200 nm, optical lenses and prisms are generally fabricated from quartz glass and optical paths are evacuated or filled by a non-absorbing gas such as Argon. In present studies, Ultima2 ICP-AES (Fig. 2.9) has been used for the determination of metal ion concentration in samples.



Fig. 2.9 Inductively Coupled Plasma-Atomic Emission Spectroscopy (ICP-AES) employed for the analysis of rare earth elements

2.3.2 Thermogravimetric analysis (TGA)

TGA is a technique in which the mass of a substance is monitored as a function of temperature or time, as the sample specimen is subjected to a controlled temperature program [138]. It can be used to study any physical or chemical process that causes a material to lose or gain mass. This technique is used to detect evaporation, sublimation, oxidation, thermal degradation and other effects of temperature that cause mass change. The processes which do not result in a change in sample mass are not detected by this technique. TGA can be carried out by using either a heating ramp (dynamic mode) or a constant test temperature (isothermal mode). Provision for changing the test atmosphere by gas switching enables polymer decomposition to be studied under inert, oxidizing, or reducing conditions. The basic instrumental requirements are simple: a precision balance, a programmable furnace, and a recorder and/or a computer instruments, however, tend to be automated and include software for data processing. In addition, provisions are made for surrounding the sample with an air, nitrogen, or an oxygen atmosphere. TG (Mettler Toledo TG/DSC STAR System) was performed by heating the samples up to 1000°C, at a heating rate of 10°C/min, in N₂ atmosphere. TG data were used to determine the weight of the encapsulated extractant per unit weight of PES.

2.3.3 Scanning electron microscopy (SEM)

Modern Morphology and internal structure of the composite beads were examined by SEM (Seron Technology AIS2300C). The internal diameter, distribution of polymer and void volume of various types of beads were evaluated from SEM images [139].

2.3.4 Fourier transforms infra-red spectroscopy (FT-IR)

The FT-IR spectra of the samples have been recorded, using Diamond ATR on IR Affinity, Shimadzu spectrophotometer. The spectra were recorded with a resolution of 4 cm⁻¹, and an average of 60 scans. In the present work FTIR spectra were used as a confirmatory

tool to substantiate the characteristic functional groups of D2EHPA and/or PC88A in the PES bead matrix. The FTIR spectra also substantiated the chemical effect of encapsulation on the functional groups present in the polymeric beads matrix.



Chapter 3

PREPARATION, CHARACTERIZATION AND EVALUATION OF D2EHPA ENCAPSULATED BEADS FOR RARE EARTH SORPTION

3 Preparation, characterization and evaluation of di-2-ethyl hexyl phosphoric acid (D2EHPA) encapsulated beads for rare earth sorption

In recent times, rare earths metals and compounds have garnered great demand due to their increased use in electronics, high tech products, processes as well as simultaneous shortfall in their supply due to various geochemical reasons [140]. However, individual separation and purification of rare earth elements is still one of the most difficult when compared with other elements present in modern periodic table. This is due to their similar chemical properties, trivalent oxidation state and low polarizability. Multistage solvent extraction and ion exchange are the most common techniques reported for the rare earths separation [141-142]. Solvent extraction technique described in section 2 is industrially accepted process for rare earth elemental separation upto a certain purity, for the production of high purity rare earth ion exchange method is being used [143]. Apart from the obvious advantages of these processes there are some associated detriments, in the case of solvent extraction multistage cycles of operation, third phase formation, finite solubility of the extractants in the aqueous phase, need of solvents and modifiers, and their loss through phase disengagement have been reported, whereas for ion exchange process low sorption rate and limitation on the metal ion concentration in the effluent to be treated, hinders the favorable purification and separation of metals [144]. In addition, solvent extraction cannot be applied to dilute metal ion solution, because of the large volume of organic extractant phase would be required [69].

In the last three decades solvent impregnated microcapsules have been widely investigated for the application in various fields such as medicine, agriculture, foods and the chemical industry. The use of solvent impregnated resins/beads in the recovery and

selectivity for the metal ions separation from dilute solutions was initially reported by Warshawsky [91]. Afterwards, various new dimensions have been explored and reported in the field of metal extraction by solvent encapsulating beads. Solvent encapsulating beads not only combine the advantages of solvent extraction and ion exchange but also provide benefits with the simplicity of operating condition with solid phase ion exchange process. The advantages of the use of polymeric beads over other processes extends due to large surface area, minimal use of organic solvents (environment friendly) and absence of phase separation phenomenon. Polyethersulfone (PES), which is an environment friendly matrix material widely used in water purification membrane can be a base matrix for the preparation of solvent impregnated bead [145]. There is scarcity of literature pertaining to the use of extractant (D2EHPA, PC88A and di nonyl phenyl phosphoric acid (DNPPA)) encapsulated PES beads in the separation of rare earths from aqueous phase [128,146]. Considering the extended advantages of composite beads in metal extraction in comparison to liquid-liquid extraction an attempt was made to develop polyethersulfone beads for the extraction of rare earths.

This chapter deals with the studies carried out on the preparation of polyethersulfone beads encapsulating organophosphorus type of extractants by phase inversion method. It elaborates the synthesis, characterization and application of polyethersulfone based organophosphorus extractant encapsulated beads. The chapter comprises two sections, depicting the synthesis of D2EHPA encapsulated beads and its application for rare earths separation from aqueous media. The first section describes the synthesis and Y(III) sorption studies performed with D2EHPA PES beads, while second section deals with optimization of

experimental parameters for Dy(III) sorption by D2EHPA –PES beads by employing Taguchi method.

3.1 **D2EHPA encapsulated beads for rare earths separation**

The present section includes preparation of novel PES beads encapsulating organophosphorus type of extractants D2EHPA by phase inversion method. In the synthesis of the beads, preparatory parameters were optimized to obtain best suited beads which were then characterized for their encapsulation capacity and micro structural investigation. These PES/D2EHPA beads were subjected for rare earths separation from aqueous medium under various experimental conditions. Subsequently an attempt has been made to modify the internal microstructure and surface morphology of PES beads by introducing various types of additives, namely, polyvinyl alcohol (PVA), multiwall carbon nanotube (MWCNT), lithium chloride (LiCl) and polyethelene glycol (PEG). The developed composite beads have been characterized by techniques like thermogravimetry (TG), scanning electron microscopy (SEM) and Fourier Transform Infra-Red (FTIR) spectroscopy. All the types of composite beads have been evaluated for the sorption of rare earths under comparable experimental conditions. The feasibility of recovering rare earths from aqueous chloride solution has also been investigated in continuous column operation mode, taking Y(III) as the representative of rare earth. Additionally, stability and reusability of MWCNT embedded composite beads have also been evaluated and reported in this section. The present work indicates the possibility of use of diluent free extractant impregnated inside the beads has been shown, which is otherwise not practiced in normal solvent extraction process.

3.1.1 Synthesis of PES/D2EHPA beads

An experimental set up shown in Fig 2.6 which is also similar to Gong's approach [116] was prepared for synthesis of extractant encapsulated polymeric beads. The method of PES beads preparation is described in section 2.2.1 of chapter 2 in detail. Five types of polymeric composite beads namely PES/PVA (as blank), PES/PVA/D2EHPA (PES-I), PES/PVA/MWCNT/D2EHPA (PES-II), PES/PEG/D2EHPA (PES-III), PES/LiCl/D2EHPA (PES-IV) with different additives were prepared by the above mentioned method.

The concentration of the constituents was optimized in such a way that the resultant composite beads resulted in spherical shape. The concentrations of additives in different polymeric beads were 1.5, 0.25, 1, and 1 % w/w for PVA, MWCNT, PEG and LiCl respectively.

3.1.2 Characterization

Morphology and internal structure of the composite beads were examined by SEM (Seron Technology AIS2300C). The internal diameter, distribution of polymer and void volume of various types of beads were evaluated from SEM images. TG (Mettler Toledo TG/DSC STAR System) was performed by heating the samples upto 1000°C, at a heating rate of 10°C/min, in N₂ atmosphere. TG data were used to determine the weight of the encapsulated extractant per unit weight of PES. Further the beads were characterized by FTIR (Shimadzu IR Affinity-1) as a confirmatory tool to substantiate the characteristic functional groups of D2EHPA in the PES bead matrix.

3.1.3 Metal ion sorption studies

Sorption (uptake) study of Y(III) or other rare earths by polymeric beads was investigated in batch as well as column mode. The procedural details of the experiments are described in

section 2.2.2 of chapter 2. The equilibrium adsorption or sorption capacity of the polymeric beads was evaluated in terms of (q_e) in mg/g and weight distribution coefficient, K_d were also evaluated using equations described in section 2.2.2. Sorption isotherm, kinetics of metal ion sorption by polymeric beads along with column studies were also performed as described in section and subsections of 2.2 of chapter 2.

3.1.4 Morphology: Role of additives

The morphology of the PES bead is an important physical characteristic which determines its usability and stability for metal ion separation from aqueous media. For metal sorption, an extractant impregnated polymeric beads should have a hollow cavity at its core, surrounded by a porous polymeric matrix structure. The central hollow core enables it to encapsulate organic solvent and the pores on the matrix provide channels for the interfacial contact of aqueous and organic phases essential for metal ion transfer. Ideally, a radial variation of pore size distribution from periphery towards the center of the bead is desired. The inner portion of the bead matrix should have high porosity with relatively bigger pore size for better mass transfer of aqueous and organic phases, while the outermost part of the bead should have a thin layer of nanoporous but relatively dense matrix, which prevents the loss of organic extractants. Fig.3.1 shows the optical images of PES/D2EHPA, PES/PVA/D2EHPA and PES/PVA/MWCNT/ D2EHPA beads respectively. Fig. 3.2(a–f) illustrates the cross sectional images of the polymeric composite beads with different additives and it is evident that the additives play vital roles in changing the internal microstructure of the bead in terms of porosity and pore size distribution which in turn affect their sorption capacity considerably.



Fig. 3.1 Optical images of PES/D2EHPA, PES/PVA/D2EHPA and PES/PVA/MWCNT/D2EHPA

Fig. 3.2 (a) shows the cross sectional image of the blank PES bead without any additive and extractant, which represent a relatively less porous structure with thick outer shell. Such kind of structure is not desirable for efficient extraction of metal ions. As soon as D2EHPA is included in the bead during preparation, the internal microstructure changes considerably (Fig. 3.2b). However, the distribution of polymer phase is very uneven and the porosity is very less at the periphery of the bead. When PVA is doped with PES along with D2EHPA, relatively thinner outer layer with finer pores along with evenly distributed porous polymer matrix is obtained (Fig. 3.2c). Noticeably, the central cavity is quite big and spherical. The addition of PEG and LiCl with PES result in reduced porosity and thick outer shell as can be observed from Fig 3.2 (d) and (e). On the other hand, polymeric composite beads embedded with PVA and MWCNT both (Fig.3.2f) has more porosity in comparison to PVA alone (Fig. 3.2 c). The above observations may be attributed to the distribution of the polymer and the additives during the phase inversion process which results in the formation of solid beads from liquid (polymer + extractant) mixture.

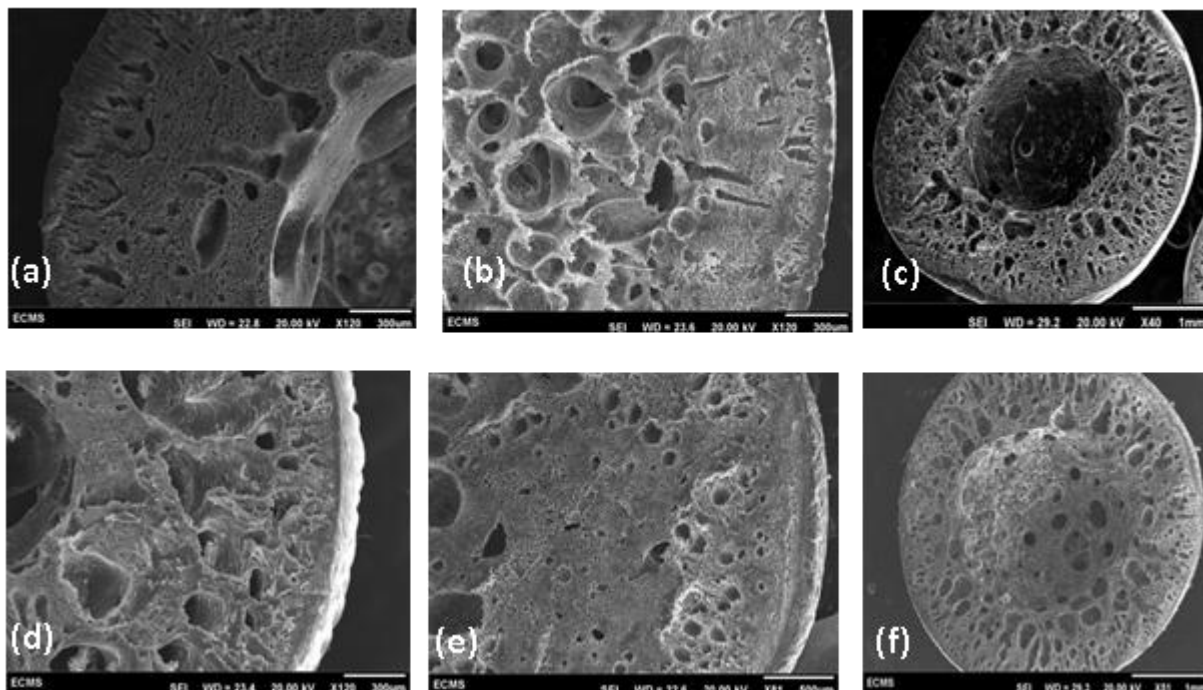


Fig.3.2 SEM images of cross-section of PES bead (a)PES blank, (b)PES/D2EHPA, (c)PES/PVA/D2EHPA, (d)PES/PEG/D2EHPA, (e)PES/LiCl/D2EHPA, (f)PES/PVA/MWCNT/D2EHPA.

During the solidification of polymeric mixture drop to bead, additive's solubility in the antisolvent (water) determines the porosity and overall distribution of polymer inside the bead [104,146]. Morphological evaluation of the beads by SEM revealed that the PES-I and PES-II beads have the microstructures close to the desired ones.

3.1.5 Thermogravimetric Studies

PES/D2EHPA beads with different extractant to polymer solution ratio were prepared. Thermo gravimetric analysis of these polymeric beads was carried out to evaluate the percentage of extractant, PES, water and NMP content in the composite material. TGA (Fig. 3.3) representing change in the weight of sample (beads) with increase in temperature showed mainly three segments of 80-160°C, 230-260°C and 460-560°C. First segment represents evaporation of water and NMP in the range of 80 to 160°C, second zone of weight

loss depicts the disintegration of D2EHPA and 460 to 560°C part of the profile shows the weight loss due to dissociation of PES and disintegrated parts of D2EHPA. Evaluation of thermograms revealed that increase in extractant to polymer solution ratio from 1:15 to 1:4 lead to increase in D2EHPA content from 9% to 25.5% in the beads, whereas polymer content in the beads was in the range of 10 to 16%.

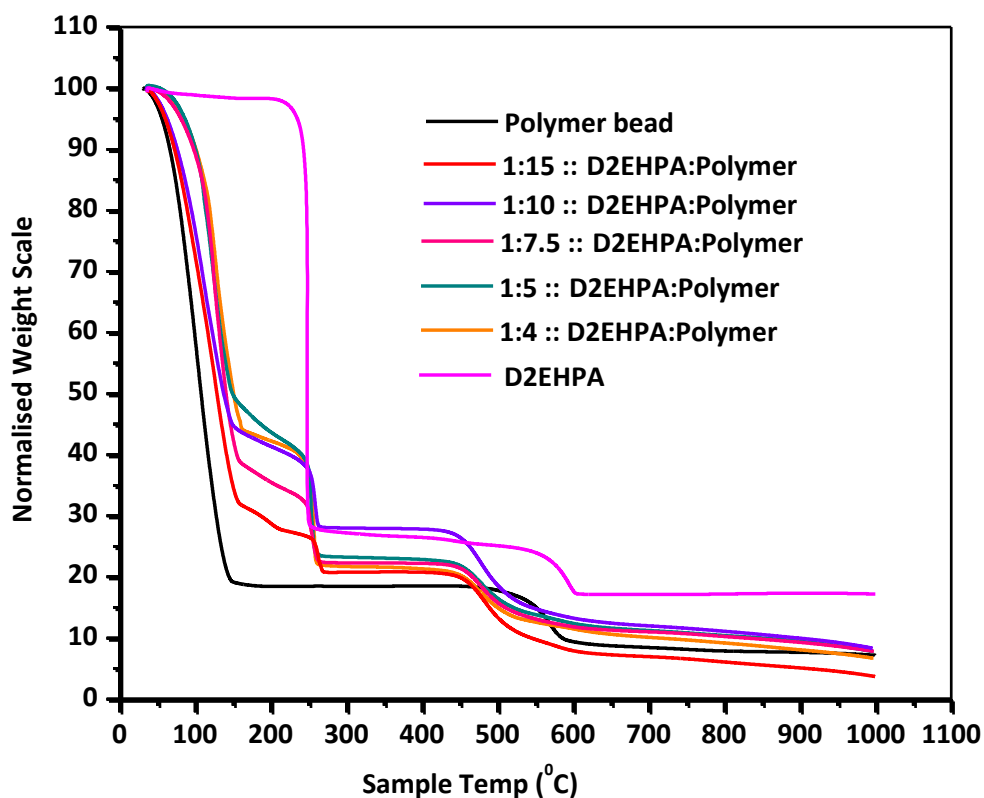


Fig. 3.3 TGA of blank polymer bead, PES/D2EHPA beads having different extractant to polymer ratios of 1:4, 1:5, 1:7.5, 1:10, 1:15 and D2EHPA (3M)

These results were in good agreement with the encapsulated amount of D2EHPA (7-25%) taken during preparation of beads. Comparison of TGA profiles of D2EHPA encapsulating beads with the profiles of D2EHPA and PES showed no shift in the mass loss vs. temperature profile of individual compound eliminating any possibility of chemical interaction among the main constituents of the extractant encapsulating beads. Subsequently

in another study involving thermogravimetry, was performed to see the role additive in encapsulation capacity. Fig. 3.4 shows the weight loss profiles of blank PES bead (line a), PES/D2EHPA/PVA bead (line b) along with PES/D2EHPA/PVA/MWCNT beads and 3M D2EHPA liquid phase (line c and d respectively) as references while heated in nitrogen atmosphere.

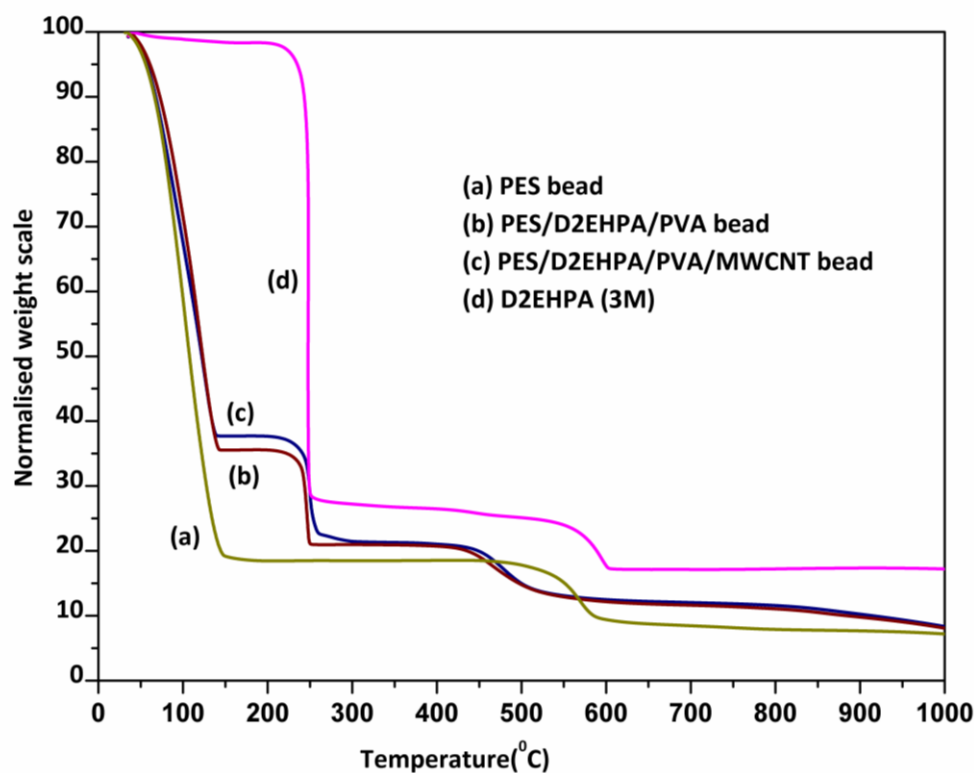


Fig. 3.4 TG profiles of (a) PES bead (b) PES/D2EHPA/PVA (c) PES/D2EHPA/PVA/MWCNT bead and (d) D2EHPA (3M)

In the case of 3M D2EHPA (line (d) in Fig.3.4), initial evaporation takes place around 230°C with a sharp loss of weight of about 70% and once again loses around 12% near 550°C. The blank PES bead loses 80% of its weight in the temperature range of 60-150°C due to evaporation of NMP and water in it (line (a) Fig. 3.4). It further loses 10% at around 500°C due to dissociation of PES followed by evaporation of volatiles. The weight loss profiles of

PES/D2EHPA/PVA and PES/D2EHPA/PVA/MWCNT beads can be divided into four zones (line (b) and (c) in Fig.3.4). The first zone in the temperature range of 60-150°C corresponds to the evaporation of NMP and water inside the polymeric beads (~60%). The second zone shows a loss of 13% weight for PES/D2EHPA/PVA beads and 16% for PES/D2EHPA/PVA/MWCNT beads which shows the evaporation/dissociation of D2EHPA in the temperature range of 230-260°C. The third zone manifests the dissociation of D2EHPA and PES (460-560°C), with a weight loss of around 12-15%. Comparing the above four TG profiles it can be concluded that the possibility of chemical interaction among the main constituents of the polymeric beads i.e. D2EHPA, PES, PVA and MWCNT are negligible. Similar observations were reported by Ozcan et al. for Cyanex 923 encapsulated polysulfonic based microcapsules [146]. Comparison of TG profiles of PES/D2EHPA/PVA and PES/D2EHPA/PVA/MWCNT beads revealed that the later beads have higher D2EHPA encapsulation capacity in comparison to the former.

3.1.6 Functional group analysis

The FTIR spectra of the pure D2EHPA, blank PES/PVA composite bead and PES-II bead are depicted in Fig. 3.5(a, b & c). The FTIR spectrum for D2EHPA in Fig. 3.6(a) shows a doublet at 1460 and 1380 cm^{-1} due to the C–H deformation vibrations. The peaks at the interval 2800–3000 cm^{-1} correspond to the presence of 2-ethylhexyl alkyl group. The most intense band is the P–O stretching, together with P–O–C between 1050 and 970 cm^{-1} . Other important peaks are P–O stretching at 1250–1210 cm^{-1} and a low intense band around 1680 cm^{-1} confirming the presence of P–OH [147].

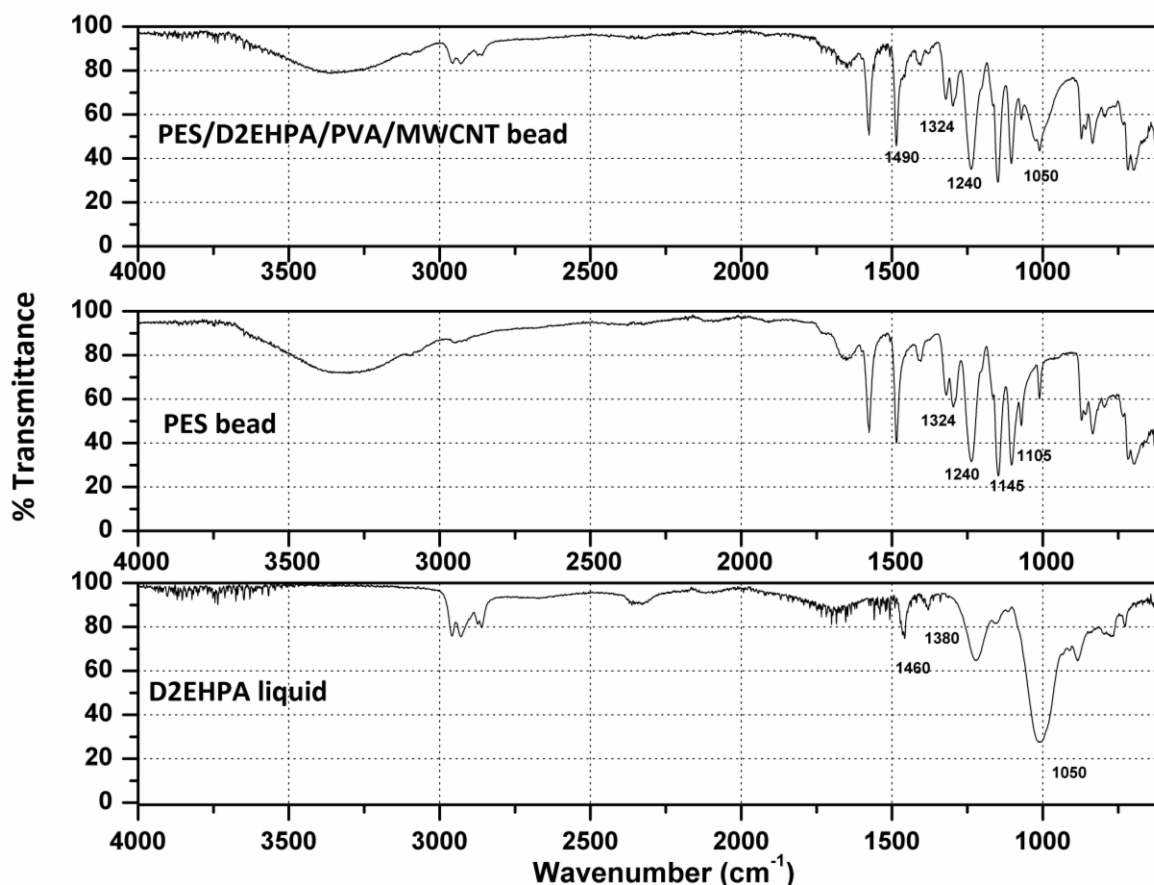


Fig. 3.5 FTIR spectra of (a) D2EHPA, (b) Blank PES bead (c) PES/D2EHPA/PVA/ MWCNT bead

In Fig. 3.5(b), three peaks between 1600 cm^{-1} to 1400 cm^{-1} are attributed to representative aromatic skeletal vibration of PES. The C-O-C stretching peaks are located between 1324 cm^{-1} to 1240 cm^{-1} . The S=O stretching peaks are present at 1145 and 1105 cm^{-1} . In Fig. 3.6(c), the peaks at $1250\text{--}1210\text{ cm}^{-1}$, which correspond to P=O group and low intense band around 1680 cm^{-1} , along with characteristic peaks of PES demonstrated that D2EHPA exist in the bead independently within the polymer matrix without any chemical interaction with PES.

3.1.7 Effect of additives in polymeric beads on Y(III) sorption

Role of different additives on the extent of sorption of Y(III) from aqueous chloride medium with PES/D2EHPA composite beads embedded with additives like PEG, PVA, LiCl and MWCNT under comparable experimental conditions was investigated. The results are shown in Fig. 3.6. The sorption of Y(III) with additive embedded composites followed the order: PES-II > PES I > PES/D2EHPA > PES III > PES IV. The addition of PEG and LiCl led to decrease in the sorption capacity due to the formation of thick layer around the encapsulated D2EHPA (Fig. 3.2d and 3.2e), which prevented the exchange of yttrium ions from aqueous solution with the hydrogen ions of the D2EHPA molecules. On the other hand, PES/PVA/D2EHPA beads resulted in an enhanced sorption of Y(III) due to its uniform pore distribution around the periphery. Interestingly MWCNT embedded composite beads resulted in significantly enhanced sorption of Y(III) compared to all other beads in the present work. The observed enhancement in sorption may presumably be due to the following two factors. Firstly, during the phase inversion of polymeric solution to polymeric beads, MWCNT acts as nucleus for the reformation of polyethersulfone inside the bead which enhances uniformity in the pore distribution with better porosity. Secondly, MWCNTs are functionalized by D2EHPA molecules on its surface, which in turn get distributed near periphery of the composite beads there by allowing the sorption of Y(III) simultaneously by ion exchange as well as adsorption. The better distribution of D2EHPA in the PES/PVA/MWCNT bead along with favorable pore size distribution resulted in the enhancement in Y(III) sorption. Not only the additive enhances or suppress the equilibrium sorption amount of Y(III) but also influences the rate of sorption.

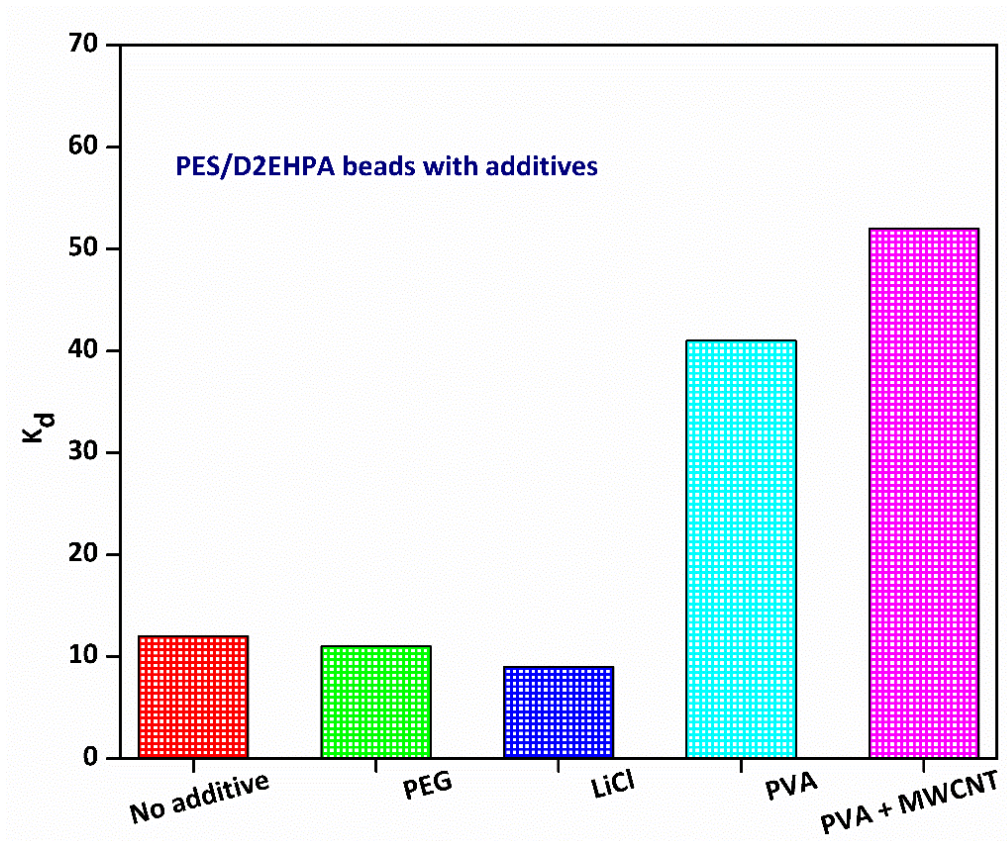


Fig. 3.6 Effect of additives in polymeric composite beads on weight distribution ratio of Y(III) by PES/D2EHPA beads. (Weight of wet PES beads: 10g, 100 mL of 0.5 N HCl solution, Y(III) concentration: 1.0 g/L stirring speed: 250rpm, temperature: 30°C, contact time: 8 hours)

To evaluate the kinetics, three types of beads namely PES/D2EHPA, PES-I and PES-II beads were contacted with 0.5M HCl solution containing 1000 mg/L Y(III) in the investigation. Fig. 3.7 shows change in Y(III) concentration in aqueous phase with time. It is evident from the results that in the case of PES/D2EHPA beads sorption of Y(III) has not attained the equilibrium even after 10 hours of contact time but for PES-I and PES-II, equilibrium was attained after 8 hours of contact with increased capacity.

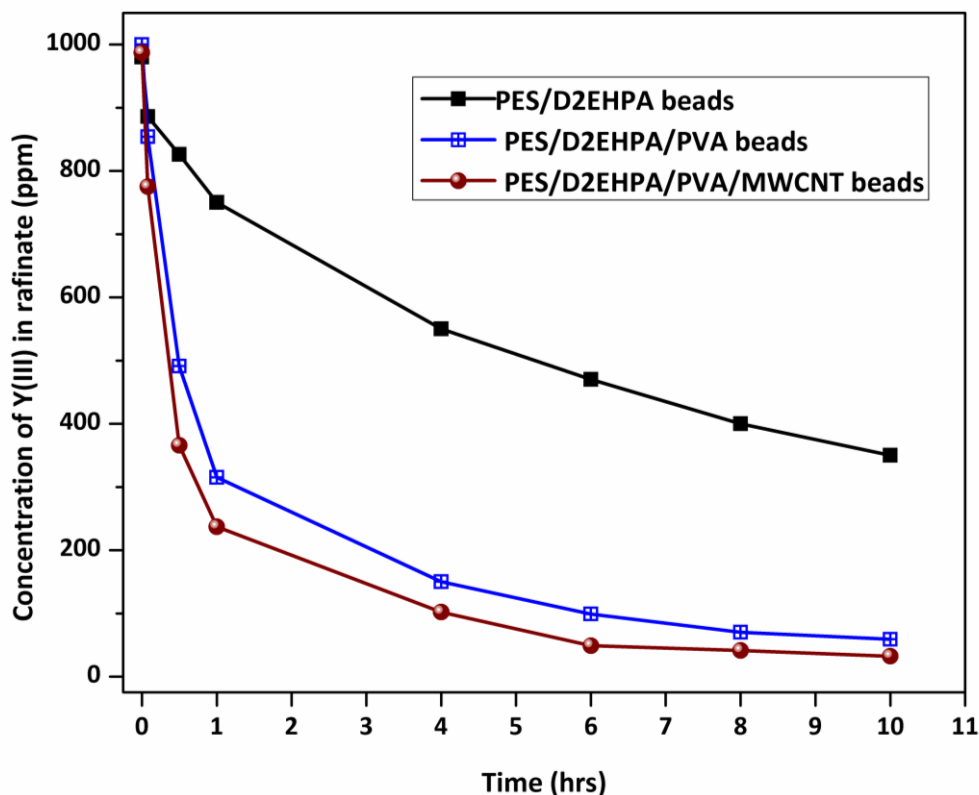


Fig. 3.7 Effect of additives in polymeric composite beads on the rate of sorption of Y(III) from aqueous media by PES/D2EHPA beads. (Weight of wet PES beads: 10g, 100 mL of 0.5 N HCl solution, Y(III) concentration: 1.0 g/L stirring speed: 250rpm, temperature: 30°C, contact time: 8 hours)

3.1.8 Effect of Yttrium ion concentration

Based on the studies on the role of additives for Y(III) sorption from chloride medium, two types of composite beads, namely, PES-I and PES-II were selected for further study under different experimental conditions. The variation of K_d as a function of Y(III) concentration in the aqueous solution at fixed L/S ratio (10/1) and acidity (0.5M HCl) is shown in Fig. 3.8. It can be observed that K_d decreased with increase in Y(III) ion concentration in aqueous solution for both the types of beads. However, MWCNT embedded composite beads was found to be superior for the recovery of Y(III) from aqueous solution.

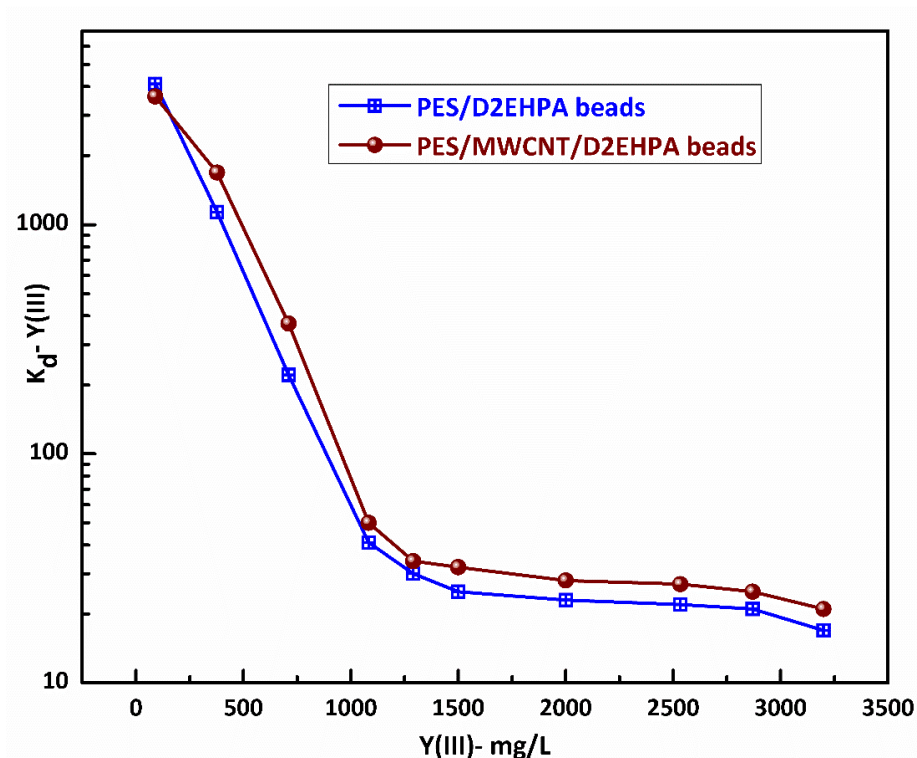


Fig.3.8 Effect of Y(III) concentration in feed solution on sorption of Y(III) by PES beads (a)PES-I (b) PES-II beads. (Weight of wet PES beads: 10g, 100 mL of 0.5 N HCl solution, stirring speed: 250rpm, temperature: 30°C, contact time: 8 hours)

The increase in K_d may possibly due to decrease in effective free concentration of D2EHPA inside the bead. Similar observations on the effect of metal ion concentration have been reported by Outkesh et al [148].

3.1.9 Effect of aqueous phase acidity

Effect of aqueous solution acidity on the sorption of Y(III) was investigated for different concentration of yttrium ion in the aqueous solution ranging from 150 to 1000 mg/L at a fixed L/S ratio (10/1) and temperature (30°C). Sorption of Y(III) decreased with increase in acid concentration for all the concentrations of Y(III) ion in the solution (Fig. 3.9).

However, the decrease in K_d at any particular acidity followed a proportional increase with increase in Y(III) concentration in the aqueous solution.

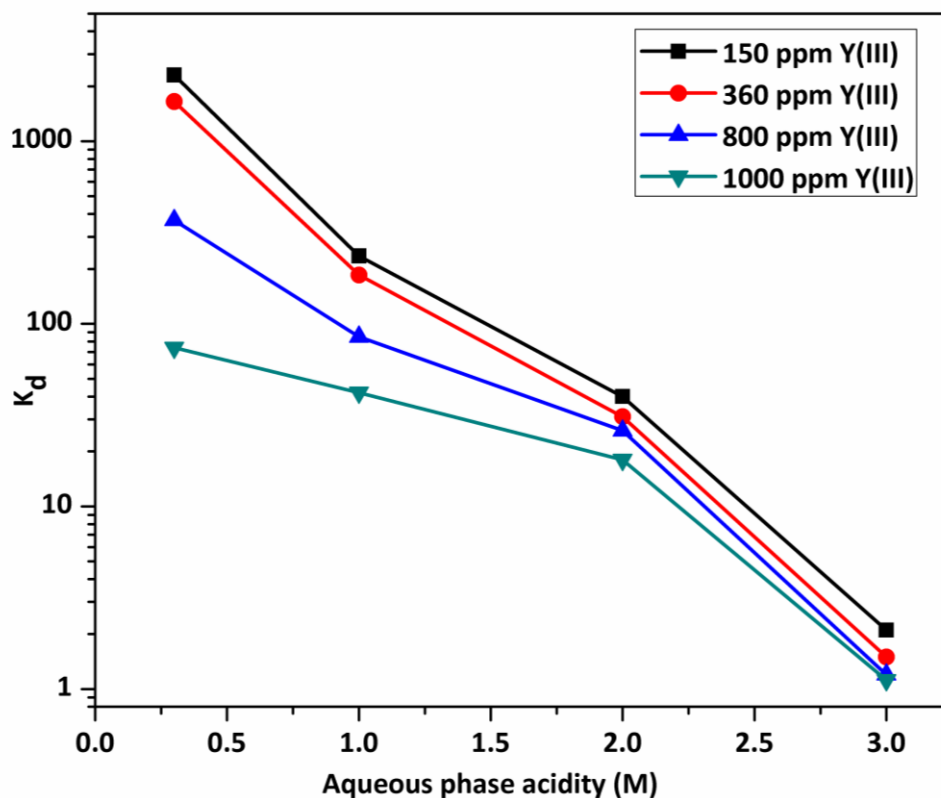


Fig. 3.9 Effect of aqueous phase acidity and Y(III) concentration in aqueous phase on Y(III) sorption by PES-II beads

The decrease in K_d with increase in acidity is exactly similar to the phenomenon observed in solvent extraction technique for the extraction of metal ion with acidic extractant like D2EHPA due to cation exchange mechanism, where hydrogen ion of D2EHPA gets replaced by metal ion of interest [149]. Similar explanation can be offered for this sorption behavior of Y(III) also, as D2EHPA molecule sit inside the composite beads, where the exchange of Y(III) with the hydrogen ion of D2EHPA takes place through the pores of the outer layer of the beads. Further, with increase in Y(III) ion concentration in aqueous

solution, the sorption decreases due to decrease in effective concentration of D2EHPA in the composite beads as a result of its complex formation with Y(III) ion.

3.1.10 Influence of temperature

After optimizing the concentration of Y(III) and aqueous acid concentration, the effect of temperature on sorption of Y(III) for both the composite beads (PES-I and PES-II) was studied under comparable experimental condition of S/L ratio 1:10, acidity 0.5M HCl and concentration of Y(III) 1000 mg/L in the aqueous solution. Fig.3.10 illustrates the variation of K_d with temperature for both the beads. K_d value of Y(III) increased from 41 to 85 with increase in temperature from 30 to 45°C, and then decreased from 85 to 43 with increase in temperature in the range of 45 to 65°C in the case of PES-I beads. Variation in K_d of Y(III) followed the similar trend with PES-II beads too. The trend of increase followed by decrease in K_d values irrespective of composition of composite beads clearly suggests that the two competitive processes are taking place simultaneously over the range of temperature studied. Firstly, the increase in K_d with increase in temperature upto 45°C may possibly be due to enhanced mass transfer as a result of decrease in viscosity and density of the liquid phases. Secondly, the decrease in K_d value in the range of 45-65°C with increase in temperature can be ascribed to the exothermic nature of the sorption reaction, whose effect is pronounced at higher temperature range. In the present case effect of temperature beyond 65°C was not investigated for sorption as the glass transition temperature of PVA is approximately 75°C at which chances of distortion in the morphology of composites beads are likely to be very high.

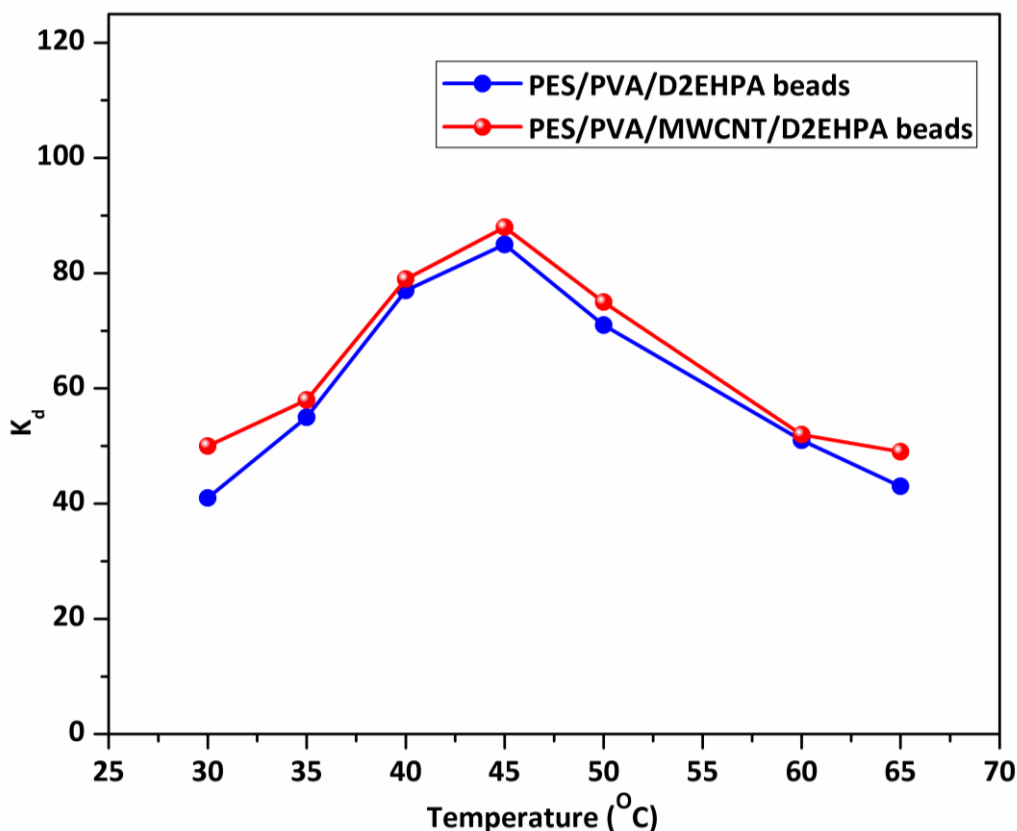
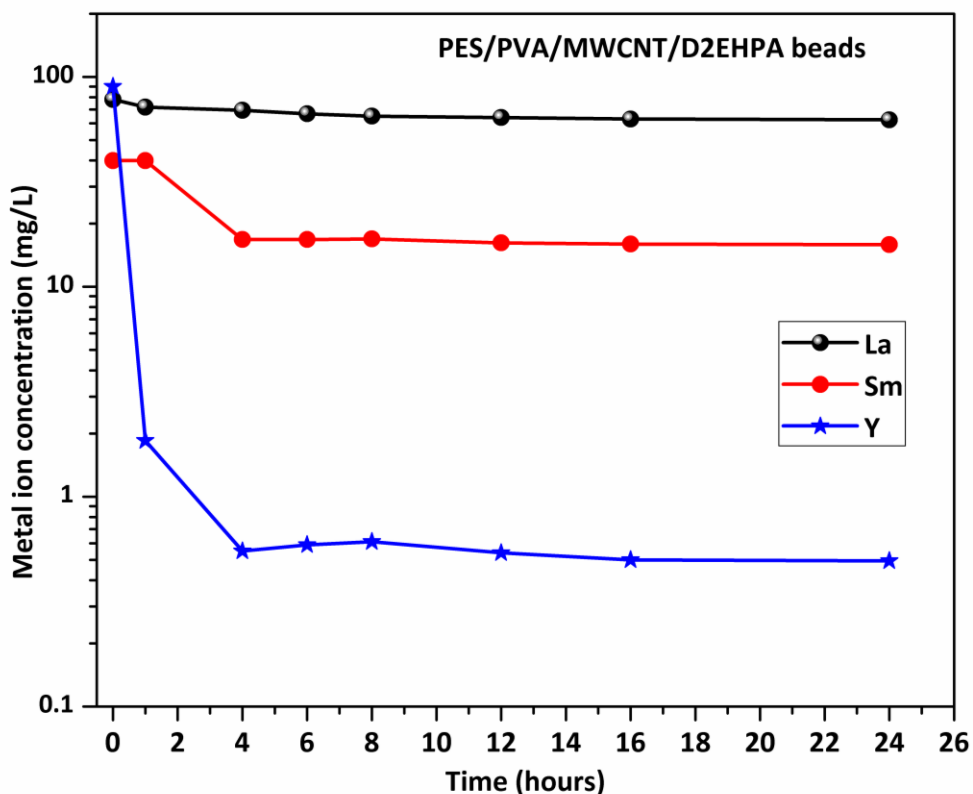


Fig. 3.10 Plots of Y(III) sorption as a function of temperature by (a)PES-I beads (b)PES-II beads. (weight of wet PES beads: 10g, aqueous phase of 0.5N HCl: 100 mL, Y(III) concentration: 2.5 g/L, stirring speed: 250rpm, contact time: 8 hours)

Further, the leaching of organic D2EHPA was noticed at higher temperature affecting the sorption ability of the composite beads.

3.1.11 Sorption of Y(III) in the presence of other rare earth ions

The effect of presence of chemically similar rare earth ions such as La(III) and Sm(III) on the sorption of Y(III) was investigated with PES-II composite beads by contacting the known amount beads with 0.5M HCl solution containing 100 mg/L of each of the three metal ions at an appropriate S/L ratio and temperature.



The

Fig. 3.11 Effect of competing rare earth ions (La, Sm) on Y(III) sorption by PES-II beads.

Experimental findings are presented in Fig.3.11 where metal ion concentrations remained in aqueous solution after equilibrium is plotted as a function of equilibration time. Recovery of rare earth ions followed the order $Y(III) > Sm(III) > La(III)$. This clearly demonstrated the ability of novel MWCNT embedded composite beads for efficient separation of Y(III) from La(III) and Sm(III). Additionally, sorption of Y(III) did not get affected by the presence of chemically similar rare earth ions in the aqueous solution.

3.1.12 Sorption isotherms

As the adsorption into the pores of the beads has vital role in Y(III) sorption additional experiments were carried out to understand the mechanism of sorption phenomenon of Y(III) by composite beads while analyzing the experimental data by Langmuir as well as Freundlich

isotherms [124,125]. Accordingly, in order to fit the sorption data in both the models, the sorption study

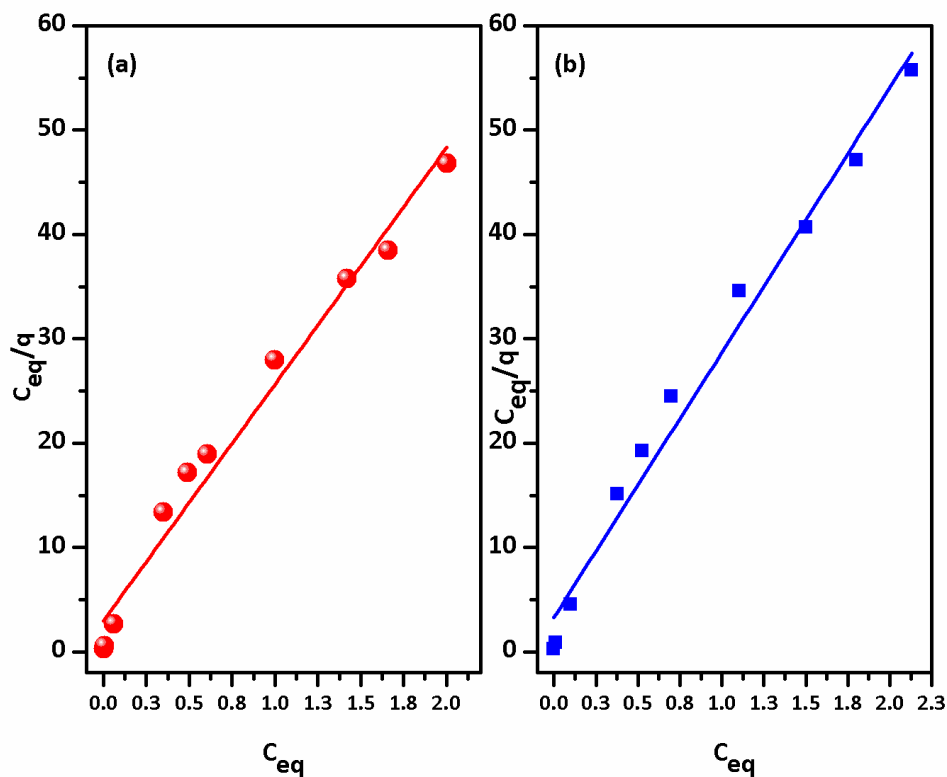


Fig. 3.12 Langmuir plot for the sorption of Y(III) on the PES-I (a) and PES-II(b) beads, aqueous phase: 0.5 M HCl, temperature: 28°C.

of Y(III) was performed from an aqueous solution containing Y(III) in the range of 0.1 to 3 g/L at 0.5M HCl concentration. The linear graphs depicted in Fig. 3.12(a) and (b) suggested that sorption data fit the Langmuir isotherm very well for PES-I and PES-II composite beads respectively. Table 3.1 depicts the Langmuir constant q_{max} and b which were obtained by fitting the experimental data in the equation 3. In the present case, Langmuir constant (b) for both the composite beads were evaluated to be 0.007, which clearly indicated that the sorption of Y(III) by PES-I and PES –II beads is a favorable process.

Table-3.1 Parameters of Langmuir isotherm model for the sorption of Y(III) by PES/D2EHPA beads, Aqueous phase: 0.5N HCl, Temperature: 28°C.				
Polymer bead	b (L mg ⁻¹)	q_{\max} (mg g ⁻¹)	R^2	q_{\max} (Exp)
PES/D2EHPA/PVA	0.007± 0.001	39.41 ± 0.23	0.98	39.28 ± 1.02
PES/D2EHPA/PVA/CNT	0.007± 0.001	44.09 ± 0.31	0.97	43.17 ± 1.27

The calculated values of q_{\max} of 39.41 ± 0.23 mg/g and 44.09 ± 0.31 mg/g for the PES-I and PES-II composite beads respectively and were found to be in good agreement with the experimental values of 39.28 ± 1.02 mg/g and 43.17 ± 1.31 mg/g. Y(III) from chloride medium is primarily a sorption phenomenon i.e the presence of monolayer chemisorptions. Fig.3.13 represents the fit of sorption data to Freundlich isotherm ($\log(x)$ vs. $\log C_{eq}$) for both the type of D2EHPA containing composite beads. The deviation from linearity of the data points indicates that the Freundlich model may not validate the presence of multilayer sorption of Y(III) onto the D2EHPA impregnated polymeric composite beads. The plots deviation from the linearity is represented as the values of correlation coefficient (R^2) were 0.940 and 0.910 for PES-I and PES-II beads respectively.

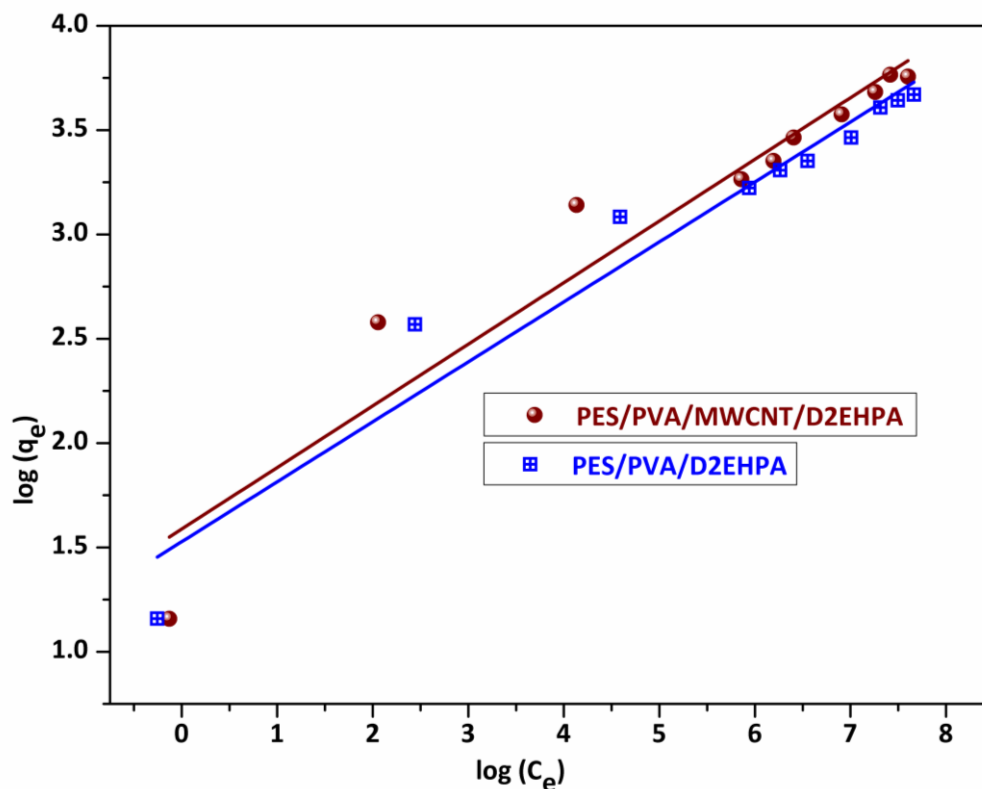


Fig. 3.13 Freundlich plot for the sorption of Y(III) on the D2EHPA containing PES beads, aqueous phase: 0.5 M HCl, temperature: 28°C.

3.1.13 Sorption kinetics

It may be noted that the evaluation of the kinetics of the sorption process plays an important role for deciding the scaling of process and designing the equipments on industrial scale level. Further it has been observed that the mechanism of the sorption / extraction of metal ion with the composite beads impregnated with organic extractant proceeds via three steps i.e. (i) diffusion of the metal ion to the surface of the beads (ii) intrabead diffusion and (iii) finally complexation of the metal ion with the extractant molecule. Therefore, the sorption isotherms and kinetic models applicable to sorption on sorbent particles, pure as well as composites, can be applied to these beads also. Accordingly, to examine the kinetic phenomenon of sorption of Y(III) with D2EHPA impregnated polymeric beads, experiments

were performed in batch mode with the aqueous solution containing different concentrations of yttrium metal ion at a particular aqueous acidity. Once the sorption data were obtained, they were analyzed utilizing different kinetic models namely pseudo first-order model, pseudo-second-order model, intra-particle diffusion model, and Boyd's expression. Table 2 presents the summary of evaluated parameters obtained by various models; it also includes the respective correlation coefficient values.

Table 3.2 Pseudo-First-Order, Pseudo-Second-Order, and Intraparticle Diffusion Constants and values of R^2 for the sorption of Yttrium

Kinetic Model	Parameters	C₀=90ppm	C₀=400ppm	C₀=750ppm	C₀=1200ppm
Pseudo-first-order	K₁(min⁻¹)	0.006	0.004	0.003	0.003
	q_e (mg g⁻¹)	1.10	7.58	13.91	11.26
	R²	0.8756	0.9970	0.9783	0.9824
Pseudo-second-order	K₂(g mg⁻¹min⁻¹)	0.0338	0.0018	0.0009	0.0011
	q_e (mg g⁻¹)	3.11	14.261	25.04	26.81
	R²	0.9999	0.99802	0.9982	0.99826
Intraparticle diffusion	K_{id}(min⁻¹)	0.0026	0.1113	0.19432	0.185
	I (μmol g⁻¹)	3.001	10.04	17.51	18.86
	R²	0.59	0.79	0.85	0.84

The description of the models and their application to define the sorption kinetics of Y(III) in the present investigation is discussed below.

3.1.13.1 Pseudo-first order model

Lagergren proposed the pseudo-first order model for describing the adsorption process of solid-liquid systems and its linear form is formulated below [150]:

$$\frac{dq}{dt} = k_1(q_e - q_t) \quad (3.1)$$

Where q_e and q_t are the amounts of yttrium adsorbed by polymeric beads in (mg/g), at equilibrium and at time t respectively. k_1 is the first order rate constant (min^{-1}).

The integrated form of eqn. 3.1 can be written as

$$\log(q_e - q_t) = \log q_e - \frac{k_1 \times t}{2.303} \quad (3.2)$$

The linear pseudo-first-order plot of $\log(q_e - q_t)$ versus t , is shown in Fig. 3.14. It has correlation coefficient (R^2) values in the range of 0.8756 to 0.9971 (Table 3.2), which indicates that the rate of sorption of yttrium ion by polymeric beads cannot be predicted by pseudo-first-order kinetic model for the entire studied range of the initial yttrium ion concentration.

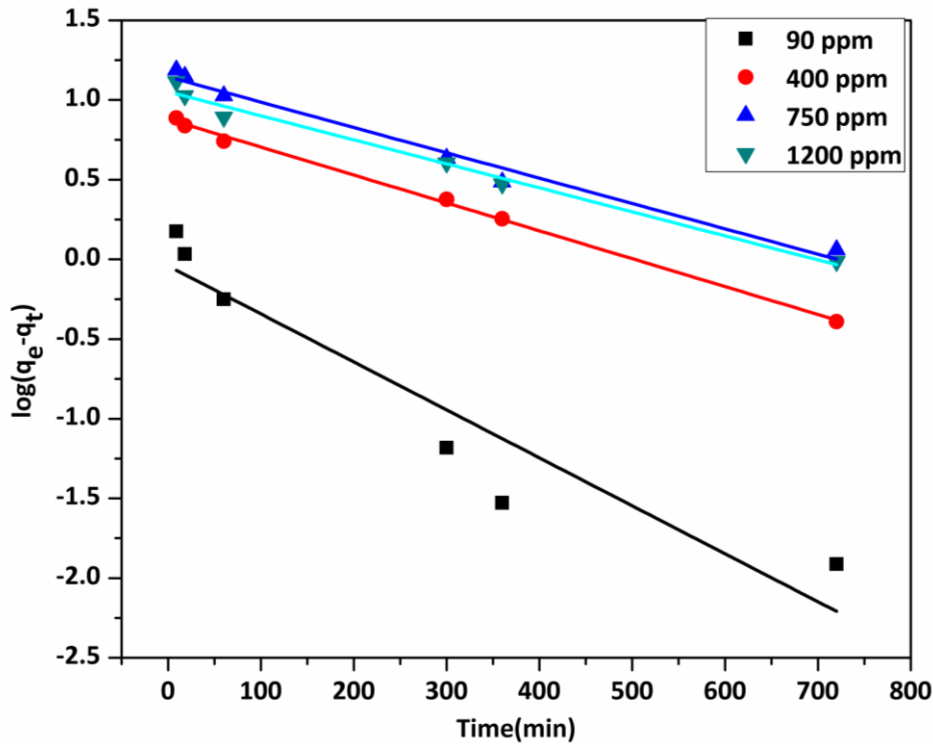


Fig. 3.14 Pseudo-first order plot for yttrium ion sorption by polymeric beads, at four different initial concentration of Y(III)

However, the pseudo-first order model was useful to describe the initial sorption periods particularly when the aqueous feed concentrations were 400, 750 and 1200 ppm Y(III) respectively. The deviation observed could be attributed to the sharp fall in gradient concentration as a consequence of a high initial yttrium sorption. The values for equilibrium sorption capacity calculated by the model were quite different from those values obtained by experiments.

3.1.13.2 Pseudo-second-order model

The pseudo-second order equation has been widely used due to the better fit of experimental data for the entire sorption period of diverse variety of systems [150]. The kinetics model can be expressed as following equation

$$\frac{dq}{dt} = k_2(q_e - q_t)^2 \quad (3.3)$$

Where q_e and q_t are the amounts of yttrium adsorbed by PVA+CNT doped polymeric composite beads in (mg/g), at equilibrium and at time t respectively, k_2 is the second-order rate constant ($\text{g mg}^{-1}\text{min}^{-1}$). Integrating and assuming boundary conditions, the rearranged linear form of the pseudo-second order model is obtained

$$\frac{t}{q_t} = \frac{1}{q_e^2 \times k_2} + \frac{t}{q_e} \quad (3.4)$$

The plot of t/q_t versus t gives straight lines, as represented in Fig 3.15. The values of R^2 for this model are 0.9999, 0.9980, 0.9982 and 0.9982 for 90, 400, 750 and 1200 mg/L of yttrium in aqueous feed, respectively. The R^2 values are higher than those for the pseudo-first-order kinetic model under comparable experimental conditions.

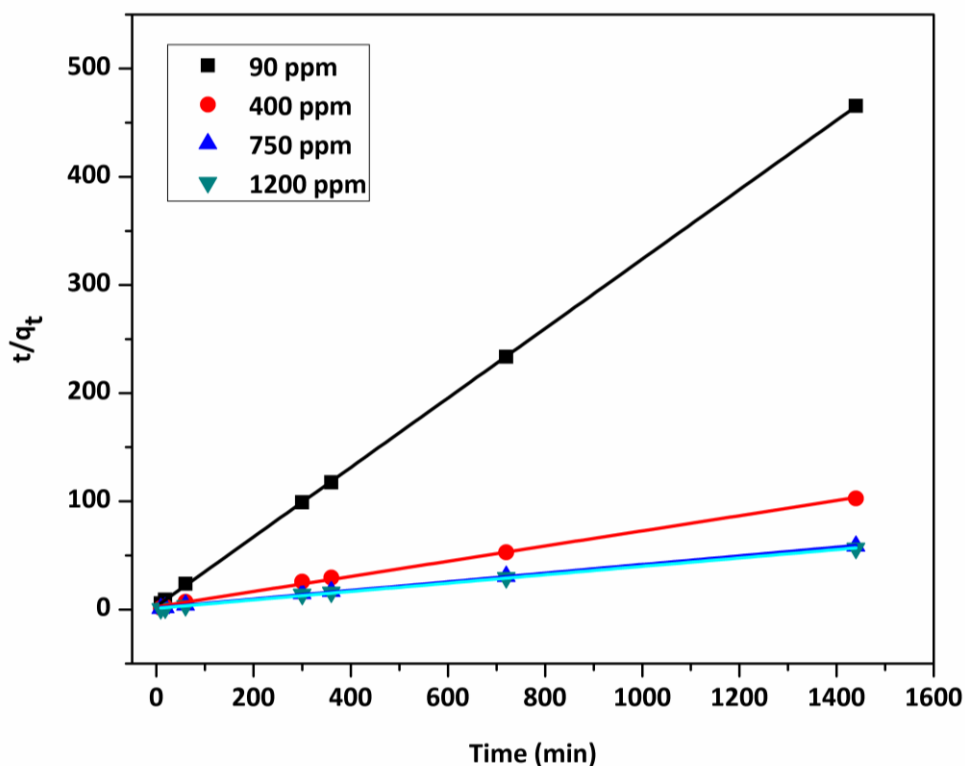


Fig. 3.15 Pseudo-second-order plot for yttrium ion sorption by polymeric beads, at four different initial concentration of Y(III)

The pseudo-second-order model assumes that chemisorption is the rate-controlling step provided that rate controlling role of the diffusion step was minimized by proper mixing. Additionally, the values of q_e obtained from the second-order model (Table 3.2) are in good agreement with the experimental q_{exp} values of 3.09, 13.05, 21.8 and 22.6 mg/g, respectively, for different initial concentrations (90, 400, 750 and 1200 mg/L) of Y (III) in aqueous solution in comparison to the first-order kinetic model. The excellent agreement of the values of q_e and q_{exp} suggests that the sorption of Y(III) by D2EHPA impregnated composite beads is well described by pseudo second order model for the entire range of initial concentration of yttrium ion.

It is also evident from Table 3.2 that the rate constant values are dependent on initial concentration of Y(III) in aqueous solution. Increase in concentration of Y(III) resulted in decrease in corresponding K values. This provides the information about the enhanced sorption at low concentration of metal ion in the aqueous solution.

3.1.14 Sorption mechanism

Though pseudo first and second order kinetic models provide useful information about sorption process, they have limitations as they cannot predict the rate-determining step of the yttrium sorption or provide information on the mechanism. In a heterogeneous process, such as the sorption of metal ion by polymeric composite beads, three subsequent steps represent the metal ion transfer: (1) transport of the yttrium ions from the bulk solution through the liquid film surrounding the external surface of the polymeric beads (film diffusion), (2) yttrium diffusion into the pores of polymeric beads (intra-particle diffusion), and (3) reaction of yttrium (sorption) at interior surface pores and capillary areas of the polymeric beads where extractant D2EHPA is impregnated (complexation). It may be noted that the rate of sorption process is controlled by the slowest step, which normally is film diffusion or intra-particle diffusion. Film diffusion often controls the rate when the sorption system has improper mixing, a low concentration of metal ion, a smaller beads size and a high affinity of the metal ions for the polymeric beads. On the contrary, intra-particle diffusion will be predominant in systems with a high concentration of metal ions in aqueous phase, proper mixing, a large polymeric beads size and a low affinity between the metal ions and the polymeric beads surface [151]. However, due to the characteristics of the polymeric beads and the experimental conditions used in the present investigation, it is possible to observe both mechanisms involved during the sorption of yttrium uptake. To elucidate the

mechanism of sorption of yttrium by the polymeric composite beads, the intra-particle diffusion model was fitted to the experimental data. The model can thus be described by the following equation:

$$q_t = k_{id} \times t^{1/2} + I \quad (3.5)$$

where k_{id} is the intraparticle diffusion rate constant, the value of intercept I give the idea about the thickness of boundary layer.

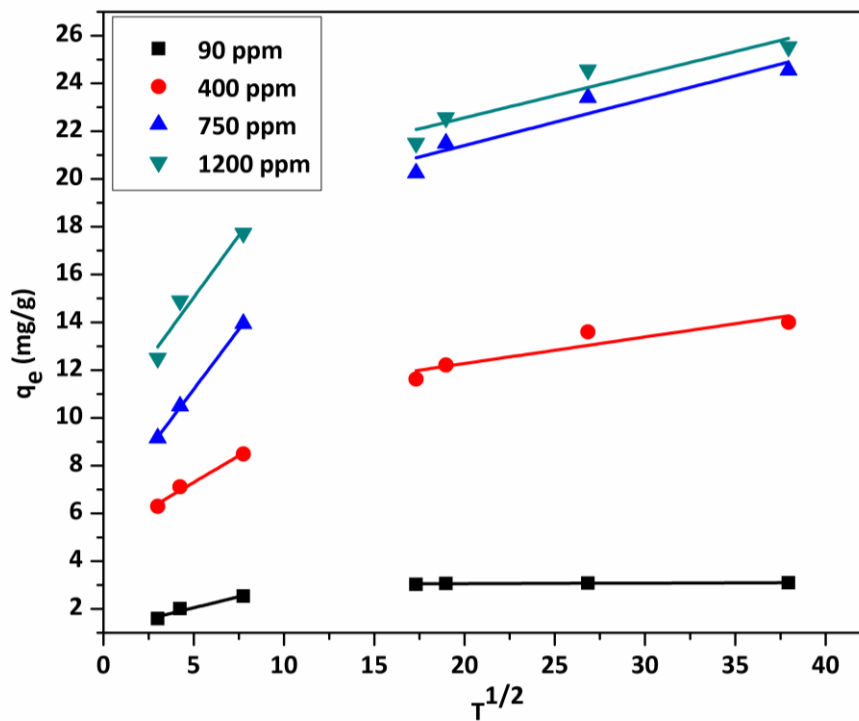


Fig. 3.16 Intraparticle diffusion plot for Y(III) sorption by polymeric beads, at different Y(III) concentration in feed.

These sorption data is fitted in the intraparticle diffusion model. The larger the intercept I (the thickness of boundary layer), the higher is the boundary layer effect. The deviation of straight line from the origin may be because of difference in initial and final stages of the sorption. The intraparticle diffusion plot for the sorption of yttrium ion is depicted in Fig.3.16. It is observed that there are two linear portions which elucidate the two

sorption stages, namely, external mass transfer at initial period followed by intraparticle diffusion of yttrium onto the polymeric beads. The slope of the second linear portion give the intraparticle diffusion rate constant, listed in Table 3.2, shows that k increases with increasing initial yttrium ion concentration. The equilibrium concentration q_e increases accordingly with the increase in initial yttrium concentration. Further, Boyd expression [127] was used to analyze the sorption kinetic data to determine that whether sorption of Y(III) by beads proceeds via film diffusion or intraparticle diffusion mechanism:

$$F = 1 - \frac{6}{\pi^2} e^{(-Bt)} \quad (3.6)$$

Where F is the fraction of solute sorbed at different time t and Bt is a mathematical function of F .

$$F = \frac{q_t}{q_e} \quad (3.7)$$

Where, q_t and q_e represent the amount sorbed (mg/g) at any time t and at infinite time (in the present study 1400 min.), respectively. Solutions to eq. (3.6), depending on the value of F , are given as eqs. (3.8) and (3.9).

$$Bt = 2\pi - \frac{\pi^2 F}{3} \quad (3.8)$$

$$Bt = 0.4977 - \ln(1 - F) \quad (3.9)$$

Bt can be calculated using both the equations (3.8) and (3.9). Equation (3.8) is used when F is upto 0.085, when it is higher > 0.85 , Eq. 3.9 is used. The linearity of Bt versus t plot provides useful information to distinguish between the film diffusion and the intraparticle diffusion mechanism of sorption.

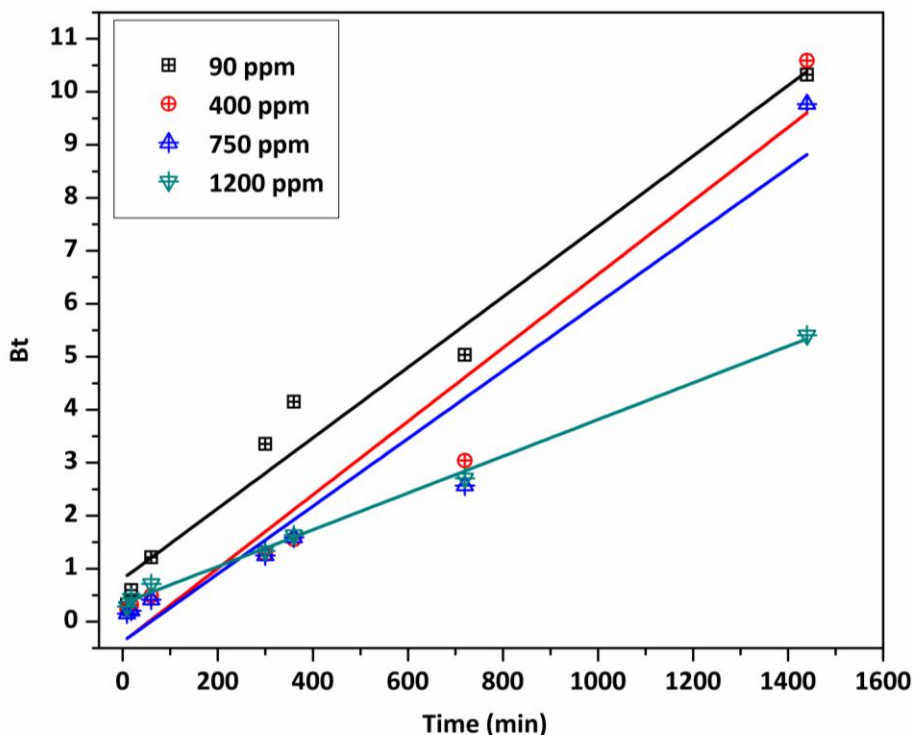


Fig. 3.17 Boyd's plot for Y(III) sorption by polymeric beads

A straight line passing through the origin is indicative of the sorption processes only governed by intraparticle diffusion mechanisms; otherwise, it is governed by film diffusion [151]. The Boyd's plot of Bt against time (t) is shown in Figure 3.17. The fitted lines, for all the concentrations studied, do not pass through the origin, indicating that the sorption process may also be governed by the external mass transport, and intraparticle diffusion may not be the only rate-controlling step in the removal of the sorbate.

3.1.15 Column study (sorption and desorption of yttrium)

The continuous column operation for both sorption and desorption were performed to evaluate the performance of these beads for the recovery of yttrium from aqueous chloride

medium. The sorption profile of Y(III) from the feed having 160mg/L at 0.3M HCl is shown in Fig. 3.18 for PES-I and PES-II beads.

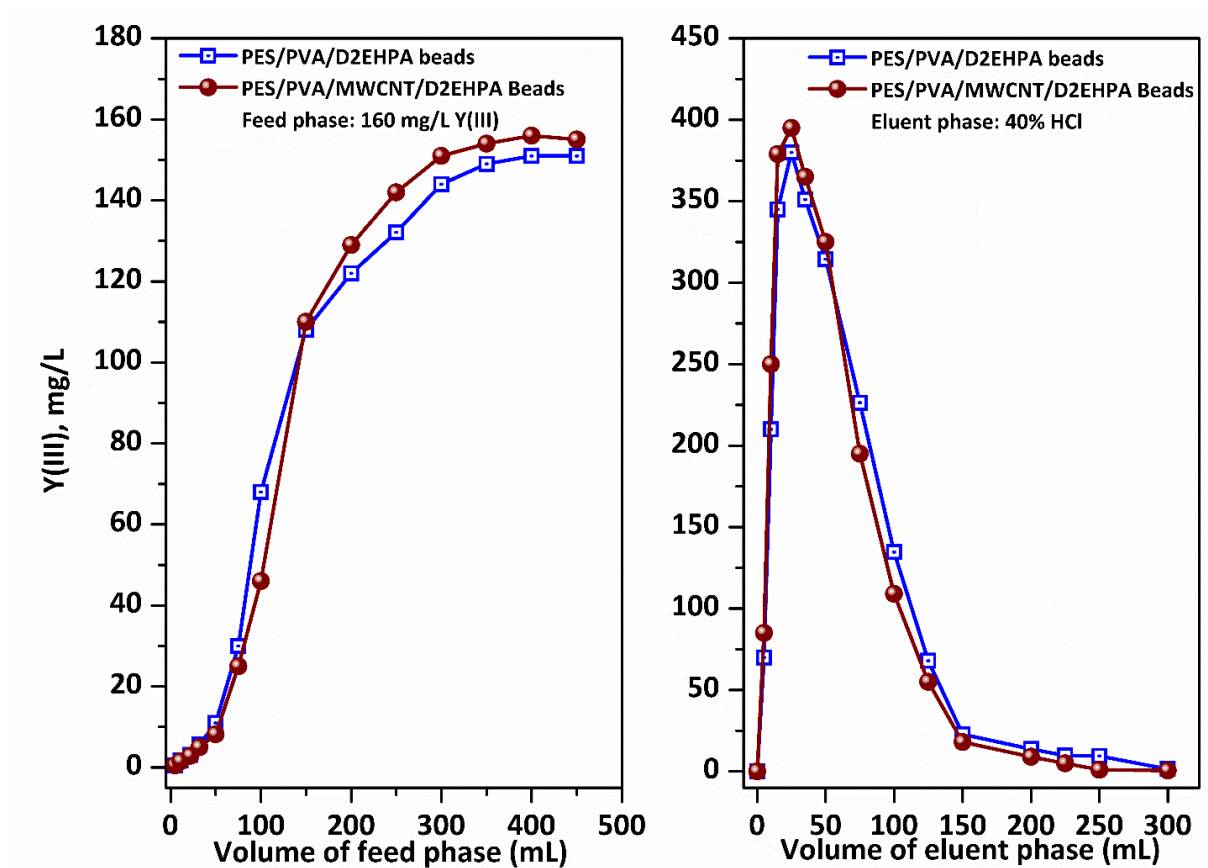


Fig.3.18(a) Breakthrough profile of Y(III) uptake by a)PES-I (b) PES-II, Feed: 160 mg/L Y(III) in 0.5M HCl, Flow rate: 2ml/min. (b) Elution profiles of loaded Y(III) beads using 40%HCl from column containing a)PES-I (b) PES-II beads

Both the types of beads showed good sorption with breakthrough points 39 and 45 ml for PES-I and PES-II beads, respectively. It was interesting that the breakthrough profiles attained saturation with 300ml of the feed solution both for PES-I and PES-II bead columns which correspond to the capacities of 19.5mg/g and 22 mg/g for them, respectively. These column sorption capacity values were lower when compared with batch sorption data. This phenomenon may be attributed to the fact that complete sorption of Y(III) is not possible in

dynamic column conditions whereas in the case of batch runs higher capacity of sorption is possible due to sufficient residence time. Mohapatra et al. have also observed the similar trend while studying the sorption of actinides by polyether ether ketone beads [152]. The desorption of sorbed Y(III) from these beads were also performed with 40% HCl solution as eluent at a rate of 2 mL per minute. The desorption pattern (Fig. 3.18(b)) indicated that elution from PES-II beads was relatively easier and had sharper peaks as compared to the elution profile of PES-I beads. In both type of beads complete elution of loaded metal ions could be achieved by passing 140 mL of eluent solution. In the separation of the Y(III) with the polymeric beads packed in the column, it was observed that better separation ability of the metals can be obtained with decrease in the flow rate of the feed solution and increase in the height of the packed column. The sorption and desorption studies indicated the suitability of these polymeric composite beads for scale up.

3.1.16 Stability of composite beads

In order to assess the feasibility of employing these composite beads for the separation of rare earths from aqueous solution on larger scale in batch or continuous column operation mode, it is desirable to evaluate the stability (recyclability/reusability) of these beads. In the present investigation the stability of both the beads (PES-I and PES-II) were determined by two ways (i) by repetitive sorption and desorption study (cyclic stability) and (ii) by keeping these beads in concentrate acidic media i.e 6M of each HCl, H₂SO₄ and H₃PO₄ separately over a period of time prior to their use in sorption for Y(III)metal ion (periodic stability).

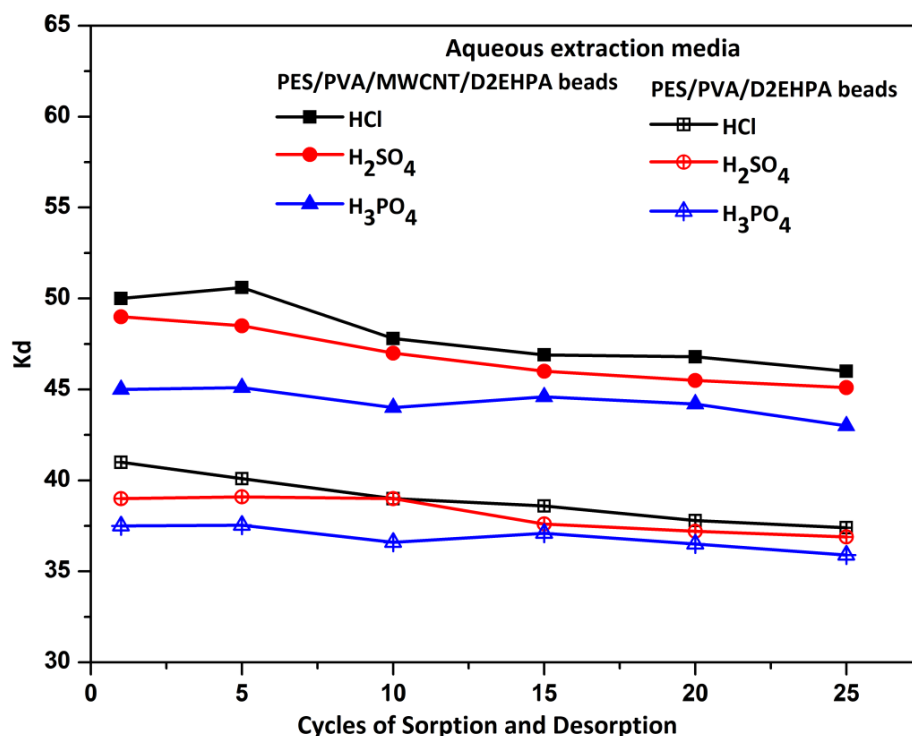


Fig. 3.19 Effect of different aqueous media on sorption of Y(III) extraction by polymeric beads (weight of PES beads: 10g, aqueous phase of 0.5N HCl /H₂SO₄/H₃PO₄: 100 mL for sorption, Y(III) concentration: 2.5g/L, stirring speed: 250rpm, Stripping: 50%HCl, temperature

In the first case, the Y(III) sorption was investigated with both the beads separately from different aqueous medium (0.5M HCl/H₂SO₄/H₃PO₄ containing 1000mg/L of yttrium) at an appropriate S/L ratio and temperature (30°C) following the desorption of Y(III) with 6M HCl prior to their reuse for sorption and desorption in a similar way. It may be noted (Fig. 3.19) that the K_d values were found to be consistent within the error limit of $\pm 5\%$ even after 20 such cycles of sorption and desorption tests. In the second case, the periodic stability of such beads were evaluated by keeping known amount of composite beads in 6M solution of HCl for a period of 15 days to 160 days and after removing and washing with distilled water these beads were tested for their sorption behavior towards Y(III) under comparable

conditions. The plots of K_d values vs. number of days for 6M HCl solution for both the beads are shown in Fig.3.20.

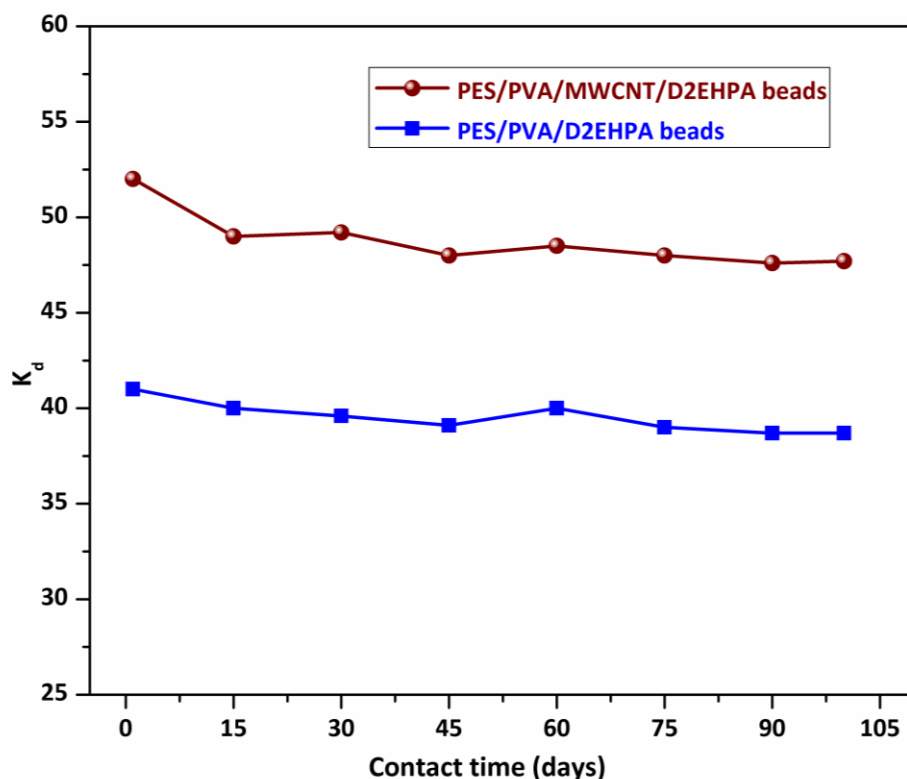


Fig. 3.20 Periodic stability of (a) PES-I (b) PES-II beads in 6M HCl

The K_d values evaluated in each case were found to be almost constant within the error limit of $\pm 5\%$.

Both these studies demonstrated that these novel beads are quite stable and have the ability for their reuse in the separation of rare earth ions from aqueous solution.

3.1.17 Evaluation of D2EHPA loss

The aim of the development of novel polymeric composite beads containing D2EHPA in the present work was directed towards not only to limit the use of D2EHPA and elimination of hazardous organic diluents, but also to restrict the leaching of extractant during hydrometallurgical operations. Accordingly, D2EHPA loss in aqueous medium during

sorption of Y(III) was monitored after each sorption and desorption cycle upto 20 cycles following the procedure described elsewhere [153].

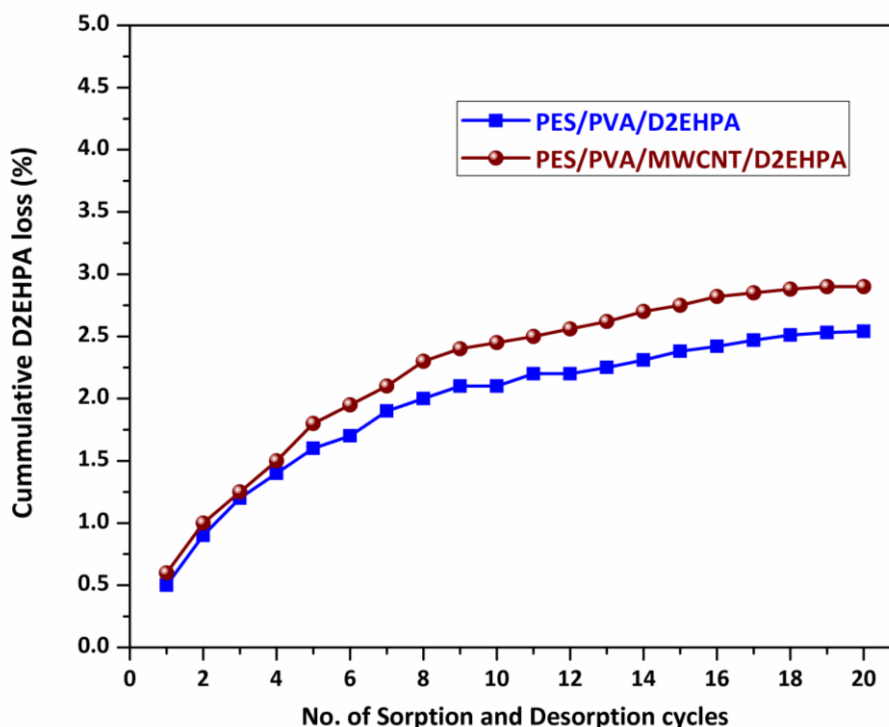


Fig. 3.21 Effect of sorption and desorption of Y(III) from PES beads on cumulative percentage loss of encapsulated D2EHPA

Leaching out of D2EHPA in the aqueous solution through the pores of the beads was found to be in the range of 1 to 1.5% (Fig.3.21). Similarly, the loss of D2EHPA was <1% in the column mode operations for sorption as well as desorption processes. This reduced loss when compared with other solvent impregnated beads is due to the presence of nanoporous dense surface layer and preferential presence of water and NMP solvent mixture near the peripheral pores of polymeric bead that prevent the loss of viscous organic extractants[154]. The non-leachability of D2EHPA suggested its prominence in the field of hydrometallurgy for the separation and concentration of metal ions from aqueous solutions.

3.1.18 Conclusions

PES based novel polymeric composite beads with different additives encapsulating 3M D2EHPA have been prepared with an aim to recover rare earths from aqueous solution. Among different beads, PES/D2EHPA/PVA/MWCNT bead has been found to be the most efficient for the separation and recovery of Y(III) from aqueous solution. The present work described herein is an environment friendly approach towards the recovery of indispensable elements from aqueous stream. The developed bead not only addresses the environmental issues but also offer selective and efficient separation of rare earths. Moreover, they have added advantage of extraordinary stability and recyclability as compared to the other conventional techniques such as solvent extraction and ion exchange. The sorption data was well described by Langmuir isotherm. The developed bead was satisfactorily employed for the recovery in continuous column operation mode and has promising potential to scale up the technology to industrial level.

3.2 Optimization of parameters by Taguchi method for Dysprosium sorption by D2EHPA beads

This section deals with the optimization of experimental parameters for Dysprosium sorption by the developed D2EHPA – PES beads.

Dysprosium (Dy) is an important member of the rare earth family, which finds numerous applications in high technology areas. Permanent magnets having Dy as additive are used in wind turbines, cell phones, data storage device etc. [155, 156]. Dysprosium cadmium chalcogenides are sources of infrared radiation used in the study of chemical reactions [157]. Dy is also used in conjunction with vanadium and other elements in making laser materials [158]. Due to its high neutron absorption cross section, Dy is used in control rods for nuclear reactors [159]. It is also used as doping material for dosimeter ($\text{CaSO}_4\cdot\text{Dy}$) for measuring ionizing radiation [160]. All these applications require Dy(III) in highly pure form (>99%). Literature on the separation of Dy(III) by polymeric beads is scanty, though some researchers have used the beads in various metal ion separation. The present studies aim at using these solvent impregnated beads with improved features for the separation of Dy(III). For effective separation/sorption of Dy(III) from the aqueous medium, the morphology of the beads plays an important role as it influences the mass transfer as well as the bead capacity. Accordingly, to modify the morphology, different additive has been added with the polyethersulfone matrix. The polymer to extractant (D2EHPA) ratio has also been varied to prepare the bead with different sorption capacities. Similarly, the effect of other important experimental parameters, including liquid to solid ratio, contact time of the beads with the solution, the concentration of Dy(III) in the feed solution, aqueous phase molarity, stirring speed of the agitator and temperature, which influence the sorption behaviour of

polymeric beads on the sorption of Dy(III) have been examined. The data generation under different experimental variables to arrive at an optimum condition is very tiring, tedious and time consuming. Taguchi mathematical approach [131] often eliminates this tiring and tedious exercise, by allowing the exact prediction of desired results with carefully and optimally selecting the most influential experimental variables there by limiting the generation of large volumes of data. It is, therefore, desirable to apply and adopt Taguchi approach in the present work also to arrive at the optimum conditions for effective sorption of Dy(III) by the solvent impregnated polymeric beads. Seven parameters, namely, contact time of the beads with the solution, nature of additive, the concentration of Dy(III) in the feed solution, aqueous phase molarity, stirring speed of the agitator, polymer to extractant ratio and the temperature have been selected and varied in three different levels. Another parameter, liquid to solid phase ratio (w/w), has been varied in two levels. Apparently this is an eight factor mixed (two and three) level system. Full factorial design [161] is not suitable for optimizing such complex system, as it would have involved thousands of experiments. Taguchi method, on the other hand, allows us to carry out only eighteen experiments in order to get the required information. With the help of these eighteen experiments the influence of the experimental parameters on Dy(III) sorption has been investigated and the optimized conditions have been evaluated and discussed in this paper.

3.2.1 Taguchi method

Taguchi method [131] is a structured approach for identifying and determining the best combination of dominant process parameters to optimize the objective function(s) with minimum number of experiments. The method is based on an orthogonal array [130] of experiments. An orthogonal array is a minimal set of experiments with various combinations

of parameter levels. Output of the orthogonal array, which indicates the relative influences of various parameters on the formation of the desired product, is used to optimize an objective function. There are three types of objective functions: larger-the-better, smaller-the-better and nominal-the-best. The influences are commonly referred in terms of S/N (signal to noise) ratio.

We aim for optimizing the recovery and equilibrium sorption of Dy(III), and for that larger-the-better type of objective function has been used. In this case the exact relation between S/N ratio and the signal is given by

$$S/N = -10 \log \left(\frac{1}{n} \sum_i^n 1/y_i^2 \right) \quad (3.10)$$

Where y_i is the signal (percentage recovery or equilibrium sorption) measured in each experiment averaged over n repetitions. The effect of a parameter level on the S/N ratio, i.e., the deviation it causes from the overall mean of signal, is obtained by analysis of mean (ANOM). The relative effect of process parameters can be obtained from analysis of variance (ANOVA) of S/N ratios. Computation of ANOM and ANOVA are done by using following relations.

$$m_i = \left(\frac{1}{N_l} \right) \sum S/N \quad (3.11)$$

$$Sum\ of\ squares\ (SoS) = \sum_{i=1}^{i=j} N_l (m_i - \langle m_i \rangle)^2 \quad (3.12)$$

Where m_i represents the contribution of each parameter level to S/N ratio, $\langle m_i \rangle$ is the average of m_i 's for a given parameter and the coefficient and N_l represents the number of times the experiment is conducted with the same factor level in the entire experimental region. SoS is obtained by using ANOVA. This term is divided by corresponding degrees of

freedom (DoF=number of parameter level minus 1) to derive relative importance of various experimental parameters by utilizing equation (3.13)

$$Factor\ effect = \frac{SoS}{\{DoF \times \sum (SoS / DoF)\}} \quad (3.13)$$

The detail about selection of Taguchi over other techniques and introduction about the same is described in section 2.2.6 of chapter 2. Several researchers [162-165] have extensively used this technique in optimization of parameters in the field of extraction or leaching. This study represents the first time evaluation of parametric sensitivity of Dy(III) sorption by extractant impregnated polymeric beads.

3.2.2 Selection of parameters for Taguchi optimization

Eight parameters have been identified for the optimization studies based on our experience. The parameter, liquid to solid phase ratio (L/S), has been varied in two levels. The other seven parameters, namely, polymer to extractant ratio (P/E), contact time of the beads with the solution, nature of additive, the concentration of Dy(III) in the feed solution, aqueous phase molarity (i.e. HCl concentration), stirring speed of the agitator and the temperature have been varied in three different levels. Table 3.3 shows the parameters and their levels. The design of experiments has been carried out based on L18 orthogonal array. The details of the experiments are shown in Table 3.4. Individual experiment was replicated three times.

Table 3.3: Selection of parameters and their levels for Taguchi method

Parameter	Level 1	Level 2	Level 3
Liquid to solid ratio (L/S)	5	10	-
Contact time (h)	1	6	24
Feed Dy (ppm)	100	500	1000
Additive	Nil	PVA	PVA+MWCNT
Polymer to extractant ratio (P/E)	4	5	7.5
Stirring speed (rpm)	100	250	500
Aqueous phase molarity	0.3	0.5	1
Temperature (°C)	30	50	65

3.2.3 Preparation and evaluation of polymeric beads

Three types of polymeric beads have been prepared by non-solvent phase inversion method under optimized preparatory conditions which is a polymer solution consisting 10-15% w/w PES in NMP was mixed with extractant and additives to obtain the desired ratio of D2EHPA to polymer solution i.e. 1:4, 1:5, 1:7.5)) as described in section 2.2.1 of chapter 2. The above mentioned mixture was employed to prepare polymeric beads by using the experimental set up and procedure developed by us [166]. The first type of bead is the basic polymeric bead containing PES as polymer matrix without any additive. The other two types of beads are composite beads having PVA and PVA+MWCNT as additives, respectively. The concentration of additive was in the range of 0.25-2% w/w. These beads were then immersed and stabilized in the water bath for 24 hours prior to their use.

Table 3.4: Design of L-18 orthogonal array for experiments

Exp. No.	Liquid to solid ratio (L/S)	Contact time (h)	Feed Dy (ppm)	Additive	(P/E)	Stirring speed (rpm)	Aqueous phase molarity	Temperature (°C)
1	5	1	100	nil	4	100	0.3	30
2	5	1	500	PVA	5	250	0.5	50
3	5	1	1000	PVA+MWCNT	7.5	500	1	65
4	5	6	100	nil	5	250	1	65
5	5	6	500	PVA	7.5	500	0.3	30
6	5	6	1000	PVA+MWCNT	4	100	0.5	50
7	5	24	100	PVA	4	500	0.5	65
8	5	24	500	PVA+MWCNT	5	100	1	30
9	5	24	1000	nil	7.5	250	0.3	50
10	10	1	100	PVA+MWCNT	7.5	250	0.5	30
11	10	1	500	nil	4	500	1	50
12	10	1	1000	PVA	5	100	0.3	65
13	10	6	100	PVA	7.5	100	1	50
14	10	6	500	PVA+MWCNT	4	250	0.3	65
15	10	6	1000	nil	5	500	0.5	30
16	10	24	100	PVA+MWCNT	5	500	0.3	50
17	10	24	500	nil	7.5	100	0.5	65
18	10	24	1000	PVA	4	250	1	30

Morphology and internal structure of the composite beads were examined by scanning electron microscope (SEM- Seron Technology AIS2300C). Thermogravimetry (TG-Mettler Toledo TG/DSC STAR System) was performed by heating the samples upto 1000°C, at a heating rate of 10°C/min, in N₂ atmosphere. TG data were used to determine the weight of the encapsulated extractant per unit weight of PES. Further the beads were characterized by

FTIR (Shimadzu IR Affinity-1) as a confirmatory tool to substantiate the characteristic functional groups of D2EHPA in the PES bead matrix. The details about above mentioned techniques have been discussed in chapter 2 of this thesis.

Sorption of Dy(III) by polymeric beads was investigated in batch mode by contacting 10 grams of polymeric beads with aqueous phase (0.3/0.5/1.0 N HCl medium) of containing Dy(III) at varying concentrations at an appropriate solid to liquid ratio for 24 hrs to make sure that the system had reached the equilibrium [167]. The solid –liquid mixture was stirred constantly to avoid mass transfer resistance. In general, the experiments were performed at ambient temperature (30±1°C) and aqueous phase was analysed for Dy(III) content by ICP-AES (Ultima JY Model 2). The percentage recovery, R and equilibrium sorption, q_e were evaluated using following equations:

$$R = \left(\frac{C_0 - C_e}{C_0} \right) \times 100 \quad (3.14)$$

$$q_e = (C_0 - C_e) \times \frac{V}{W} \quad (3.15)$$

Where C_0 , and C_e are concentrations of Dy(III) at initial time and at equilibrium, respectively; W is the weight of polymeric beads (polymer, additive and extractant); and V is the volume of aqueous phase in litre. R and q_e are the two input objective functions which need to be maximized by Taguchi method.

3.2.4 Taguchi Analysis on sorption

The objective of applying Taguchi method is to determine the optimum conditions at which R and q_e are maximized. The results of the experiments as per the L-18 array and the corresponding S/N ratios for R and q_e are given in Table 3.5. The effect of each parameter on R as calculated by equation (1-4) is shown in Table 3.6. It can be observed from Table 3.6

that the aqueous phase molarity has the maximum effect (24.4%) on the effective percentage recovery(R) of Dy(III).

Table 3.5: Percentage recovery (R) and equilibrium sorption (e_q) data for L-18 arrays and corresponding S/N ratio

Exp. No.	R			S/N (dB) (for R)	e_q			S/N (dB) (for e_q)
	Trial 1	Trial 2	Trial 3		Trial 1	Trial 2	Trial 3	
1	97.44	97.5	97.3	39.772	3.07	3.08	3.072	9.754
2	69.5	69	69.1	36.801	9.05	9.06	9.058	19.138
3	40.1	40.12	41.2	32.141	11.21	11.01	11.2	20.936
4	47.45	47.44	47.15	33.505	1.57	1.59	1.575	3.963
5	94.18	94.2	94.22	39.481	12.7	12.75	12.745	22.097
6	94.81	94.55	94.28	39.512	26.3	26.2	26.28	28.385
7	97.82	96.98	97.51	39.774	3.08	3.1	3.18	9.88
8	74.14	74.25	74.55	37.421	10.6	10.51	10.55	20.467
9	90.59	91.2	90.22	39.149	23.3	23.38	23.5	27.381
10	72.12	72.25	72.21	37.169	4.6	4.7	4.49	13.244
11	20.53	20.55	20.65	26.267	5.78	5.81	5.72	15.222
12	29.15	29.41	29.2	29.323	15.6	15.61	15.55	23.855
13	49.5	49.12	49.25	33.855	3.27	3.22	3.25	10.228
14	90.69	90.715	90.25	39.137	25.01	25.3	25.18	28.015
15	45.9	45.2	45.28	33.151	25.36	25.1	25.2	28.034
16	94.47	94.5	95.1	39.525	5.97	5.9	5.2	15.05
17	86.98	86.25	86.59	38.75	23.9	23.91	23.1	27.468
18	59.94	59.28	59.1	35.481	33.1	32	32.5	30.244

The effects of polymer to extractant ratio (P/E), stirring speed of the agitator and the temperature are insignificant on R as calculated by ANOVA. The ANOVA also depicts that the relative effect of 'Error' is about 44.1%. The percent influence of the 'Error' term represents the combined influence of (a) factors not included in the study, (b) noise factors,

and (c) any experimental unintended anomalies. Generally, ‘Pooling of factor’ is performed on the insignificant factors, to reduce the error.

Table 3.6 Effect of different parameters on the percentage recovery (R) of Dy(III)

Factor	DoF	SoS	%Effect	Modified % Effect after 1 st pooling	Modified % Effect after 2 nd pooling
Liquid to solid ratio (L/S)	1	34.436	9.826	10.484	10.57
Contact time (h)	2	69.192	19.771	21.087	21.27
Feed Dy (ppm)	2	18.675	1.05	2.336	2.55
Additive	2	18.092	0.834	2.15	2.33
Polymer to extractant ratio (P/E)	2	12.317	0	0.01	0.19
Stirring speed (rpm)	2	10.803	0	0	pooled
Aqueous phase molarity	2	81.749	24.424	25.74	25.92
Temperature (°C)	2	8.739	0	Pooled	pooled
Error	2	15.838	44.095	38.163	37.15

As, out of the insignificant factors, ‘Temperature’ has minimum SoS, it was pooled. It is worth noting that the effect of ‘Error’ was reduced to 38.16% after removing the effect of temperature. The modified % effect after pooling of temperature is also shown in Table 3.6. Further pooling of the factor ‘stirring speed’ was performed as it was found insignificant after first pooling. The effect of the remaining factors is shown in the rightmost column of Table 3.6. The ‘Error’ was subsequently reduced to 37.15%. Any further pooling resulted in increase in the error value. Table 3.6 shows that the factor effect on *R* followed the sequence:

aqueous phase molarity > contact time > L/S ratio > Dy(III) concentration in feed > additives > P/E ratio. The S/N ratios for different factors at different levels are shown in Figure 3.22.

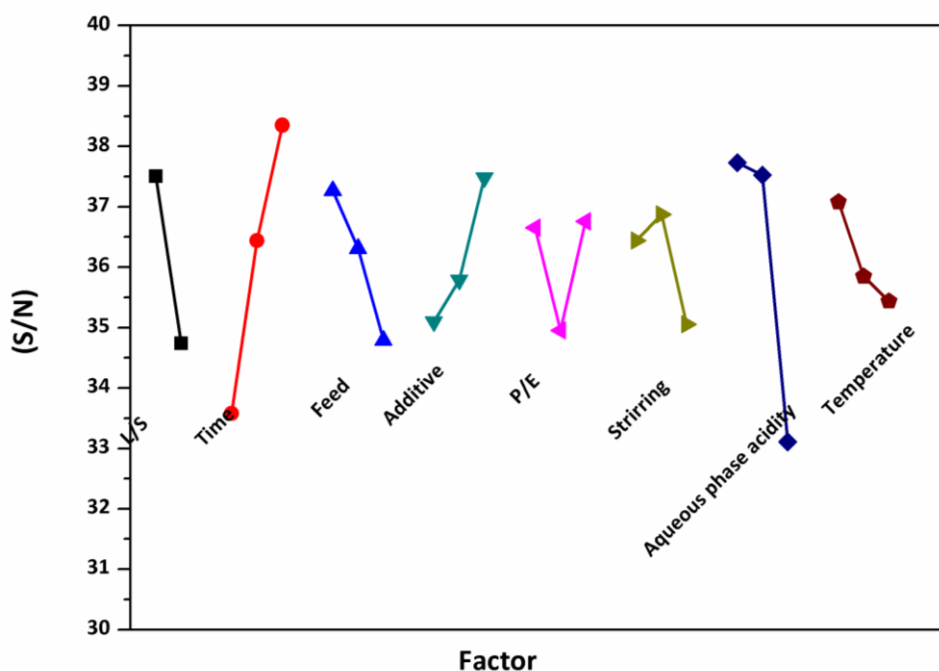


Fig. 3.22 Plot of S/N ratios for different factors for R

Since larger-the-better is the objective for R , the optimum operating conditions can be set up as L/S ratio 5, contact time 24 h, Dy(III) in feed 100 ppm, additive PVA+MWCNT, P/E ratio 7.5, stirring speed 250 rpm, aqueous phase molarity 0.3 and temperature 30°C. A variation reduction plot at the optimum condition is shown in Figure 3.23, which shows the improvement of the performance. The standard deviation in S/N is predicted to come down from 25 to 7.9. Experiment carried out at the optimum conditions as determined by Taguchi analysis yielded an average recovery of 98.6% (three trials) with a standard deviation of 7.3. The enhanced percentage recovery with excellent reproducibility shows the accuracy of this analytical method in predicting the optimized conditions.

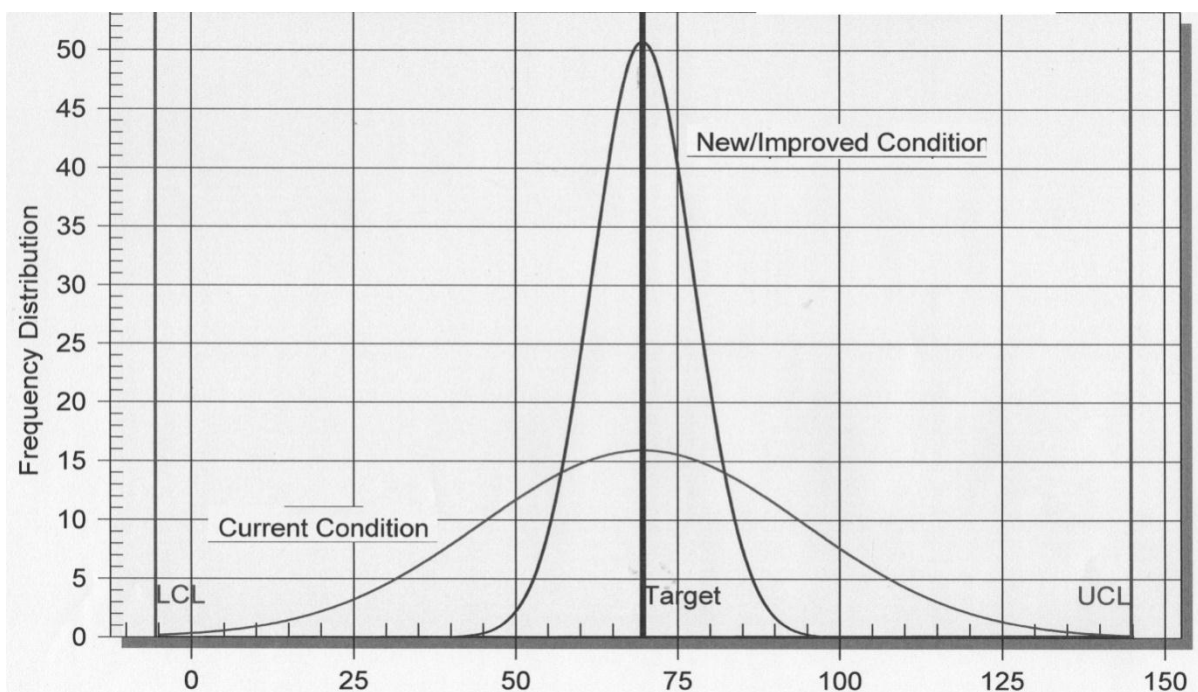


Figure 3.23: Variation Reduction plot for R

Table 3.7 depicts the effect of various parameters on q_e . In this case it can be observed that Dy(III) concentration in feed has the maximum effect (75.4%). Like previous one, the effect of temperature and stirring speed being least important, they were pooled. The revised factor effects are shown in the rightmost column of Table 3.7, which followed the sequence: Dy(III) concentration in feed > aqueous phase molarity > contact time > L/S ratio > additives > P/E ratio. The S/N ratios for different factors at different levels are shown in Figure 3.24. Since larger-the-better is the objective for q_e , the optimum operating conditions can be set up as L/S ratio 10, contact time 24 h, Dy(III) in feed 1000 ppm, additive PVA+MWCNT, P/E ratio 4, stirring speed 250 rpm, aqueous phase molarity 0.3 and temperature 30°C. A variation reduction plot at the optimum condition is shown in Figure 3.23, which shows the

improvement of the performance. The standard deviation in S/N is predicted to come down from 9.8 to 1.6.

Table 3.7: Effect of different parameters on the equilibrium sorption (q_e) of Dy(III)

Factor	DoF	SoS	%Effect	Modified % Effect after 1 st pooling	Modified % Effect after 2 nd pooling
Liquid to solid ratio (L/S)	1	47.878	3.757	3.869	3.9
Contact time (h)	2	69.098	5.058	5.282	5.3
Feed Dy (ppm)	2	832.947	75.397	75.621	75.64
Additive	2	18.356	0.387	0.61	0.63
Polymer to extractant ratio (P/E)	2	13.25	0	0.14	0.16
Stirring speed (rpm)	2	11.058	0	0	pooled
Aqueous phase molarity	2	69.945	5.137	5.361	5.38
Temperature (°C)	2	9.296	0	pooled	pooled
Error	2	14.15	10.264	9.117	9

The actual experiment under the predicted optimum conditions shows the value of q_e to be 37.9 mg/g with a standard deviation of 1.8 (three trials).

It is worth noting that for the percentage recovery of Dy(III), R , aqueous phase molarity is the main contributing factor, whereas for equilibrium sorption, q_e , feed concentration is the main contributing factor. Also the values of L/S ratio, Dy(III) feed concentration, and P/E ratio are different for maximizing R and q_e . The Dy(III) concentration in feed is at minimum value for maximizing R , but it is at maximum value for maximizing q_e .

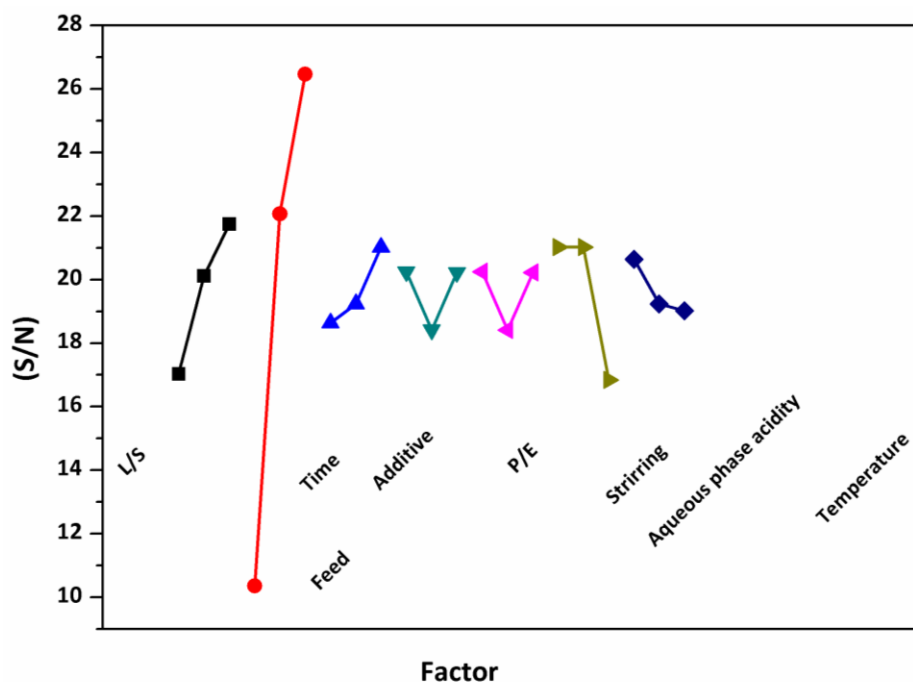


Fig. 3.24 Plot of S/N ratios for different factors for q_e

These observations will be explained in the ‘Discussion’ section after analyzing the microstructure of the beads.

As can be observed from above, the percentage recovery of Dy(III), R , greatly depends on aqueous phase molarity; whereas for equilibrium sorption, q_e , feed concentration is the main contributing factor. The sorption takes place via exchange of Dy(III) ion with hydrogen ion of D2EHPA. Therefore, the percentage recovery R is guided by the hydrogen ion concentration and R decreases with increase in aqueous phase molarity. On the other hand, q_e depends on the availability of Dy(III) ion in the aqueous phase and is therefore strongly influenced by the feed concentration. Higher the feed concentration, higher will be the value q_e . However, higher the feed concentration, lower is the value of R due to saturation of the available sites. More the contact time (24 h) better is the values of R and q_e . Lower is the L/S ratio (5), better will be the value of R due to more extractant quantity with

respect to available Dy(III) ions. On the other hand, higher the L/S ratio, higher is the amount of Dy(III) in the solution resulting in increase in sorption capacity (q_e) of the bead. Again low aqueous phase molarity (0.3) favours R and q_e for enhanced cation exchange.

The bead without any additive (Figure 3.3b) formed a non-uniform less porous microstructure which prevented the exchange of Dy(III) ions from aqueous solution with the hydrogen ions of the D2EHPA molecules. On the other hand, addition of PVA+MWCNT resulted in significantly enhanced sorption of Dy(III) due to the following two factors. Firstly, during the phase inversion of polymeric solution to polymeric beads, MWCNTs acted as the nuclei for the reformation of polyethersulfone inside the bead which enhanced uniformity in the pore distribution with better porosity. Secondly, MWCNTs were functionalized by D2EHPA molecules on its surface, which in turn got distributed near periphery of the composite beads thereby allowing the sorption of Dy(III) simultaneously by ion exchange as well as adsorption. The better distribution of D2EHPA in the PES/PVA/MWCNT bead along with favourable pore size distribution resulted in the enhancement in R and q_e .

The effects of P/E, stirring speed and temperature are not very significant. However, higher stirring speed eliminates mass transfer resistance and lower temperature favours adsorption, which is exothermic in nature. Decrease in P/E results in more extractant and thus improves q_e . On the other hand, increase in P/E increases R .

3.2.5 Conclusions

The percentage recovery and the equilibrium sorption of Dy(III) from aqueous phase have been studied using novel polymeric beads encapsulating D2EHPA. The effects of

various operational and structural parameters have been analyzed by Taguchi method using L18 orthogonal array. Feed concentration of Dy(III) has been found to be the most influential factor for equilibrium sorption capacity, whereas aqueous phase acidity influences the percentage recovery most. Addition of PVA and MWCNT in the polymer bead changes the pore structure and distribution of D2EHPA, thereby enhances the recovery. The analysis of variance predicted the optimum conditions where the performance was enhanced with minimum standard deviation. Experiments carried at optimum conditions verified the predicted data.



Chapter 4

SYNTHESIS AND EVALUATION OF EHEHPA ENCAPSULATED BEADS FOR RARE EARTHS SEPARATION

4 Synthesis and evaluation of carbon nanotube embedded EHEHPA encapsulated beads for rare earths separation

Rare-earth elements (REE) are a group of 17 elements which include 15 lanthanides along with yttrium and scandium owing to their similar chemical characteristics. They find critical utility in multitude of arenas ranging from hybrid and electric cars, compact fluorescent lamps, wind turbines to HDD's, optical glasses and lasers [22,168]. The multidimensional applicability of these REE is due to their excellent electrical, magnetic and optical properties derived from their partially filled f orbital. The constant increase in applicability of REE in various fields created a huge demand for constant supply of these elements [169]. The supply risk of REE have necessitated the need of recovering rare earths from other important sources such as e-wastes, tailing of mines and lean solutions of processing plants to augment the supply through regular mines [169]. Apart from these supply related concerns, rare earths separation and purification of individual elements is itself one of the most difficult task in analytical chemistry due to their very close chemical and physical properties. Multistage solvent extraction and ion exchange are the most common techniques used for the rare earths separation at industrial level [142, 170]. As discussed in chapter 1 and chapter 3 these processes have some associated detriments, such as multistage cycles of operation, third phase formation, finite aqueous solubility of the extractants, solvents and modifiers, and their loss through phase disengagement have been reported, whereas for ion exchange process low extraction rate and limitation on the metal ion concentration in the effluent to be treated, hinders the favorable purification and separation of metals. In solvent extraction process, use hazardous organic extractants, diluents and modifiers, leads to severe environmental concerns [171,172].

In the Chapter 3, I have reported application of PES as matrix material for synthesizing composites beads encapsulating extractants like D2EHPA (di-2-ethyl hexyl phosphoric acid) for

separation of rare earths from acidic medium [166-167, 173-174]. D2EHPA is a well-known organic extractant in separation industry, it forms very strong complex with metal cations and hence requires a relatively high concentration of HCl (~6M) for back extraction of metal ions [175]. To avoid the use of high concentration of corrosive HCl fumes which have detrimental effect on the equipment's in the down-stream of process, 2-ethylhexyl phosphonic acid mono-2-ethylhexyl ester (EHEHPA also known as PC88A industrial trade name) was proposed for rare earths separation and recovery. The advantage of using EHEHPA as extractant is that it requires low HCl concentration (~3.5M) for complete stripping of rare earths from organic phase as well as it is a good rejecter of Ca [176]. Use of EHEHPA containing polymeric beads for metal ion separation is scanty [177].

Therefore, it is desirable to develop an environment friendly EHEHPA encapsulated PES beads which can be employed for effective separation of rare earths from aqueous solutions. The present work emphasizes with the investigations on the synthesis, characterization as well as evaluation of PES encapsulated with EHEHPA for the separation of rare earths from aqueous solution. Effect of various experimental process variables such as aqueous phase acidity, organic extractant concentration inside the beads, temperature, metal ion concentration and morphology has been investigated on the extraction of rare earths. The role of different additives including multiwall carbon nanotube (MWCNT), polyvinyl alcohol (PVA), lithium chloride (LiCl) and polyethylene glycol (PEG) on the internal morphology of composite beads have been studied to allow the understanding mass transport of rare earth metal ions into EHEHPA encapsulated polymeric beads through the pore. Extraction and stripping profiles of different rare earths have also been obtained.

4.1 Synthesis of PES/EHEHPA beads

Total five varying type of polymeric composite beads namely PES/PVA (as blank), PES/PVA /EHEHPA, PES/PEG/EHEHPA, PES/LiCl/EHEHPA, PES/PVA/MWCNT/EHEHPA with different additives were prepared by non-solvent phase inversion method under optimized preparatory conditions using similar experimental set up described in chapter 2 and 3 [144]. The concentration of additives was optimized in such a way that the resultant composite beads had spherical shape. The concentration of additive was found to be optimum at 1% w/w of polymer solution, where as in the case of MWCNT, the optimum concentration was 0.25% w/w of polymer solution. The developed polymeric beads were characterized by SEM, TGA and FT-IR to evaluate their structural, physical and chemical properties. The details regarding the experimental condition were described in chapter 3 section 3.1.2.

Extraction/sorption study of rare earths such as La, Nd, Sm, Dy and Y by EHEHPA polymeric beads was investigated in batch mode of operation. The procedural details of the experiments are described in section 2.2.2 of chapter 2. The equilibrium adsorption or sorption capacity of the polymeric beads was evaluated in terms of (q_e) in mg/g and weight distribution coefficient, K_d were also evaluated using equations described in section 2.2.2. Sorption isotherm, kinetics of metal ion sorption by polymeric beads along with column studies were also performed as described in section and subsections of 2.2 of chapter 2.

4.2 Effect of additives on beads morphology:

The morphology of the polyethersulfone bead is a significant characteristic which influences its applicability and stability for metal ion separation from aqueous media. For metal extraction, an ideal extractant encapsulated polymeric bead should have a central cavity

circumvented by a porous polymeric structure. Fig. 4.1 (a–f) illustrates the cross sectional images of the polymeric composite beads with different additives.

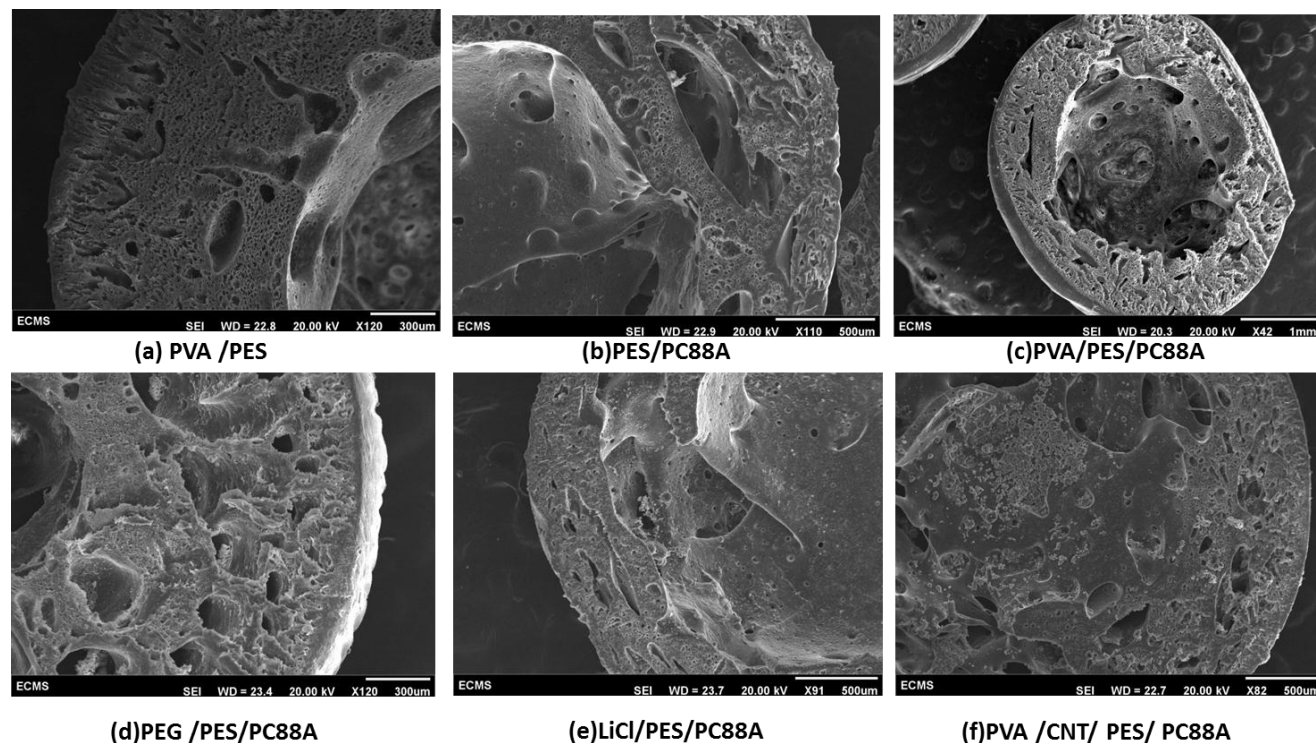


Fig.4.1 SEM images of cross-section of PES based bead (a)PES blank, (b)PES/PC88A, (c)PES/PVA/PC88A, (d)PES/PEG/PC88A, (e)PES/LiCl/PC88A, (f)PES/PVA/MWCNT/PC88A

It is evident from the figure that additives play critically important role in altering the internal microstructure of the bead in terms of porosity and pore size distribution which in turn affect their extraction capacity considerably. Fig. 4.1(a) shows the cross sectional image of the PES bead having PVA as an additive, with porous structure and thick outer shell. The second image (Fig. 4.1b) is cross-sectional view of EHEHPA encapsulated PES bead, the internal microstructure changes considerably in terms of uneven distribution of polymer when compared to Fig.4.1 (a). However, the distribution of polymer phase is uneven and even at the periphery

the matrix formed by PES seems to be broken. Fig. 4.1(c) depicts cross sectional image of PVA doped EHEHPA encapsulated PES bead, having relatively thinner outer layer with porous polymer matrix up to periphery when compared with fig. 4.1 (b). Noticeably, the core cavity is big and spherical when compared to beads shown in fig 4.1 (a, b). The addition of PEG and LiCl with PES resulted in detriment in terms of porosity and distribution of polymer fig 4.1 (d) and (e). On the other hand, polymeric beads with PVA and MWCNT both as additives (Fig.4.1f) also show porous and even distribution of polymer with gradual increase in polymer content at periphery. The above observations may be attributed to the distribution of the polymer and the additives during the phase inversion process; during the solidification additive's solubility in the antisolvent (water) determines the porosity and overall distribution of polymer inside the bead [146]. Morphological evaluation of the beads by SEM revealed that the PES/PVA/EHEHPA and PES/PVA/MWCNT/EHEHPA beads have the desired microstructures.

4.3 Thermo gravimetric Analysis

Fig. 4.2 represents mass loss profiles of blank PES bead, two types of PES/PVA/MWCNT/EHEHPA bead having different extractant to polymer ratio (1:5 and 1:15) and 3M EHEHPA liquid phase while heated in nitrogen atmosphere. In the case of 3M EHEHPA mass loss profile initial evaporation takes place around 210- 400°C with a two-step loss of weight of about 85%. The blank PES bead loses 82% of its weight in the temperature range of 60-130°C due to evaporation of NMP and water in it. It further loses 10% at around 520°C due to dissociation of PES followed by evaporation of volatiles. The weight loss profiles of PES/PVA/MWCNT/EHEHPA beads (1:5 and 1:15) can be divided into three zones. The first zone in the temperature range of 60-130°C corresponds to the evaporation of NMP and water inside the polymeric beads (~65 and 75%).

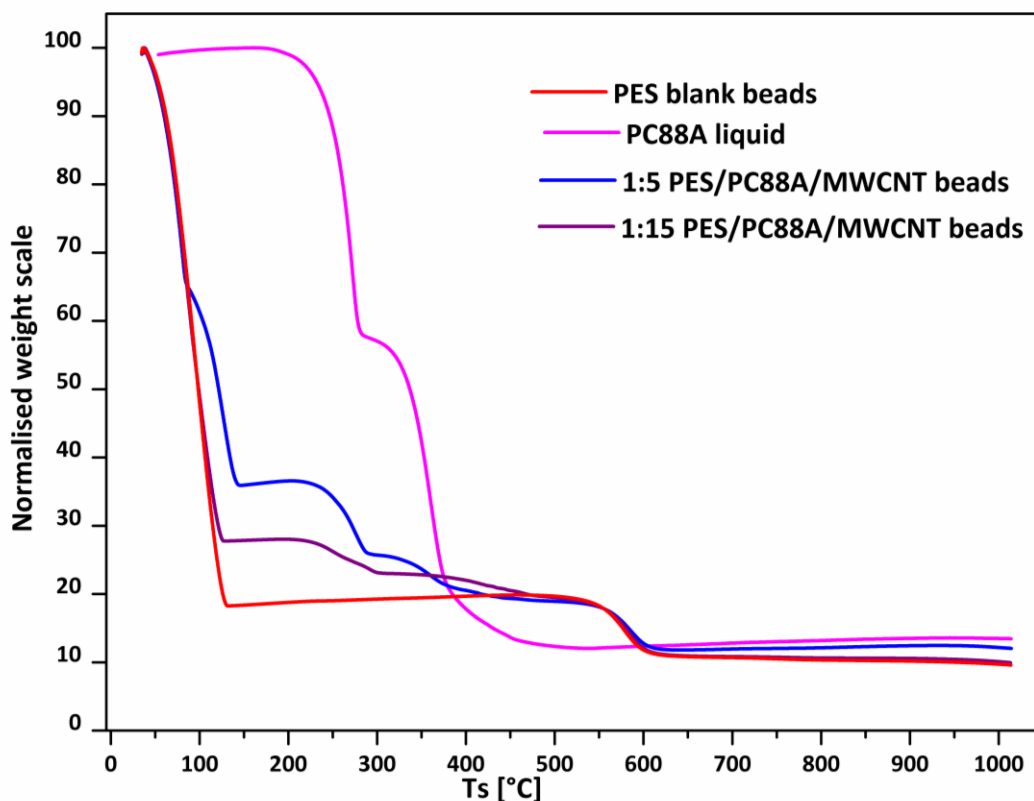


Fig. 4.2 TG of PES/PC88A bead, PC88A (3M), Blank polymer bead

The second zone (210-400°C) shows a loss of 18% weight for PES//PVA/MWCNT/EHEHPA beads with 1:5 extractant to polymer ratio and 13% for 1:15 extractant to polymer ratio beads which corresponds to the dissociation and evaporation of EHEHPA. The third zone manifests the dissociation of PES around 520-600°C, with a weight loss of around 7%. Comparing the depicted four TG profiles in figure 4.2, it can be concluded that there is no chemical interaction among water, NMP, EHEHPA, PES, PVA and MWCNT the main constituents of the polymeric beads. Similar observations were reported by Ozcan et al. for Cyanex 923 encapsulated polysulfonic based microcapsules and Yadav et al. for D2EHPA encapsulated polyethersulfone beads [174,146].

4.4 Functional group studies

The FTIR spectra of the pure EHEHPA, blank PES/PVA composite bead and two types of PES/PVA/MWCNT/EHEHPA bead having different extractant to polymer ratio (1:5 and 1:15) are shown in Fig. 4.3 (a, b, c & d).

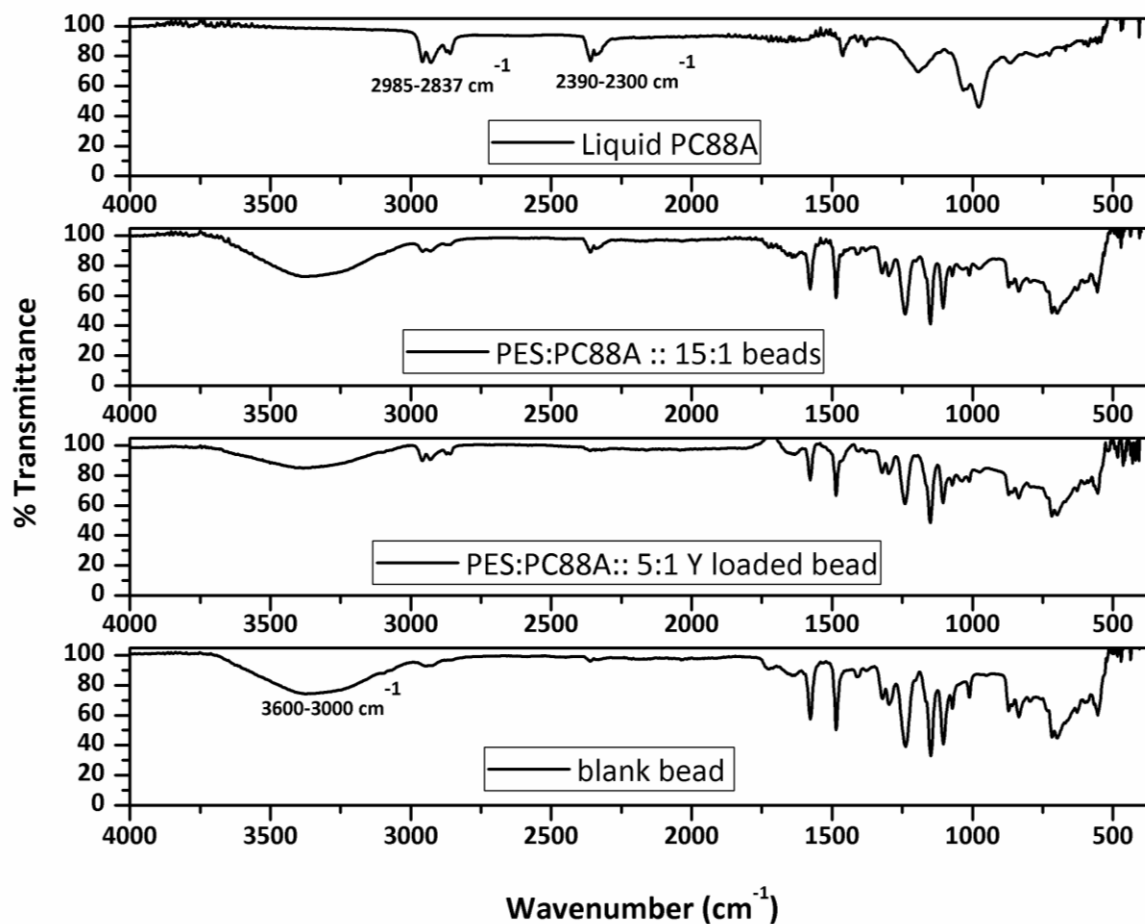


Fig. 4.3 FTIR spectra of PC88A (3M), PES/PC88A (15:1) bead, PES/PC88A (5:1)bead, blank PES bead

The FTIR spectrum for pure EHEHPA in Fig. 4.3(a) shows peaks at the interval 2800–3000 cm⁻¹ correspond to the radical 2-ethylhexyl and C-H stretching of methyl. The most intense band is the P–O stretching, together with P–O–C between 1050 and 970 cm⁻¹. Other important bands are P–O stretching at 1250–1210 cm⁻¹ and a low intense peak around 1500

cm^{-1} confirming the presence of P-OH [15]. In Fig. 4.3(d), three peaks between 1600 cm^{-1} to 1400 cm^{-1} are attributed to representative aromatic skeletal vibration of PES. The C-O-C stretching peaks are located between 1324 cm^{-1} to 1240 cm^{-1} . The S=O stretching peaks representing polyethersulfone are present at 1145 and 1105 cm^{-1} . In Fig. 4.3(b, c) the peaks at $1250\text{-}1210\text{ cm}^{-1}$, which represent P=O group and low intense band around 1680 cm^{-1} , along with peaks of polyethersulfone shows that EHEHPA encapsulated inside the bead is present within the polymer matrix without any chemical interaction with PES.

4.5 Effect of additives in polymeric beads on Y(III) extraction

All the types of EHEHPA encapsulated polymeric beads differing only in terms of additive (PEG, PVA, LiCl and MWCNT) were evaluated for their Yttrium sorption capacity from aqueous media under comparable experimental condition to assess the role of different additives. The extraction of Y(III) by different types of EHEHPA polymeric beads is evaluated as weight distribution ratio (k_d) and equilibrium sorption capacity (q_e). The results shown in Fig 4.4(a) and 4.4(b) confirms that additives in the polymeric beads not only alter the morphology of polymeric beads but also plays a significant role on its rare earths sorption capacity, polymeric beads having additives such as PVA or PVA+CNT showed marked increase in term of sorption of Yttrium whereas additives such as PEG, LiCl hampers the beads Y(III) sorption capacity. The decrease in the sorption capacity of EHEHPA/PES beads doped with PEG and LiCl can be attributed to the uneven distribution of polymer (Fig. 4.1d) and presence of thick outer layer around the encapsulated extractant EHEHPA (Fig. 4.1e) respectively when compared to EHEHPA beads without additive beads (Fig. 4.1b), which ultimately affects the interfacial contact area between aqueous and organic phases. On the other hand two types of beads i.e. PES/PVA/EHEHPA and PES/PVA/MWCNT/EHEHPA beads showed an increased Y(III)

sorption capacity due to their better encapsulation and enhanced porosity (Fig. 4.1c and Fig. 4.1f).

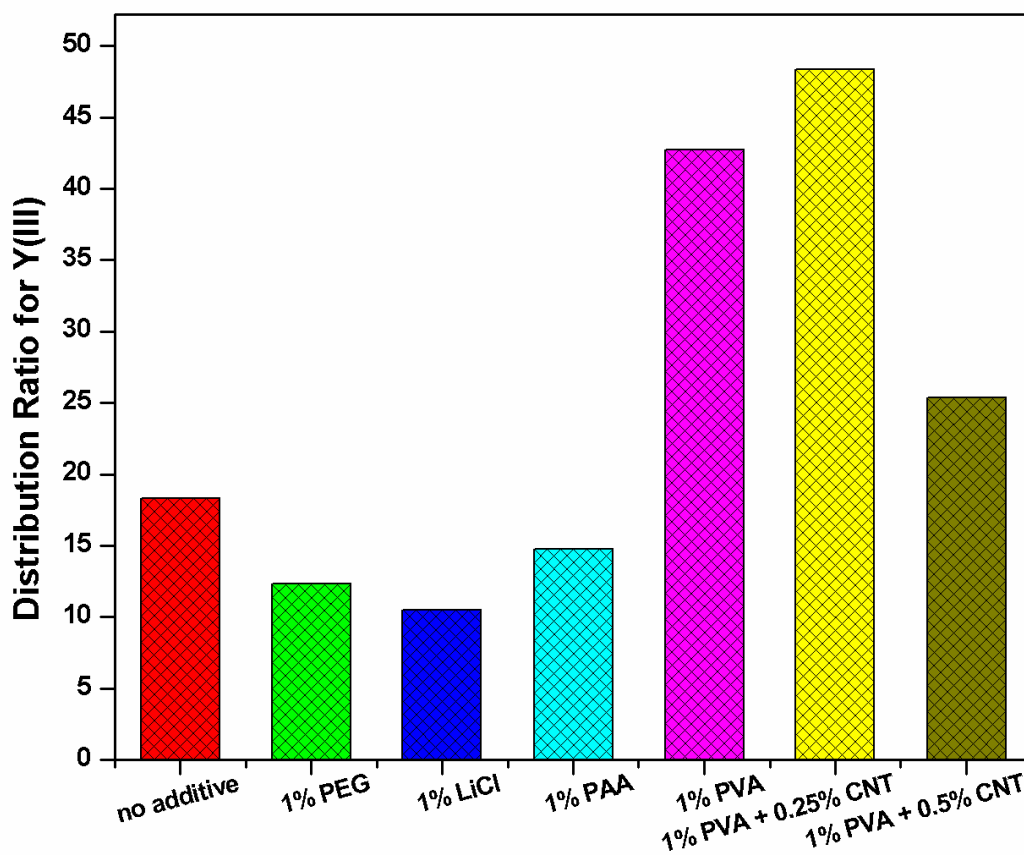


Fig. 4.4 (a) Effect of additives in polymeric composite beads on sorption of Y(III) by PES/EHEHPA beads

The observed enhancement in Y(III) sorption of PES/PVA/EHEHPA beads by addition of MWCNT may be due to the fact that MWCNT may acts as nucleus for the reformation of polyethersulfone inside the bead during the process of phase inversion, ultimately enhancing uniformity in the pore distribution with better porosity.

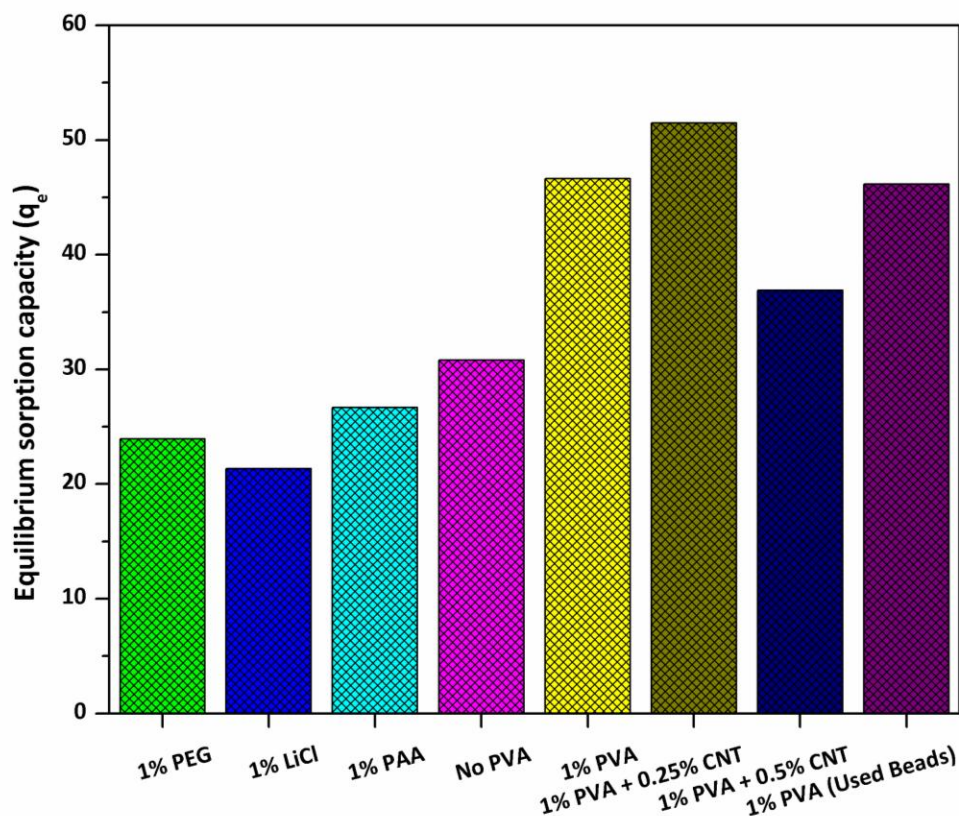


Fig. 4.4 (b) Effect of additives in polymeric composite beads on equilibrium sorption capacity of Y(III) by PES/EHEHPA beads

4.6 Effect of extractant concentration

The concentration of organic extractants in the diluents plays crucial role in metal extraction phenomenon as the presence of diluents not only determines physical characteristics of organic phase (viscosity, density and solubility) but also determines chemical reactivity by changing the dielectric constant and available concentration of organic solvent for extraction [178]. Effect of EHEHPA concentration inside the bead on yttrium sorption capacity was evaluated by preparing polymeric beads encapsulating variable concentration of EHEHPA (0.5 to 3.0 M) in petrofin, and subsequently evaluating the same for rare earths sorption. The shape of polymeric beads having 0.5 M and 1.0 M concentration of EHEHPA have been distorted sphere when compared with beads encapsulating 3M EHEHPA. The spherical morphology obtained

with high concentration of EHEHPA (3M) may presumably be due to the viscous nature of the solvent in absence of any diluent as compared to 0.5M and 1.0 M EHEHPA.

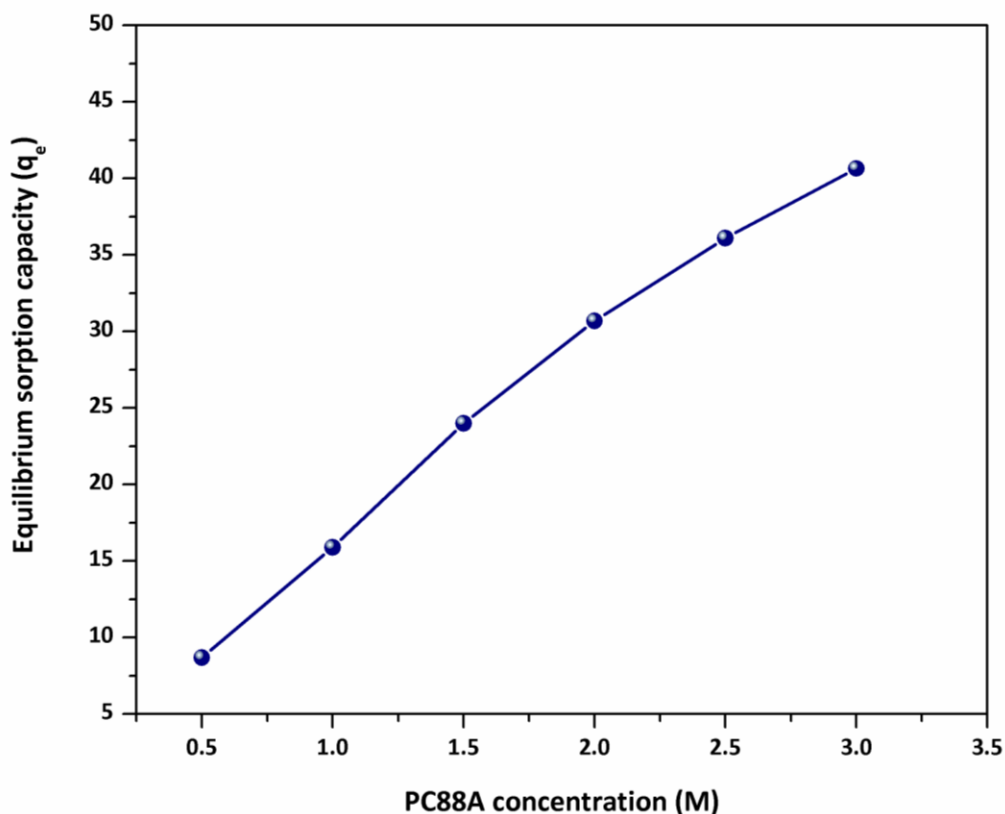


Fig. 4.5 Effect of extractant (PC88A i.e. EHEHPA) concentration inside the bead on Y(III) extraction. (EHEHPA diluted by petrofin, weight of PES/PVA/MWCNT/ EHEHPA beads: 10g, aqueous phase of 0.3N concentration of the acid used: 100 mL, Y(III) concentration: 2.1g/L, stirring speed: 250rpm, temperature: 30°C)

Fig.4.5 represents the effect of extractant concentration encapsulated inside the bead on the extraction of Y(III) from aqueous phase. The q_e values increased from 8 to 43 mg/g with increase in the concentration of EHEHPA from 0.5M to 3M inside the polymeric beads. Similar behavior was observed during solvent extraction process, where the metal ion distribution ratio between organic to aqueous phase also increased with increase in EHEHPA concentration [177]. However, continuous operating conditions in solvent extraction process do not allow extractant

concentrations beyond 1.5M for EHEHPA due to increase in density and viscosity of extractant phase affect the phase separation and mass transfer kinetics. On the contrary, in the present investigation 3M EHEHPA encapsulated polymeric beads (as prepared) can be used without any practical difficulties (phase separation and third phase formation) making the full utilization of concentrated extractant inside the beads.

4.7 Effect of Yttrium ion concentration

The experimental results of Y(III) extraction by different types of polymeric beads embedded with different additives from chloride medium revealed that PES/PVA/MWCNT/EHEHPA (PES-EHEHPA) were best suited for rare earth recovery and subsequently employed for further studies to optimize other different experimental variables. Effect of metal ion concentration Y(III) on the equilibrium sorption capacity q_e of PES-EHEHPA beads were evaluated at fixed aqueous/polymer (L/S) beads ratio (100ml/10gram) and acidity (0.3M HCl). Results shown in fig. 4.6 indicated that q_e values increased (16 to 50 mg/g) with increase in Y(III) ion concentration (600 to 3000 mg/L) in aqueous solution. The increase in sorption capacity is due to increase in effectively available metal ion in aqueous streams. Experimental results reported by Outokesh et al confirm our findings on the effect of metal ion concentration on q_e values. [148].

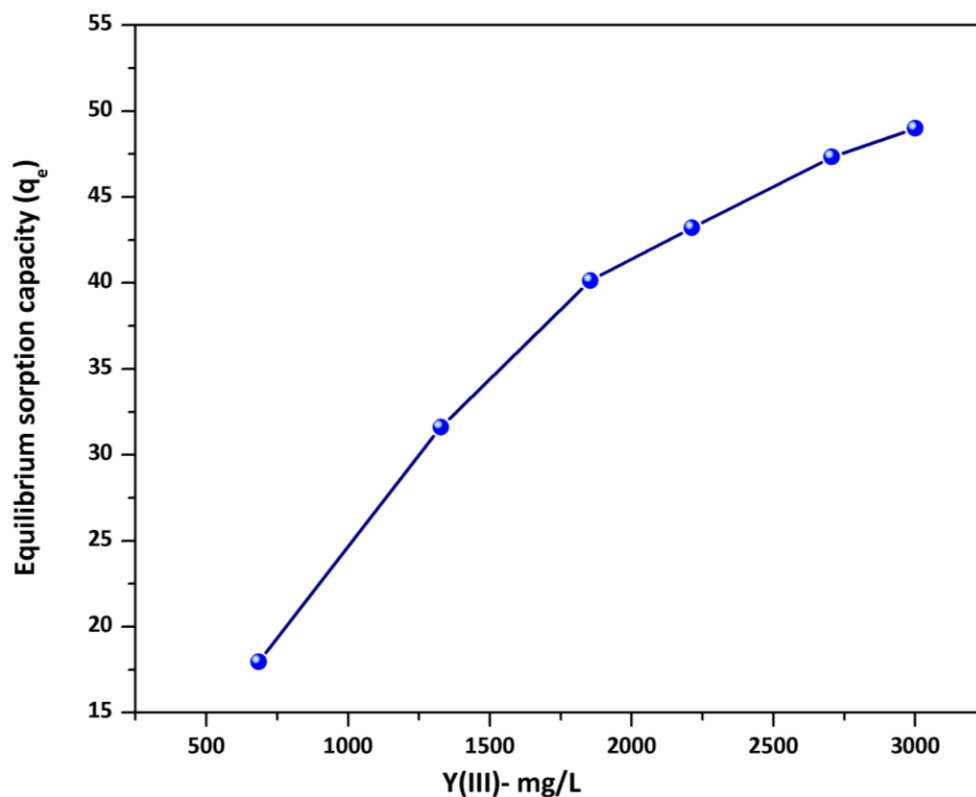


Fig. 4.6 Effect of Y(III) concentration in feed solution on equilibrium sorption capacity of Y(III) by PES/PVA/MWCNT/ EHEHPA beads (Weight of wet PES beads: 10g, 100 mL of 0.3N HCl solution, stirring speed: 250rpm, temperature: 30°C, contact time: 8 hours).

4.8 Effect of aqueous phase acidity

Effect of aqueous solution acidity on the extraction of Y(III) by PES-EHEHPA beads was investigated for different concentration of yttrium ion in the aqueous solution ranging from 150 to 750 mg/L at a fixed L/S ratio (10/1) and temperature (30°C). Sorption capacity of PES-EHEHPA for Y(III) decreased with increase in acid concentration for all the concentrations of Y(III) ion in the solution (Fig. 4.7a). However, the decrease in q_e at a particular acidity followed a proportional increase with increase in Y(III) concentration in the aqueous solution. In another set of experiments, aqueous feed acidity was varied from 0.3M to 3M HCl keeping the

concentration of Y(III) fixed at 2500 mg/L to evaluate the effect of feed acidity on equilibrium sorption capacity of polymeric beads.

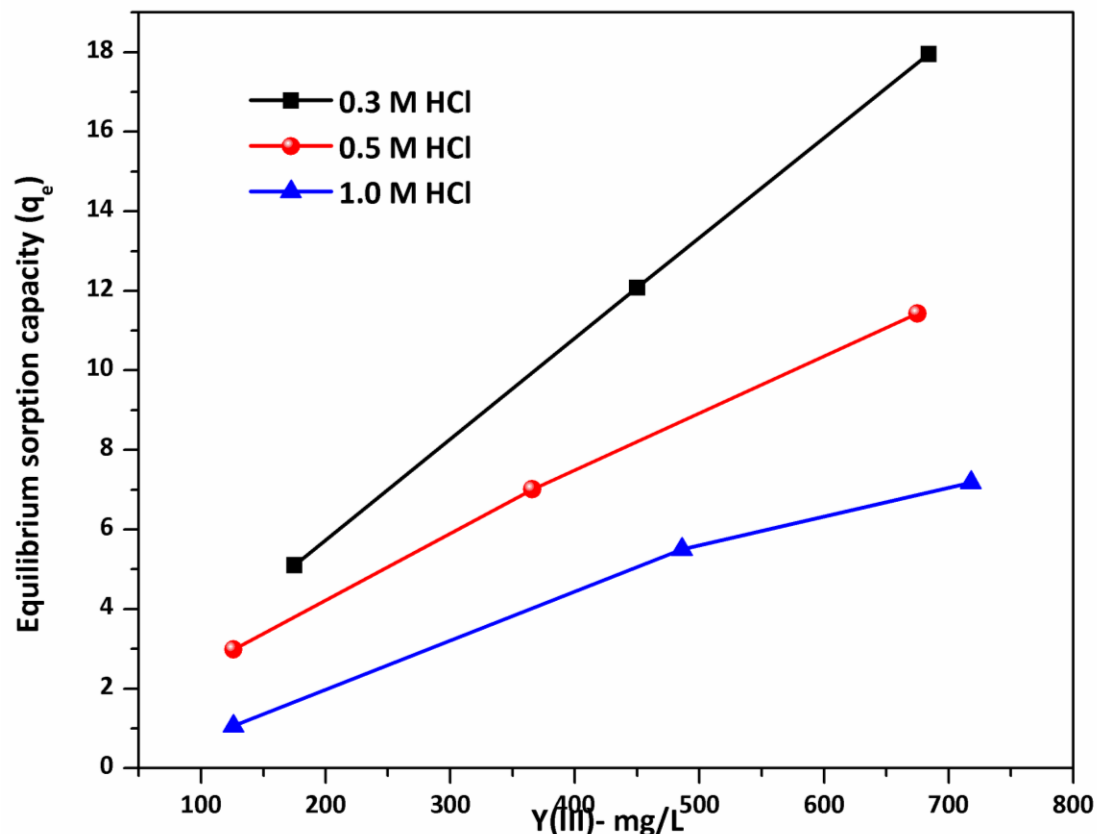


Fig. 4.7(a) Plots of Y(III) uptake as a function of aqueous phase hydrochloric acid concentration and Y(III) concentration in aqueous phase by PES/PVA/MWCNT/ EHEHPA beads

Results illustrated in fig 4.7(b) indicate that increase in acidity of aqueous solution, led to decrease in q_e value for PES-EHEHPA beads. The decrease in q_e with increase in acidity is a similar phenomenon observed in solvent extraction technique for the extraction of metal ion with acidic organophosphoric extractant like EHEHPA due to the ion exchange mechanism, where H^+ ion of EHEHPA gets displaced by metal ion of interest [176].

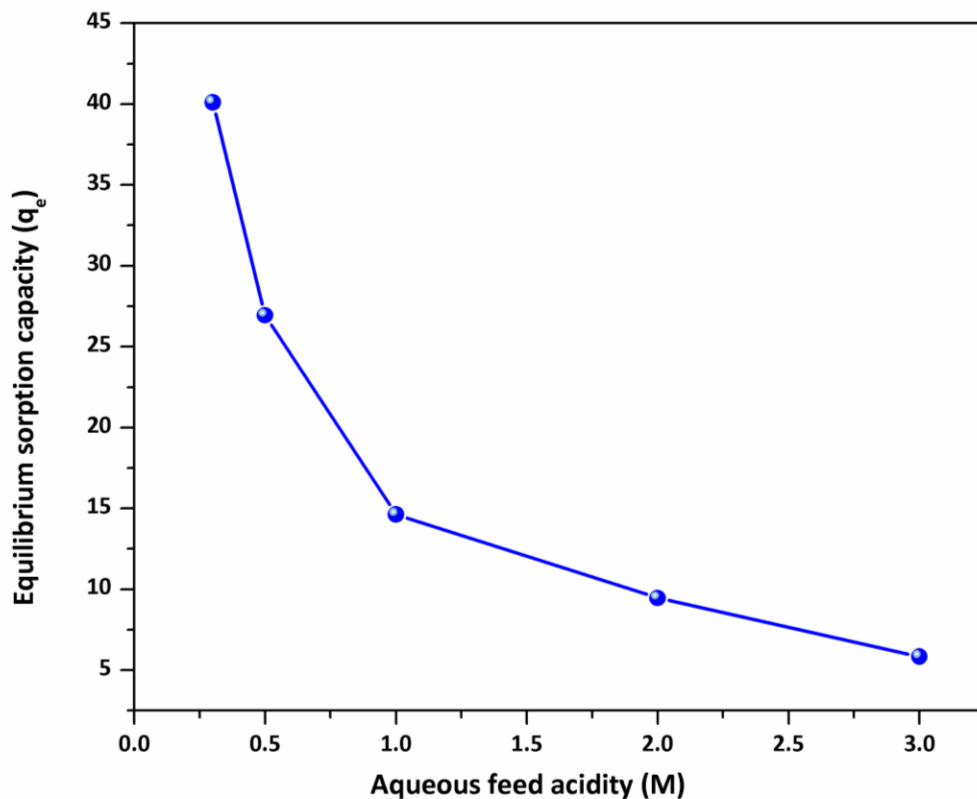
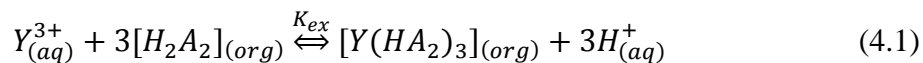


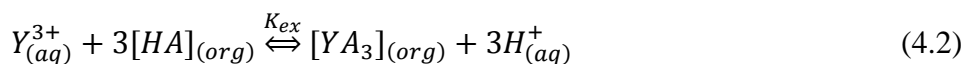
Fig. 4.7(b) Effect of aqueous feed acidity in terms of HCl concentration on Y(III) sorption capacity by PES/PVA/MWCNT/ EHEHPA beads (Weight of wet PES beads: 10g, Y(III) concentration in Feed: 2.5 g/L, stirring speed: 250rpm, temperature: 30°C, contact time: 8 hours)

4.9 Y(III) extraction mechanism from aqueous medium

Literature reports and slope analysis experiments indicate that EHEHPA exists as a dimer in paraffinic hydrocarbon based diluents [176]. The liquid liquid extraction of Y(III) from acidic medium by EHEHPA results in the formation of extracted species consisting 3 EHEHPA dimers shown in equation 4.1.



where H_2A_2 represents the dimer form of EHEHPA in nonpolar diluents, K_{ex} denoted in the equation is the equilibrium constant for the chemical reaction shown in eq. 4.1 while subscripts (aq.) and (org.) depicts the aqueous and organic phase respectively. However, in the present investigation the EHEHPA encapsulated polymeric beads do not contain any diluent and thereby, it is likely that EHEHPA will be present in monomeric form where its hydrogen ion will be replaced by yttrium ion from the aqueous solution and the exchange of H^+ ion with the metal ion takes place through the pores of the beads and the formation of $[YA_3]$ complex can be represented by the following equation:



The complex formation initially occurs at the periphery of the polymeric bead at the interface between aqueous and organic phase. Then the complexed ion diffuses inside the pore through concentration gradient. Similar observations were reported by Kamioet. al., [106], while studying the extraction of gallium and indium with extractant-impregnated microcapsule.

4.10 Influence of temperature

The effect of temperature on the sorption capacity of PES-EHEHPA beads for Y(III) for was studied under similar experimental condition of S/L ratio 1:10, aqueous phase acidity 0.3M HCl and concentration of Y(III) 2500 mg/L in the aqueous solution. Fig.4.8 represents the variation of q_e with change in temperature for PES-EHEHPA beads. Equilibrium sorption values for Y(III) sorption by PES-EHEHPA beads were decreased from 54 to 30 mg/g with increase in temperature of aqueous feed solution from 30 to 70°C. The decrease in q_e values with increase in temperature can be ascribed to the exothermic nature of the extraction reaction. In the present case effect of temperature beyond 70°C was not investigated for extraction as the glass transition

temperature of PVA is approximately 75°C at which chances of distortion in the morphology of composites beads are likely to be very high.

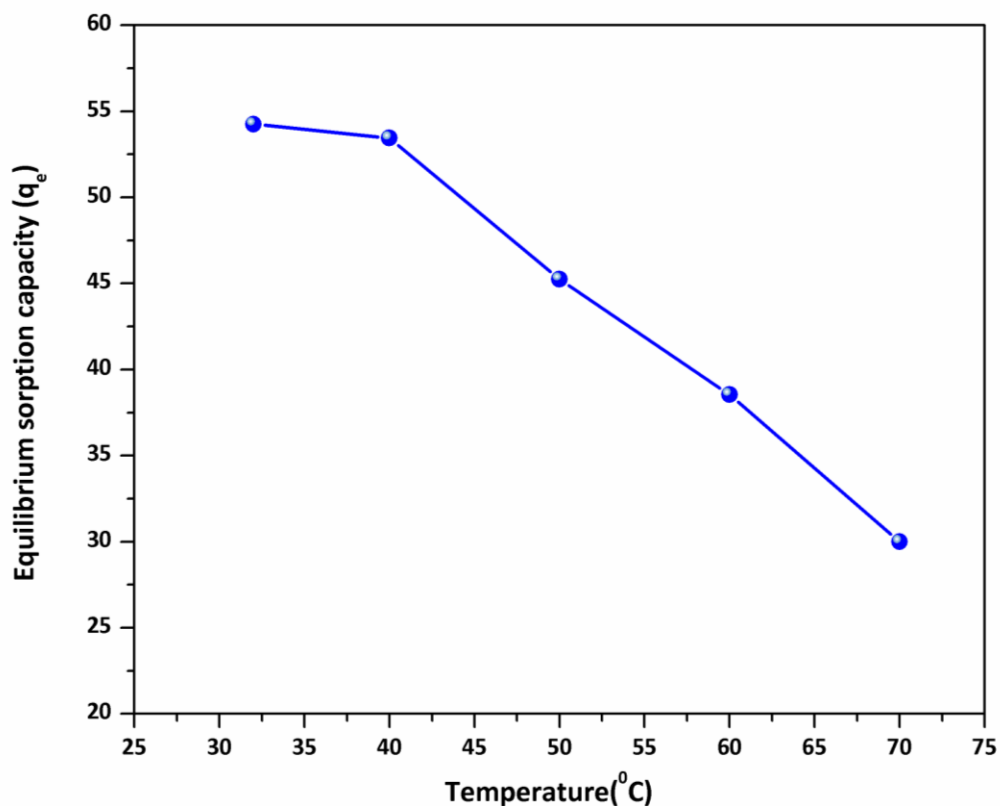


Fig. 4.8 Effect of temperature on Y(III) equilibrium sorption capacity by PES/PVA/MWCNT/EHEHPA beads (weight of PES beads: 10g, aqueous phase of 0.3N HCl: 100 mL, Y(III) concentration: 2.5 g/L, stirring speed: 250rpm, contact time: 8 hours)

4.11 Extraction of Y(III) in presence of competing rare earth ions: individual and mixture

The effect of chemically similar rare earth ions such as Lanthanum: La(III), Neodymium: Nd(III), Samarium: Sm(III), Dysprosium: Dy(III) on the extraction of Y(III) by PES-EHEHPA beads from aqueous media having different composition in terms of mixture of rare earths or individual elements was investigated. The first set of experiments were performed by contacting

the known amount PES-EHEHPA beads with 0.3M HCl solutions containing individual rare earths (2500 mg/L) i.e. La, Nd, Sm, Dy and Y at an appropriate S/L ratio and temperature.

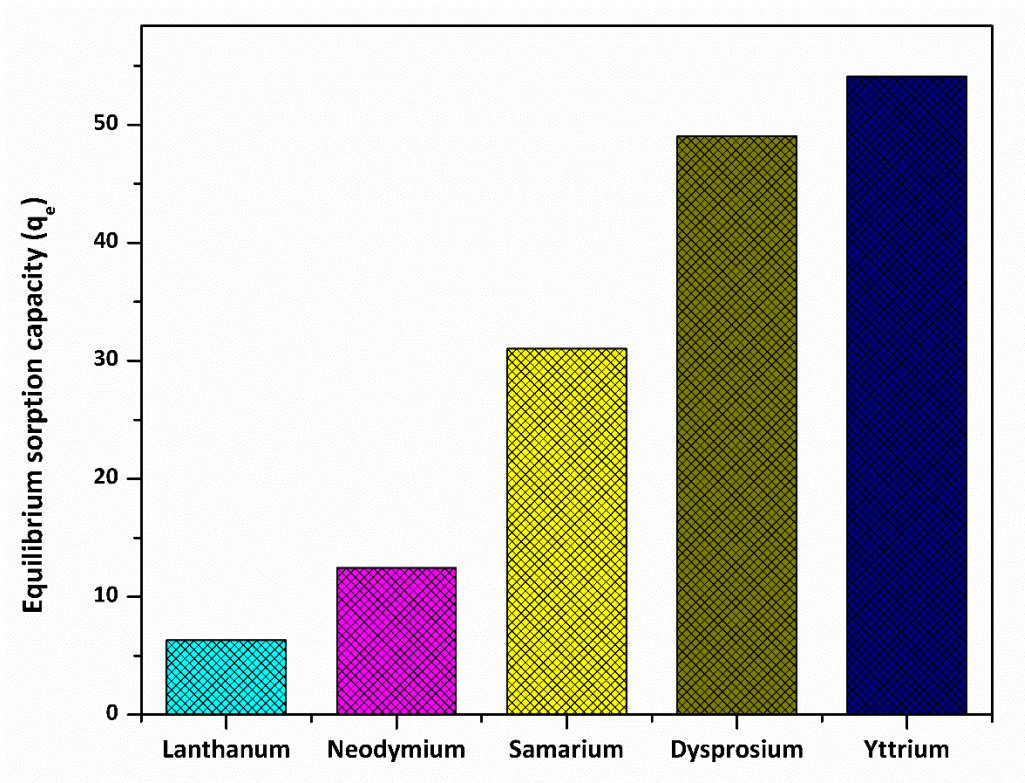


Fig. 4.9 Equilibrium sorption capacity for different rare earths (La, Nd, Sm, Dy, Y) sorption by PES/PVA/MWCNT/ EHEHPA beads (Feed phase:100 mL of 0.3N HCl, Rare Earth element concentration: 2.5 g/L, Stirring speed: 250rpm, Contact time: 8 hours)

The experimental findings are presented in Fig.4.9, where equilibrium sorption capacity of PES-EHEHPA for individual rare earth elements is depicted. PES-EHEHPA beads equilibrium sorption capacity for rare earths followed the order $Y > Dy > Sm > Nd > La$ respectively. Polymeric beads were also tested for individual rare earths extraction from aqueous feed solution consisting mixed rare earths i.e. La: 514; Nd: 522; Sm: 558; Dy: 612; Y: 654 mg/L in 0.3M HCL aqueous feed phase.

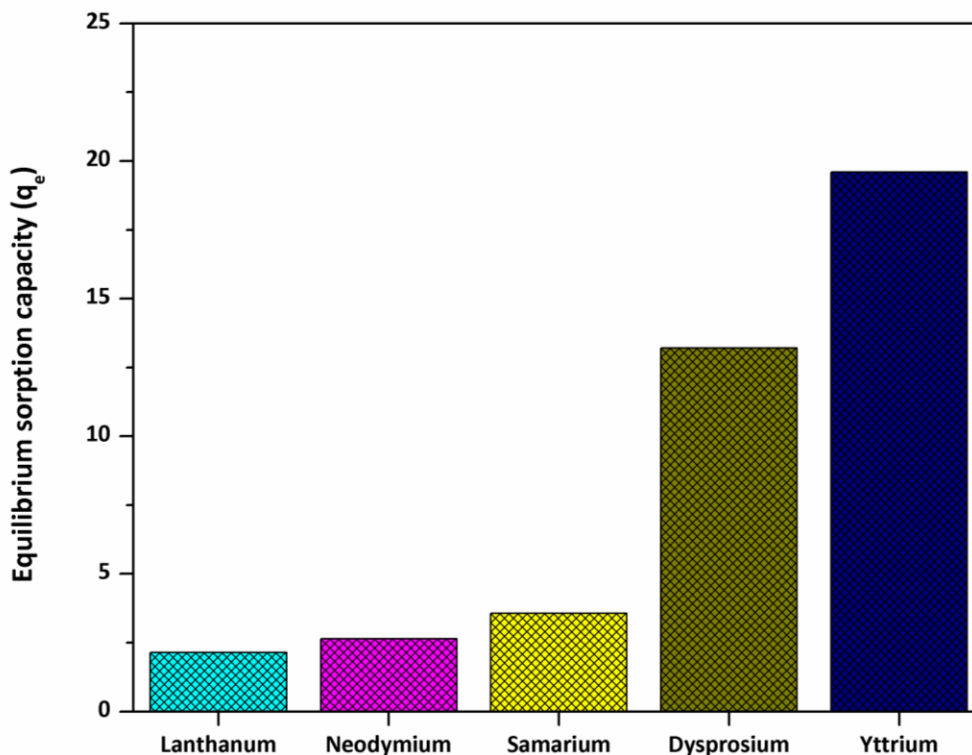


Fig. 4.10 Equilibrium sorption capacity(mg/g) for different rare earths (La, Nd, Sm, Dy, Y) sorption by PES/PVA/MWCNT/PC88A beads from Mixed RE feed (Feed phase:100 mL of 0.3N HCl, Rare Earth concentration in feed: La: 514; Nd: 522; Sm: 558; Dy: 612; Y: 654 mg/L, Stirring speed: 250rpm, Contact time: 8 hours)

Results (Fig. 4.10) indicated that PES-EHEHPA beads had higher sorption capacity for heavier rare earths (Y and Dy) in the mixture whereas minimum sorption capacity for lighter rare earths (La, Nd, Sm). This clearly demonstrated the ability of novel MWCNT embedded PES-EHEHPA beads for efficient separation of Y(III) and Dy(III) from La(III), Nd(III) and Sm(III).

4.12 Yttrium recovery from loaded EHEHPA beads

Subsequent to the optimization of sorption parameters, experiments were carried out to evaluate the stripping agents for the recovery of Y(III) from RE loaded EHEHPA/PES beads.

Varying concentration of HCl (25%, 40% v/v) were screened for the stripping of rare earths from loaded beads.

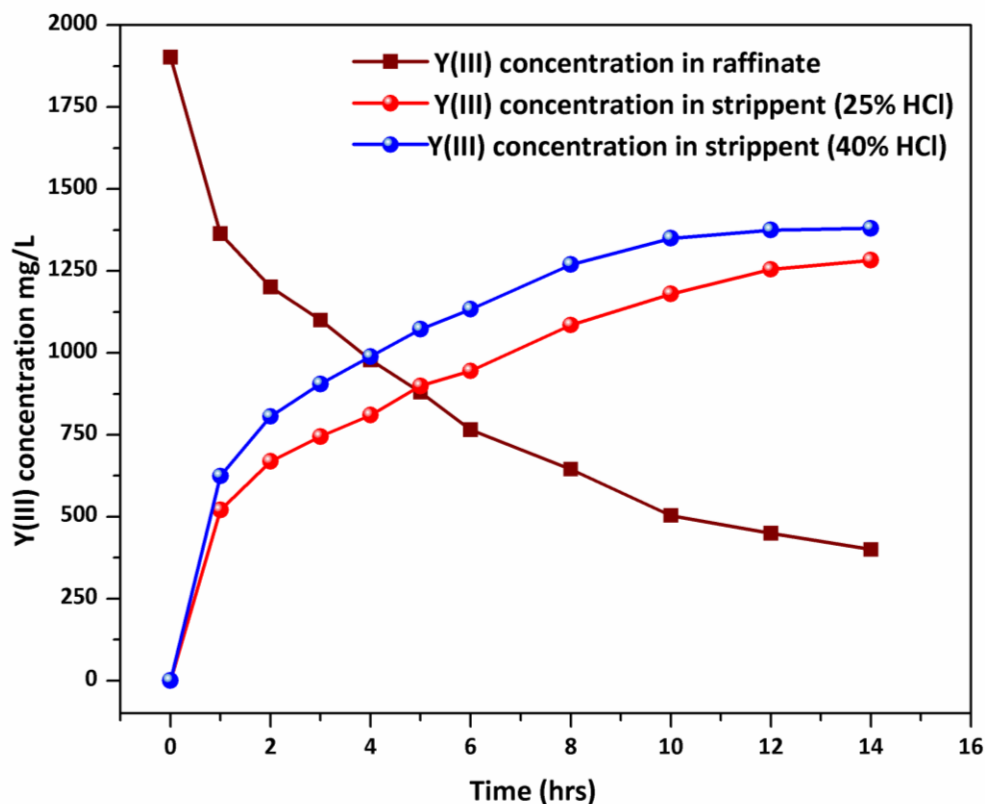


Fig. 4.11 Effect of stripping agent on Y(III) stripping from loaded beads (weight of PES/PVA/EHEHPA beads: 10g, strip phase: 100 mL, Y(III) loading in beads with aqueous phase: 1.9 g/L Y(III) 0.3 N HCl, stirring speed: 250rpm, contact time: 14 hours)

Fig. 4.11 shows that increase in concentration of HCl from 25 to 40% (v/v) resulted enhancement in Y(III) stripping from EHEHPA polymeric beads loaded with yttrium from feed solution containing 1850 mg/L. In the case of stripping by sulphuric acid, 30% H_2SO_4 was found to optimum for Y(III) extraction from loaded beads as further increase in concentration decreases the stripping efficiency due to increase in viscosity of stripping agent. The above observation led to the conclusion that both 30% H_2SO_4 and 40% HCl were suitable for stripping of rare earths

from polymeric beads. HNO_3 was not explored as a medium for extraction due to its oxidative nature towards polymeric material (PVA).

4.13 Reusability and stability of EHEHPA composite beads

The effect of reuse and recycling of EHEHPA encapsulating polymeric beads on the sorption of Y(III) from aqueous streams and subsequent loss of encapsulated extractant EHEHPA from the beads during the reuse was evaluated.

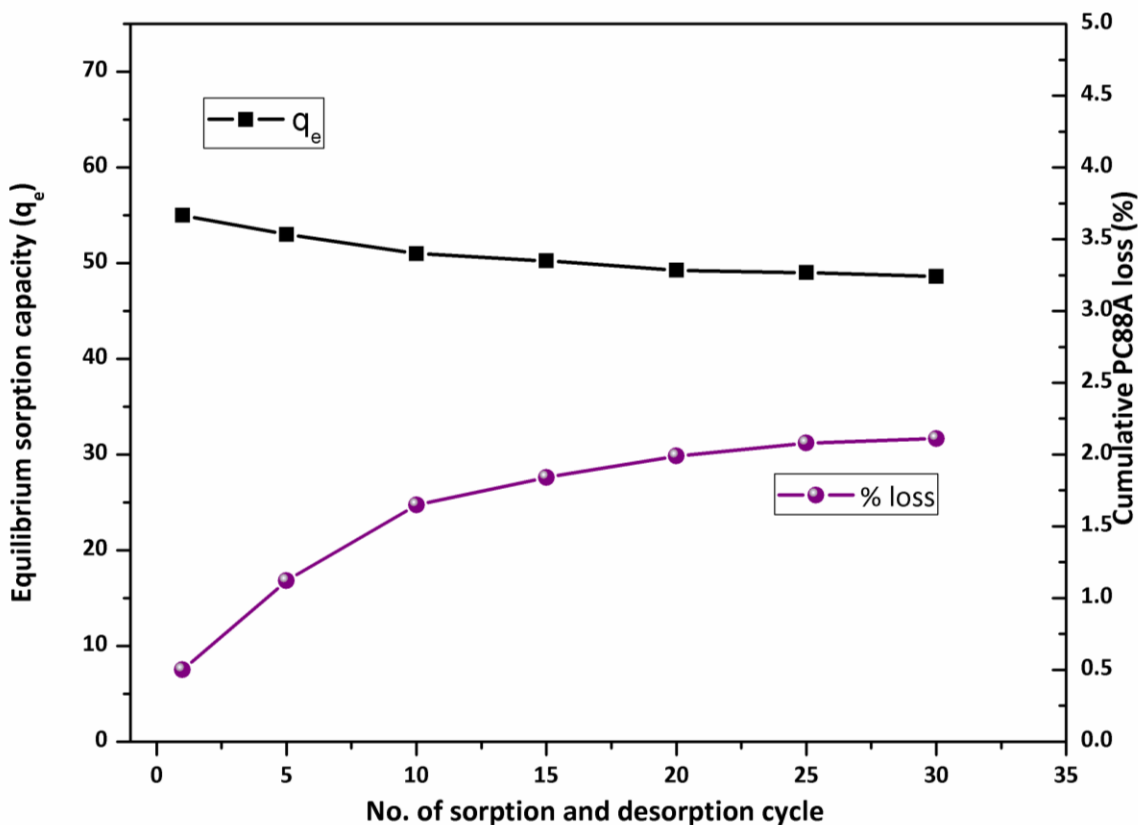


Fig. 4.12 Effect of sorption and desorption of Y(III) from PES/ EHEHPA beads on cumulative percentage loss of encapsulated EHEHPA and on equilibrium sorption capacity(q_e).

To investigate the cyclic stability of polymeric beads, the Y(III) sorption was investigated with EHEHPA/PES beads from (0.3M HCl containing 1000 mg/L of yttrium) at an appropriate 1: 10:: S:L ratio and temperature (30°C) followed by the stripping of Y(III) with 6M HCl,

subsequently the same beads were reused for 30 cycles of extraction and stripping in a similar way. The results shown in Fig. 4.12 indicate that the EHEHPA/PVA/MWCNT/PES beads show little deviation from their q_e values (56 to 49mg/g) for Y extraction even after reused for 30 cycles.

Fig. 4.12 also represents the cumulative loss of EHEHPA after repeated use of these EHEHPA/PES beads. EHEHPA loss in aqueous medium during extraction of Y(III) was monitored after each extraction and stripping cycle upto 30 cycles following the procedure reported by Pullianen et. al [153]. Leaching out of EHEHPA in the aqueous solution through the pores of the beads was found to be in the range of < 2.1% (Fig.4.12). This loss of EHEHPA from the pores of polymeric beads is significantly less (< 2.1% after 30 cycles) when compared with other XAD based solvent impregnated resins (5-25% after 10 cycles)[179]. This can be attributed to the presence of nanoporous dense surface layer and presence of water and NMP solvent (section 3.2 and 3.3) near the peripheral pores of polymeric bead. This presence of aqueous layer around the organic phase in polymeric beads prevent the loss of viscous organic extractants[154]. The reduced loss or non-leachability of EHEHPA from EHEHPA/PES beads indicate its employability in the field of hydrometallurgy for the separation and concentration of metal ions from aqueous solutions.

4.14. Conclusions

Polyethersulfone beads encapsulating EHEHPA and were prepared by phase inversion method. The synthesized EHEHPA-PES beads morphology and internal microstructure is modified and optimized by introducing suitable additives namely, multiwall carbon nanotube (MWCNT), polyvinyl alcohol (PVA) in polymeric beads matrix. The developed polymeric beads consisting PES/EHEHPA/PVA/MWCNT found to be most efficient to recover yttrium along

with rare earths from aqueous solution with minimum loss of encapsulated extractants. The developed 3 M EHEHPA-PES beads not only recovers rare earths values (with Q_e values as high as 56 mg/g) from aqueous phase but also addresses to the problems of environmental hazards originating from the use of organic diluents in conventional solvent extraction process. Moreover, these developed EHEHPA-PES beads offers added benefit of extraordinary stability and recyclability of beads as compared to the other conventional methods.



Chapter 5

TRANSPORT STUDIES ON RARE EARTHS BY HOLLOW FIBRE LIQUID MEMBRANE

5 Transport studies on rare earths by Hollow Fibre Liquid membrane

Rare earth metals (REMs) consist of fourteen lanthanides and three elements which are Sc, Y and La. Thus, the total number of REMs is 17. In the last decade, these rare earths elements which have unique physical and chemical properties have been highly in demand for their application in almost all walks of life. Rare earth metals have been also widely used in petrochemical, glass, ceramics, fluorescent materials, electronic material, medicine, agriculture department, a lot of modern science and technology field [180]. In China, there are abundant rare earth resources. With the development of rare earth industry, the application of rare earth elements widely for transport and enrichment has become more and more necessary [181]. Various methods can be used to recover these metals from aqueous solutions. Traditional methods, such as ion exchange, precipitation and solvent extraction also have been some inherent disadvantages along with their ineffectiveness to recover a very low concentration of contaminated metal ions [182, 183]. In earlier chapters; I have elaborated the importance of alternative methods for the separation and purification of rare earths. Chapter 3 and 4 of the present thesis elaborate the development and application of polyethersulfone based solvent encapsulated beads for this purpose. In this regard, another important technique i.e. liquid membrane methods offers separation schemes, this combines the characteristics of solvent extraction with solid membrane separation. Membrane separation processes are used in a wide variety of industrial and medical applications for separation of ions, macromolecules, colloids, and cells. The most important advantages of membrane processes are their unique separation capabilities and ability to adapt in diversified conditions including easy scale-up. In some fields membranes are already proven technology and are incorporated in various production lines or purification processes [184-187]. Membrane technology dealing with various applications has

generated businesses totaling more than one billion U.S. dollars annually [188]. Systems based on hollow fiber membrane contactors can make chemical plants more compact, more energy efficient, cleaner, and safer by providing a lower equipment size-to-production capacity ratio, by reducing energy requirements, by improving efficiency, and by lessening waste generation, with the correct choice of membrane material. The loss of organic from the membrane (by entrainment) can be reduced to levels lower than those expected in other type of contactors. In addition, traditional stripping, scrubbing, absorption, and liquid-liquid extraction processes can be carried out in this new configuration. It has several potential advantages compared to the conventional methods of solvent extraction technique. Liquid membrane transport of rare earth metals is characterized by a short process, high speed, great enrichment ratio, little reagent consuming and low cost, which has extensive industrial application prospect.

In particular, a hollow fiber liquid membrane (HFLM) contactor is an excellent system for the extraction of metal ions at very low concentration from various solutions. This method allows for both simultaneous extraction and stripping of target ions in one single-step operation or non-dispersive mode of metal extraction which is similar to conventional liquid-liquid extraction[189]. Many advantages of HFLM over traditional methods include lower energy consumption, lower capital and operating costs, and less solvent use. It also offers a higher mass transfer rate per unit surface area [190]. The application of HFLM was considered for rare earths separation studies due to the previous success of radioactive, alkali metal and lanthanide metal separation by various research groups [191-194]. In this chapter the transport behavior of rare earths (Dy, La, Sm etc) in Hollow Fibre Membrane is evaluated.

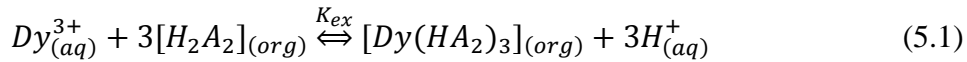
The Non-dispersive solvent extraction (NDSX) and supported liquid membrane (HFSLM) are the two mode of operation evaluated for these transport studies. In the NDSX

method, an organic phase passing through one side of the membrane wets the microporous hydrophobic membrane. A non-wetting aqueous phase is passed through other side of the membrane at a pressure higher than that of the organic phase, but lower than that needed for the aqueous phase to displace the organic phase in the pores of the membrane. The aqueous–organic (aqueous–membrane) interface is essentially immobilized at the pore mouth of the hydrophobic membrane support through which the solute mass transfer takes place. Here, the membrane support does not function as a size selective sieve, but it merely prevents the dispersion of one phase into the other. Moreover, with hollow fiber based NDSX, the limitations of hollow fiber supported liquid membrane based methods such as membrane stability are largely overcome. The batch solvent extraction experiments suggested that PC88A in petrofin is a suitable carrier solvent for polypropylene hollow fibre membrane. Various experiments were carried out to evaluate the effect of feed acidity, metal ion concentration, carrier concentration, feed composition, flow rates and phase ratio on the transport of rare earths metal ions across the membrane. The experimental findings discussed in this chapter revealed that in non-dispersive mode of operation with 0.5M EHEHPA as carrier solvent, ~98% of Dy(III) in aqueous feed has been transported across the membrane. Similarly, in the case of stripping of loaded carrier by this mode resulted in ~96% recovery in 1 hour under optimized condition. In another set of experiments Dy(III) transport has been investigated by Hollow fibre supported liquid membrane containing EHEHPA as carrier solvent. Various process variables such as feed acidity, metal ion concentration, carrier concentration, feed composition, flow rates and phase ratio were altered to achieve an optimized experimental conditions to achieve maximum Dy(III) recovery. Under optimized experimental condition >94% recovery of Dy(III) from aqueous feed solution can be attained in 2 hours of operation. Quantitative transport of rare earths was also achieved during

non-dispersive as well as supported liquid membrane mode of operation, when EHEHPA was used as a carrier. Studies on the effect of interfering rare earth ions on the transport of Dy(III) has been also discussed in this chapter.

5.1 Batch Extraction of Dy(III) by EHEHPA

Literature reports and slope analysis experiments indicate that EHEHPA exists as a dimer in paraffinic hydrocarbon based diluents [195]. The liquid liquid extraction of Dy(III) from nitric acid medium by EHEHPA results in the formation of extracted species consisting 3 EHEHPA dimers shown in equation 1.



Where H₂A₂ shows the dimer form of EHEHPA in nonpolar diluents, K_{ex} denoted in equation 5.2 is the equilibrium constant for the chemical reaction shown in eq. 5.1 while subscripts (aq.) and (org.) depicts the aqueous and organic phase respectively.

$$K_{ex} = \frac{[Dy(HA_2)_3]_{(org)}[H^+]_{(aq)}^3}{[Dy^{3+}]_{(aq)}[H_2A_2]_{(org)}^3} \quad (5.2)$$

The distribution coefficient of the metal ion (D) is the ratio of Dy(III) concentration in the organic phase to that of in the aqueous phase as represented in equation 5.3.

$$D = \frac{[Dy(HA_2)_3]_{(org)}}{[Dy^{3+}]_{(aq)}} \quad (5.3)$$

The distribution coefficient values for Dy(III) extraction by 0.5M PC88A as function of nitric acid concentration were evaluated and shown in table 1. Results indicated that with increase in aqueous phase acidity from 0.1 to 0.75M HNO₃ distribution ratio for Dy extraction by PC88A decreases from 53 to 0.3. It is reported that increase in feed acidity decreases the D value because of the protonation of EHEHPA. The distribution data indicated that the extraction of Dy(III) can only be performed below the acidity value of 0.3 M HNO₃.

Table 5.1: Distribution Coefficient (D) for Dy(III) extraction by EHEHPA from different aqueous phase acidities: Organic Phase: 0.5 M EHEHPA in petrofin, aqueous phase: 1089 mg/L Dy

[HNO₃], M	D
0.1	53.48
0.3	3.91
0.5	1.15
0.75	0.35

5.2 Membrane based transport studies

In view of various advantages of Holow Fibre Membrane based liquid membranes over other methods, the aim of the present study was to develop suitable liquid membrane technique for the recovery of rare earth values from aqueous acidic solutions. In the present work, transport behaviour of Dy(III) by employing hollow fibre membrane contactor in both NDSX and HFSLM mode was investigated. Subsequently various system parameters were studied to optimize the experimental conditions.

5.2.1 Non-dispersive solvent extraction by hollow fibre membrane

A commercial module measuring 2.5"×8" described in section 2.2.7 of chapter 2 with about 10,000 microporous hydrophobic hollow fiber of polypropylene lumens was used in the present work. During the experiment aqueous and organic phases were contacted in counter-current mode in the hollow fibre module in recycling mode. Since the membrane is hydrophobic and the organic phase easily wets the polypropylene fibers, to prevent the dispersion of the organic phase into the aqueous feed phase a trans-membrane pressure of 3 psi in the lumen side

is applied [196]. The aqueous and organic solutions in the reservoir were agitated continuously to provide uniform concentration of metal ion. Samples from aqueous feed and organic phase were removed from bulk of the reservoir at different time intervals for analysis.

5.2.1.1 Effect of aqueous phase acidity on Dy extraction

In the case solvent extraction by organophosphorus based acidic extractants, aqueous phase acidity plays key role in extraction as well as stripping of metal ion. Effect of aqueous phase acidity was investigated for Dy (III) extraction by 0.5M PC88A organic extractant at phase ratio of 1:1 in non-dispersive mode of operation. Results indicated in Figure 5.1 illustrates that increase in acidity from 0.1 to 0.5 M HNO_3 decreases percentage extraction of Dy(III) from 99.5 to 45.2 when extracted by 0.5M PC88A across the membrane in non-dispersive mode of operation. Increase in acidity also affects the equilibration time required from 30 to 60 minutes to achieve the quantitative transport of Dy(III) from aqueous phase to organic phase. The loaded organic phase of 0.5M PC88A with Dy(III) resulted from this experiment was quantitatively stripped by equilibrating the organic phase with 3.5 M HNO_3 in separating funnel. The regenerated 0.5M PC88A was reused for the repeat experiments and results obtained showed excellent reproducibility in terms of Dy(III) extraction and no degradation of solvent system/membrane.

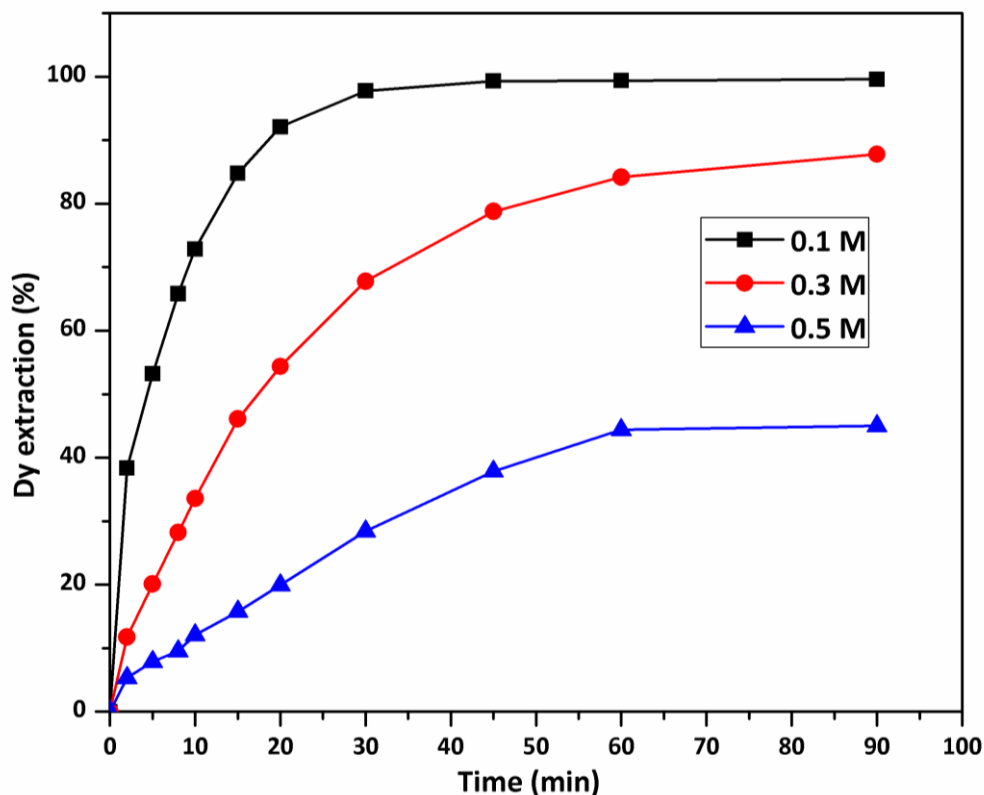


Fig. 5.1 Effect of Aqueous phase acidity on the extraction of Dy(III) by 0.5 M PC88A; aqueous phase: 1000mg/l; flow rate: 100mL/min, Phase ratio: 1:1

5.2.1.2 Effect of flow rate

In order to study the mechanism of mass transfer in NDSX mode of operation in HFM and determinate the rate determining part of part of total mass transfer resistance, it is necessary to investigate the hydrodynamic characteristics of current system. The flow rates in both feed phase and extractant phase play a vital role in the transport of metal ion from the feed side to the organic side. Flow rates of both organic and aqueous phases in non-dispersive solvent extraction carried out in hollow fibre membrane affects the contact time of organic and aqueous phase at the interface. In the case of Dy(III) extraction by 0.5M PC88A effect of organic phase flow rate was examined by varying them in the range of 50 to 200 mL/min while keeping aqueous phase flow rate constant at 100 mL/min. Results shown in fig 5. 2. indicates that though the extraction

of Dy(III) in organic phase was quicker at lower flow rate in the initial stages of the experiment (< 10 min of run) but after 30 min of contact time extraction Dy(III) was almost unaffected by the flow rate.

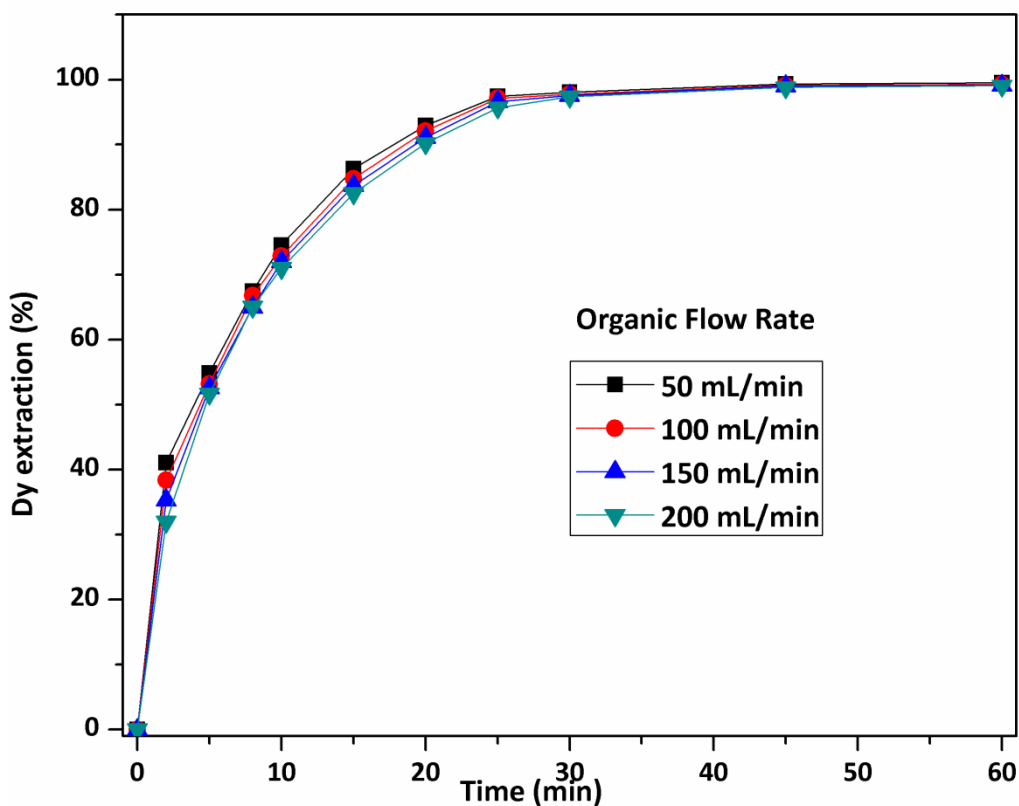


Fig. 5.2 Effect of organic phase flow rate on the percentage extraction of Dy(III) at fixed aqueous phase flow rate (100ml/min); organic phase: 0.5 M PC88A; aqueous phase: 1000mg/l of Dy(III) at 0.1M HNO₃; Phase ratio: 1:1

The result indicated that >99.1% Dy(III) could be transported in the organic phase i.e. 0.5M PC88A in 35 min at the differing flow rates. Similar kind of results were also observed when aqueous phase flow rate was varied between 50 to 200 mL/min keeping organic phase flow rate at 100 mL/min. Due to the insignificant effect of aqueous and organic phase flow rates on

equilibrium extraction of Dy(III), all subsequent experiments were performed at 100 mL/min flow rate of both the phases.

5.2.1.3 Effect of Dy(III) concentration

Effect of Dy(III) concentration in aqueous feed phase on its transport across the membrane and extraction by 0.5 M PC88A organic phase was evaluated in NDSX mode by employing HFM contactor.

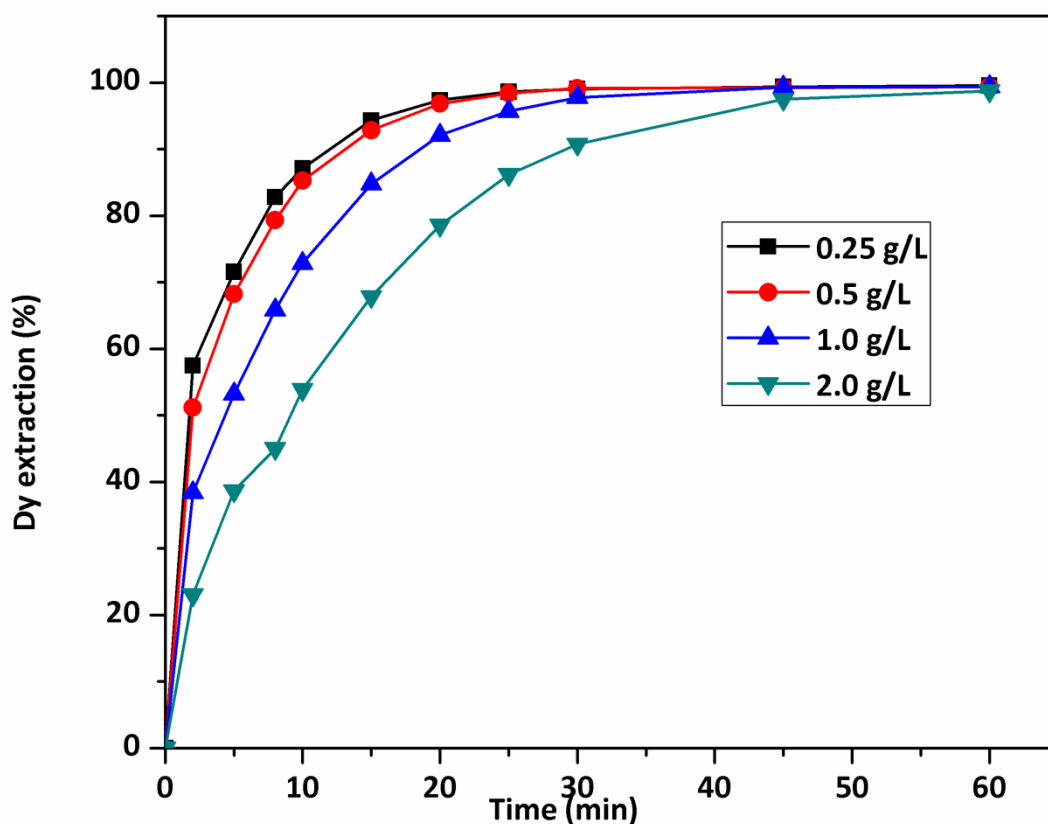


Fig. 5.3 Effect of Dy(III) concentration on its extraction by 0.5M PC88A organic phase and 0.1M HNO₃ aqueous phase at flow rates of 100 mL/min for both the phases

Figure 5.3 represent that increase in Dy(III) concentration from 250 to 2000 mg/L increases the time required for the quantitative (99%) transport across the membrane. However,

in all the cases >98% extraction of Dy(III) from aqueous phase was observed in 60 minutes even with 2000 mg/L Dy (III) in the feed phase. The loaded organic phase of 0.5M PC88A with Dy(III) resulted from this experiment was quantitatively stripped by equilibrating the organic phase with 3.5 M HNO₃ in separating funnel. The strippent was later analyzed for Dy(III) content by ICP AES and subsequently stripping results were used to ascertain the mass balance of extraction by NDSX experiment.

5.2.1.4 Influence of organic extraction on Dy(III) extraction

PC88A concentration in the organic phase plays a significantly important role in transport of Dy(III) from feed to organic side. Effect of PC88A concentration on percentage transport of Dy(III) was studied in the extractant concentration range from 0.2 mol/L to 0.83 mol/L.

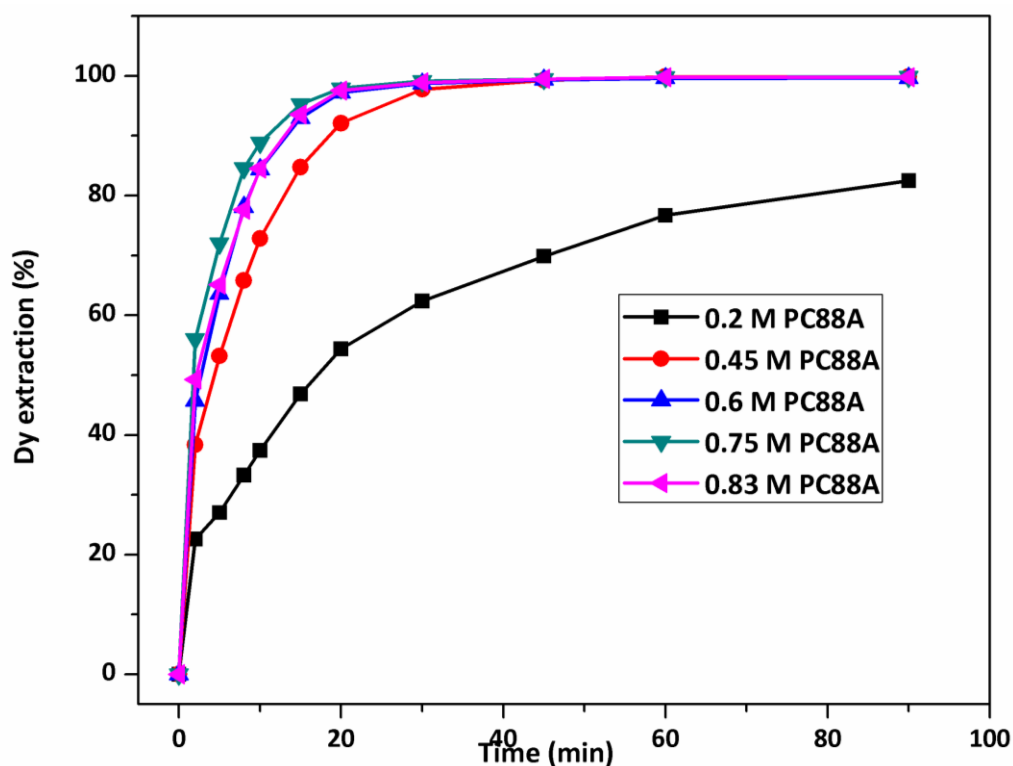


Fig. 5.4 Effect of Dy(III) concentration on its extraction by 0.5M PC88A organic phase and 0.1M HNO₃ aqueous phase at flow rates of 100 mL/min for both the phases

The results of percentage Dy(III) transport obtained from varying concentration of PC88A are shown in Fig. 5.4. With the increasing of concentration of carrier in the organic phase from 0.2 mol/L to 0.45 mol/L, the % transport of Dy(III) after 90 minutes of equilibration, increased from 82 to 99, however, when PC-88A concentration increased from 0.45 mol/L to 0.83 mol/L, the increase in % extraction of Dy(III) was not obvious. Within this concentration of PC-88A range from 0.2 mol/L to 0.45 mol/L, the availability of PC88A at the feed–membrane–organic interfaces increased with the increasing of concentration of carrier. The chemical equilibrium moved toward left, vice versa, when concentration of PC88A became low, the equilibrium moved toward the right [190]. When the PC-88A concentrations were 0.2, 0.45, 0.6, 0.75 and 0.83 mol/L, the percentage extraction values were 82.49, 99.60, 99.65, 99.81 and 99.80, respectively. The optimum concentration of PC88A to perform further experiments was chosen to be 0.5mole/L in petrofin.

5.2.1.5 Effect of phase ratio

Loading of Dy(III) in the organic solvent phase i.e. 0.5M PC88A were performed by varying phase ratio of organic to aqueous phase in the range of 0.25 to 1. Experimental results depicted in figure 5.5 suggest that the time required to achieve quantitative recovery of Dy(III) from aqueous to organic phase increased with decrease in organic to aqueous phase volume ratio. At organic to aqueous phase ratio of 1, about 25 min were required for the quantitative extraction of Dy(III) from a feed phase containing 1.0 g/L Dy(III) in 0.3 M HNO₃. Under the comparable experimental conditions with only variation in phase ratio (O/A) of 0.5 and 0.25, quantitative extraction of Dy from aqueous phase to organic took around 80 and 130 minutes respectively. It is also observed that ~96% extraction of Dy(III) could be achieved in the case O/A of 0.25 which is relatively less than the recovery obtained in phase ratios of 0.5 or 1.

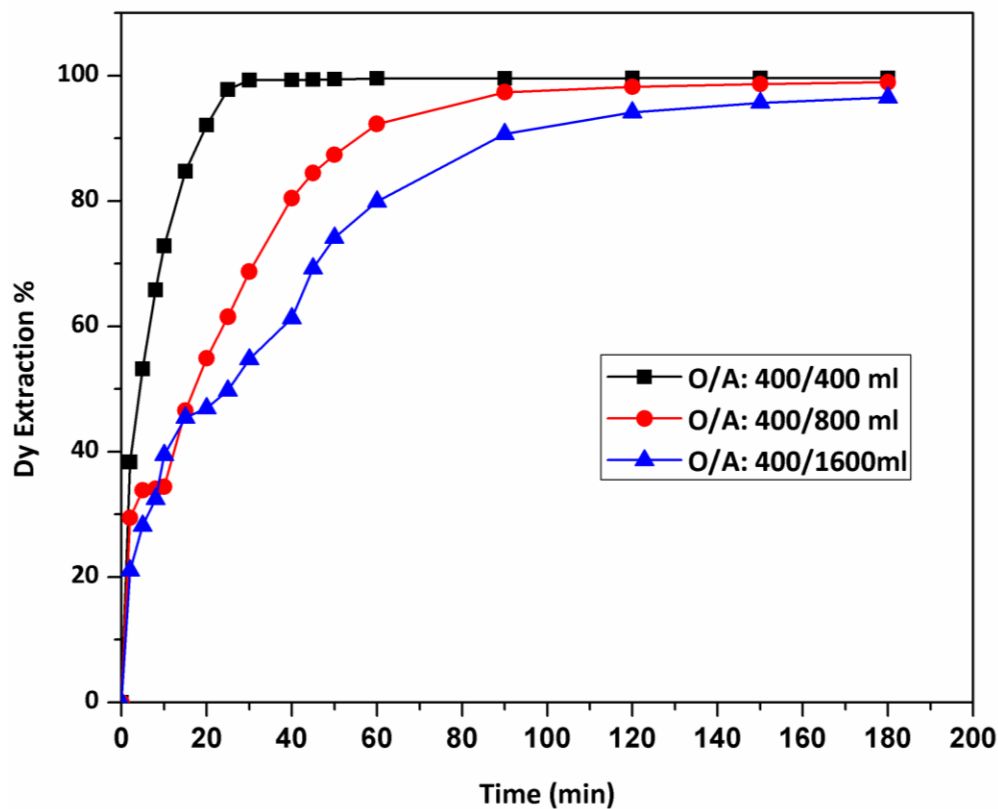


Fig. 5.5 Extraction of Dy(III) at different organic to aqueous phase volume ratios; organic phase: 0.5M PC88A; aqueous phase: 1.0 g/L Dy(III) at 0.3M HNO₃; flow rate: 100 mL/min.

5.2.1.6 Effect of competing metal ions

To evaluate the transport phenomenon of Dy(III) in presence of other rare earths such as La and Sm, an aqueous feed solution consisting 1 g/L each of La, Sm, Dy in 0.3 M HNO₃ was equilibrated in HFM module with 0.5 M PC88A. Experimental results depicted in figure 5.6 indicates the possibility of separating as well as purifying Dy from the mixture of other lighter and middle rare earths by employing hollow fibre membrane contactor. Dysprosium purification from the mixture of Sm and La by using PC88A in hollow fibre membrane was found to be time dependent. Fig 5.6 shows that initially % extraction of Dy(III) in organic phase increased and

rose upto 74 % in 10 minutes of contact time, however competing ions La and Sm were extracted <1.7 and <2.8 % respectively in same amount of time. This finding leads the way to recover high pure Dy from the mixture of light and middle rare earths. After complete equilibration, % extraction of Dy, La and Sm by 0.5 M PC88A in HFM contactor in NDSX mode were found to be 98.88, 54.13 and 9.28 respectively.

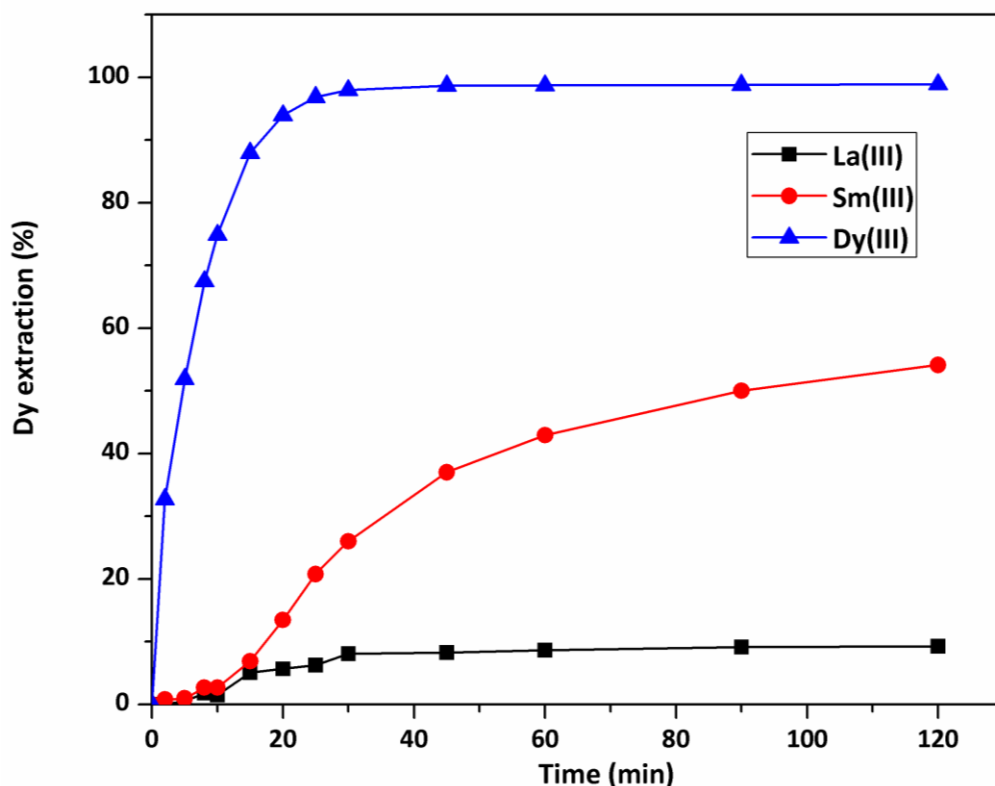


Fig. 5.6 Extraction of Dy(III) in presence of competing rare earths ions; organic phase:0.5M PC88A; aqueous phase: 1.0 g/L of Dy(III), La(III) and Sm(III) each in 0.3M HNO₃; flow rate:100 mL/min.

5.2.1.7 Stripping of Dy(III) from loaded PC88A by HFM

Stripping investigations were also performed to establish the viability of non-dispersive mode of operation by employing hollow fibre contactor to separate Dy from aqueous phase in

continuous mode operation. Furthermore, the effect of contact time at a definite flow rate of strip phase i.e. 1.5M HNO_3 on the transport of Dy(III) from loaded organic phase i.e. 0.5M PC88A was evaluated. Figure 5.7 depicts the stripping of 0.5 M PC88A loaded with 3.3 g/L Dy(III) with 1.5 M HNO_3 phase. It is evident from the results that complete stripping could be achieved with 150 minutes of equilibration through the pores of HFM.

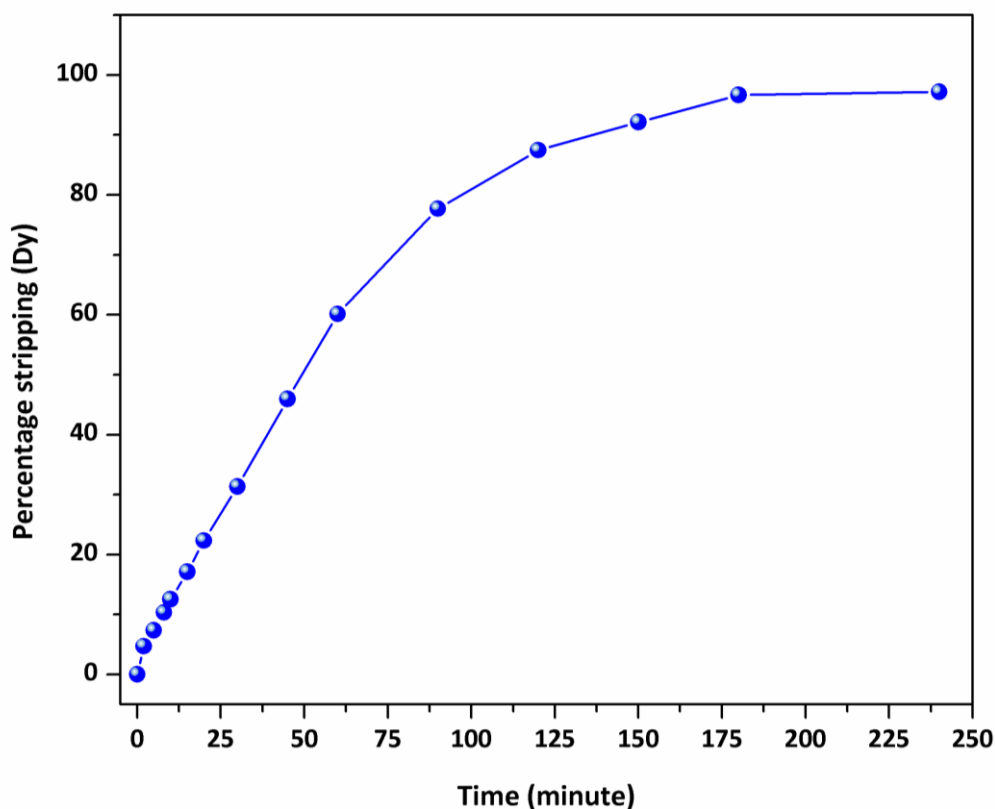


Fig. 5.7 Stripping of Dy(III) from loaded 0.5 M PC88A phase; strip phase: 1.5 M HNO_3 ; flow rate: 100 mL/min, phase ratio 1:1, organic phase 0.5 M PC88A having 3.3g/L Dy(III)

5.2.2 Hollow Fibre supported liquid membrane studies

After standardizing the process to recover Dy by employing hollow fibre membrane in Non-dispersive mode of operation which require more organic phase for loading as its being run

through shell side, I have evaluated Dy(III) separation via hollow fiber supported liquid membrane (HFSLM). In this technique carrier-mediated transport through HFSLM takes place with extraction and stripping process of target ions occurs in a single step operation. Relatively higher selectivity is obtainable from this technique by controlling (1) the extraction and stripping equilibrium at the interfaces and (2) the kinetics of transported species under non equilibrium mass transfer process [197, 198]. One of the most important advantages of such a system and possibility to use this for rare earths separation is the possibility for selectivity and its ability to tune the transport by controlling the pH of the aqueous feed and/or receiving phases. The HFSLM process has several advantages, such as low energy consumption and a lower amount of extractant solution used, when compared with non-dispersive solvent extraction [199]. It also has a larger mass transfer per unit surface area [200]. HFSLM offers unique simultaneous extraction and recovery applications [201]. This method is suggested as a viable technique for achieving metal extraction at very low concentrations [202]. A commercial module measuring 2.5"×8" described in section 2.2.7 of chapter 2 with about 10,000 microporous hydrophobic hollow fiber of polypropylene lumens was used in the present work.

The hollow fiber supported liquid membrane (HFSLM) was prepared by pumping organic extractant 0.5M PC88A solution through the lumen side of module at a pressure of 5 kPa in recirculation mode. To ensure the complete soaking of the membrane pores, the extractant phase was circulated for ~15 min when the solution started percolating from lumen side to the shell side. The excess of organic phase was washed out completely with sufficient distilled water, prior to the introduction of the feed and strip solutions. For all the experiments, the feed solution was passed through the lumen side while strip solution was passed through the shell side of the module in recirculation mode. Both feed and receiver phases were contacted inside the

hollow-fiber module in counter-current flow for the effective transport of metal ions.

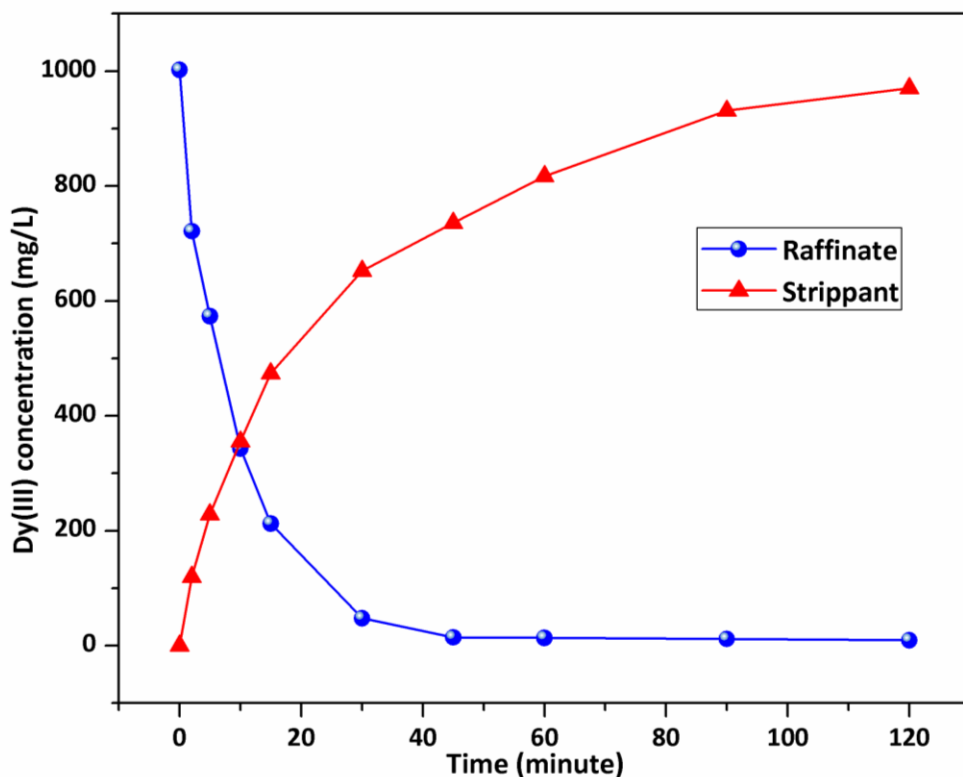


Fig. 5.8 Simultaneous extraction and stripping of Dy by PC88A as carrier in HFSLM mode Carrier: 0.5 M PC88A in petroffin; feed, 1 g/L Dy (400 mL); strippant, 3M HNO₃ (400 mL); flow rate, 100 mL/min; temperature, 25 °C.

The flow rates of the feed and strip solutions were maintained constant at 100 mL/min with the help of gear pumps equipped with precise flow controllers. A schematic diagram of hollow fiber unit is shown in Figure 2a. The transport behavior of Dy (III) was evaluated by varying experimental parameters. Initial studies performed to optimize the minimum experimental conditions revealed that flow rate of 100 ml/min along with 1 g/L Dy(III) in aqueous nitrate media may be employed for the experiments. PC88A was chosen as an carrier solvent in the present studies. Fig. 5.8 represents the extraction and stripping against time scale when 1 g/L of Dy solution having 0.1 M HNO₃ was equilibrated against the carrier concentration

of 0.5 M PC88A and 3 M HNO₃ on the strip side of the HFSLM setup. As evident from fig 5.8 quantitative transport of Dy from aqueous feed side to carrier side is attained around 30 in minute whereas at least 60-90 minutes of recirculation is required to completely strip the loaded carrier phase.

5.2.2.1 Effect of aqueous Feed Acidity

The effect of aqueous feed acidity on the transport of Dy(III) was investigated from a feed solution containing 1 g/L Dy(III) and the results are shown in Figure 5.9.

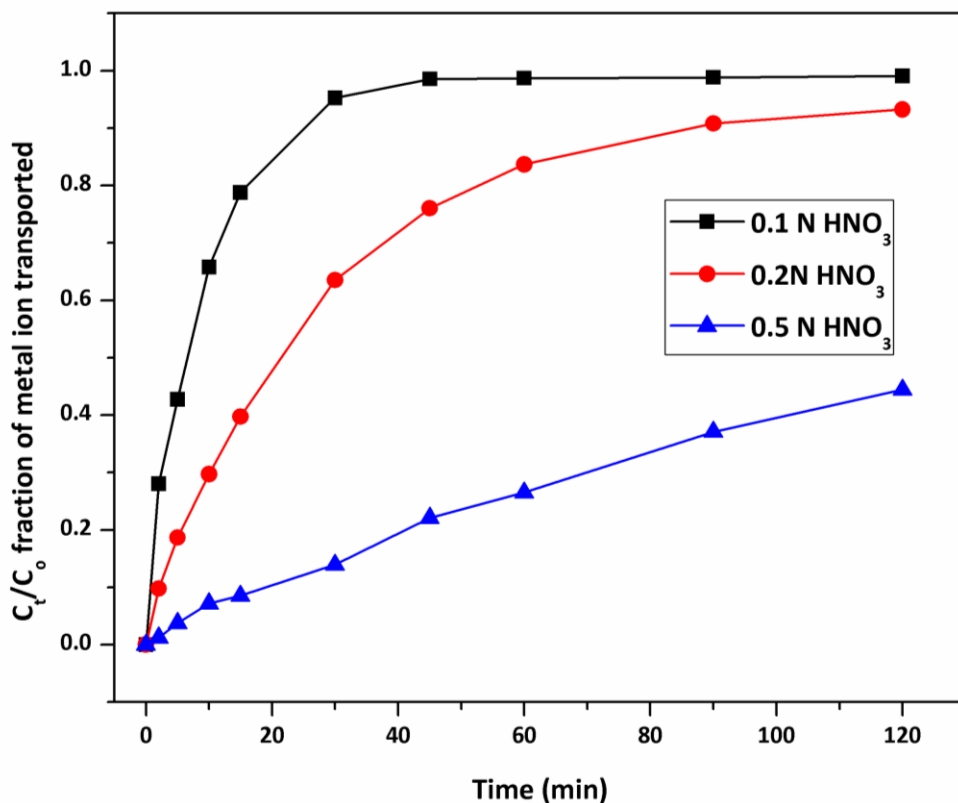


Fig. 5.9 Influence of feed acidity on the permeation of Dy(III) by HFSLM. Carrier, 0.5 M PC88A in petroffin; feed, 1 g/L Dy (400 mL); strippant, 3M HNO₃ (400 mL); flow rate, 100 mL/min; temperature, 25 °C.

The results revealed decrease in permeation of Dy(III) with the feed acidity being increased up to 0.5 M HNO₃. With increased nitric acid concentration, the H⁺ concentration is also increased and, therefore, equilibrium reaction 5.1 is favored toward the reverse side. Higher concentration of HNO₃ in strip side assured the complete transport of Dy metal ions loaded in the carrier phase. Results depicted in figure 5.9 shows that >98% of Dy is being transported from the feed phase to strip side when the feed acidity was kept at 0.1 M HNO₃. On the other hand increase in the feed acidity to 0.5 M HNO₃ resulted in reduction (45 %) of Dy transport into the strip phase.

5.2.2.2 Effect of Carrier Concentration

Solvent extraction studies on Dy(III) partitioning is shown in section 5.1 by employing PC88A as the extractant. The similar study was also performed and depicted in 5.2.1.4 to evaluate the effect of organic extractant on Dy transport in non-dispersive mode of operation by HFM module. In the same context effect of PC88A concentration on Dy transport from feed side to strip side has been investigated in HFSLM mode (Fig. 5.10). Feed composition is 0.3 M HNO₃ along with 1 g/L Dy and strip side aqueous phase was fixed at 3M HNO₃. It was observed that the transport of Nd increased significantly with increase in PC88A concentration. Results shown in figure shows that increase in PC88A concentration from 0.25 M to 1.5 M enhanced the Dy metal ion transport from 85 to 98%. Interestingly the equilibration time required for quantitative transport of metal ion also increased with decrease in extractant concentration. In the case of organic extractant concentration > 0.5 M PC88A the equilibration time was 30 minutes whereas for 0.25M PC88A equilibration time was found to be > 60min.

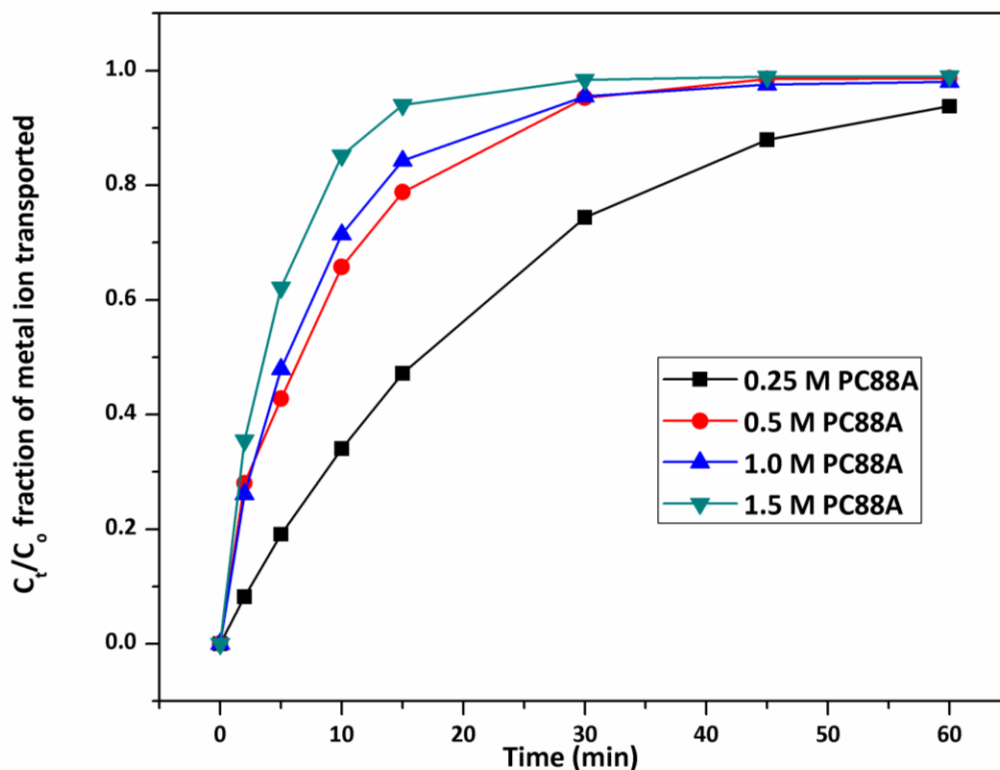


Fig. 5.10 Effect of extractant concentration on the permeation of Dy(III) by HFSLM. Aqueous feed: 0.1 M HNO₃ consisting 1 g/L Dy (400 mL); strippant, 3M HNO₃ (400 mL); flow rate, 100 mL/min; temperature, 25 °C.

5.2.2.3 Effect of competing metal ions on Dy transport in HFSLM mode

The main objective of these investigations is to achieve a reasonable separation and purification of rare earths from other competing ions. Section 5.2.1.6 represented the Dy separation from the mixture of La and Sm by employing non dispersive mode of solvent extraction in hollow fibre membrane module. The similar set of experiments has been performed to see the effect of competing ion when PC88A has been used as carrier solvent in HFSLM mode. Figure 5.11 shows the results obtained from the study, which indicate that in the case of hollow fibre supported liquid membrane the separation of Dy from the mixture is even easier when compared with the non-dispersive method.

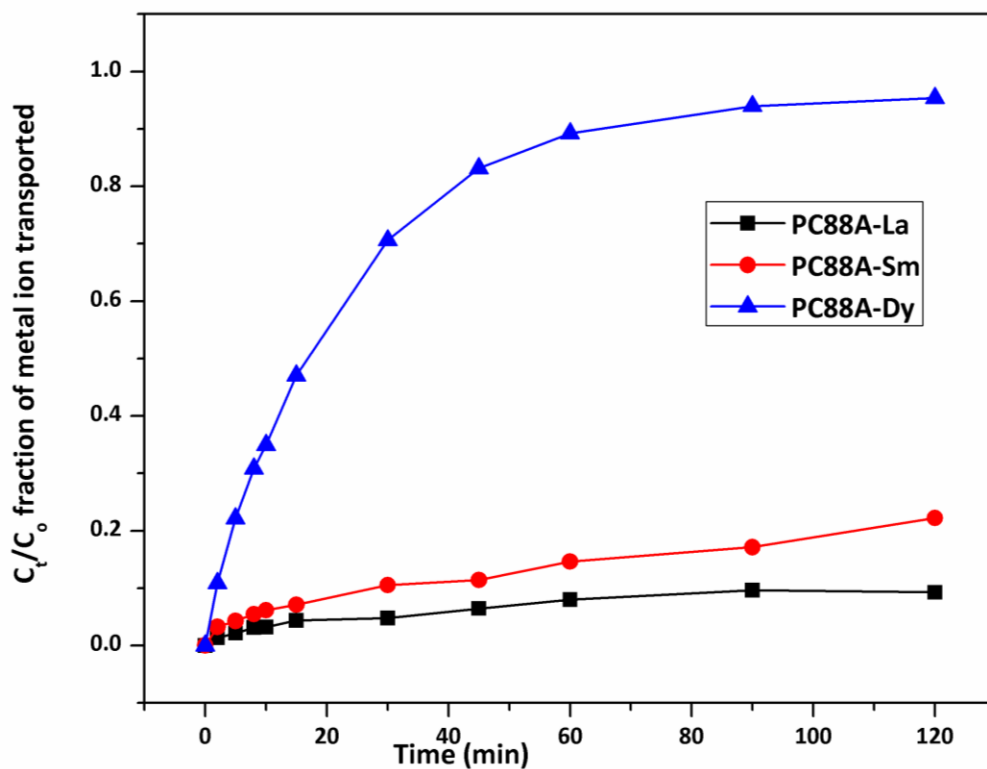


Fig. 5.11 Transport of Dy(III) in presence of competing rare earths ions; organic carrier phase: 0.5M PC88A; aqueous feed phase: 1.0 g/L of Dy(III), La(III) and Sm(III) each in 0.3M HNO_3 ; flow rate: 100 mL/min, strip phase 3 M HNO_3

Quantitative transport (~70%) of Dy has been achieved after 30 minutes of recirculating the feed phase which also consisted Sm and La. After 20 minute of equilibration the strip phase composition revealed that >90% pure Dy(III) with almost 65 % recovery could be achieved from the HFSLM mode of operation. Complete equilibration and quantitative transport could only be achieved after 120 minutes of contact among aqueous feed, carrier phase and strip phase in the module.

5.2.2.4 Evaluation of permeation coefficient for Dy transport

The permeability coefficient is calculated by using the following equation 5.4 as suggested by Danesi[203-205],

$$\ln \frac{C_t}{C_0} = -P \left(\frac{Q}{V} \right) \left(\frac{\varphi}{\varphi+1} \right) t \quad \text{----- 5.4}$$

where, P is the overall permeability coefficient of the transported species, C_t and C_0 are the respective concentrations of the metal ions in the feed solution at an elapsed time t (min) and at zero time, and V is the total volume of the feed solution (mL). Here, the parameter A represents the total effective surface area of the hollow fibre (cm²) which is calculated from the following equation:

$$A = 2\pi r_i L N \epsilon \quad 5.5$$

where, r_i is the internal radius of the fibre (cm), L is the length of the fibre (cm), N is the number of fibres and ϵ is the membrane porosity. The parameter, φ for a module containing N number of fibres is expressed as follows,

$$\varphi = \frac{Q_T}{P r_i L N} \quad 5.6$$

where, Q_T is the total flow rate of the feed solution (mL/min). By plotting $\ln(C_t/C_0)$ as a function of time t a straight line is expected, and according to Eqs. (5.5) and (5.6), the P value for the given system can be obtained from the fitted slope of Eq. (5.4). Fig. 5.12 represents evaluation of permeation constant for Dy transport across the membrane. For the sake of comparison data for the evaluation of P values for Erbium transport has also been depicted in the fig. 5.12 and Table 5.2 depicts percentage transport in 30 minutes along with permeability coefficient across the membrane for both the metal ions.

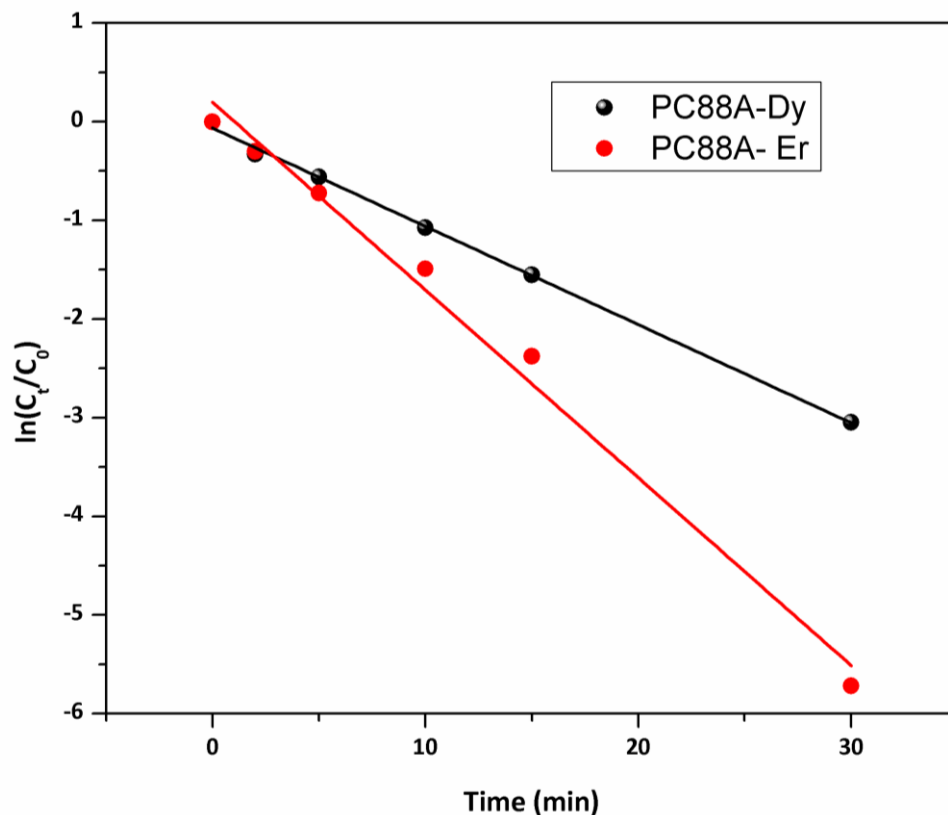


Fig. 5.12 Evaluation of P values for Erbium and Dy transport

Table 5.2 Permeability Coefficient (P) of Dy(III) and Er(III) by HFSLM System

Metal ion-PC88A	P (cm/min)	% transport in 30 minutes
Dy ³⁺	2.84×10^{-3}	75.3%
Er ³⁺	5.43×10^{-3}	88.1%

5.3 Conclusions

Transport behavior of lanthanides (La, Sm, Dy and Er) across the hollow fibre membrane pores with PC88A as an extractant have been studied by employing two types of transport methodologies i.e. non-dispersive solvent extraction and hollow fibre supported liquid

membrane. In the case of NDSX mode of operation, the extraction of Dy(III) was found to be affected by various experimental variables such as aqueous phase acidity, organic phase concentration, metal ion concentration and presence of competing ions. Successful stripping of loaded organic phase in non-dispersive mode of solvent extraction indicate the possibility of using this method in continuous operation mode even at large scale for rare earth separation. The recycling of the organic phase 0.5M PC88A resulted in excellent reproducibility of the extraction results. Under optimized conditions dysprosium could be successfully separated by using NDSX method from the mixed rare earth feed upto 95% purity and >75% recovery. While in the case of HFSLM mode 0.5 M PCC88A in petrofin was optimized as a suitable carrier for maximum transport and separation of rare earth elements from aqueous feed solution. The permeability of Dy(III) was found to be 2.84×10^{-3} cm/min with >75 % transport in 30 minutes of contact time. The % transport achieved quantitative value of 98% after 60 minutes of recirculation. The stability of the HFSLM was found to be good even after 5 successive runs.

The results obtained with the present study indicate that hollow fibre membrane module not only offers a better separation method but also have the potential to be up scaled for rare earth separation and purification.



Chapter 6

SUMMARY AND CONCLUSIONS

6 Summary and Conclusions

The aim of the present thesis work was to develop alternative techniques which require minimal amount of organic extractant, offers simultaneous extraction and stripping of rare earths and also eliminate the use of organic diluents in the process of recovering rare earths from aqueous phase. The rare-earth elements (REEs) are becoming increasingly important due to their essential role in permanent magnets, lamp phosphors, catalysts, rechargeable batteries etc. Careful examination of the current scenario in the field of rare earths separation and purification including environmental concerns, there is an urgent need to develop effective and efficient processes which not only maximizes the separation but also minimizes the environmental hazard associated with the conventional processes [22]. Presently, the most commonly used hydrometallurgical concentration and purification methods in the mining industry for rare earths separation are precipitation, liquid- liquid extraction and ion exchange [23]. However, the traditional solvent extraction process has limitations such as requirement of large volumes of organic solvents, diluents and saponification agent. Solvent extraction is a complex process and creates environmental concerns due to the use of hazardous diluents [64]. Another drawback of this process lies with the difficulty in automation as the liquid phases may form emulsions which at times leads to delay in phase separation. The work summarized in this thesis consist development of two environment benign separation techniques i.e. solvent encapsulated polymeric beads and application of hollow fibre membrane module for the recovery of rare earths (La, Sm, Dy, Y) from various aqueous streams. The brief summary of the results is given below.

This thesis reports development of novel polymeric composite beads encapsulating organic extractant (di-2-ethyl hexyl phosphoric acid (D2EHPA) and 2-ethyl hexyl phosphonic

acid (PC88A)) to separate and purify rare earths (Yttrium, Dysprosium) from lean and secondary sources. The polymeric beads were synthesized by non-solvent phase inversion technique. This one step synthesis method consists of both preparations of porous polymeric matrix and encapsulation of desired organic solvent inside the porous matrix, in one-step. The developed D2EHPA encapsulated polymeric beads act as a better alternative to the ion exchange process in terms of kinetics and mass transfer with >97% Y(III) and Dy(III) recovery. These beads can also recover rare earths from lean sources and secondary sources having rare earths concentration in ppm range. The developed beads have shown higher loading capacity (100mg of Dy / gram of dry beads) in comparison to conventional solvent extraction process. These polymeric beads also have excellent stability and reusability under harsh experimental conditions (vigorous mixing, strong acidity >50% HCl/H₂SO₄ and 100 cycle application) with minimal loss of encapsulated extractant (<2%).

This thesis also describes optimized experimental details of a stable, semipermeable, reusable and leak proof porous solvent encapsulated beads made by modifying the internal microstructure and surface morphology. The modifications were carried out with suitable additives such as polyvinyl alcohol and carbon nanotube (CNT). The modified extractant encapsulated beads have shown better separation of Yttrium and Dysprosium from aqueous streams over conventional methods. The polymeric beads have the dual advantage of liquid-liquid extraction and conventional ion exchange in terms of comparatively faster mass transfer rates and better selectivity for rare earths recovery from aqueous phase. Based on the batch experimental results, the developed polymeric beads were successfully deployed for the recovery of rare earths in continuous column operation mode, to establish its potential to industrial level scale up.

The work reported in this thesis also concludes the critical significance of optimization of various variables i.e. system compositions (polymer, additive, extractants etc.), preparatory parameters and process variables (aqueous media, metal ion, temperature, solid to liquid ratio etc.) to obtain the best suited beads by design of experiments. Taguchi, which is a multi-parameter optimization procedure, was successfully employed in the present developmental work to identify and optimize process parameters with a minimum number of experiments. The analysis of variance predicted the optimum conditions where the performance was enhanced with minimum standard deviation. Experiments carried out at optimum conditions verified the predicted data. The effects of various operational and structural parameters were analyzed by Taguchi method using L18 orthogonal array. Feed concentration of Dy(III) has been found to be the most influential factor for equilibrium sorption capacity, whereas aqueous phase acidity influences the percentage recovery most.

The work carried out in this thesis has led to the development of a process for rare earths recovery (Dy from La and Sm) by employing hollow fibre membrane (HFM) contactor module having organophosphorus type of extractant. The results obtained indicate successful optimization of conditions for dysprosium purification by using HFM module from the mixed rare earths feed upto 98% purity and >85% recovery. Rare earths separation from aqueous phase was obtained by employing HFM module in two different mode of operation i.e. non-dispersive solvent extraction and hollow fibre supported membrane. The stability and reusability of the HFSLM was found to be good even after 5 successive runs.

The studies on the synthesis, characterization, evaluation and application of polymeric beads for the recovery of REEs have promising potential to be harnessed in the fields like toxic metal removal, concentration of metal ions from lean sources and removal of entrained

impurities. HFM technique has been explored as an emerging technique for the separation of valuable rare earths from acidic feed solutions. All the above developed process and materials have the potential to be up scaled for industrial level applications.

Future direction drawn from the present work

- **The developed method reported in this thesis can be employed to prepare PES based beads encapsulating wide class of organic extractants for use in vast spectrum of separation science.**
 - **PES based matrix may find use in encapsulating ionic liquid inside the polymeric beads; this can lead to development of environmental friendly process for metal ion recovery.**
 - **Hollow fibre membrane based work can be further fine-tuned and scaled up for continuous operation which include extraction, scrubbing and stripping for individual rare earths separation and purification.**
-



REFERENCES

References

1. Voncken, JHL. The rare earth elements an introduction, Springer, AG Switzerland; 2015.
2. Jones AP, Wall F, Williams CT, Rare earth minerals: chemistry, origin and ore deposits. Chapman & hall, London; 1996.
3. McLennan SM. Geology, geochemistry and natural abundances of the rare earth elements. In: Atwood DA (ed) The rare earth elements—fundamentals and applications. Wiley, New York; 2012:1–19.
4. Auer von Welsbach C. Über die Erden des Gadolinites von Ytterby. Monatshefte für Chemie und verwandter Teile anderer Wissenschaften. 1883;4(1):630–642 (now Chem. Monthly)
5. Haxel GB, Boore S, Mayfield S. U.S. geological survey. Fact Sheet 087-02. Rare earth elements—critical resources for high technology; 2005.
6. Gadolin J. Undersökning av en svart tong stenart från Ytterby stenbrott i Roslagen, Kungliga Svenska Vetenskapsakademien, Handlingar. 1794;137–155.
7. Gadolin J. Von einer schwarzen, schweren Steinart aus Ytterby Steinbruch in Roslagen in Schweden, Crell's Annalen. 1796; 313–329.
8. Weeks ME. Discovery of the Elements (7th edition, Ch. 16). J Chem Educ Am Chem Soc. 1968; 667–699.
9. Gupta CK, Krishnamurthy N. Extractive metallurgy of the rare earths. CRC Press, Boca Raton; 2005:484.
10. Marinsky JA, Glendenin LE, Coryell CD. The chemical identification of radioisotopes of Neodymium and of element 61. J Am Chem Soc. 1947;69(11):2781–2785.
11. Autschbach J, Siekierski S, Seth M, Schwerdtfeger P, Schwarz WHE. J. Comput. Chem. 2002; 23:804.

12. Baerends EJ, Schwarz WHE, Schwerdtfeger P, Snijders J G, J. Phys. B: At. Mol. Opt. Phys. 1990; 23: 3225.
13. Diemann E. Prax. Naturwiss. Chem. 1994; 43: 36.
14. Spedding FH, Beaudry BJ, The effect of impurities, particularly hydrogen, on the lattice parameters of the “ABAB” rare earth metals, J. Less Common Met. 1971; 25:61.
15. Taylor KNR, Darby MI. Physics of Rare Earth Solids, Chapman and Hall, London; 1972:1 – 324.
16. Shannon RD, Prewitt CT. Effective ionic radii in oxides and fluorides, Acta Crystallogr. Sect. B. 1969:25:925.
17. Petzel T, Greis O, Anorg Z. Über die Anwendung eines neuartigen Reduktionsverfahrens zur Reindarstellung von SmF_2 , EuF_2 , YbF_2 , SmS , YbS und EuO , Allg. Chem.; 1973; 396:95.
18. Henderson P. The rare earth elements: introduction and review. In: Rare earth minerals, chemistry, origin and ore deposits, The Mineralogical Society Series, Chapman and Hall, London; 1996: chapter 1:1–19.
19. Van Vleck JH. The Theory of Electric and Magnetic Susceptibilities. Oxford University Press, Oxford; 1932:1 – 395.
20. Chen JY. Handbook of hydrometallurgy. Metallurgical Industry Press, Beijing, China; 2005.
21. Wernick J. Magnetic materials. In Kroschwitz, J.I. and Grant, M.H. (eds.), Kirk-Othmer Encyclopedia of Chemical Technology, John Wiley & Sons, New York; 1995:4:15: 723–788.
22. Alonso E, Sherman AM, Wallington TJ, Everson MP, Field FR, Roth R, Kirchain RE. Evaluating Rare Earth Element Availability: A Case with Revolutionary Demand from Clean Technologies. Environ. Sci. Technol. 2012; 46: 3406– 3414.

23. Zhang J, Zhao B, Schreiner B. Separation Hydrometallurgy of Rare Earth Elements, Springer International Publishing, Switzerland; 2016.
24. Welsbakh CAV. Pyrophoric Alloy, US Patent; 1906:837017.
25. Yung Y, Bruno K. Low rare earth catalysts for FCC Operations. Pet Technol Q. 2012; 1–10.
26. Emsley J. Nature's building blocks: an A-Z guide to the elements. Oxford University Press, Oxford; 2001:538.
27. Liu G, Chen X, Spectroscopic properties of lanthanides in nanomaterials. In: Gschneidner KA, Büinzli Jr JCG, Pecharsky VK. (Eds.), Handbook on the Physics and Chemistry of Rare Earths. 2007; 37: 99–169.
28. Tu D, Liang Y, Liu R, Li D. Eu/Tb ionsco-doped white light luminescence Y₂O₃ phosphors. Journal of Luminescence. 2011; 131: 2569–2573.
29. Fauchera MD, Morlottib R, Moune OK. The effects of added foreign ions in Gd₂O₂S: Tb³⁺; crystal field calculations, lifetimes, photo-luminescence and absorption spectra. Journal of Luminescence. 2002; 96: 37–49.
30. Karsu EC, Popovici EJ, Ege A, Morar M, Indrea E, Karali T, Can N,. Luminescence study of some yttrium tantalate-based phosphors. Journal of Luminescence. 2011; 131:1052–1057.
31. Liu J, Vora P, Walmer M. Overview of Recent Progress in Sm-Co Based Magnets. In: Proceedings of 19th International Workshop on Rare Earth Permanent Magnets & Their Applications, Journal of Iron and Steel Research.13. (Supplement) 2006; 319–323.

32. Hu ZH, Lian FZ, Zhu MG, Li W. Effect of Tb on the intrinsic coercivity and impact toughness of sintered Nd–Dy–Fe–B magnets. *Journal of Magnetism and Magnetic Materials*. 2008; 320: 1735–1738.
33. Xu F, Zhang L, Dong X, Qiongzen, Liu Q, Komuro M. Effect of DyF₃ additions on the coercivity and grain boundary structure in sintered Nd–Fe–B magnets. *ScriptaMaterialia*. 2011; 64: 1137–1140.
34. European Commission. Critical raw materials for the EU, Report of the Ad-hoc working group on defining critical raw materials; 2010.
35. U.S. Department of Energy 2011 critical materials strategy; 2011.
36. Binnemeans K, Jones PT, Blanpain B, Van Gerven T, Yang YX, Walton A, Buchert M. Recycling of rare earths: a critical review. *J Clean Prod*. 2013;51:1–22
37. USEPA, Rare earth elements: a review of production, processing, recycling, and associated environmental issues; 2012. Web page: <http://nepis.epa.gov/Adobe/PDF/P100EUBC.pdf>
38. USGS. Rare earth elements — critical resources for high technology;2012. Web page: <http://pubs.usgs.gov/fs/2002/fs087-02/> (Sept. 2014).
39. Ferron CJ, Henry P. A review of the recycling of rare earth metals. In: *Rare Earth Elements 2013*. Met Soc of CIM, Montreal, QC. 2013; 517–531.
40. Gomez I, Van Damme G. The unique Umicore closed loop solution. Umicore S.A, Hoboken, Belgium; 2009.
41. Hitachi, Hitachi develops recycling technologies for rare earth metals. Hitachi press release, Japan; 2010.

42. Trombe F, Loriers J, Gaume-Mahn P, La Blanchetais Ch. H. Scandium-Yttrium-Elements des Terres Rares-Actinium in P. Pascal (ed.): *Nouveau Traite De Chimie Minerale*, Paris; 1959.
43. Adams JW, Iberall ER. Bibliography of the Geology and Mineralogy of the Rare Earths and Scandium to 1971. *Geological Bulletin*, Washington; 1973: 1366.
44. Wang D, Chi R. Rare earth processing and extraction technology. Scientific Press, Beijing; 1996:63–111.
45. Cheng J, Hou Y, Che L. Making rational multipurpose use of resources of RE in baiyuanebo deposit. *Chinese Rare Earths*. 2007; 28: 70–74.
46. Breithaupt. Über den Monazit, eine neue Specie des Mineral Reichs. *J für Chemie und Physik*; 1829:55:301–303
47. Berzelius JJ, Account of two newly discovered mineral species. *Edinb J Sci*. 1825; 3: 327–332.
48. Tanaka M, Oki T, Koyama K, Narita H, Oishi T. Recycling of rare earths from scrap. In: *Handbook on the Physics and Chemistry of Rare Earths*, vol. 43. Elsevier B.V, Amsterdam, Holland; 2013: 159–211.
49. Habashi F. Extractive metallurgy of rare earths. *Can Metall Q*; 2013:52:3:224–233.
50. McGill I. Rare Earth Elements, Ullman's Encyclopedia of Industrial Chemistry. 2012; 183-224.
51. Spedding FH, Powell JE. In Nachod FC, Schubert J. (eds.): *Ion Exchange Technology*, Academic Press, New York; 1956: 359 – 390.
52. Scott CD, Spence RD, Sisson WG. Pressurised Annular Chromatography for Continuous Separation. *J. Chromatogr*. 1976; 126: 381 – 400.

53. Begovich JM, Sisson WG. A Rotating Annular Chromatograph for Continuous Metals Separation and Recovery. *Resour. Conserv.* 1982; 9: 219 – 229.
54. Begovich JM, Byers CH, Sisson WG. A High Capacity Pressurised Continuous Chromatograph. *Sep. Sci. Technol.* 1983; 18: 1167 – 1191.
55. Taniguchi VT, Doty AW, Byers CH. Large Scale Chromatographic Separations using Continuous Displacement Chromatography (CDC) in Bautista RG, Wong MM. (eds.) *Rare Earths; Extraction, Preparation and Applications*. The Minerals, Metals and Materials Soc. Las Vegas. 1989; 147 – 161.
56. Surls JP, Choppin GR. Equilibrium Sorption of Lanthanides, Americium and Curium on Dowex-50 Resin, *J. Am. Chem. Soc.* 1957; 79:855 – 859.
57. Spedding FH, Powell JE, Wheelwright EJ. The use of copper as the retaining ion in the elution of rare earths with ammonium ethylene diamine tetra acetate solutions. *J Am Chem Soc.* 1954; 76: 2557–2560.
58. Fischer W, Dietz W, Jubermann O. *Naturwissenschaften* 1937; 25: 348.
59. Fischer W, Biesenberger K, Heppner J, U. Neitzel, *Chem. Ing. Tech.* 1964; 36: 85 – 99.
60. Horn F. Zur Theorie der multiplikativen Verteilungsverfahren, *Chem. Ing. Tech.* 1964; 36: 99 –111.
61. Kislik VA. *Solvent extraction: classical and novel approaches*. Elsevier; 2012:555.
62. Reuters, Inner Mongolia Baotou Steel Rare-Earth announces fire in factory. 2007.
63. Peppard DF, Mason GW, Maier JL. Fractional extraction of the lanthanides as their di-alkyl orthophosphates. *J InorgNucl Chem.* 1957;4:(5–6):334–343.

64. Sun XQ, Waters KE. Development of industrial extractants into functional ionic liquids for environmentally friendly rare earth separation. *ACS Sustainable Chem Eng.* 2014; 2: 1910–1917.
65. Guo L, Chen J, Shen L. Highly selective extraction and separation of rare earths (III) using bifunctional ionic liquid extractant. *ACS Sustainable Chem Eng.* 2014; 2: 1968–1975.
66. Mulder M. *Basic Principles of Membrane Technology.* Kluwer Academic: Norwell, MA. 1992.
67. Ho WSW, Sirka KK, Eds. *Membrane Handbook.* Chapman & Hall: New York. 1992.
68. Lee K, Evans DF, Cussler EL. Selective copper recovery with two types of liquid membranes, *AIChE J.* 1978; 24: 860-868.
69. Danesi PR, Separation of Metal Species by Supported Liquid Membranes, *Sep Sci Technol.* 1984-85; 19: 857-894.
70. Dworzak WR, Naser AJ. Pilot-Scale Evaluation of Supported Liquid Membrane Extraction, *Sep Sci Technol.* 1987; 22: 677-689.
71. Guerreiro R, Meregalli L, Zhang, X. Indium recovery from sulphuric solutions by supported liquid membranes, *Hydrometallurgy.* 1988; 20: 109-120.
72. Kopunec R, Manh TN. Carrier-mediated transport of actinides and rare earth elements through liquid and plasticized membranes, *J Radioanal Nucl Chem.* 1994; 183:181-204.
73. Uragami T, *Membrane Science and Technology*, Eds. Osada Y, Nakagawa T, Marcel Dekker: New York; 1992.
74. Parthasarathy N, Pelletier M, Buffle J. Hollow fiber based supported liquid membrane: a novel analytical system for trace metal analysis, *Anal. Chim. Acta.* 1997; 350: 183-195.

75. Prasad R, Sirkar KK. Hollow fiber solvent extraction: Performances and design, J. Membr. Sci. 1990; 50: 153-175.
76. Zhang Q, Cussler EL. Microporous hollow fibers for gas absorption. I. Mass transfer in the liquid, J. Membrane Sci. 1985; 23: 321–332.
77. Zhang Q, Cussler EL. Microporous hollow fibers for gas absorption. II. Mass transfer across the membrane, J. Membrane Sci. 1985; 23: 333–345.
78. Kiani A, Bhavé RR, Sirkar KK, Solvent extraction with immobilized interfaces in a microporous hydrophobic membrane, J. Membrane Sci. 1984; 20: 125–145.
79. D’Elia NA, Dahuron L, Cussler EL. Liquid–liquid extractions with microporous hollow fibers. J. Membrane Sci. 1986; 29: 309–319.
80. Gyves J, San Miguel ER. Metal ion separations by supported liquid membranes. Ind. Eng. Chem. Res. 1999; 38: 2182–2202.
81. Dahuron L, Cussler EL. Protein extractions with hollow fibers. AIChE J. 1988; 34: 130.
82. Prasad R, Sirkar KK. Hollow fiber solvent extraction: Performances and design, J. Membrane Sci. 1990; 50: 153–175.
83. Cooney DO, Poufos MS. Liquid–liquid extraction in a hollow-fiber device. Chem. Eng. Commun. 1987; 61: 159–167.
84. Basu R, Prasad P, Sirkar KK. Nondispersive membrane solvent back extraction of phenol, AIChE J. 1990; 36: 450–460.
85. Yun CH, Prasad R, Sirkar KK. Membrane solvent extraction removal of priority organic pollutants from aqueous waste streams. Ind. Eng. Chem. Res. 1992; 31: 1709.
86. Yun CH, Prasad R, Guha AK, Sirkar KK. Hollow fiber solvent extraction removal of toxic heavy metals from aqueous waste streams. Ind. Eng. Chem. Res. 1993; 32: 1186.

87. Alonso A, Urtiaga AM, Irabien A. Extraction of Cr(VI) with Aliquat 336 in hollow fiber contactors: Mass transfer analysis and modeling, *Chem. Eng. Sci.* 1994; 49: 901.
88. Escalante H, Alonso AI, Ortiz I, Irabien A. Separation of L-phenylalanine by nondispersive extraction and backextraction: Equilibrium and kinetic parameters, *Sep. Sci. Tech.* 1998; 33: 119.
89. Urtiaga AM, Ortiz MI, Salazar E, Irabien I. Supported liquid membranes for the separation-concentration of phenol. 1. Viability and mass-transfer evaluation, *Ind. Eng. Chem. Res.* 1992; 31: 877; Supported liquid membranes for the separation-concentration of phenol. 2. Mass-transfer evaluation according to fundamental equations, *Ind. Eng. Chem. Res.* 1992; 31: 1745.
90. Hale DK, *Chelating Resins*, Research (London). 1956; 9: 104.
91. Warshawsky A. Polystyrenes impregnated with ethers—A polymeric reagent selective for gold. *Talanta*. 1974; 21: 962-965.
92. Warshawsky A. Solvent impregnated resins in hydrometallurgical applications, *Inst. Min. & Metal. (London) Trans. Sect. C.* 1974; 83: 101.
93. Grinstead RR, Jones KC. Aliphatic amidines: A new solvent extraction system, *J. Nucl. Inorg. Chem.* 1974; 36: 391.
94. Warshawsky A. *Ion Exchange and Solvent Extraction* vol. 8, ed. Marinsky JA, Marcus Y. Marcel Dekker, New York; 1981: 229.
95. Cortina JL, Warshawsky A. *Ion Exchange and Solvent Extraction*, vol. 13, ed. Marinsky JA, Marcus Y. Marcel Dekker, New York; 1996: 209.
96. Tiravanti G, Petruzzelli D, Passino R. Low and non waste technologies for metals recovery by reactive polymers, *Waste Mangement.* 1996; 16: 597–605.

97. Bart HJ, Schoneberger A. Reactive processes for recovery of heavy metals in miniplants, *Chem. Eng. Technol.* 2000; 23: 653–660.
98. Ritcey GM, Ashbrook AM. *Solvent Extraction: Principles and Applications to Process Metallurgy, Part 1*, Elsevier, Amsterdam: 1984.
99. Rovira M, Hurtado L, Cortina JL, Arnaldos J, Sastre AM. Recovery of palladium (II) from hydrochloric acid solutions using impregnated resins containing Alamine 336, *Reactive and Functional Polymers*. 1998; 38: 279–287.
100. Wakui Y, Matsunga H, Suzuki TM. Distribution of Rare earth elements between (2-ethylhexyl hydrogen 2-ethylhexylphosphonate)-Impregnated resin and acid aqueous solution, *Anal. Sci.* 1988; 4: 325-327.
101. Abdeltawab A, Nii S, Kawaizumi F, Takahashi K. Separation of La and Ce with PC-88A by counter-current mixer-settler extraction column, *Sep. Purif. Technol.* 2002; 26: 265–272.
102. Xiao DS, Yuan YC, Rong MZ, Zhang MQ, Hollow polymeric microcapsules: Preparation, characterization and application in holding boron trifluoride diethyl etherate, *Polymer*. 2009; 50: 560–568.
103. Berg van den C, Roelands CPM, Bussmann P, Goetheer ELV, Verdoes D, Wielen LAMVD. Preparation and analysis of high capacity polysulfone capsules, *React. Funct. Polym.* 2009; 69: 766–770.
104. Wang GJ, Chu LY, Zhou MY, Chen WM. Effects of preparation conditions on the microstructure of porous microcapsule membranes with straight open pores, *J. Membr. Sci.* 2006; 284: 301–312.

105. Reyes LH, Medina IS, Mendoza RN, Vazquez JR, Rodriguez MA, Guibal E, Extraction of cadmium from phosphoric acid using resins impregnated with organophosphorus extractants, *Ind. Eng. Chem. Res.* 2001; 40:1422-1433.
106. Kamio E, Matsumoto M, Valenzuela F, Kondo K, Sorption behavior of Ga(III) and In(III) into a microcapsules containing long chain alkylphosphonic acid monoester, *Ind. Eng. Chem. Res.* 2005; 44: 2266-2272.
107. Kamio E, Matsumoto M, Kondo K. Uptakes of rare metal ionic species by a column packed with microcapsules containing an extractant, *Sep. Purif. Technol.* 2002; 29: 121–130.
108. Dara MT, Belaid T, Benamor M. Extraction of Pb(II) by XAD7 impregnated resins with organophosphorus extractants (DEHPA, IONQUEST 801, CYANEX 272), *Sep. Purif. Technol.* 2002; 40: 77-86.
109. Cortina JL, Miralles N, Sastre A, Aguilar M, Profumo A, Pesavento M. Solvent impregnated resins containing Cyanex 272. Preparation and application to the extraction and separation of divalent metals, *Reactive Polymers.* 1992; 18: 67-75.
110. Ciftci H, Separation and solid phase extraction method for the determination of cadmium in environmental samples, *Desalination.* 2010; 263: 18-22.
111. Lee GS, Uchikoshi M, Mimura K, Isshiki M, Distribution coefficients of La, Ce, Pr, Nd, and Sm on Cyanex 923-, D2EHPA-, and PC88A-impregnated resins, G.S. Lee, M. Uchikoshi, K. Mimura, *Sep. Purif. Technol.* 2009; 67: 79–85.
112. Nishihama S, Sakaguchi N, Hirai T, Komasaawa I. Extraction and separation of rare earth metals using microcapsules containing bis(2-ethylhexyl) phosphinic acid, *Hydrometallurgy.* 2002; 64: 35–42.

113. Kondo K, Kamio E. Separation of rare earth metals with a polymeric microcapsule membrane, *Desalination*. 2002; 144: 249-254.
114. Sun X, Peng B, Ji Y, Chen J, Li D. The solid–liquid extraction of yttrium from rare earths by solvent (ionic liquid) impregnated resin coupled with complexing method, *Sep. Purif. Technol.* 2008; 63: 61-68.
115. Lee GS, Uchikoshi M, Mimura K, Isshiki M. Separation of major impurities Ce, Pr, Nd, Sm, Al, Ca, Fe, and Zn from La using bis(2-ethylhexyl)phosphoric acid (D2EHPA)-impregnated resin in a hydrochloric acid medium, *Sep. Purif. Technol.* 2010; 71: 186–191.
116. Gong XC, Luo GS, Yang WW, Wu FY, Separation of organic acids by newly developed polysulfone microcapsules containing trioctylamine, *Sep. Purif. Technol.* 2006; 48: 235–243.
117. Horwitz EP, Mcalister DR, Bond AH, Barrans Jr. RE, Novel extraction of chromatographic resins based on tetra alkyl diglycoamides: Characterization and potential applications, *Sol. Ex. Ion Exc.* 2005; 23: 319-344.
118. Zhao CS, Liu T, Lu ZP, Cheng LP, Huang J. An evaluation of a polyethersulfone hollow fiber plasma separator by animal experiment. *Artif Organs* 2001; 25: 60–63.
119. Tullis R H, Duffin RP, Zech M, Ambrus JL. Affinity hemodialysis for antiviral therapy. I. Removal of HIV-1 from cell culture supernatants, plasma, and blood. *TherApher Dial* 2002; 6: 213–20.
120. Samtleben W, Dengler C, Reinhardt B, Nothdurft A, Lemke HD. Comparison of the new polyethersulfone high-flux membrane DIAPES HF800 with conventional high-flux membranes during on-line haemodia filtration. *Nephrol Dial Transpl* 2003; 18: 2382–6.

121. Barth C, Gonçalves MC, Pires ATN, Roeder J, Wolf BA. A symmetric polysulfone and polyethersulfone membranes: effects of thermodynamic conditions during formation on their performance. *J Membrane Sci* 2000; 169: 287–99.
122. Cevasco G, Chiappe C. Are ionic liquids a proper solution to current environmental challenges? *Green Chem.* 2014;16: 2375-2385.
123. Dasgupta K, Joshi JB, Singh H, Banerjee S. Fluidized bed synthesis of carbon nanotubes: reaction mechanism, rate controlling step and overall rate of reaction, *AIChE J.* 2014; 60:2882–2892.
124. Langmuir I, The adsorption of gases on plane surfaces of glass, mica and platinum, *J. Am. Chem. Soc.* 1918; 40: 1361–1403.
125. Freundlich HMF. Uber die adsorption in losungen, *Z. Phys. Chem.* 1906; 57: 385–471.
126. Ho YS, Ng JCY, McKay G. Kinetics of pollutant sorption by biosorbents: A review. *Sep. Purif. Methods.* 2000; 29: 189–232.
127. Boyd GE, Adamson AW, Meyers LS. The exchange adsorption of ions from aqueous solutions by organic zeolites. II. Kinetics, *J. Am. Chem. Soc.* 1947; 69: 2836–2848.
128. Singh KK, Pathak SK, Kumar M, Mahtele AK, Tripathi SC, Bajaj PN. Study of uranium sorption using D2EHPA impregnated polymeric beads. *J. Appl. Polym. Sci.* 2013;130 (5): 3355–3364.
129. Adler YP, Markova EV, Granovsky YV, *The Design of Experiments to Find Optimal Conditions*, Mir Publication, Moscow;1975.
130. Taguchi G, Konishi S, *Orthogonal Arrays and Linear Graphs*, ASI Press, Dearborn, MI; 1987.

131. Taguchi G. Introduction to Quality Engineering: Designing Quality into Products and Processes, Asian Productivity Organization; 1986.
132. Sirkar KK. Membrane separation technologies: Current developments, Chem. Eng. Commun., 1997; 157: 145.
133. Gabelman A, Hwang ST. Hollow fiber membrane contactors, J. Membrane Sci. 1999; 159: 61.
134. Sengupta A, Reed BW, Seibert F. Liquid–liquid extraction studies on semi commercial scale using recently commercialized large membrane contactors and systems, Paper presented at the AIChE annual meeting, San Francisco, CA (November 16, 1994).
135. Thompson M, Walsh JN. Inductively Coupled Plasma Spectrometry. Blackie; 1989.
136. Moore VGL, Introduction to Inductively Coupled Plasma Atomic Emission Spectroscopy. Elsevier Amsterdam; 1989: ISBN: 0-444-43029-6.
137. Brown ME. Introduction to Thermal Analysis: Techniques and Applications, Kluwer Academic Publishers; 2001.
138. Goodhew PJ, Humphreys FJ, Beanland R. Electron Microscopy and Analysis. Taylor and Francis London; 1988.
139. Humphries M. Rare earth element, global supply chain, Congressional Research Service; 2011: 3-6.
140. Bochinski J, Smutz M, Spedding FH, Separation of Monazite Rare Earths by Solvent Extraction, Ind. Eng. Chem. Res. 1958; 50: 157-160.
141. Brown CG, Sherrington LG. Solvent extraction used in industrial separation of rare earths, J. Chem. Tech. Biotechnol. 1979; 29: 193-209.

142. Spedding H, Voigt AF, Gladrow EM, Sleight NR. The Separation of rare earths by ion exchange. I. Cerium and Yttrium, *J. Am. Chem. Soc.* 1947; 69: 2777–2781.
143. Wellens S, Goovaerts R, Möller C, Luyten J, Thijs B, Binnemans K. A continuous ionic liquid extraction process for the separation of cobalt from nickel, *Green Chem.* 2013; 15: 3160-3164.
144. Zhao C, Xue J, Ran F, Sun S. Modification of polyethersulfone membranes – A review of methods. *Prog. Polym. Sci.* 2013; 58: 76-150.
145. Wijimans JG, Kant J, Mulder MHV, Smolders CA, Phase separation phenomena in solutions of polysulfone in mixtures of a solvent and a nonsolvent: relationship with membrane formation, *Polymer.* 1985; 26: 1539-1545.
146. Ozcan S, Tor A, Aydin ME. Removal of Cr(VI) from aqueous solution by polysulfone microcapsules containing Cyanex 923 as extraction reagent, *Desalination.* 2010; 259: 179-186.
147. Ooi K, Handa YT, Abe Y, Wakisaka A. Lanthanide ion exchange properties of a coordination polymer consisting of di(2-ethylhexyl) phosphoric acid and trivalent metal ions (Ce³⁺, Fe³⁺, or Al³⁺), *Dalton Trans.* 2014; 43: 4807-12.
148. Outokesh M, Tayyebi A, Khanchi A, Grayeli F, Bagheri G. Synthesis and characterization of new biopolymeric microcapsules containing DEHPA-TOPO extractants for separation of uranium from phosphoric acid solutions, *J. Microencapsulation.* 2011; 28: 248-257.
149. Yoshizuka K, Sakamoto Y, Baba Y, Inoue K, Nakashio F. Solvent extraction of holmium and yttrium with bis(2-ethylhexyl)phosphoric acid, *Ind. Eng. Chem. Res.* 1992; 31: 1372–1378.
150. Ho YS, Ng JCY, McKay G. Kinetics of pollutant sorption by biosorbents: review, *Sep. Purif. Methods.* 2000; 29: 189–232.

151. Urbano BF, Rivas BL, Martinez F, Alexandratos SP. Equilibrium and kinetics study of arsenic sorption by water-insoluble nanocomposite resin of poly[N-(4-vinylbenzyl)-N-methyl-D-glucamine]-montmorillonite, *Chem. Eng. J.* 2012; 193-194: 21-30.
152. Gujar RB, Lakshmi DS, Figoli A, Mohapatra PK. Polymeric beads containing Cyanex 923 for actinide uptake from nitric acid medium: Studies with uranium and plutonium. *J. Chromatography A*. 2013; 1305: 48–54.
153. Pullianen TK, Wallian HC. Determination of total phosphorus in foods by calorimetric measurement of phosphorus as molybdenum blue after dry ashing: NMKL inter-laboratory studies, *J. AOAC Int.* 1994; 77: 1557-1561.
154. Matsunaga H, Ismail AA, Wakui Y, Yokoyama T. Extraction of rare earth elements with 2-ethylhexyl hydrogen 2-ethylhexyl phosphonate impregnated resins having different morphology and reagent content, *React. Funct. Polym.* 2001; 49: 189-195.
155. Behrendt DR, Legvold S, Spedding FH. Magnetic Properties of Dysprosium Single Crystals, *Phys. Rev.* 1958; 109: 1544-1547.
156. Goot ASV, Buschow KHJ. The dysprosium-iron system: Structural and magnetic properties of dysprosium-iron compounds, *J. Less-Common Metals.* 1970; 21(2): 151-157.
157. Lide R, David, Dysprosium, *CRC handbook of Chemistry and Physics.* CRC Press., New York; 2007-2008: 11.
158. Krebs E, Robert. "Dysprosium". *The History and Use of our Earth's Chemical Elements.* Greenwood Press; 1998: 234–235.
159. Singh RK, Kakodkar A, *Indian Nuclear Society News Letter*, 2003; 16: 3-10.
160. Emsley J, *Nature's Building Blocks.* Oxford University Press. Oxford; 2001: 129–130.

161. Yadav KK, Anitha M, Singh DK, Singh H. Statistical study of factors affecting the phase separation kinetics in solvent extraction for uranium recovery from phosphoric acid, *Desalination and Water Treatment*. 2012; 38: 15-21.
162. Chee KK, Wong MK, Lee HK. Optimization of microwave-assisted solvent extraction of polycyclic aromatic hydrocarbons in marine sediments using a microwave extraction system with high-performance liquid chromatography-fluorescence detection and gas chromatography-mass spectrometry, *J. Chromatogr. A*. 1996; 723: 259-271.
163. Dasgupta K, Singh DK, Sahoo DK, Anitha M, Awasthi A, Singh H. Application of Taguchi method for optimization of process parameters in decalcification of samarium-cobalt intermetallic powder, *Sep. Purif. Technol.* 2014; 124: 74-80.
164. Nasab ME, Sam A, Milani SA. Determination of optimum process conditions for the separation of thorium and rare earth elements by solvent extraction, *Hydrometallurgy*. 2011; 106: 141-147.
165. Taghizadeh M, Ghasemzadeh R, Ashrafizadeh SN, Saberyan K, Ghanadi M. Determination of optimum process conditions for the extraction and separation of zirconium and hafnium by solvent extraction, *Hydrometallurgy*. 2008; 90: 115-120.
166. Yadav KK, Singh DK, Anitha M, Varshaney L, Singh H. Studies on separation of rare earths from aqueous media by polyethersulfone beads containing D2EHPA as extractant, *Sep. Purif. Technol.* 2013; 118: 350-358.
167. Yadav KK, Dasgupta K, Singh DK, Anitha M, Lenka RK, Varshaney L, Singh H. Sorption behavior of Y(III) from chloride medium with polymer composites containing di-2-ethyl hexyl phosphoric acid and multiwall carbon nanotube, *Sep. Sci. Tech.* 2015; 50:463-470.

168. Critical Raw Materials for the EU; Report of Adhoc Working group on defining critical raw materials, European Commission, Enterprise and Industry: Bruxelles, Belgium; 2010.
169. Binnemans K, Jones PT, Blanpain B, Van Gerven T, Yang Y, Walton A, Buchert M. Recycling of rare earths: a critical review. *J. Cleaner Product.* 2013; 51.
170. Xu L, Xiao Y, Li D. An expert system for solvent extraction of rare earths. *J. Chem. Inf. Comput. Sci.* 1992; 32 (5): 437–442.
171. Noble RD, Stern SA. *Membrane Separations Technology: Principles and Applications*; Elsevier: New York; 1995.
172. *Separation and Purification: Critical Needs and Opportunities*; National Research Council; 1987.
173. Yadav KK, Dasgupta K, Singh DK, Varshney L, Singh H. Dysprosium sorption by polymeric composite bead: Robust parametric optimization using Taguchi method. *J. of Chromatography A.* 2015; 1384: 37-43.
174. Yadav KK, Dasgupta K, Singh DK, Anitha M, Varshney, L.; Singh, H. Solvent impregnated carbon nanotube embedded polymeric composite beads: An environment benign approach for the separation of rare earths. *Sep. Purif. Technol.* 2015; 143: 115-124.
175. Beltrami D, Cote G, Mokhtari H, Courtaud B, Moyer BA, Chagnes A. Recovery of Uranium from Wet Phosphoric Acid by Solvent Extraction Processes. *Chem. Rev.* 2014; 114 (24): 1202–1202. .
176. Xiea F, Zhanga TA, Dreisingerb D, Doyle F. A critical review on solvent extraction of rare earths from aqueous solutions. *Mineral Eng.* 2014; 56: 10-28.

177. Pathak SK, Tripathi SC, Singh KK, Mahtele AK, Kumar M, Gandhi PM. Removal of americium from aqueous nitrate solutions by sorption onto PC88A—Impregnated macroporous polymeric beads. *J. Haz. Mat.* 2014; 278: 464–473.
178. El-Nadi YA. Effect of diluents on the extraction of praseodymium and samarium by Cyanex 923 from acidic nitrate medium. *J. Rare Earths.* 2010; 28: 215–220.
179. Ahmad A, Siddique JA, Laskar MA, Kumar R, Mohd-Setapar SH, Khatoon A, Shiekh RA, New generation Amberlite XAD resin for the removal of metal ions: A review. *J. Environ. Sci.* 2015; 31: 104–123.
180. Crow JM. 13 exotic elements we can't live without, *The New Sci.* 2011; 2817: 36–41.
181. Yu J, Yao ST, Chi SJ. Rare earth separation techniques in the development, *J. Shenyang Univ. Technol.* 1999; 21: 83–85.
182. Pei L, Yao BH, Fu XL, Wang L M. Transport and separation of Cerium (IV) in dispersion supported liquid membrane system, *Chin. J. Proc. Eng.* 2008; 8: 851–858.
183. Suren S, Wongsawa T, Pancharoen U, Prapasawat T, Lothongkum AW. Uphill transport and mathematical model of Pb(II) from dilute synthetic leadcontaining solutions across hollow fiber supported liquid membrane. *Chem. Eng. J.* 2012; 191: 503–511.
184. Hägg MB. Membranes in chemical processing: A review of applications and novel developments, *Separ. Purif. Method.* 1998; 27: 51–168.
185. Kumar A, Sastre AM. Developments in non-dispersive membrane extraction separation processes, in A. K. Sengupta and Y. Marcus, eds., *Ion Exchange and Solvent Extraction*, Marcel Dekker, New York; 2001: 331–469.
186. Sastre AM, Kumar A, Shukla JP, Singh RK. Improved techniques in liquid membrane separations: An overview, *Separ. Purif. Method.* 1998; 27: 213–298.

187. Ho W, Sirkar KK. Membrane Handbook, New York: Van Nostrand Reinhold; 1992.
188. Drioli E, Romano M. Progress and new perspectives on integrated membrane operations for sustainable industrial growth, *Ind. Eng. Chem. Res.* 2001; 40: 1277–1300.
189. Pabby AK, Sastre AM. Developments in dispersion-free membrane – based extraction – separation processes, Marcus Y, Sengupta AK, (Eds.), *Ion Exchange and Solvent Extraction*, 15, Marcel Dekker, New York; 2002.
190. Kocherginsky NM, Yang Q, Seelam L, Recent advances in supported liquid membrane technology. *Sep. Purif. Technol.* 2007; 53(2); 171–177.
191. Panja S, Mohapatra PK, Tripathi SC, Gandhi PM, Janardan P. Supported liquid membrane transport studies on Am(III), Pu(IV), U(VI) and Sr(II) using irradiated TODGA, *J. Hazard. Mater.* 2012; 237–238: 339.
192. Wannachod P, Chaturabul S, Pancharoen U, Lothongkum AW, Patthaveekongka W. The effective recovery of praseodymium from mixed rare earths via a hollow fiber supported liquid membrane and its mass transfer related, *J. Alloys Compd.* 2011; 509: 354.
193. Kandwal P, Dixit S, Mukhopadhyay S, Mohapatra PK, Mass transport modeling of Cs(I) through hollow fibre supported liquid membrane containing calyx-[4]-bis(2,3-naphtho)-crown-6 as mobile carrier, *Chem. Eng. J.* 2011; 174: 110.
194. Ansari SA, Mohapatra PK, Manchanda VK. Recovery of Actinides and lanthanides from high level waste using hollow fibre supported liquid membrane with TODGA as the carrier, *Ind. Eng. Chem. Res.* 2009; 48: 8605-8612.
195. Li D, Zhang J, Xu M, Studies of extraction mechanism of rare earth compounds with MONO (2-ethyl hexyl) -2 ethyl hexyl phosphonate (HEH/EHP). *Chinese Journal of Applied Chemistry.* 1985; 2(2): 17–23.

196. Patil CB, Ansari SA, Mohapatra PK, Manchanda VK. Non-dispersive solvent extraction and stripping of neodymium(III) using a hollow fiber contactor with TODGA as the extractant, *Sep. Sci. Technol.* 2011; 46: 765–773.
197. Yang XJ, Fane AG. Facilitated transport of copper in bulk liquid membrane containing LIX 984 N, *Sep. Sci. Technol.* 1999; 34: 1873–1890.
198. Coelho IM, Cardoso MM, Viegas RMC, Crespo JPSG. Transport mechanism and modeling in liquid membrane contactors, *Sep. Purif. Technol.* 2000; 19: 183–197.
199. Lothongkum AW, Pancharoen U, Prapasawat T, in: J. Markos (Ed.), *Mass Transfer in Chemical Engineering Process*. 2011; 177–204.
200. Pancharoen U, Poonkum W, Lothongkum AW, Treatment of arsenic ions from produced water through hollow fiber supported liquid membrane, *J. Alloys Compd.* 2009; 482: 328–334.
201. Ramakul P, Supajaroen T, Prapasawat T, Pancharoen U, Lothongkum AW, Synergistic separation of yttrium ions in lanthanide series from rare earths mixture via hollow fiber supported liquid membrane, *J. Ind. Eng. Chem.* 2009; 15: 224–228.
202. Lothongkum AW, Ramakul P, Sasomsab W, Laoharochanapan S, Pancharoen U, Enhancement of uranium ion flux by consecutive extraction via hollow fiber supported liquid membrane, *J. Taiwan Inst. Chem. Eng.* 2009; 40: 518–523.
203. Danesi PR, Permeation of metal ions through hollow fibre supported liquid membrane: concentration equations for once-through and recycling module arrangement. *Solv. Extr. Ion Exch.* 1984; 2: 115.
204. Amrani FZ, Kumar A, Beyer L, Sastre AM, Mechanistic study of active transport of silver(I) using sulphur containing novel carriers across liquid membrane. *J. Membr. Sci.* 1999; 152: 263.

205. Danesi PR. A simplified model for the coupled transport of metal ions through hollow-fiber supported liquid membranes. *J. Membr. Sci.* 1984; 20: 231.